USE OF A DIRECT, POSITIVE SELECTION STRATEGY TO GENERATE IMPROVED PRODRUG-ACTIVATING ENZYMES FOR CANCER GENE THERAPY

SHELLEY LOUISE BAKER

A thesis submitted to

The University of Birmingham

for the degree of

DOCTOR OF PHILOSOPHY

CRUK Institute for Cancer Studies

Division of Cancer Studies

The University of Birmingham

March 2011

I would like to dedicate this to the two men in my life.
Mark my wonderful husband, who has been my rock throughout and Logan my son who brings me joy every day.

ABSTRACT

E. coli NfsB nitroreductase (NTR) is currently being studied in combination with the prodrug CB1954, as a gene directed enzyme prodrug therapy. NTR reduces CB1954 at either the 2- or 4-nitro groups to produce highly cytotoxic hydroxylamine derivatives, using either NADH or NADPH as cofactor. Initial clinical trials suggest activity, with reduction in PSA and apparent delayed progression in some patients. This thesis is concerned with engineering the NTR enzyme to improve the efficiency of CB1954 activation, since this would be expected to improve the potential clinical efficacy. Site directed mutagenesis has been used to generate four libraries of NTR mutants with three small libraries having a maximum diversity of 6.4 $x10^1$ – 8.2 x 10^3 and a large library of 6.3 x 10^6 possible nucleotide combinations. A direct positive selection strategy, which utilises bacteriophage lambda and the SOS response, was used to select NTR variants with increase sensitivity for CB1954 from each library. NTR mutants with greatest sensitivity were analysed by bacterial IC_{50} assays. Despite considerable work to generate and optimise the large library, only one NTR enzyme was improved over WT. However the best mutant (T41G N71S) came from a small library, with an IC_{50} of 8 µM. The most promising NTR enzyme variants were column purified and their kinetic parameters and activity determined. T41G N71S showed good activity for CB1954 (0.52 µM s^{-1}), being the second best mutant to date behind T41L N71S (0.90 µM s^{-1}). Adenoviral vectors were generated and their ability to sensitise SKOV3 cancer cells tested. T41G N71S was ~2-fold improved relative to WT NTR. Purified enzymes were also tested with SKOV3 cells, with T41G N71S being ~2.6-fold improved relative to WT NTR. My best enzyme should be considered when planning future clinical trials using prodrug activation gene therapy with NTR.

ACKNOWLEDGMENTS

I would firstly like to thank Dr Peter Searle for his encouragement and support during this study, particularly during the hard times when things seemed impossible. I would also like to thank the gene therapy group both past and present, in particular Dr Chris Guise for all his help and support when I was a complete novice and for all his hard work on the system that was integral to this study. Many thanks go to Dr Simon Vass and Dr David Onion for their help with virus work. To Dr Jane Grove and Dr Mansooreh Jaberipour whose work laid the foundations for this project.

I would also like to thank several people from Biosciences Dr Eva Hyde for her help with my kinetics chapter and NMR data, Rosemary Parslow for her help purifying enzymes and Martin Day for helping with structural images.

I would finally like to thank the Medical Research Council for funding this project and Cancer Research UK for financing Birmingham's Cancer Research Institute.

TABLE OF CONTENTS

LIST OF FIGURES

1. INTRODUCTION

2. MATERIALS AND METHODS

3. GENERATION AND CB1954 PRODRUG SELECTION OF THREE SMALL LIBRARIES OF NTR MUTANTS

4. GENERATION AND CB1954 PRODRUG SELECTION OF A LARGE LIBRARY OF NTR MUTANTS

5. KINETIC STUDIES OF WT AND MUTANT NTR

6. COMPARISON OF WT AND MUTANT NTR IN HUMAN CELLS

7. DISCUSSION

8. APPENDIX

9. REFERENCES

LIST OF TABLES

1. INTRODUCTION

2. MATERIALS AND METHODS

3. GENERATION AND CB1954 PRODRUG SELECTION OF THREE SMALL LIBRARIES OF NTR MUTANTS

4. GENERATION AND CB1954 PRODRUG SELECTION OF A LARGE LIBRARY OF NTR MUTANTS

5. KINETIC STUDIES OF WT AND MUTANT NTR

6. COMPARISON OF WT AND MUTANT NTR IN HUMAN CELLS

7. DISCUSSION

8. APPENDIX

9. REFERENCES

LIST OF ABBREVIATIONS

282	N71S A113V R121V F123N F124V A125C K179R
2-HA	5-aziridin-1-yl-4-nitro-2-hydroxlaminebenzamide
2 NB	2-Nitrobenzamide
3D	Three dimensional
3D-CRT	Three dimensional conformal radiation therapy
3'	3 prime strand
4-HA	5-aziridin-1-yl-2-nitro-4-hydroxlaminebenzamide
4 NB	4-Nitrobenzamide
5-FC	5 fluorocytosine
5-FU	5 fluorouracil
5-FUMP	5 fluorouracil monophosphate
5'	5 prime strand
A	Alpha
B	Beta
Γ	Gamma
Λ	Lambda
Å	Angstrom
^{o}C	Degrees centigrade
%	Percentage
[ ]	Concentration
~	Approximately
Aa	Amino acid
AAV	Adeno-associated virus
AAV-2	Adeno-associated virus serotype 2
ACV	Acyclovir
Ad5	Adenovirus serotype 5
ADA	Adenosine deaminase
ADEPT	Antibody directed enzyme prodrug therapy
Amp	Ampicillin
APS	Ammonium persulfate
Bp	Base pair
BSA	Bovine serum albumin
CAP	Calf alkaline phosphatase
CB1954	5-(aziridin-1-yl)-2,4-dinitrobenzamide
CD	Cytosine deaminase
cDNA	Complementary DNA
CEA	Carcinoembryonic antigen
CF	Cystic fibrosis

CFTR	Cystic fibrosis transmembrane conductance regulator
Cm	Centimetre
CMDA	4-[(2-chloroethyl)(2-mesoyloxyethyl)amino]benzoyl-L-glutamic acid
CML	Chronic myeloid leukaemia
CMV	Cytomegalovirus
CPE	Cytopathic effect
CPG2	Carboxypeptidase G2
CRAd	Conditionally replicating adenoviral vector
CRT	Conformal radiation therapy
CRUK	Cancer Research United Kingdom
CsCl	Caesium chloride
CTL102	Replication deficient Ad5-CMV-NR
dGTP	Deoxyguanosine triphosphate
dH_2O	De-ionised water
D_2O	Deuterium Oxide
DME(M)	Dulbecco's modified Eagle (medium)
DMSO	Dimethyl sulphoxide
DNA	Deoxyribonucleic acid
DNase I	Deoxyribonuclease I
DNBM	Dinitrobenzamide mustards
DTT	Dithiothreitol
dTTP	Deoxythymidine triphosphate
E1	Adenovirus early region 1
E2	Adenovirus early region 2
E3	Adenovirus early region 3
E-boxes	Enhancer Box sequence
EBV	Epstein-Barr virus
E. coli	*Escherichia coli*
EDTA	Ethylenediamine tetra acetic acid
Env	Envelope protein
FAD	Flavin adenine dinucleotide
FBS	Foetal bovine serum
FMN	Flavin mononucleotide
G	Acceleration due to gravity
Gag	Group Antigens
G1	Phase of cell cycle
GCV	Ganciclovir
GCK	Gene construction kit software
GDEPT	Gene directed enzyme prodrug therapy
EGFP	Enhanced green fluorescent protein
GM-CSF	Granulocyte-macrophage colony stimulating factor

GMP	Good Manufacturing Practice
H_2O	Water
HBV	Hepatitis B Virus
HCC	Hepatocellular Carcinoma
HEK 293	Human embryonic kidney cells
HER 911	Human embryonic retinoblast cells
HEPES	4-(2-hydroxyethyl)-1-piperazineethanesulfonic acid
HLA	Human leukocyte antigen
HPV	Human Papilloma virus
Hr	Hour
HSV 1	Herpes simplex virus 1
HSV-TK	Herpes simplex virus thymidine kinase
hTERT	Human telomerase reverse transcriptase
HT	Hormone therapy
HTLV-1	Human T cell leukaemia virus
IC_{50}	Inhibitory concentration 50
IFN	Interferon
Ifu	Infectious unit
IL 2	Interleukin two
IPTG	Isopropyl β-D-1-thiogalactopyranoside
ITRs	Inverted terminal repeat
IV	Intravenous
K	Kelvin
Kan	Kanamycin
Kb	Kilobase
K_{cat}	Turnover number
K_m	Michaelis Menton constant
K_{cat}/K_m	Specificity constant
kDa	kilo-Dalton
Kg	Kilogram
LB	Luria broth
LH7	Acyclic 4-nitrobenzyl phosphoramide mustard
LMO2	LIM domain only 2
M	Molar
M^{-1} cm^{-1}	Molar to the minus one centimetre to the minus one
MD	Menadione
Mg	Milligram
MHC	Major histocompatability complex
MHz	Megahertz
Ml	Millilitre
mM	Millimolar

MOI('s)	Multiplicity of infection (s)
mRNA	Messenger ribonucleic acid
MTT	3-(4,5-Dimethylthiazol-2-yl)-2,5-diphenyltetrazolium bromide
MVA	Modified Vaccinia Ankara
NaCl	Sodium Chloride
NAD^+	Nicotinamide adenine dinucleotide (oxidised form)
NADH	Nicotinamide adenine dinucleotide (reduced form)
$NADP^+$	Nicotinamide adenine dinucleotide phosphate (oxidised form)
NADPH	Nicotinamide adenine dinucleotide phosphate (reduced form)
Nfs*A*	*Escherichia coli* major nitroreductase *A*
Nfs*B*	*Escherichia coli* major nitroreductase *B*
Nfs*C*	*Escherichia coli* major nitroreductase *C*
NFZ	Nitrofurazone
NHL	Non-hodgkin's lymphoma
NK	Natural Killer cells
Ng	Nanogram
nM	Nanomolar
Nm	Nanometre
NMR	Nuclear Magnetic Resonance
NSCLC	Non-small cell lung carcinoma
NTR	Nitroreductase
NQO1	Mammalian NAD(P)H quinone oxidoreductase 1
Nt	Nucleotide
OC	Osteocalcin promoter
OD	Optical density
ORF	Open reading frame
OTC	Ornithine transcarbamylase
PAGE	polyacrylamide gel electrophoresis
PAMAM	Polyamidoamine
PBMCs	Peripheral blood mononuclear cells
PBS	phosphate buffered saline
PCR	Polymerase chain reaction
PDB	Protein Data Bank
PEG	Polyethylene glycol
Pfu	Plaque forming unit
Pg	Picogram
P:I	Particle to Infectivity ratio
pM	Picomolar
PMSF	Phenylmethylsulphonyl fluoride
PNP	Purine nucleotide phosphorylase
Pol	Reverse Transcriptase Polymerase

Ppm	Parts per million
PSA	Prostate specific antigen
RB	Retinoblastoma gene
RNA	Ribonucleic acid
RNAi	Interfering ribonucleic acid
RNAP	RNA Polymerase
RNase A	Ribonuclease A
Rpm	Revolutions per minute
RSV	Rous sarcoma virus promoter
RT	Radiotherapy
s^{-1}	Seconds to the minus one
SCID	Severe combined immunodeficiency
SCID-X1	Severe combined immunodeficiency – X linked
SDS	Sodium dodecyl sulphate
SiRNA	Small interfering RNAs
SKOV3	Ovarian carcinoma cells
$T_{10}E_1$	10 mM Tris, 1 mM EDTA pH 8
$T_{10}E_1N_{100}$	10 mM Tris, 1 mM EDTA, 100 mM NaCl, pH 8
TAE	242 g of Tris HCl, 57.1 ml glacial acetic acid, 18.2 g disodium EDTA (1 litre)
TEMED	Tetramethylethylenediamine
TNF-α	Tumour necrosis factor alpha
Tris	Tris(hydroxymethyl) methylamine
TRUS	Trans rectal ultrasound scan
Tween	Polyoxyethylene-sorbitan mono oleate
µg	Microgram
µm	Micrometre
µM	Micromolar
µM s^{-1}	Micromolar seconds to the minus one
UPRT	Uracil phosphoribosyl transferase
USA	United States of America
UV	Ultraviolet light
V	Volts
VCV	Valacyclovir
VDEPT	Virus directed enzyme pro-drug therapy
VV	Vaccinia virus
v/v	Volume by volume
w/v	Weight by volume
WT	Wild type
XMRV	Xenotropic murine leukaemia related virus
YieF	*Escherichia coli* Chromate reductase
YwrO	*Bacillus amyloliquefaciens* nitroreductase

CHAPTER 1: INTRODUCTION

1.1 CANCER

Cancer is a complex group of diseases that affect a wide range of cells and tissues. A genetic link to cancer was first put forward in the 20th century, and is currently one of the major foundations of cancer research. Mutations which increase or decrease the expression of certain genes are common features of cancers.

1.1.1 Incidence

One in three people will be diagnosed with cancer at some point in their life and a quarter of all deaths are due to cancer. Cancer tends to affect older people with 74 percent of diagnoses occurring in people over 60 years. Figure 1.1 shows the number of new cases and rates in the UK based on age and sex.

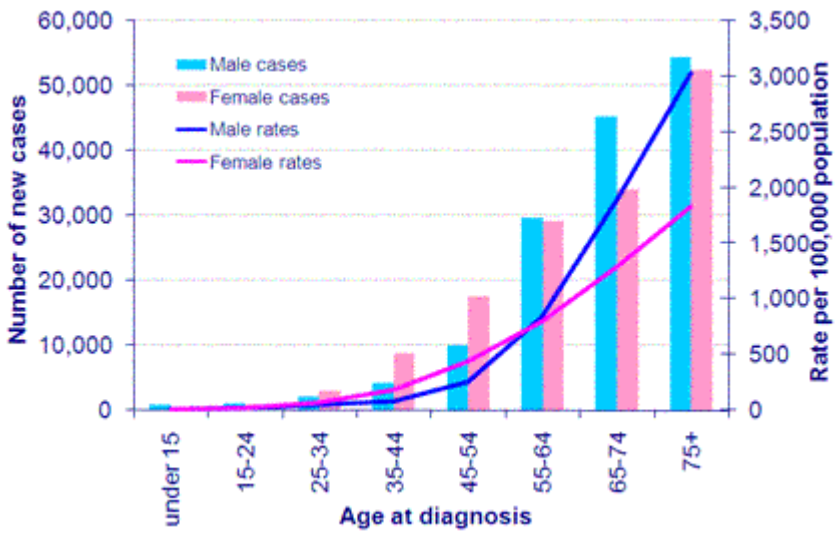

Figure 1.1 Number of new cases and rates by age, sex and type of cancer, UK 2007
(CRUK website info.cancerresearchuk.org October 2009)

Less than 1 percent of cancers are in children (0-14 years) which accounts for around 1,400 cases. Leukaemia makes up a third of all child cases and brain and spinal tumours account for more than a fifth. A further 1,875 teenagers and young adults (15-24 years) were diagnosed in 2006. In this age group Hodgkin's lymphoma, testicular cancer, malignant melanoma, leukaemia and bone cancer are common. Around 10 percent of all cancer cases are in adults between the ages of 25-49 years. In this age group breast, malignant melanoma, colorectal and cervical cancers are most common.

In 2006 293,601 people were diagnosed with cancer in the UK with 147,223 cases in men (Figure 1.2a) and 146,378 cases in women (Figure 1.2b). Prostate cancer is the most commonly diagnosed cancer in males. In women breast cancer is the most common.

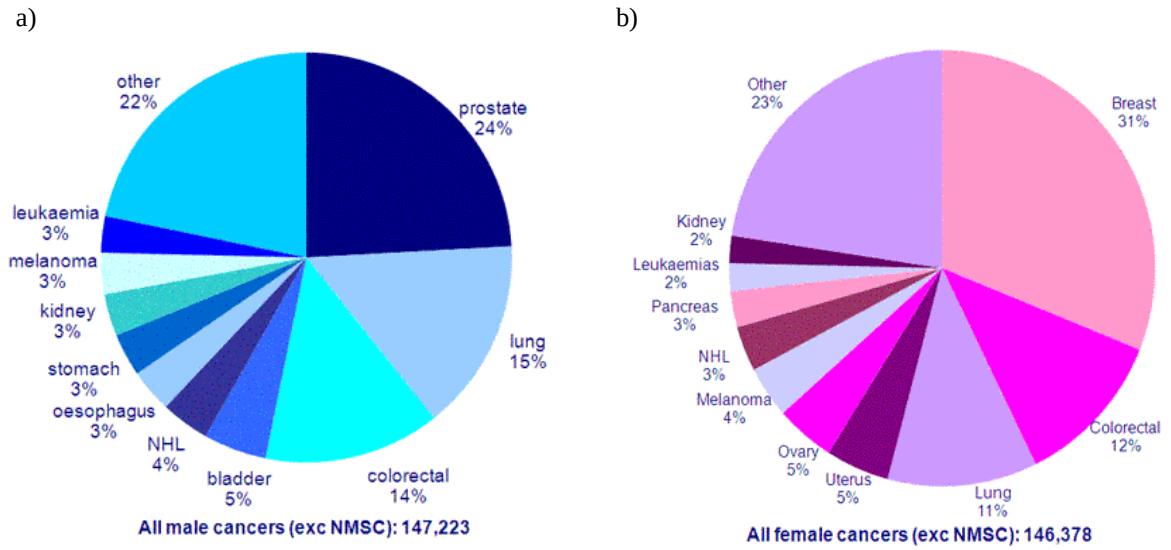

Figure 1.2 Ten most common cancers in the UK for males and females in 2006
a) Ten most common male cancers, b) Ten most common female cancers. This table excludes non-melanoma skin cancer (CRUK website info.cancerresearchuk.org October 2009)

There are more than 200 different types of cancer, however 54 percent of all cancer diagnoses were breast, lung, colorectal and prostate cancer. Breast cancer is the most common cancer in the UK (see Figure 1.3).

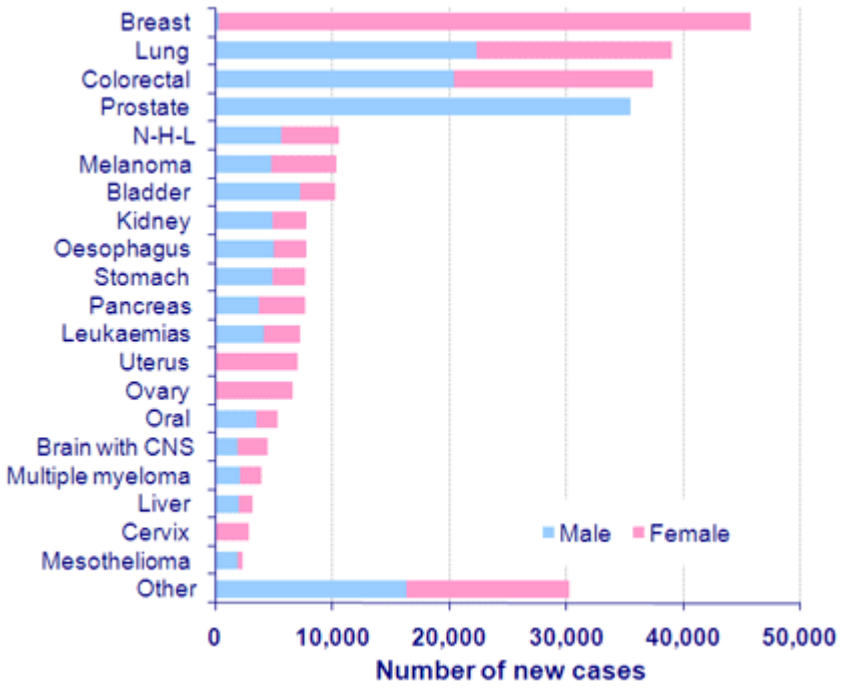

Figure 1.3 Twenty most common diagnosed cancers in the UK in 2006
This table excludes non-melanoma skin cancer and N-H-L stands for non-hodgkin's lymphoma (CRUK website info.cancerresearchuk.org October 2009)

1.1.2 Mortality

The second largest cause of death in the UK is cancer only slightly behind heart disease with 155,484 deaths in 2007. The vast majority of deaths from cancer occur in the elderly with 76 percent occurring in people aged 65 years and over. Figure 1.4 shows the number of deaths and specific mortality rates based on age and sex.

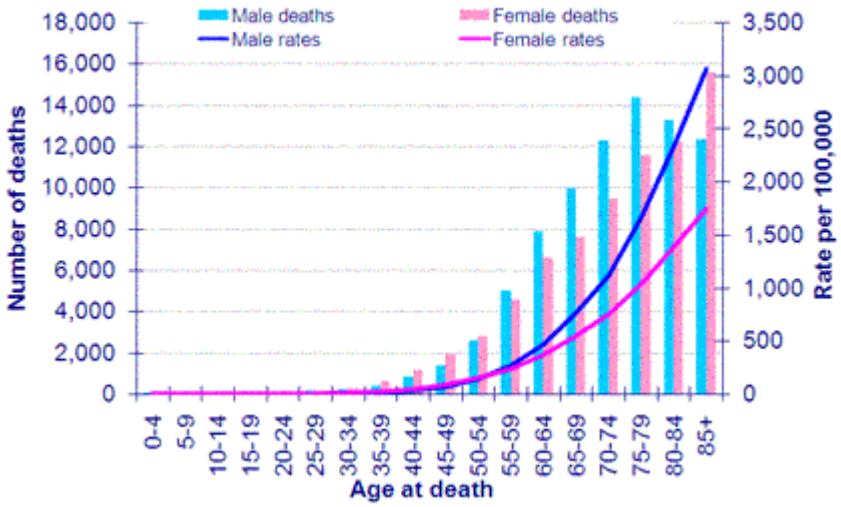

Figure 1.4 Number of deaths and mortality rates by age, sex and type of cancer, UK 2007
(CRUK website info.cancerresearchuk.org October 2009)

In 2007 155,484 people died from cancer in the UK with 80,907 cases in men (Figure 1.5a) and 74,577 cases in women (Figure 1.5b). Lung cancer is the most common cause of both male and female deaths from cancer.

a)

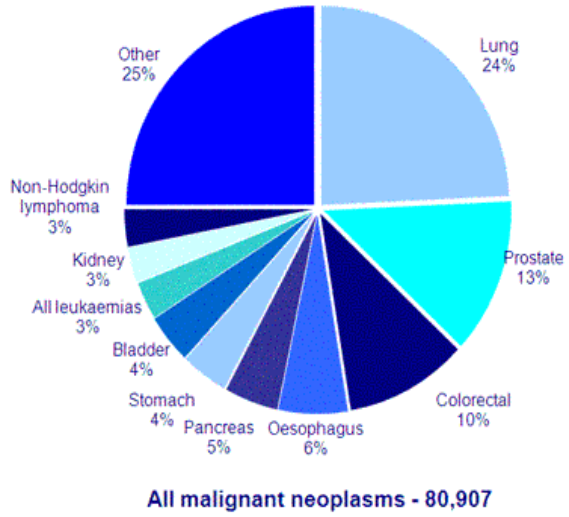

b)

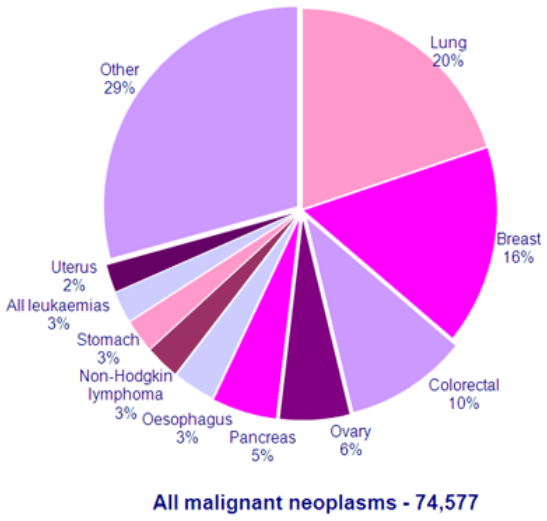

Figure 1.5 Ten most common causes of cancer deaths in the UK for males and females in 2007
a) Ten most common causes of cancer death in males, b) Ten most common causes of cancer death in females (CRUK website info.cancerresearchuk.org October 2009)

47 percent of all cancer deaths in the UK in 2007 were from lung, bowel, breast and prostate cancer. Lung cancer causes the most cancer deaths accounting for 22 percent. This was followed by colorectal cancer with 10 percent and breast cancer with 8 percent. Figure 1.6 shows the most common causes of death from cancer.

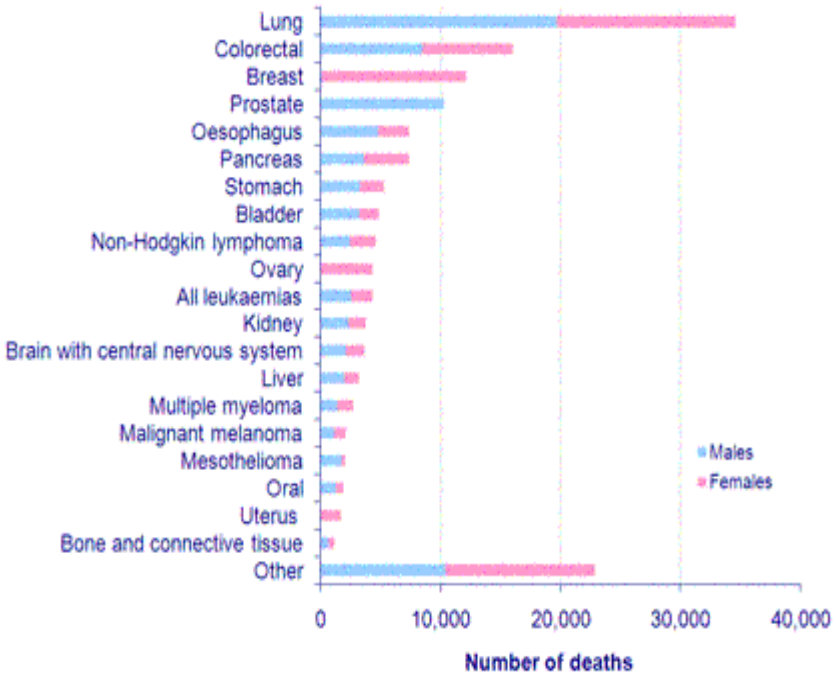

Figure 1.6 Twenty most common diagnosed cancers in the UK in 2007
(CRUK website info.cancerresearchuk.org October 2009)

1.1.3 Risk Factors

Many factors may contribute to the development of cancer. These can generally be divided into cellular (intrinsic) and environmental (extrinsic) factors.

1.1.3.1 Cellular (Intrinsic)

Cancerous cells lose the ability to regulate growth leading to an imbalance between proliferation, differentiation and cell death. Control of cell division is regulated by two broad classes of genes, firstly by genes which suppress cell division known as tumour suppressor genes and secondly by genes which promote cell division, these genes are known as proto-oncogenes.

Tumour suppressor genes encode proteins that can inhibit inappropriate cell cycle progression (for example: following DNA damage). In general for a tumour suppressor gene to contribute to cancer, both copies of the gene must lose their function or be lost. Studies have identified approximately 10 tumour suppressor gene that when mutated lead to a predisposition for specific cancers (Lewin 2000). The tumour suppressor gene *RB* when mutated leads to retinoblastoma, a cancer of the retinal cells in the eyes (Alberts *et al.* 1994). About 40 percent of cases are dominantly inherited affecting both eyes and the remaining 60 percent are sporadic affecting a single eye (Sudbery 2002). In normal cells retinoblastoma tumour suppressor protein (*pRB*) regulates cell proliferation by binding and sequestering transcription factors essential for progression to S phase. Specifically *RB* binds to the transcription factor E2F in the G1 phase of cell cycle. Following growth signal transduction pRB becomes phosphorylated; this triggers dissociation from E2F at the end of G1, allowing transcription of E2F regulated genes and S-phase entry.

It is well known that in many cancers the transcription factor *p53* is faulty or absent. Protein *p53* mutations have been associated with many cancers including breast, lung, bladder and colon cancer. In fact approximately 50 percent of all cancers can be associated with mutations in the *TP53* gene which encodes p53 (Campbell *et al.*1999 and Griffiths *et al.* 2002).

The *p53* gene encodes a phosphoprotein that plays a critical role in both regulation of the cell cycle and apoptosis. Following DNA damage, *p53* activates the *p21* gene; *p21* halts the cell cycle by binding to cyclin-dependent kinases allowing time for the cell to repair the DNA. When DNA damage is irreparable *p53* can activate genes whose protein products cause cell death via apoptosis.

The gene *BRCA1* is associated with breast cancer, as a dominant inherited trait. Approximately 60 percent of women carrying a mutation will go on to develop breast cancer by age 50 and 82 percent by 70. The comparable figures for women who inherit two normal copies are 2 percent and 7 percent respectively (Purves *et al.* 1999). Mutations in *BRCA1* also increase the risk of ovarian cancer. A further breast cancer gene called *BRCA2* can also be inherited as a dominant trait. Both *BRCA1* and *BRCA2* play important roles in DNA double strand break repair (Campbell *et al.* 1999).

Proto-oncogenes when expressed have a positive function on cell signalling and the cell cycle, these genes are under strict regulation. Upon mutation proto-oncogenes can become oncogenic, typically retaining their positive function but losing the appropriate regulatory control. Approximately 100 oncogenes have been identified (Lewin 2000).

There are at least three mechanisms associated with the conversion of proto-oncogenes to oncogenes, point mutation, translocation or over-expression. The most well known proto-oncogenes would be the *ras* gene family. Three well-characterised genes of the *ras* gene family H-*ras,* K-*ras* and N-*ras,* code for related monomeric guanosine triphosphate-binding proteins (G proteins) that have a role in the transduction of growth signals between growth factor receptors and the cytoplasmic MAP kinase pathway (Hurley *et al.* 1984, Bos *et al.* 1985 and Rodenhuis and Slebos 1990). Most *ras* mutations are single nucleotide substitutions which lead to constitutive activation of downstream signalling pathways. Approximately 30 percent of cancers carry a *ras* mutation (Zhang *et al.* 1993 and Campbell *et al.*1999).

Another well characterised oncogene is *c-abl* which is activated by translocation and is associated with chronic myeloid leukaemia (CML). This proto-oncogene encodes a cytoplasmic and nuclear protein tyrosine kinase, which plays a role in cell differentiation, cell division, cell adhesion and stress responses (Zipfel *et al.* 2000 and Qiu *et al.* 2009).

In human tumours, members of the *myc* proto-oncogene family are often amplified by over-expression; there can have up to several hundred times greater expression. *myc* encodes a transcription factor that regulates the expression of approximately 15 percent of all genes by binding through Enhancer Box sequences (E-boxes). The cancer Burkitt's lymphoma is associated with *myc* upregulation as a result of chromosome translocation to the immunoglobulin loci (Walhout *et al.* 1997, Tsuneoka *et al.* 1997 and Kim *et al.* 2004).

1.1.3.2 Environmental (Extrinsic)

Epidemiology shows that environmental factors are the leading cause of cancer. Variations of cancer differ from place to place, time to time and depend on peoples activities. There are several environmental factors which affect a person's risk of cancer including radiation, diet, smoking, chemical carcinogens and viruses.

Both ionising and non-ionising radiation can physically damage DNA within the human body leading to mutation. In the case of ionising radiation target molecules lose electrons. These electrons can cause extensive chemical alterations in DNA, including strand breaks and base and sugar destruction (Turner *et al.* 1997). Examples of ionising radiation include x-rays, α-rays, β-rays and γ-rays (Hartl and Jones 1999). Non-ionising radiation causes molecular vibrations within the target molecules. This can lead to the formation of new chemical bonds (Turner *et al.* 1997). Non-ionising radiation can damage DNA by causing thymidine dimers in single stranded DNA. An example of non-ionising radiation would be ultraviolet light.

A variety of cancers such as bowel, stomach, mouth and breast can be affected by a diet. A diet high in red and processed meats, saturated fat and salt increases cancer risk, where as a diet high in fibre, fruit and vegetables is associated with a reduced risk of cancer. Experts think that up to a quarter of cancer deaths are caused by unhealthy diet (CRUK website info.cancerresearchuk.org October 2009). Excessive alcohol consumption increases the risk of mouth, throat and oesophageal cancer. Alcoholics also have an increased risk of liver and bowel cancer.

Smoking is the single biggest cause of cancer in the world and causes one in four UK cancer deaths. Nine out of ten cases of lung cancer are caused by smoking (CRUK website info.cancerresearchuk.org October 2009). Smoking is also a risk factor for many other cancers including bladder, kidney, cervical, throat, mouth, oesophagus, stomach and pancreas cancer.

Many chemicals are considered to be carcinogens that cause cancer. Some examples of chemical carcinogens are 2-naphthylamide, ethidium bromide, trichloroethylene, benzene, arsenic and acrylamide. In particular 2-naphthylamide is associated with the development of bladder cancer.

Certain viruses have been shown to have a relationship with cancer. Approximately 15 percent of human cancers are thought to be caused by viruses (Alberts *et al.* 1994 and Campbell *et al.* 1999). Individuals who develop liver cancer known as hepatocellular carcinoma (HCC) tend to also have hepatitis B virus (HBV) infection. The presence of HBV infection can increase the risk of cancer a hundred fold.

The human papilloma virus (HPV) has been associated with carcinoma of the uterine cervix and the herpes virus Epstein-Barr (EBV) is associated with cancer of the B lymphocytes known as Burkitt's lymphoma and in the cancer nasopharyngeal carcinoma. A rare form of leukaemia is caused by the human T cell leukaemia virus (HTLV-1) (Purves *et al.* 1999).

1.1.4 Cancer Treatments

The three major treatment modalities for cancer are surgery, chemotherapy and radiotherapy.

Tumours that are localised to a single area can be removed by surgery. Surgery is often used before other forms of treatment to remove the vast majority of cancerous tissue and increase the success rate of chemotherapy and radiotherapy.

Chemotherapy drugs are used for most forms of cancer, as the drugs can be transported through the blood to all areas of the body. Some chemotherapy drugs can even cross the blood-brain barrier for the treatment of brain tumours. Multiple drugs are often used in combination allowing different stages of the cancer cell life cycle to be targetted. This permits tumour attack from several mechanisms increasing the percentage of cells killed, reducing systemic toxicity and helping to avoid drug resistance. Some examples of chemotherapy drugs include cyclophosphamide, cisplatin, methotrexate, fluorouracil and doxorubicin (Rang *et al.* 2003). Chemotherapy treatment can be used with the intention to cure, or for palliative care. Hormones can significantly affect the growth of some tumours, which are considered as hormone dependent. Therefore a number of hormones are used in cancer chemotherapy including corticosteroids, estrogens, and androgens. Alternatively a number of hormone antagonists can also be used such as tamoxifen an anti-estrogen and flutamide an androgen antagonist (Rang *et al.* 2003).

Radiotherapy is an effective way of killing tumour cells. A high dose of ionizing radiation is aimed directly at the tumour. Radiotherapy is also sometimes given as a form of palliative care for inoperable cancers, to shrink the size of a tumour.

Two different types of cancer and their treatments will be discussed in greater detail below. Both of these cancers could benefit from the development of new and improved treatment strategies.

1.1.4.1 Prostate Cancer

Prostate cancer is the most common form of cancer for men in the UK with more than 34,000 new cases per year. This accounts for 24 percent of all new male cancer diagnoses (CRUK website www.cancerhelp.org.uk October 2009). Prostate cancer is quite rare in men that are under 50 years of age. 63 percent of cases are in men over the age of 70. Prostate cancer can run in families, with several gene changes identified that increase the risk.

A strong risk factor for prostate cancer is age; however a family history of prostate cancer in a first degree relative increases the risk up to three fold. The risk further increases if the relative is young and if more than one relative has the condition. It is estimated that a predisposing gene may be responsible for 10 percent of all prostate cancer cases (Elo and Visakorpi 2001). The tumour suppressor gene PTEN is the most frequently inactivated gene in prostate cancer resulting in an increased activation of Akt. (McCall *et al.* 2008 and Van Duijn et al. 2010). PTEN is associated with the regulation of the P13K cell survival pathway (Mabjeesh *et al.* 2002). PTEN expression is often low or absent in hormone refractory prostate tumours and is associated with shorter time to relapse in hormone sensitive prostate tumours (McCall *et al.* 2008). Other tumour suppressor genes associated with prostate cancer include p53, RB and BRCA2.

Scientists have recently produced evidence that the Xenotropic murine leukaemia related virus (XMRV) can be linked to prostate cancer in humans. It is already known that gamma retroviruses are oncogenic in animals, but this is the first gamma retrovirus known to infect humans. The virus was found in 30 percent of prostate cancers tested with protein expression in 23 percent. Protein expression was primarily in malignant epithelial cells, suggesting that the retrovirus may be directly linked to tumorigenesis. The virus was also associated with more aggressive high grade tumours (Schlaberg *et al.* 2009). However a study in Germany failed to detect the virus in greater than 200 prostate cancers (Hohn *et al.* 2009). Therefore the contribution of XMRV to prostate (or potentially other cancers) remains to be confirmed.

The prostate is a small gland the size of a walnut, which is divided into two small lobes that sit left and right of a central groove. The prostate gland produces a thick clear fluid used for the production of semen. Prostate tumours can be both benign (non-cancerous) or malignant. The symptoms for both forms are very similar.

Prostatectomy surgery and radiotherapy are the only forms of curative treatment currently available. However many patients treated with prostatectomy and radiotherapy get local recurrent cancer within 10 years. Few alternative treatments are available once first line treatment has failed. Most prostate cancers are androgen dependent, and respond well to androgen blockade. However many go on to develop androgen-independence within 2 years, leading inevitably to metastatic spread. Hormonal therapy using anti-androgens has been used for over 50 years; however these significantly affect the quality of life without offering a cure (Goktas *et al.* 1999).

The prognosis for prostate cancer is very difficult to determine and is based on several different factors. Approximately 99 percent of patients diagnosed with localised prostate cancer will live for more than 5 years.

Advanced prostate cancer is much more complicated to predict. When radiotherapy and hormone therapy is used for treatment 70 to 80 percent will live for at least 5 years. Advanced metastatic prostate cancer has much lower survival rates with only 30 percent of patients living for at least 5 years after diagnosis. (CRUK website info.cancerresearchuk.org October 2009)

Better treatments are needed for aggressive forms of localised disease and hormone-refractory metastatic disease. Several gene therapy strategies have raised the possibility that gene therapy may have the potential to affect both localised and metastatic disease.

Gene therapy for localised prostate cancer has progressed rapidly from replication deficient adenoviruses encoding a single therapeutic gene, to replication competent oncolytic adenoviruses lacking a therapeutic gene, to replication competent oncolytic adenoviruses encoding multiple therapeutic genes. See Table 1.1 for details of clinical trials for localised prostate cancer.

Both *in vivo* and *ex vivo* gene therapy strategies have been used to target metastatic prostate cancer disease. A range of vectors have been trialled including adenovirus, retrovirus and vaccinia virus. See Table 1.2 for details of trials for metastatic prostate cancer.

There are currently 30 clinical trials recruiting prostate cancer patients in the UK. These range from adapting current treatments regimes, trying out new drugs to improving diagnostic techniques (CRUK website www.cancerhelp.org.uk October 2009).

Treatment	Description	Results	Reference
HSV-TK + GCV	Replication defective adenovirus (E1/E3 deleted) containing wild-type HSV-TK under RSV promoter	Minimal toxicity (grade 1-2), three patients fall in PSA ≥ 50 percent Follow up with repeat treatment showing prolonged PSA doubling time	Herman *et al.* 1999 Miles *et al.* 2001
HSV-TK + GCV	Replication deficient adenovirus type 5 (E1/E3 deleted) containing wild-type HSV-TK under RSV promoter	Minimal toxicity (grade 1-2), prolonged PSA doubling time	Shalev *et al.* 2000
HSV-TK + GCV	Replication deficient adenovirus containing wild-type HSV-TK	Nine courses of treatment, prolongation of median serum PSA doubling time from 2.9 to 6.2 months	Nasu *et al.* 2007
HSV-TK + VCV + RT ± HT	Replication deficient adenovirus type 5 (E1/E2 deleted) containing wild-type HSV-TK under RSV promoter	Minimal toxicity (grade 1-2) PSA levels declined rapidly, remaining low at 14 months post treatment	Teh *et al.* 2001 Teh *et al.* 2004
NTR + CB1954	Replication deficient adenovirus CTL102 containing wild-type NTR	NTR expression seen upon immunohistochemistry staining Minimal toxicity, at 6 months patients 10-50% reduction, and 2 out of 19 showed greater than 50% reduction in PSA	Searle *et al.* 2004 Patel *et al.* 2009
IL-2	Replication deficient adenovirus AdCAIL-2	Minor adverse reactions, pathology consisted of $CD3^+$ $CD8^+$ T lymphocytes, areas of tumour necrosis. PSA levels fell in patients	Trudel *et al.* 2003
p53	Replication deficient adenovirus INGN 201 containing wild-type *p53* under CMV promoter	Immunohistochemistry staining showed wild-type *p53* and an increase in apoptotic index from 0.39 to 1.18 was observed indicating some cancerous tissue had undergone apoptosis	Pisters *et al.* 2004
CV706	Replication competent PSA selective adenovirus CV706	Minimal toxicity, five patients ≥ 50 percent reduction in PSA	DeWeese *et al.* 2001
HSV-TK + CD + GCV + 5-FC ± 3D-CRT	Replication competent adenovirus containing CD/HSV-TK fusion gene	Minimal toxicity (grade 1-2), seven patients ≥ 25 and three patients ≥ 50 percent reduction in PSA. Two patients cancer free at 1 year Minimal toxicity, shorter PSA half lives than expected 5 year follow up, PSA doubling time from 17 to 31 months	Freytag *et al.* 2002a Freytag *et al.* 2003 Freytag *et al.* 2007

Table 1.1 Prostate cancer gene therapy trials for localised disease
Abbreviations: 3D-CRT – 3 dimensional conformal radiation therapy, 5-FC – 5-fluorocytosine, CD – cytosine deaminase, CMV – cytomegalovirus, GCV – ganciclovir, HSV-TK – Herpes simplex virus thymidine kinase, HT – Hormone therapy, IL-2 – Interleukin-2, NTR – Nitroreductase, PSA – Prostate-specific antigen, RT – Radiotherapy and RSV – Rous sarcoma virus.

Treatment	Description	Results	
HSV-TK + VACV	Replication defective (E1/E3 deleted) adenovirus containing wild-type HSV-TK under OC promoter	No serious adverse events, local cell death in treated lesions, stabilisation of lesion for 317 days in one patient	Kubo *et al.* 2003
HSV-TK + VACV	Replication defective adenovirus (Ad5) containing WT HSV-TK, OC promoter	Minimal toxicity, patient 1 and 3 PSA continued to rise, patient 2 PSA dramatically dropped, metastasis density became lower	Hinata *et al.* 2006
HSV-TK + VACV	Replication defective adenovirus containing WT HSV-TK, OC promoter	No serious adverse events, 1 patient PSA dropped time to progress 12 months	Shirakawa *et al.* 2007
CG7870	Replication competent PSA selective adenovirus CG7870	Adverse events (grade 1- 3), no partial or complete PSA response seen, 5 patients PSA fall > 25-49 percent	Small *et al.* 2006
GM-CSF vaccine	Autologous tumour cells transduced with replication-defective retrovirus encoding GM-CSF	No serious adverse events, evidence of T cell activation, no PSA response	Simons *et al.* 1999
PSA vaccine ± GM-CSF	Recombinant vaccinia virus expressing PSA (PROSTVAC)	Low toxicity, no PSA response Minimal toxicity, one patient undetectable PSA > 8 months	Sanda *et al.* 1994 Sanda *et al.* 1999
PSA vaccine ± GM-CSF	Recombinant vaccinia virus expressing PSA (PROSTVAC)	Minimal toxicity (grade 1-2), PSA levels stable > 6-25 months, 6 patients progression free with stable PSA	Eder *et al.* 2000
PSA vaccine ± GM-CSF	Recombinant vaccinia virus expressing PSA (PROSTVAC)	Minimal toxicity, PSA specific T-cells present, able to lyse PSA-expressing tumour cells	Gulley *et al.* 2002
PSA vaccine	Combination of vaccinia virus expressing PSA and fowl pox virus expressing PSA	Few adverse events, 45.3 percent remained free of PSA progression at 19.1 months, 78.1 percent progression-free survival. 46 percent of patients show increased PSA-reactive T-cells	Kaufman *et al.* 2004
PSA + B7-1 + ICAM + LFA-3 vaccine	Recombinant vaccinia virus expressing PSA (PROSTVAC-VF) and recombinant fowl pox virus expressing co-stimulatory molecules B7-1, ICAM and LFA-3 (TRICOM)	Minimal toxicity (grade 1-2), four patients had stable disease (≤ 25 percent increase in PSA) at week 8	DiPaola *et al.* 2006

Table 1.2 Prostate cancer gene therapy trials for metastatic disease
Abbreviations: GM-CSF – Granulocyte-macrophage colony-stimulating factor, HSV-TK – Herpes simplex virus thymidine kinase, OC – Osteocalcin, PSA – Prostate-specific antigen and VACV – Valacyclovir

1.1.4.2 Ovarian Cancer

For women, ovarian cancer is the fifth most common form of cancer in the UK with around 6,800 new cases per year. 5 percent of cancers diagnosed in women will be ovarian cancer. In fact the UK has one of the highest incidence rates across Europe (CRUK website www.cancerhelp.org.uk October 2009). Ovarian cancer is hard to diagnose due to vague signs and symptoms in early stages of the disease. Many of the symptoms can be related to other less serious conditions therefore, up to three quarters of women are in the late stage of the disease when they are diagnosed. Survival rates for women at this stage are very poor despite advances in surgical techniques.

There are two main types of ovarian cancer epithelial and germ cell. Eighty to 90 percent of ovarian tumours are epithelial where the cancer started in the surface layer of the ovary, whereas germ cell tumours originate from the egg making cells and make up approximately 10 percent of ovarian cancers. However some rare cases of sarcomas of the ovary have been seen (CRUK website www.cancerhelp.org.uk October 2009).

Current treatments used for ovarian cancer include surgery, radiotherapy and chemotherapy. The amount and type of surgery used depends on several factors including the stage, grade and type of tumour to be treated. In early stage disease surgery can be used alone, with the removal of the affected ovary and fallopian tube. As the disease progresses, surgery to remove both ovaries and womb would be recommended to reduce the risk of cancerous cells remaining. In some cases adjuvant chemotherapy is offered.

If the cancer is more advanced, surgery will be used to remove the ovaries, womb, omentum and as much visible tumour as possible. Following surgery, a course of chemotherapy will almost certainly be used to further reduce the number of remaining cancer cells. With final stage ovarian cancer, chemotherapy may be used first to shrink the tumours before surgery is used to remove as much as possible known as 'debulking'. Following surgery chemotherapy may be repeated to try and shrink any remaining tumours. In some cases the cancer is too advanced and surgery is no longer an option. In these cases a combination of chemotherapy and radiotherapy is often used (CRUK website www.cancerhelp.org.uk October 2009). Currently carboplatin alone or in combination with paclitaxel are the most commonly used chemotherapy drugs for ovarian cancer treatment (CRUK website www.cancerhelp.org.uk October 2009).

From the 6,800 women diagnosed with ovarian cancer in the UK each year overall approximately 36 out of each 100 will live for at least five years after their diagnosis. However the stage of the cancer when diagnosed is highly important when predicting survival. It is likely that for women diagnosed with early stage ovarian cancer 7 out of 10 will live for more than 5 years, but for women whose cancer has spread to surrounding tissue and lymph nodes the 5 year survival rate is about 3 out of 10 (CRUK website www.cancerhelp.org.uk October 2009).

Ovarian cancer is considered as a potential target for gene therapy as it is initially confined to the peritoneal cavity, where it can be directly targeted away from critical organs. See Table 1.3 for recent clinical trials for ovarian cancer.

Treatment	Description	Results	Reference
BRCA1*sv*	Retrovirus encoding BRCA1*sv*	Minimal toxicity, 8 patients stable disease for 4-16 weeks, 3 patients showed tumour reduction No response, no disease stabilisation, little or no vector stability, trial terminated after 6 patients	Tait *et al.* 1997 Tait *et al.* 1999
Anti-*erb-2*	Anti-*erb-2* Single-Chain Antibody-encoding Adenovirus (AD21)	Minimal toxicity (grade 1-2), 5 patients stable disease, 8 patients progressive disease	Alvarez *et al.* 2000a
HSV-TK + GCV	Replication incompetent adenovirus (Ad5 E1a/E1b deleted) encoding HSV-TK	Minimal toxicity, 5 patients stable disease, 8 patients progressive disease	Alvarez *et al.* 2000b
HSV-TK + ACV + Topotecan	Replication deficient recombinant adenovirus encoding HSV-TK	Some toxicity (grade1-4)	Hasenburg *et al.* 2000
E1A	Cationic Liposome-Mediated E1A	E1A detected by immunohistochemistry staining, HER-2/neu downregulation, increased apoptosis, reduced proliferation	Hortobagyi *et al.* 2001
p53	Replication deficient adenovirus encoding human *p53* cDNA	Some toxicity (grade 1-3), 2 patients had mixed response, 4 patients had stable disease for 4 courses, 5 patients had progressive disease after 1-2 courses	Wolf *et al.* 2004
Adoptive T cells	T-cells with high dose IL-2 or dual specific T-cells (FR and allogeneic cells)	Some toxicity (grade 1-4), no reduction in tumour burden seen in any patient	Kershaw *et al.* 2006
IFN β	Replication incompetent adenoviral vector encoding IFN β	Minimal toxicity (grade 1-2), regression of tumour in thorax and abdomen observed 2 months post treatment to thorax, indicating a system response	Sterman *et al.* 2006

Table 1.3 Ovarian cancer gene therapy trials
Abbreviations: ACV – Acyclovir, GCV – Ganciclovir, HSV-TK – Herpes simplex virus thymidine kinase, IFN β – Interferon β, IL-2 – Interleukin-2 and *sv* – splice variant

There are currently 10 clinical trials recruiting ovarian cancer patients in the UK. These range from adapting current treatments regimes to trying out new drugs (CRUK website www.cancerhelp.org.uk October 2009).

1.2 GENE THERAPY

'Gene therapy' can be defined as the transfer of genetic material into a patient's cells for therapeutic purposes (Bansal and Engelhard 2000). The last 20 years have shown rapid progress from concept to reality with a rapid advancement in molecular biology and a greater understanding of disease. Gene modified cells were first used in 1989 and the first gene therapy trial was performed in 1990. A diverse array of treatments that utilise gene therapy have been attempted including gene transfer for modulation of the immune system, enzyme prodrug therapy, oncolytic therapy, replacement gene transfer and antisense therapy (Bansal and Engelhard 2000). As our knowledge of gene therapy has progressed larger more complex therapies are being devised away from single gene defects (monogenic disease) towards more complex diseases such as cardiovascular disease and cancer.

Gene therapy can be categorised into two broad categories ex vivo and in vivo. Ex vivo gene therapy usually involves the collection of cells from the patient, the correction of the defect by gene transfer into the isolated cells and the return of the cells to the patient by infusion or transplantation (Glick and Pasternak 1998). A good example of ex vivo gene therapy would be the treatment of severe combined immunodeficiency (SCID-X1) which will be discussed further later.

In vivo gene therapy involves the direct delivery of a therapeutic gene to targeted cells and tissue within the patient. In this case either viral or non-viral vectors are required to deliver the therapeutic gene (Glick and Pasternak 1998). A good example of in vivo gene therapy is the treatment of cystic fibrosis (CF) which will be discussed further later.

1.2.1 Gene Delivery Vectors

Several different types of delivery vectors can be used for the insertion of DNA into a cell. The vector can be either viral or non-viral and the advantages and disadvantages of the different types will be discussed below. The ideal delivery vector should be capable of targeting the cell of interest and achieving a sufficient level of expression. There are currently 1537 active gene therapy trials worldwide. Approximately 69 percent of these ongoing clinical trials use viral vectors, with 24 percent being adenovirus and a further 20.9 percent being retrovirus. The most widely used non-viral vector is naked/plasmid DNA which makes up 17.9 percent of worldwide gene therapy vectors (see Figure 1.7).

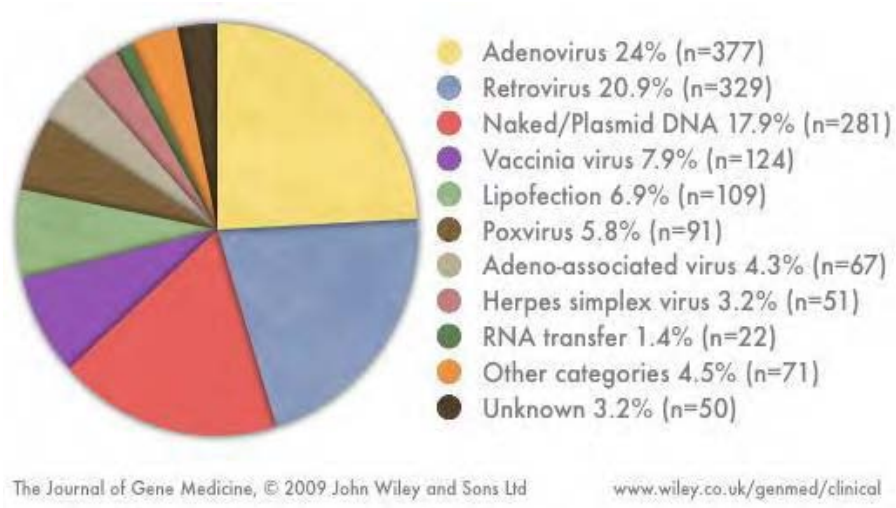

Figure 1.7 Current active gene therapy clinical trials 2009
(Wiley website www.wiley.co.uk/genmed/clinical October 2009)

1.2.1.1 Viral Vectors

Many different types of viral vectors have been used for cancer gene therapy. Therapeutic genes and their regulatory elements are inserted in to the viral DNA. The viruses can be either replication competent where the virus is able to replicate in the host cells or replication deficient where essential viral genes have been removed. Replication deficient viruses need to be grown in helper cell lines that contain the removed genes allowing the viruses to grow. There are several advantages to viral vectors; they can have selectivity for certain cells such as a preference for dividing cells and generally achieve greater transduction efficiencies than non-viral methods. In some cases such as retroviruses and adeno-associated viruses they are capable of integrating the gene of interest in to the host genome. However there are several disadvantages to viral vectors: they can be toxic to tissues causing immunological and inflammatory responses and there is a limit on the size of gene that can be inserted.

1.2.1.1.1 Retrovirus

Retroviruses are lipid enveloped single stranded RNA viruses (Buchschacher 2001). Upon infection by the retroviral particle, the virion core enters the host cell and RNA is reverse transcribed into double stranded linear DNA by reverse transcriptase. The DNA gains access to chromatin when the nuclear membrane dissolves during mitosis and integrates at a random place in the host genome. The provirus DNA is transcribed by the cellular machinery. The WT retroviral genome encodes three essential genes *gag*, *pol* and *env* (Brenner and Malech 2003).

All retroviruses have long terminal repeats (LTR) which are comprised of three regions U3, R and U5. These three regions are essential for reverse transcription and provirus integration. Retroviruses can be classified into seven different groups based on nucleotide sequence homology (Brenner and Malech 2003). The first retroviral vectors developed were gamma-retroviruses derived from the Moloney murine leukaemia virus and until recently retroviral vectors were the most common vectors used for gene therapy clinical trials. This is mainly due to their ability to stably integrate their DNA into the host cell genome. This allows prolonged expression of the gene. Retroviruses are generally used as replication deficient vectors, with deletion of *gag*, *pol* and *env*, allowing the insertion of transgenes of up to approximately 7.5 kb. In order to generate the retrovirus particles a packaging cell line providing the essential *gag*, *pol* and *env* proteins would be used. More recently lentivirus vectors have become increasingly common because of their ability to infect both dividing and non-dividing cells. Recent focus has concentrated on the human immunodeficiency virus type 1 (HIV-1).

1.2.1.1.2 Herpes Simplex Virus

Herpes Simplex Viruses (HSV) are linear double stranded virus with a large genome of about 150 kb, they are able to carry up to 20 kb of additional DNA and have many dispensable genes. Most vectors originate from Herpes Simplex Viruses 1 (HSV-1) which has a genome of 152 kb (Krisky *et al.* 1998). HSV-1 infection can be either latent or lytic. The ability of HSV-1 to establish lifelong latent infection in neurones, in which the viral genome forms a stable episome showing no evidence of damage to the host cell, makes these vectors ideal for some gene therapy systems (Efstathiou and Minson 1995 and Krisky *et al.* 1998).

Following HSV-1 expression more than 80 viral genes are expressed in a well ordered cascade. High titres of these viruses can be easily generated and both dividing and non-dividing cells can be infected.

1.2.1.1.3 Adeno-Associated Virus

Adeno-Associated viruses (AAV) are single stranded icosahedral non-enveloped DNA viruses which belong to the parvovirus family. AAVs are among the smallest known viruses with a genome of 4.7 kb. Five serotypes have been identified the most extensively studied being AAV-2 which has identical inverted repeats (ITRs) at each end. AAV-2 particles contain two open reading frames *rep* and *cap* which code for regulatory elements and structural proteins respectively (Goncalves 2005). Adenovirus-Associated viruses require a helper virus in order to replicate, these helper viruses tend to be adenoviruses however vaccinia, herpes simplex and human papilloma viruses have also been known to complement. AAV viruses are able to infect both dividing and non-dividing cells and tissue (Tal 2000 and Li *et al.* 2005). These viruses have emerged as potential vectors for gene therapy as they are apparently non-pathogenic in the absence of helper virus, with no immune response against host infected cells (Tal 2000). A broad range of tissues such as brain, liver, muscle, lung, retina and cardiac muscle can gain long term expression. They are able to give prolonged transgene expression via episomal concatamer formation (Li *et al.* 2005). One of the biggest downsides to AAV vectors is their inability to carry large genes. Genes of up to 4.5 kb can be inserted which is too small for many gene therapy applications. Also the production of AAV vectors is difficult, due to a requirement for helper virus which must subsequently be removed.

Nevertheless AAV vectors have been tested for several diseases, with the first clinical trial for the treatment of cystic fibrosis (Flotte *et al.* 1996). Most success using AAV as a vector was seen for the transfer of RPE65 gene to the eye of patients with Leber's congenital amaurosis, giving improvement in vision (Bainbridge *et al.* 2008).

1.2.1.1.4 Vaccinia Virus

Vaccinia virus (VV) is a large complex enveloped virus which belongs to the pox virus family. This virus is a linear double stranded DNA virus of 200 kb. VV was the first virus used as a vaccine which resulted in the eradication of smallpox (Mastrangelo *et al.* 2000). This virus is capable of infecting a wide range of cell types and remains in the cytoplasm having little or no effect on the host genome. Until recently vaccinia virus was dismissed as a potential vector due to lack of immune control in immuno compromised patients (Mastrangelo *et al.* 2000). VV may be ideal for immunotherapy applications against solid tumours. Genetically modified vaccinia vectors have been generated with few side effects (Moroziewicz and Kaufman 2005). Modified Vaccinia Ankara (MVA) is less virulent allowing infection but not replication in human cells (Sutter and Moss 1992 and Paoletti 1996). A recombinant vaccinia vector expressing GM-CSF has been used for a melanoma cancer trial. Seven patients were treated, two showing no response, four with a partial response and one, complete remission. The only side effect seen rarely was mild flu-like symptoms, showing safe use of vaccinia vector (Mastrangelo *et al.* 1998).

1.2.1.1.5 Adenovirus

Adenovirus is a non-enveloped icosahedral virus with a linear double stranded DNA genome (Shenk 1996). The capsid comprises 252 capsomeres of which 240 are hexavalent and the remaining 12 are situated at the apices and are pentavalent (Ginsberg *et al.* 1966). In 1953 adenoviruses were first isolated from human adenoid and tonsil tissue (Rowe *et al.* 1953). These viruses are linked to several human diseases including respiratory tract infections, gastroenteritis and conjunctivitis. These infections are generally transient and therefore self-limiting. There are over 50 different human adenoviral serotypes. One of the main advantages of using adenovirus as a vector is that viral infection doesn't require the host cell to be dividing (Horwitz 1996). Very rarely adenoviral infections lead to mortality in healthy individuals. However there is a significant risk in immuno-compromised patients. The vast majority of vectors are based on species C serotypes 2 and 5 (Horwitz 1996).

Wild-type adenovirus types 4 and 7 were successfully used as oral vaccines to provide protection from acute respiratory disease in US military recruits (Grabenstein *et al.* 2006). Very few side effects have been seen. This has suggested that adenovirus could be a safe vector for gene therapy. Since then adenoviruses have been successfully used as vectors for many clinical trials and in recent years adenoviruses have increasingly become the vector of choice due to high transgene transfer efficiency and the ability to infect a large range of dividing and non-dividing cell types (Hardy *et al.* 1997). WT adenoviruses can only hold an additional 2 kb of genetic material without affecting the virus infectivity and stability. Therefore much work has been undertaken on replication defective adenoviruses.

The vast majority of replication defective adenoviruses are E1 deleted preventing replication. Further deletion of E3 has made it possible to incorporate genes of up to 7.5 kb in size. This allows the packaging of approximately 105 percent of the normal adenovirus genome (Horwitz 1996).

Replication after the removal of the E1 region (E1A and E1B genes) requires the use of helper cells for virus propagation eg: HEK 293 or 911 cells. Both of these cell lines contain adenovirus type 5 E1A and E1B functions (Graham *et al.* 1997 and Fallaux *et al.* 1998). More recently, 'gutless' replication defective adenoviral vectors have been generated with all viral genes removed. Only the viral inverted repeats and packaging signals remain. This allows the insertion of up to 35 kb (Hardy *et al.* 1997). Helper virus is also required for these viruses to replicate (Parks *et al.* 1996). The main advantages of 'gutless' vectors are the large capacity they can hold.

Recent development of conditionally replicating adenoviral vectors allows a combination of inserting a therapeutic gene while still allowing cytolytic effects due to adenovirus replicating. Several approaches have been designed for tumour specific replication by controlling early adenovirus genes using tumour specific promoters. Examples are the use of prostate specific antigen promoter to control replication for the treatment of prostate cancer (Rodriguez *et al.* 1997) and exploiting tumour specific defects such as the loss of functional p53 proteins, originally proposed to provide tumour selectivity to the E1B 55K-deleted adenovirus mutant *dl*1520 (ONYX 015) (Barker and Berk 1987, Heise *et al.* 1997 and Freytag *et al.* 1998).

During normal adenovirus infections, E1B 55K protein sequesters p53, thereby preventing apoptosis and allowing viral replication. However when E1B 55K is absent, viral replication could only take place in cells which have non-functional p53; this is often the case with tumours (Heise *et al.* 1999 and Vollmer *et al.* 1999). However, the tumour suppressor selectivity of ONXY 015 has subsequently been shown to be more complex, being attributed to late viral RNA export functions (O'Shea *et al.* 2004).

E1 promoters have also been replaced with the human telomerase reverse transcriptase (hTERT) promoter which restricts viral replication to cells that express telomerase. This enzyme is often highly expressed in cancer cells allowing the replacement of chromosomes ends that are normally lost after several cycles of cell division. It is usually this replacement that allows cancer cells to divide indefinitely (Lanson *et al.* 2003, Bilsland *et al.* 2003 and Irving *et al.* 2004).

1.2.1.2 Non-viral Vectors

In some clinical trials non-viral vectors have been used for the delivery of therapeutic DNA. The main advantage of non-viral vectors is the absence of an immune response allowing repeat treatment. However this form of vector usually express at lower levels when compared with viral vectors and are often less efficiently delivered.

1.2.1.2.1 Cationic Liposomes and lipids

Cationic liposomes are a mixture of plasmid DNA with lipid which leads to the formation of large DNA-reagent aggregates that have positively charged side chains which are used for gene transfer.

Colloidal stability of lipid/DNA aggregation is a major requirement for lipid mediated transfection, particularly at high concentration which is needed for gene delivery (Pitard *et al.* 2001). Cationic lipid DNA complexes also known as 'lipoplexes' have been used for many clinical trials and are currently the most promising non-viral vectors, however only low levels of gene transfer have been achieved. Several immunotherapy trials have been performed using lipid/DNA complexes (Roth and Cristiano 1997).

1.2.1.2.2 DNA polymer conjugates

In 1987 DNA polymer complexes were first used for gene therapy using poly-L-lysine to make the first conjugate (Wu and Wu 1987). Current DNA polymer complex delivery systems use cationic polymers polylysine, polyethylenimine and polyamidoamine. These confer resistance to nuclease enzymes and large size genes can be incorporated.

Polylysine has been used for the majority of cationic polymer vectors. In some cases ligands or antibodies have been incorporated allowing targeting to specific receptors. Polyethylenimine has endosomolytic properties which may enhance transfection efficiency.

Polyethylenimine complexes attach to the cell surface and migrate into clumps that can enter the cell by endocytosis. They become deaggregated within lysosomes and are then free to enter the nucleus (Merlin *et al.* 2002). A relatively successful gene therapy trial used a polyethylenimine vector for aerosol inhalation. The treatment was non-invasive and effectively transferred the gene to the respiratory tract. Permanent gene transfer was observed without expression in other tissues (Ferrari *et al.* 1999). Polyamidoamine (PAMAM) dendrimer has been used as a vector to target the brain (Liu *et al.* 2009).

One main constraint is that the DNA must be condensed; currently up to 45 kb of DNA has been successfully condensed without damage. One of the biggest problems with polymer complexes is that polycation can lead to cytotoxicity. A balance between polymer cationic density and endosomal escape resulted in less cytotoxic vectors by using two side chains, one being polylysine, which makes the vector cationic and the second contained an imidazole group allowing endosomal escape of the vector (Putnam *et al* 2001).

1.2.1.2.3 Naked DNA

Gene transfer of naked DNA was first demonstrated in 1990 when RNA and DNA expression vectors were separately injected into mouse skeletal muscle. Protein expression was readily detected in all cases (Wolff *et al.* 1990). This method has potential safety benefits because most side effects are usually caused by the vector.

The biggest problem with injecting naked DNA is the low efficiency of gene expression. A variety of tissues such as skin (Titomirov *et al.* 1991), liver (Suzuki *et al.* 1998), lung (Yang and Huang 1996) and muscle (Kon *et al.* 1999) have been investigated as target tissue. A variety of naked DNA delivery methods have been put forward including direct injection, electroporation and particle mediated transfection.

For electroporation small pores are made in the cell membrane by generating short electric pulses. This allows entry of the DNA into the cell. Electroporation has been used to insert DNA in to murine spleen cells (Tupin *et al.* 2003). Particle mediated transfection was first used to transfer genetic material into plants but has since been used for mammalian cells.

This technique is also referred to as 'gene gun'. Gold or tungsten particles of 0.5-3 μm are coated in the therapeutic gene and shot into the target cells with either a helium gas pulse acceleration gun or high voltage electrical discharge. This method has been used to introduce genes for IL-12 into murine tumours (Rakhmilevich *et al.* 1997) and GM-CSF into a mouse myeloma model. These methods are considered as easy and cost efficient and controls on their use are less stringent than when using viruses.

1.2.2 Gene Therapy for Genetic Disorders

The identification of single genes responsible for genetic disease first showed the potential for gene therapy. Following the development of gene delivery vectors many gene therapy trials for genetic disorders have been undertaken. Below are two examples of genetic disease which have been treated by gene therapy.

1.2.2.1 Human Severe Combined Immunodeficiency (SCID)-X1 Disease

Severe combined immunodeficiency (SCID-X1) is an X-linked inherited disease which is caused by a range of mutations within a 4.2 kb gene IL2RG (Noguchi *et al.* 1993 and Puck *et al.* 1993). This gene encodes the common gamma chain, a subunit of several cytokine growth factor receptors.

SCID-X1 patients lack T and Natural killer cells, but tend to have normal B cells that are unable to perform immunoglobin class-switching and are unable to produce antibodies (Buckley *et al.* 1997 and Cooper *et al.* 2003). The failure to produce T and NK cells is thought to result from loss of signalling through the γc receptors for interleukin 7 and 15 (Cavazzana-Calvo *et al.* 1996).

This condition only affects boys leading to severe immune compromise which results in bacterial, viral and fungal pathogenic infections. SCID-X1 is usually fatal, if left untreated; most patients die within the first few years of life (Cooper *et al.* 2003). The current treatment for SCID-X1 is immune reconstitution by bone marrow transplantation of haematopoietic stem cells from a HLA matched relative. Not all patients have a relative with perfect matching HLA, which initially led to the use of patient isolation in a germ free gnotobiotic environment. Transplantation from a mismatched haploidentical HLA donor has since been used with varying success. Mismatched donors are known to result in increased mortality and complication rate partly due to graft versus host disease and the requirement of chemotherapy to prevent rejection (Buckley *et al.* 1999 and Gaspar *et al.* 2004). SCID-X1 was considered an ideal disease for gene therapy. In the first clinical trial for this disease ex vivo transduction of $CD34^+$ haematopoietic stem cells with a retroviral vector expressing the cytokine growth factor receptor γc was used. During a 10 month follow up T cell immunity was seen at three months. Evidence was seen of recovery of both B and Natural killer cells (Cavazzana-Calvo *et al.* 2000).

Further clinical trials have since been performed. In one clinical trial four out of five treated patients showed generation of T-cells within 6-12 weeks of treatment. At three year follow up correction of the deficiency was maintained (Fischer *et al.* 2002 and Hacein-Bey-Abina *et al.* 2002). In another trial at another centre, four children were treated with a similar gammaretroviral vector encoding the cloned human γc region; all the children showed clinical and immunological improvement. Two of the children no longer required antibiotic medication and lived normal lives (Gaspar *et al.* 2004).

However two adverse events have been seen relating to SCID trials. Three years after treatment two patients showed uncontrolled exponential clonal proliferation of mature T cells (Hacein-Bey-Abina *et al.* 2003a and Hacein-Bey-Abina *et al.* 2003b). Both patients showed retroviral vector integration on the short arm of chromosome 11 within the LMO2 proto-oncogene promoter, which lead to over expression of LMO2 resulting in childhood acute lymphoblastic leukaemia. A third patient has since developed the condition. One of the three children died from the resulting leukaemia.

1.2.2.2 Cystic Fibrosis

The most common genetic disease in the Caucasian population is cystic fibrosis (CF). This disease effects 1 in 2500 live births in the UK (Johnson 1995 and Wilson *et al.* 1994). Cystic fibrosis results from a single gene defect which is recessive in nature, therefore two defective genes must be inherited to have the condition. Mutations in the CFTR gene are responsible for this condition. Multiple mutations in the gene have been detected which lead to a CFTR protein that is abnormally metabolised, dysfunctional or sometime both (Boucher *et al.* 1994). This makes this disease an ideal target for gene therapy treatment. The disease usually manifests in early childhood leading to progressive loss of lung function, eventually leading to an early death. More than 95 percent of CF patients die from lung disease (Boucher *et al.* 1994). Other organ systems can also be involved eg: the pancreas. Treatment involves physiotherapy, antibiotics and steroid treatment. This has improved the life expectancy for CF sufferers; however mean survival is still only 30 years in developed countries with good health care. The disease manifests because of decreased chloride ion conductance across epithelial cells leading to thick mucus, chronic airway infections and inflammation. *Staphylococcus aureus* and *Pseudomonas aeruginosa* infections are common for CF sufferers.

Attempts to restore the CFTR function were first attempted in the early 1990's. In the first trial an E1 deficient adenovirus encoding CFTR was administered to the nasal airway epithelia of three CF sufferers. Chloride ion transport was corrected allowing normal responses. There was no evidence of viral replication (Zabner *et al.* 1993) however inflammation was seen. Further trials have been performed (Boucher *et al.* 1994, Wilson *et al.* 1994 and Crystal *et al.* 1995). It has been found that as few as 6-10 percent corrected cells within an epithelial sheet are able to generate chloride transport similar to 100 percent corrected cells (Johnson *et al.* 1992). In some trials inflammatory responses were seen most probably from the adenoviral vector used. Due to concerns over the inflammation potential of viral vectors, most attention has turned to non-viral approaches, although adeno-associated viral vectors are also of interest. A phase I study for CF patients with mild lung disease was performed with an adeno-associated vector (Flotte *et al.* 1996). A DNA/liposome vector was tested on ten CF patients. Modest gene expression was observed, however repeat administration was required for long-term expression. There was no evidence of inflammation and toxicity. Six of the ten patients showed some CFTR gene correction in nasal cells (Hyde *et al.* 2000).

1.3 CANCER GENE THERAPY

In order for gene therapy to be effective for cancer treatment it is essential for 100 percent of cancer cells to be killed requiring either highly efficient gene delivery or additional mechanisms to kill non-transduced cancer cells. Over the last 10 years research and clinical trials developing gene therapy as a form of cancer treatment have increased greatly with more than 50 percent of all gene therapy trials being for cancer. Four main different strategies for cancer gene therapy treatment have been developed and each will be discussed below.

1.3.1 Immunotherapy

Immunotherapy as a cancer treatment utilises the ability of the immune system to recognise and kill cancer cells. Cytokines control and regulate many aspects of the immune response. The cytokine interleukin-2 (IL-2) is an important stimulator of T cell proliferation and has been used for several clinical trials for the treatment of metastatic melanoma. In one study forty-seven patients were treated with recombinant IL-2. Responses were seen in ten patients, two had complete responses and eight partial responses (Parkinson *et al.* 1990). In another study patients were divided into four groups IL-2 alone, IL-2 with chemotherapy, IL-2 with IFNα and IL-2, chemotherapy and IFNα. The addition of IFNα to IL-2 was associated with prolonged survival but the effect of chemotherapy was less obvious (Keilholz *et al.* 1998). Tumour necrosis factor (TNF-α) has also been tested in clinical trials and has been found to have cytolytic activity against tumour cells (Meany *et al.* 2008).

However there have been some side-effects from cytokine treatment with flu like symptoms seen following systemic administration. Gene therapy has the potential to overcome dose limiting toxicity by producing the cytokine only within the target cells. Adenovirus and modified vaccinia Ankara vectors have been used to express IL-2 and IFN-γ. In each case the virus was directly injected intratumorally. Higher cytokine levels were achieved in the tumour than was possible by systemic administration and stabilisation of melanoma was seen in several patients treated. Research is now working towards using virally administered IL-2 in combination with chemotherapy (Liu *et al.* 2004).

1.3.2 Tumour Suppressor Genes

Studies have shown that restoring *p53* function in tumours could lead to controlled cell death and prevention of tumour growth. A clinical trial using a retroviral vector encoding wild-type *p53* has been undertaken. The virus was delivered by direct intratumoral injection into human non small cell lung carcinoma (NSCLC). In total of nine male patients were treated, with tumour regression seen in three patients and stabilisation of the tumour observed in another three patients (Roth *et al.* 1996).

A phase I clinical study has used an adenoviral vector encoding wild-type *p53*. In this case twenty eight NSCLC patients were treated. These were patients where other treatments had failed to stop progression of the cancer. Again direct intratumoral injection was used as the method for introducing the virus. Therapeutic activity was observed in twenty five patients with a partial response in two and disease stabilisation in a further sixteen patients. The remaining seven patients showed disease progression (Swisher *et al.* 1999).

A further clinical study assessed the effect of recombinant adenovirus-*p53* combined with radiotherapy for the treatment of nasopharyngeal carcinoma. Patients were divided into two groups; 42 patients received rAd-*p53* with radiotherapy and a further 40 patients radiotherapy alone. Postinjection tumour biopsy showed downregulation of vascular endothelial growth factor. An 11.7 percent increase in 5 year disease free survival rate was seen when rAd-*p53* and radiotherapy were used in combination (Pan *et al.* 2009). rAs-*p53* is commercially licensed in china under the name Gendicine and is used for a large range of cancers (Guo and Xin 2006).

1.3.3 Oncogenes

Studies have shown that direct alteration of oncogene expression in human cancer cells can decrease cell proliferation and tumorigenicity. A retroviral vector system has been developed for the transduction of a fragment of antisense K-*ras* into human cancer cells. The vector was allowed to infect a lung carcinoma cell line with defective K-*ras*. Transcription of the defective K-*ras* RNA was specifically inhibited. The proliferation of the cancer cell line was inhibited 10-fold (Zhang *et al.* 1993).

An alternative approach involves the use of either small interfering RNAs (SiRNA) or small hairpin RNAs (ShRNA). SiRNA is a class of double stranded RNA molecules of approximately 20-25 nucleotides in length. SiRNA has potential for human therapy, without producing an interferon response. SiRNA has been used to overcome drug resistance in cancer with tamoxifen (Iorns *et al.* 2009) and doxorubicin (Chen *et al.* 2010). A phase I human clinical trial involving the systemic administration of SiRNA to patients with solid cancers using a targeted, nanoparticle delivery system has been undertaken. Results showed that SiRNA administered systemically to a human can produce specific gene inhibition (reduction in messenger RNA and protein) by an RNAi mechanism of action (Davis *et al.* 2010). ShRNA are sequences of RNA that make tight hairpin turns, and use RNA interference to silence gene expression (Bernards *et al.* 2006). Stable transfection of heparanase-specfic shRNA has been used to knockdown herparanase, leading to a decrease in invasiveness and angiogenesis of human gastric cancer cells (Zheng *et al.* 2009).

1.3.4 Prodrug Activation Therapies

Chemotherapy is currently one of the best forms of treatment for cancer. However chemotherapeutic agents have limited selectivity affecting all rapidly dividing cells. Therefore healthy tissue that rapidly divides will also be targeted. In the early 1990's an alternative approach to standard chemotherapy was put forward; antibody-directed enzyme prodrug therapy (ADEPT). This approach allows a prodrug-activating enzyme to be targeted to a tumour using a tumour specific monoclonal antibody, followed by systemic delivery of a non-toxic prodrug. The prodrug is activated to its toxic form in the presence of the antibody/prodrug activating enzyme conjugate. Therefore the active drug is only activated within the tumour vicinity reducing systemic toxicity. Not all tumour cells are required to have bound the antibody/prodrug activating enzyme conjugate as the active drug can diffuse locally to kill other surrounding tumour cells, a phenomenon known as the 'bystander effect'. Essential requirements for ADEPT include the use of small high affinity monoclonal antibodies which are able to penetrate tumour quickly and be rapidly cleared from the rest of the body. The choice of enzyme used is subject to several constraints; the optimum pH should be close to the pH of the target tumours' extracellular fluid and the enzyme should be non-immunogenic and specific (Bagshawe *et al.* 1994). A clinical trial using ADEPT to target carcinoembryonic antigen (CEA) has been used for the treatment of colorectal, breast, peritoneal and oesophageal cancer. This antigen is abundant in a variety of adenocarcinomas. 31 patients with CEA-expressing tumours were treated. The best response seen at 6 weeks after treatment was a 10 percent reduction in tumour diameter in a patient that had peritoneal cancer. At 6 weeks 11 patients showed stable disease the rest showed disease progression (Mayer *et al.* 2006).

A variation on this theme is that of gene-directed enzyme prodrug therapy (GDEPT) also referred to as 'suicide' gene therapy. This follows a similar principle to ADEPT except a gene encoding an activating enzyme is delivered to the tumour cells, which then express the enzyme. If a virus is used to administer the gene to the tumour cells it is also referred to as virus-directed enzyme prodrug therapy (VDEPT) (see Figure 1.8).

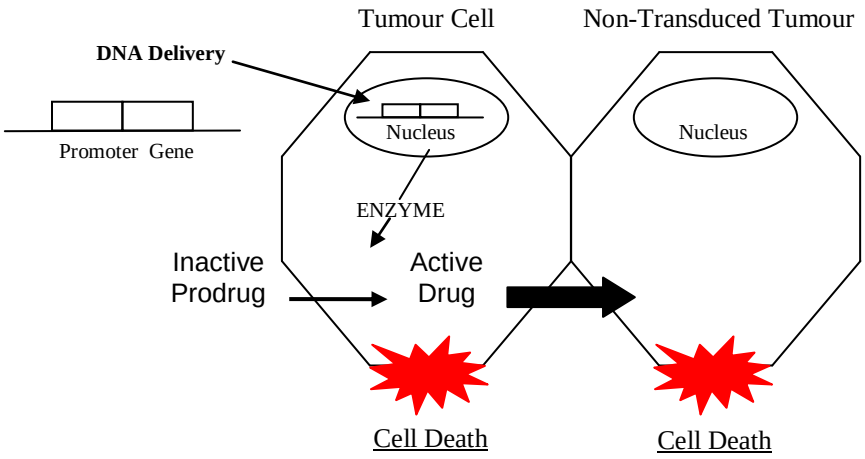

Figure 1.8 Mechanism of Virus Directed Enzyme Prodrug Therapy
Adapted from (McNeish *et al.* 1997)

The most important consideration for any VDEPT strategy is the method of delivery to tumour cells, the choice of enzyme and prodrug combination and how to regulate the enzyme's expression. Non-toxic prodrugs which are converted intracellularly to highly cytotoxic metabolites that are not cell cycle-specific in their mechanism of action are ideal for GDEPT.

The active drugs released should also be readily diffusible and exert a good bystander effect. Bacterial and viral enzymes tend to be ideal for VDEPT because they tend to have little or no endogenous effect on normal human cells (Connors 1995).

The enzyme should ideally consist of a single polypeptide species of reasonably low molecular weight and be independent of post-translational modifications. The desirable parameters for the enzyme-prodrug combinations are a high differential toxicity of the active species relative to the prodrug with a low K_m and high k_{cat} (McNeish *et al.* 1997). Current prodrug activating enzymes systems being studied for VDEPT will be discussed below.

1.3.4.1 Herpes simplex virus thymidine kinase with ganciclovir

The most widely studied and used gene directed enzyme prodrug therapy system is herpes simplex virus thymidine kinase (HSV-TK) enzyme with the prodrug ganciclovir. This system was first described in 1986. Murine cell lines bearing HSV-TK gene were exposed to 9-{[2-hydroxy-1-(hydroxymethyl)ethoxy]methyl}guanine (HHEMG) or ganciclovir drug leading to the loss of the cells' clonogenic potential. Mouse studies also showed complete regression of tumours (Moolten 1986).

Ganciclovir is most toxic to cells in the triphosphate state as it competes with deoxyguanosine triphosphate for incorporation into DNA during S phase of the cell cycle. HSV-TK can phosphorylate ganciclovir to ganciclovir monophosphate. Then cellular enzymes can phosphorylate ganciclovir monophosphate to ganciclovir diphosphate and ganciclovir triphosphate. It should be noted that cellular enzymes are unable to convert ganciclovir to ganciclovir monophosphate (see Figure 1.9).

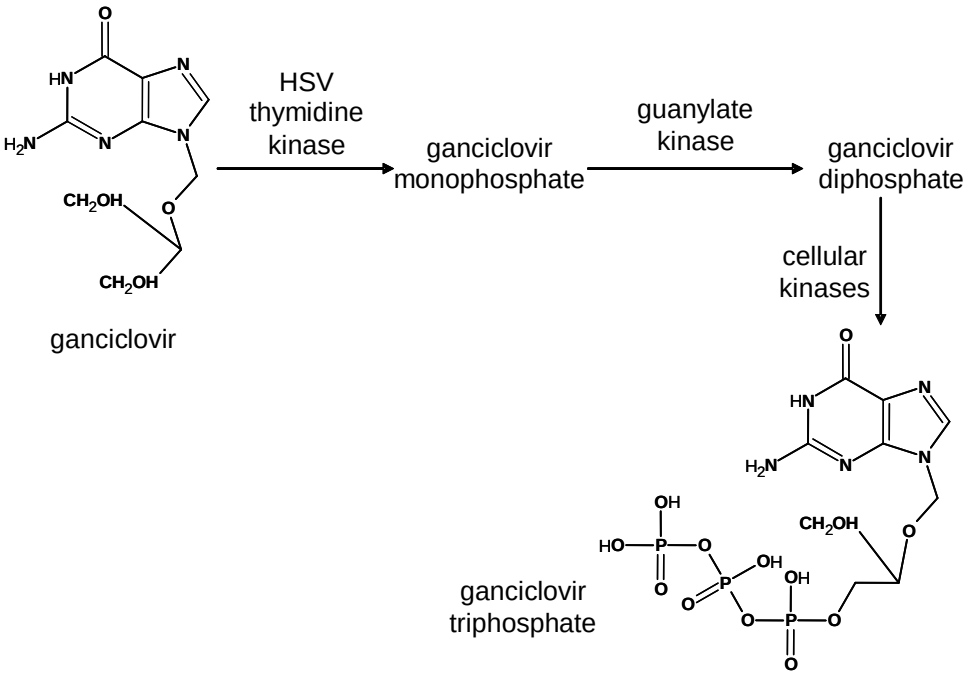

Figure 1.9 Activation of ganciclovir by thymidine kinase
Adapted from (McNeish *et al.* 1997)

When incorporated into DNA ganciclovir inhibits DNA polymerase leading to DNA strand breaks and ultimately cell cycle arrest and death by apoptosis (Mesnil and Yamasaki 2000). HSV-TK is also capable of phosphorylating several other drugs including acyclovir and bromovinyl-deoxyuridine.

A good bystander effect can be seen with HSV-TK and ganciclovir; however the active drug requires gap junctions for cell-to-cell spread (Ishii-Morita *et al.* 1997, Mesnil and Yamasaki 2000 and Wilson *et al.* 2004). This enzyme prodrug system is particularly good for rapidly dividing glioblastoma, as it only targets proliferating cells leaving the surrounding normal brain tissue undamaged.

HSV-TK in combination with ganciclovir was first approved for gene therapy trials in 1991. Since then many trials using this combination have been performed. In 2000 the first phase III clinical trial was completed for glioblastoma. The HSV-TK was delivered by a retroviral vector. This large scale trial treated two hundred and forty eight patients in three test groups treated with either surgery alone, radiotherapy alone or HSV-TK with ganciclovir in combination with surgery and radiotherapy. No benefit was seen relative to surgery and radiation. However the therapy was well tolerated and very little toxicity was seen. It was concluded that vector delivery was a limiting factor in this trial as very little HSV-TK gene was delivered to the tumour cells (Rainov 2000). In 2004 a further clinical trial for malignant glioma treated 17 patients with AdHSV-TK gene therapy by local injection, followed by intravenous ganciclovir (GCV). Median time of survival increased relative to radiotherapy (Immonen *et al.* 2004). Adenovirally delivered HSV-TK in combination with ganciclovir has since has been granted Orphan Drug Status under the name of Cerepro (Arktherapeutics website www.arktherapeutics.com/CEREPRO October 2009).

1.3.4.2 Cytosine deaminase with 5-fluorocytosine

The enzyme cytosine deaminase is found in both bacteria and fungi but absent in higher eukaryotes. The enzyme is able to catalyse the conversion of cytosine to uracil by the process of deamination. Cytosine deaminase can convert a clinically used anti-fungal agent 5-fluorocytosine to the active drug 5-fluorouracil (see Figure 1.10).

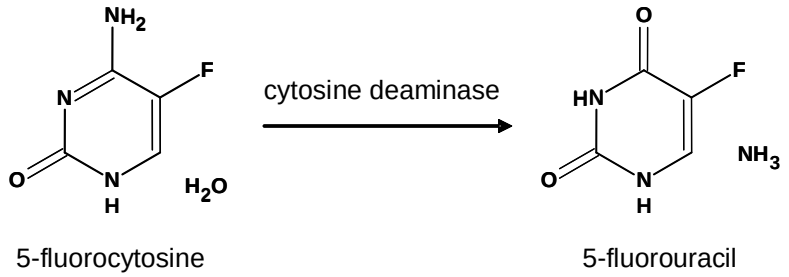

5-fluorocytosine 5-fluorouracil

Figure 1.10 Conversion of 5-fluorocytosine into 5-fluorouracil by cytosine deaminase
Adapted from (McNeish *et al.* 1997)

Recent studies have shown that the cytosine deaminase from fungi significantly increases the conversion of 5-fluorocytosine into 5-fluorouracil relative to bacterial cytosine deaminase (Kievit *et al.* 1999 and Kievit *et al.* 2000). 5-flourouracil is a widely used anticancer agent, in mammalian cells the 5-flourouracil is metabolised to 5-flouro-deoxyuridine-5'-triphosphate. This in turn inhibits thymidylate synthase preventing DNA synthesis and ultimately leading to cell death. The incorporation of 5-fluorouracil metabolites into nucleic acid also has a toxic effect. High doses of 5-fluorouracil are required for tumour regression, leading to high systemic toxicity when used for chemotherapy. However using a prodrug system for efficient targeting of tumour cells could greatly reduce the systemic toxicity and therefore improve efficacy. A good bystander effect is also seen with this system; in this case the metabolite is able to diffuse across the cell membrane (Wilson *et al.* 2004). Cytosine deaminase with 5-fluorocytosine has been used for a variety of cancers including colorectal (Huber *et al.* 1993 and Kievit *et al.* 2000) and breast cancer (Pandha *et al.* 1999).

1.3.4.3 Combination cytosine deaminase/Herpes Simplex Virus thymidine kinase with 5-fluorocytosine and ganciclovir

A novel system looking for synergistic cytotoxicity using double suicide gene therapy has been investigated over the last 7 years. A combination of cytosine deaminase and herpes simplex virus thymidine kinase enzymes was used with the addition of both prodrugs 5-fluorocytosine and ganciclovir. Prostate cancer was the target of this treatment. A replication competent Ad5 CD/TK adenovirus delivering the two enzymes as a fusion gene was used for expression. Two days later 5-fluorocytosine and ganciclovir were administered for a week (Freytag *et al.* 2002a). This system was put into phase I clinical trial for prostate cancer. The virus was intraprostatically injected using transrectal ultrasound guidance to sixteen patients. Two days later patients were given 5-flourocytosine and ganciclovir for one to two weeks. Seven of the patients showed a 25% decrease in prostate specific antigen (PSA) and a further three 50% decrease. Two patients were negative for adenocarcinoma one year after treatment (Freytag *et al.* 2002b). A similar study included three-dimensional conformal radiation therapy (3D-CRT) has also been through phase I clinical trials. In this case fifteen patients were treated, and patients were given 5-fluorocytosine and valganciclovir for one to three weeks along with 3D-CRT. PSA levels significantly declined. The results demonstrated that double suicide gene therapy could be successfully combined with 3D-CRT. (Freytag *et al.* 2003). In 2006 a slightly different approach was taken; prostate carcinoma cells were infected by adenovirus containing a CD/HSV-TK fusion gene. The cells were incubated for 24 hours with 5-fluorocytosine followed by 24 hours with ganciclovir. This gave greater growth inhibition compared with simultaneous administration of the prodrugs. It was proposed that CD/5-FC reduction of dTTP also results in decreased dGTP production.

dGTP is the endogenous competitor for ganciclovir triphosphate. Therefore more ganciclovir triphosphate was incorporated in the DNA allowing greater cell killing. This shows synergistic cytotoxicity interaction (Boucher *et al.* 2006).

1.3.4.4 *Escherichia coli* purine nucleoside phosphorylase with 6-methylpurine-2'deoxyribonucleoside

Purine nucleoside phosphorylase (PNP) can catalyse the phosphorolysis of purine nucleosides. The human nucleoside phosphorylase is a homotrimeric enzyme which is highly specific for 6-oxopurine nucleosides (Agarwal *et al.* 1975). By contrast *E. coli* DeoD nucleoside phosphorylase is a homohexameric enzyme, which allows phosphorolysis of a large range of substrates including 6-oxopurines and 6-aminopurines. This allowed the construction of prodrugs that are not substrates for the human PNP enzyme but that can be phosphorolysed by the *E. coli* enzyme. For example the prodrug 6-methylpurine-2'deoxyribonucleoside is readily converted by the *E. coli* PNP enzyme to 6-methylpurine (see Figure 1.11).

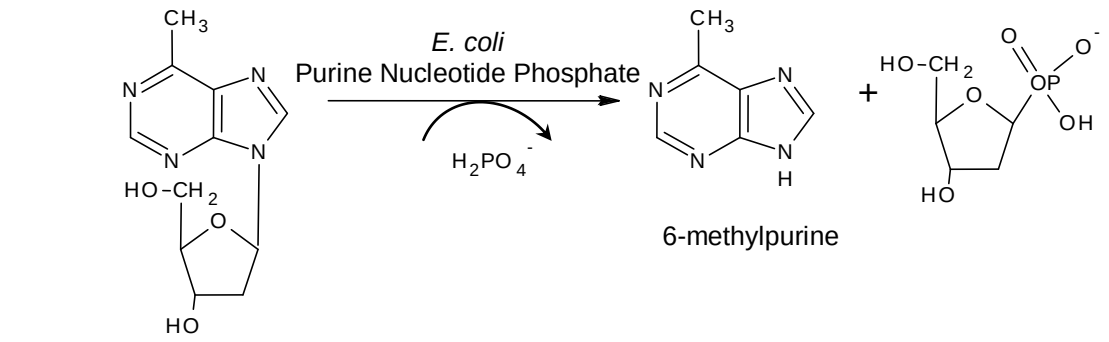

6-methylpurine-2'-deoxyriboside

Figure 1.11 Conversion of 6-methylpurine-2'deoxyribonucleoside into 6-methylpurine by *Escherichia coli* purine nucleoside phosphorylase
Adapted from (Hughes *et al.* 1995)

The resulting cytotoxic purine bases inhibit protein, RNA and DNA synthesis and are membrane permeable allowing effective killing of neighbouring cells (Hughes *et al.* 1995). Research has shown that expression of *E. coli* PNP in less than 1% of human colon carcinoma cells leads to the death of virtually all bystander cells following treatment with 6-methylpurine-2'deoxyribonucleoside (Sorscher *et al.* 1994).

1.3.4.5 Cytochrome P450 with cyclophosphamide

Cyclophosphamide is a commonly used chemotherapy agent which becomes bioactivated in the liver by cytochrome P450 enzymes. The active metabolite 4-hydroxy-cyclophosphamide is then transported round the body via the bloodstream. Further metabolism results in phosphoramide mustard and acrolein which alkylate DNA and protein respectively (see Figure 1.12).

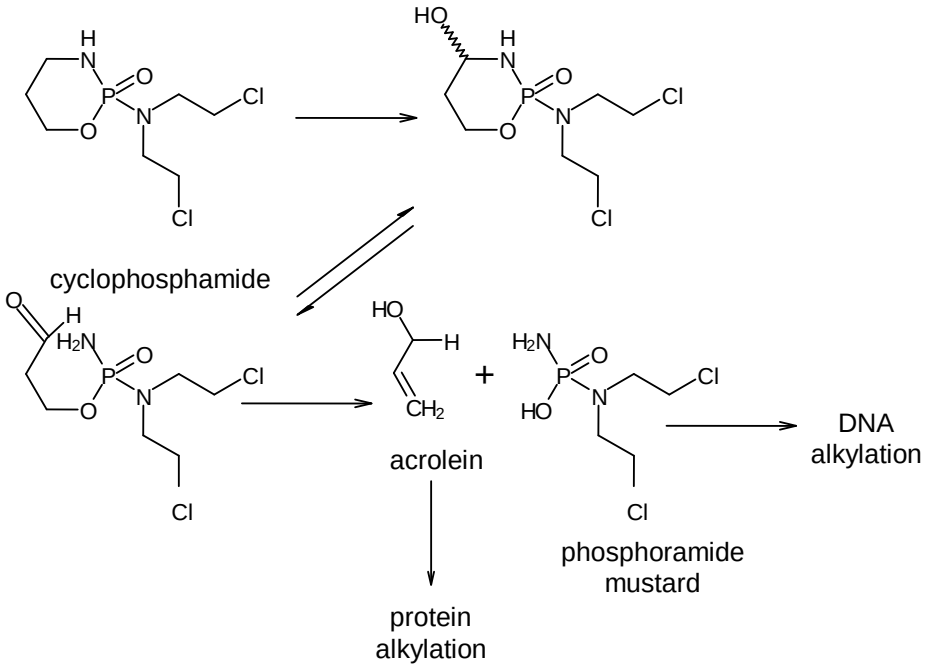

Figure 1.12 Conversion of cyclophosphamide into phosphoramide mustard and acrolein by cytochrome P450
Adapted from (Chen and Waxman 1995)

As a GDEPT approach cytochrome P450 enzyme is delivered directly to the tumour for localised prodrug activation. A strong bystander effect is seen for phosphoramide metabolites which are stable and diffuse easily between cells. A phase I clinical trial for breast cancer used recombinant retroviral vector encoding human cytochrome P450 enzyme. The vector was intratumorally injected followed by oral administration of cyclophosphamide. Twelve patients were treated, one patient showed a partial response, four showed stable disease for more than three months and the remaining four patients showed progressive disease (Braybrooke *et al.* 2005).

1.3.4.6 Carboxypeptidase G2 with aromatic mustard compounds

Carboxypeptidase enzymes hydrolyse peptides, resulting in the formation of shorter peptides and amino acids. Several prodrugs have been designed using aromatic mustard compounds which are stabilised by a glutamic acid residue. The active mustard compound is then released by the cleavage of the glutamic acid by the bacterial enzyme carboxypeptidase G2 (CPG2). The active mustards behave as alkylating agents and are therefore able to kill both dividing and non-dividing cells. They are also relatively lipophilic and can therefore pass directly through cell membranes (Hedley *et al.* 2007). The first report of CPG2 based GDEPT was in 1996. The system was tested using a range of different human cancer cell types that had been transduced with CPG2. The cells were found have greater sensitivity to the nitrogen mustard prodrug 4-[(2-chloroethyl)(2-mesoyloxyethyl)amino]benzoyl-L-glutamic acid (CMDA) relative to control cells which expressed bacterial β-galactosidase (Marais *et al.* 1996). A substantial bystander effect was seen for many of the cell lines with between 5-12% of cells needed to express CPG2 for total cell killing to be observed (Marais *et al.* 1996).

In 2002 three alternative prodrugs have been designed for use with mutant CPG2. These new drugs can be readily converted and give greater cell killing than CMDA (Friedlos *et al.* 2002). An adenoviral vector has been used for the expression of glycosylphosphatidylinositol (GPI) anchored CPG2. Greater than 50% cell killing was observed in all the cell lines tested following exposure to the prodrug [4-[bis(2-iodethyl)-amino]phenyl oxy carbonyl]-L-glutamic acid. A phase I clinical trial has been conducted using the prodrug CMDA and CPG2 enzyme. The prodrug was well tolerated and in some of the patients an anti-tumour response was observed (Cowen *et al.* 2002).

In 2008 an attenuated *Salmonella typhimurium* bacterium vector was used to target the delivery of CPG2 delivery to tumours. CPG2 was expressed within the bacterial periplasm. Prodrugs were activated inducing cytotoxicity in human tumour cells but not in the bacteria. After systemic administration to tumour bearing mice the bacteria multiplied preferentially in the tumour. The bacteria alone reduced tumour growth and addition of the prodrug further significantly reduced the tumour (Friedlos *et al.* 2008).

1.3.4.7 *Escherichia coli NfsB* Nitroreductase with CB1954

The prodrug 5-(aziridin-1-yl)-2, 4 dinitrobenzamide (CB1954) can be converted to cytotoxic 2- and 4-hydroxlamine derivatives by *E. coli NfsB* Nitroreductase. The 4-hydroxlamine derivative can then subsequently react with cellular thioesters to produce a potent cytotoxic difunctional alkylating agent that is capable of introducing interstrand crosslinking into cellular DNA (see Figure 1.13) (Knox *et al.* 1988a).

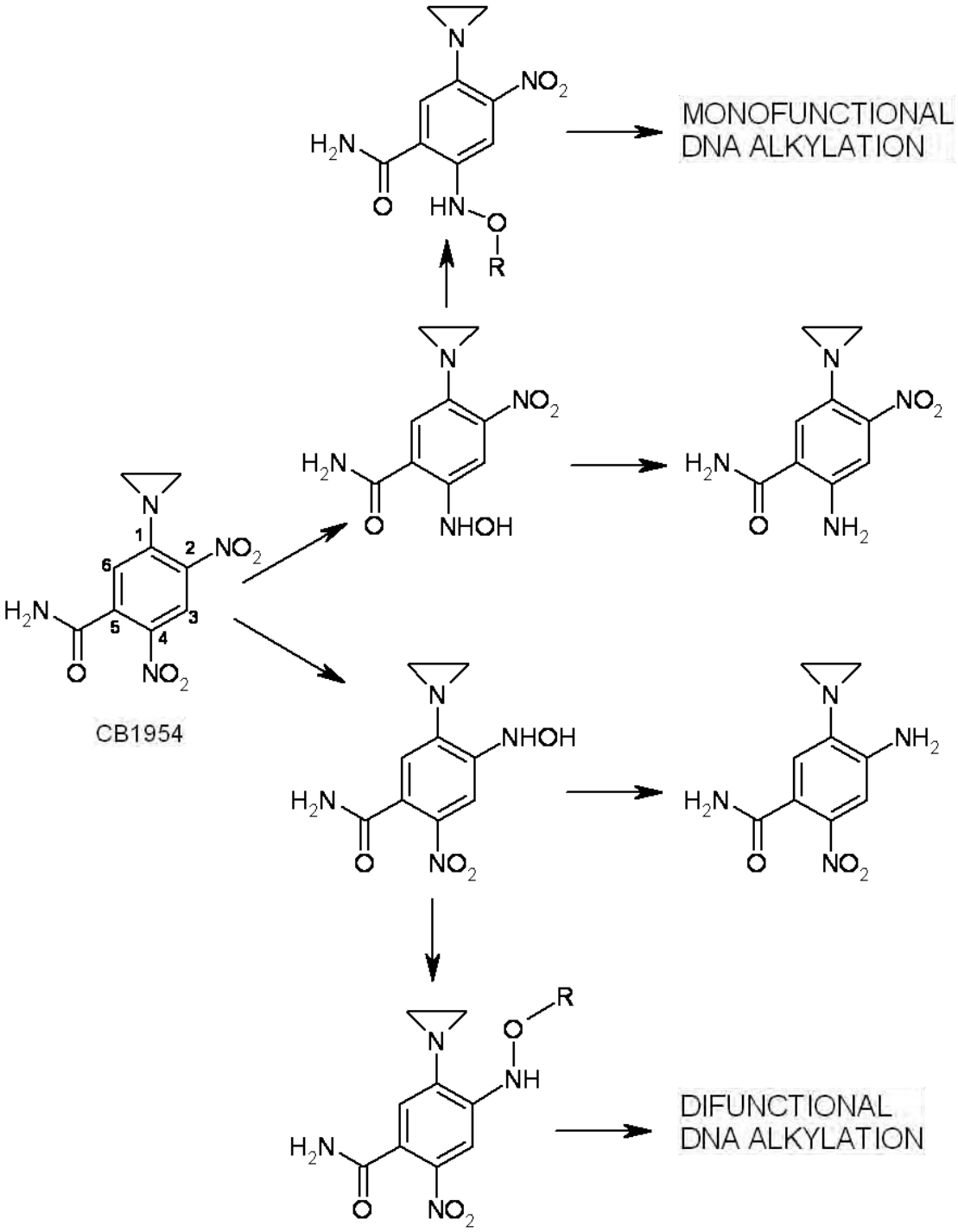

Figure 1.13 Products of CB1954 nitroreduction
Two equimolar products the cytotoxic 4-hydroxylamine derivative and the relatively non-toxic 2-hydroxylamine are yielded.

Initial investigations for the potential of *E. coli NfsB* nitroreductase (NTR) with CB1954 as a VDEPT system used a recombinant retrovirus for the delivery of the *NfsB* NTR gene. Upon systemic administration of CB1954, NTR encoding cells were killed (Bridgewater *et al.* 1995). A significant bystander effect was also observed in a mixing experiment. Similar killing potential has been seen in human melanoma, ovarian carcinoma and mesothelial cells using a retrovirally delivered *NfsB* NTR gene (McNeish *et al.* 1998). More recent investigations using replication-defective adenoviral vectors have been used to express *NfsB* NTR in a large range of tumour cell types (Weedon *et al.* 2000).

Both CB1954 and *E. coli* enzyme *NfsB* NTR will be discussed in detail as this system forms the basis for this thesis.

1.4 NITROREDUCTASE FOR PRODRUG ACTIVATION

Nitroreductases form a family of flavoenzymes which are defined by their dependence on a flavin cofactor for catalysis. Nitroreductases catalyse the reduction of a broad range of quinone and nitroaromatic compounds to either quinone or hydroxylamine derivatives. These enzymes use either NADH or NADPH as an electron donor (Anlezark *et al.* 1992). A wide range of nitroreductases have been identified in prokaryotic organisms including *Escherichia coli*, *Enterobacter cloacae* (Bryant *et al.* 1991a and Bryant *et al.* 1991b), *Salmonella typhimurium* (Watanabe *et al.* 1990 and Watanabe *et al.* 1998) and *Helicobacter pylori* (Jenks and Edwards 2002).

The role of nitroreductase is not fully known. It has been proposed that NTR plays a role in the metabolism of xenobiotics (Lovering *et al.* 2001). The theory behind this is nitroreductases are able to metabolise a large range of antibiotics and foreign compounds preventing toxicity to the bacteria.

1.4.1 Discovery of the flavoenzyme nitroreductase

In the late 1940's it was first noted by Smith and Worrel that *E. coli* are capable of reducing the nitro group from the antibiotic chloramphenicol. By the mid 1950's it was confirmed that an NADH specific flavoenzyme was present that could reduce nitroaromatic compounds including the antibiotics nitrofurazone and nitrofurantoin (Saz and Slie 1954). Further analysis later showed the presence of two types of *E. coli* nitroreductases (Asnis 1957). These were later termed as type I nitroreductase and type II nitroreductase (McCalla *et al.* 1970).

1.4.1.1 Type I Nitroreductases

Type I NTR's are insensitive to oxygen (can perform the reaction in the presence and absence of oxygen) using NADH or NADPH as electron donor (Asnis 1957 and McCalla *et al.* 1970). Type I NTR catalyses redox reactions where pairs of electrons are transferred. *E. coli* has three type I NTR's which will be discussed below.

1.4.1.1.1 *Escherichia coli NfsA* Nitroreductase

The first type I NTR is known as the major *E. coli* oxygen-insensitive nitroreductase encoded by the *NfsA* gene. The *NfsA* enzyme is a physiological homodimer with each subunit having a flavin mononucleotide (FMN) cofactor. The subunit mass of *NfsA* is 26.8 kDa. This enzyme has a marked preference for NADPH as electron donor (Bryant *et al.* 1981, Zenno *et al.*1996a and Vass *et al.* 2009).

1.4.1.1.2 *Escherichia coli NfsB* Nitroreductase

The second type I NTR is known as the minor *E. coli* oxygen-insensitive nitroreductase encoded by the *NfsB* gene. The *NfsB* enzyme is a physiological homodimer with each subunit having a FMN cofactor. The subunit mass of *NfsB* is 23.9 kDa. This enzyme can use either NADPH or NADH as electron donor with similar efficiency (Bryant *et al.* 1981 and Michael *et al.*1994).

1.4.1.1.3 *Escherichia coli NfsC* Nitroreductase

The third type I *E. coli* oxygen-insensitive nitroreductase is encoded by the *NfsC* gene. *NfsC* enzyme can use either NADPH or NADH as electron donor. Very little else is known about this enzyme (Bryant *et al.* 1981).

1.4.1.2 Type II Nitroreductases

In contrast type II NTR is sensitive to oxygen using NADH as an electron donor. Type II NTR's use two single-electron transfer reactions to reduce their substrates allowing the formation of superoxide radicals. Two type II NTR have been identified these are termed IIa and IIb. Very little research has been undertaken on these enzymes (McCalla *et al.* 1975).

Type I NTR *NfsB* enzyme was used for this study therefore all information following this point will concern *NfsB* nitroreductase unless otherwise stated.

1.4.2 CB1954

5-(aziridin-1-yl)-2, 4 dinitrobenzamide (CB1954) was originally identified from a series of N-substituted ethylamine derivatives synthesised in the early 1950's. The first indication of its potential as an anti-cancer agent came when it was seen that the compound was able to inhibit tumour growth of the Walker 256 rat carcinoma cell lines. The therapeutic potential of CB1954 was greater than many clinical agents available at that time such as cyclophosphamide and cisplatin. However CB1954 was later found to be ineffective in many animal and human tumours (Cobb *et al.* 1969). It was proposed that toxicity stemmed from activation of the drug by an enzyme that was present in the Walker cells. DT-diaphorase enzyme was purified from Walker rat cells and found to reduce CB1954 when in the presence of NADH/NADPH. The reduction of CB1954 by DT-diaphorase resulted in a 4-hydroxylamine derivative that reacted with cellular thioesters to form a highly cytotoxic agent (Knox *et al.* 1988b).

Hopes of using CB1954 for the treatment of human tumours was halted when it was discovered the human form of the enzyme was unable to reduce CB1954. However in 1992 it was found that *E. coli NfsB* nitroreductase can reduce CB1954 and has much better kinetic parameters compared to both the rat and human enzymes (Anlezark *et al.*1992). See Table 1.4 for kinetics parameters for rat and human NQO1 and *E. coli NfsB* NTR.

Enzyme	$K_{m\ CB1954}$ (μM)	k_{cat} (s^{-1})	$k_{cat}/K_{m\ CB1954}$ ($\mu M^{-1}\ s^{-1}$)
Rat NQO1	826	0.0683	0.00008
Human NQO1	1403	0.0107	0.000008
NfsB NTR	862	6	0.007

Table 1.4 CB1954 Kinetic parameters for rat and human NQO1 and *E. coli NfsB* NTR
(Anlezark *et al.* 1992 and Knox *et al.* 1992)

A more recent kinetic study here in Birmingham has shown that *NfsB* NTR global kinetics for both k_{cat} and K_m for CB1954 are approximately twenty-fold higher than previously estimated, however the measured specificity constant, k_{cat}/K_m remains the same (Jarrom *et al.* 2009).

Enzyme	k_{cat} (s^{-1})	$K_{m\ CB1954}$ (μM)	k_{cat}/K_m ($\mu M^{-1}\ s^{-1}$)	$K_{m\ NADH}$ (μM)	k_{cat}/K_m ($\mu M^{-1}\ s^{-1}$)
NfsB NTR	140 ± 32	17200 ± 4800	0.007 ± 0.0006	40 ± 12	3.46 ± 0.6

Table 1.5 CB1954 and NADH kinetic parameters for *E. coli NfsB* NTR
(Jarrom *et al.* 2009)

1.4.3 Catalytic Mechanism

NTR catalyses the reduction of quinone and nitroaromatic compounds using NADH and NADPH, via a ping pong bi-bi mechanism. The 'bi-bi' indicates a two substrate, two product reaction, while the 'ping pong' indicates the order in which the substrates are bound and the products released. A single substrate is bound to the active site at any one time being released as product before the second substrate is bound.

In the case of NTR the first step ('ping') involves a reaction between oxidised NTR and NADH or NADPH, resulting in two electron reduction of the FMN cofactor. Reduced NTR and NAD/$NADP^+$ products are released. The second step ('pong') involves a reaction between the reduced NTR and the second substrate eg: quinone or nitroaromatic compound. The quinone or nitroaromatic compound undergoes a two or four electron reduction respectively, which returns the NTR enzyme to its oxidised form. See Figure 1.14 for a schematic of the ping pong mechanism of NTR.

It was originally proposed that NTR followed a ping pong mechanism in 1992 after initial kinetic analysis (Anlezark *et al.* 1992). Further evidence was provided after extensive kinetic analysis and inhibition studies were performed, these showed that the k_{cat}/K_m of the first substrate was independent of the second substrate (Zenno *et al.* 1996b).

Crystallographic study of NTR has also shown that the active site is too small to accommodate both NADH/NADPH and its substrate at the same time, providing clear evidence that a ping pong mechanism must be used (Parkinson *et al.* 2000, Lovering *et al.* 2001 and Haynes *et al.* 2002). A reduced form of NTR has also since been crystallised (Johansson *et al.* 2003).

a)

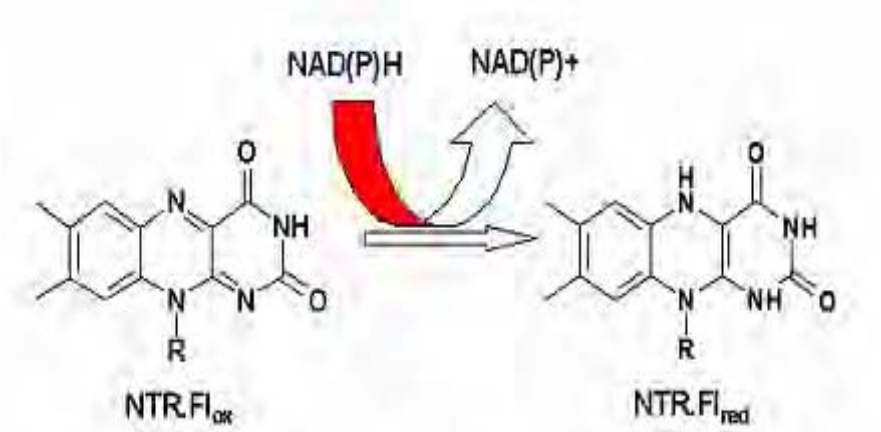

b)

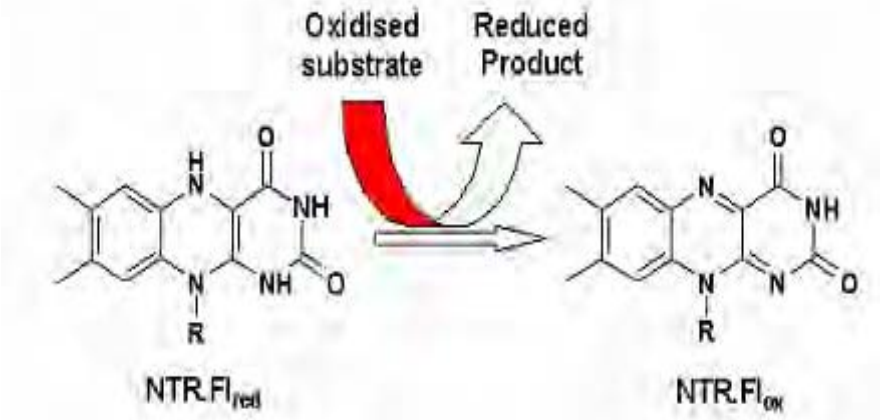

c)

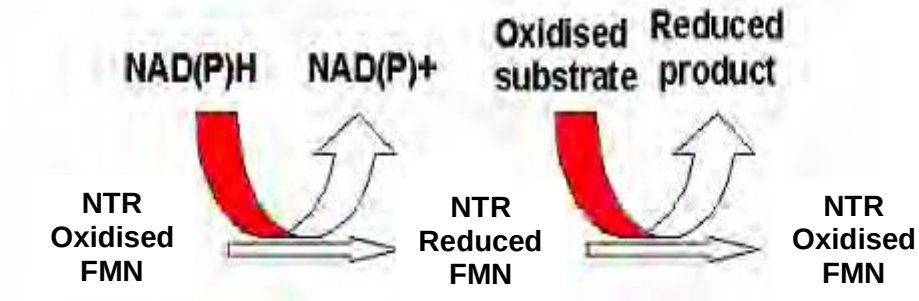

Figure 1.14 Schematic of ping pong mechanism for NTR showing flavin cofactor
a)'ping' step – electron donation by NADH/NADPH and production of the reduced FMN, b) 'pong' step- re-oxidation of FMN cofactor after electron donation to an oxidised substrate, c) Complete NTR ping pong mechanism. Adapted from (Race 2003)

1.4.3.1 Reduction of Quinones

NTR can catalyse the two-electron reduction of quinone compounds eg: Menadione and 1,4-Benzoquinone yielding quinol products (see Figure 1.15) (Anlezark *et al.* 1992).

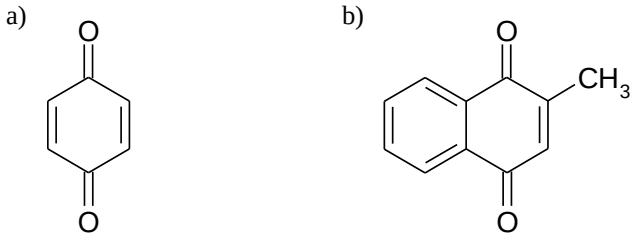

Figure 1.15 Quinone substrates of NTR
a) Menadione, b) 1,4-Benzoquinone

1.4.3.2 Reduction of Nitroaromatic Compounds

NTR can catalyse the four-electron reduction of nitroaromatic compounds eg: Nitrofurazone, CB1954, 2-Nitrobenzamide (2-NB) and 4-Nitrobenzamide (4-NB) to their hydroxylamine derivatives (see Figure 1.16) (Anlezark *et al.* 1992).

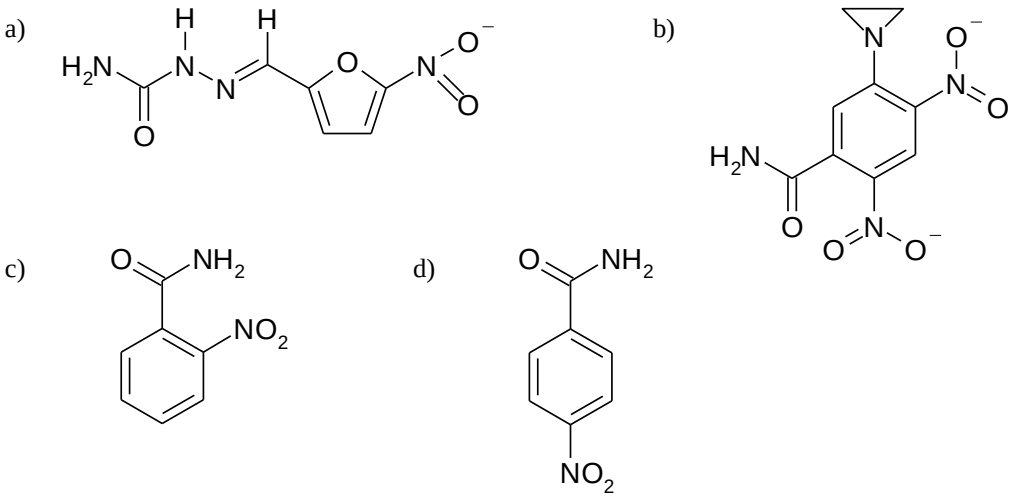

Figure 1.16 Nitroaromatic substrates of NTR
a) Nitrofurazone (NFZ), b) CB1954, c) 2-Nitrobenzamide (2-NB), d) 4-Nitrobenzamide (4-NB)

The reduction of nitroaromatic compounds is believed to be performed in two sequential steps. The first step involves the two electron reduction of the nitro group to produce a nitroso intermediate followed by a second step where the two electron reduction of the nitroso intermediate yields the hydroxylamine product (see Figure 1.17) (Anlezark *et al.* 1992).

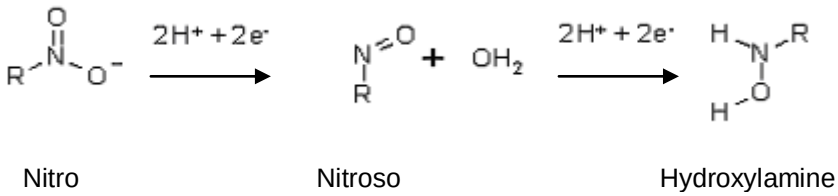

Figure 1.17 Four electron reduction of a nitro group to its hydroxylamine product
Conversion from nitro to nitroso intermediate, then nitroso to hydroxylamine

However it has also been observed that the nitroso compound can also be converted to the hydroxylamine product non-enzymatically by NADH/NADPH in solution (Anlezark *et al.* 1992). Therefore it is possible that the second step may not always be enzyme catalysed.

1.4.4 Crystallographic studies

The determination of *NfsB* NTR crystal structure has provided information on its structure, substrate binding, conformational changes and catalytic mechanism.

1.4.4.1 Structure

The structure of *NfsB* NTR was first published in 2000, showing that the enzyme consists of a dimer of two identical monomers with each subunit having a mass of 24 kDa (Parkinson *et al.* 2000). This study generated a low resolution structure by comparison with the FMN oxidoreductase from *Vibrio fisheri* (*FRase* I), based on its high sequence identity to *NfsB* NTR (Parkinson *et al*. 2000).

The following year a high resolution structure for *NfsB* NTR was published. The enzyme structure was determined when bound to the substrate analogue nicotinic acid. From this structure it was possible to determine that the enzyme has a large hydrophobic core, each monomer consists of a five-stranded β sheet surrounded by α helices. Two active sites lie on opposite sides of the molecule, in solvent-exposed clefts at the dimer interface. The FMN is in a butterfly conformation as seen in other flavoenzymes. The nicotinic acid stacks between the re face of FMN and residue Phe 124 (Lovering *et al.* 2001).

Further reduced *NfsB* NTR crystal structures have since been published bound with the inhibitor dicoumarol and three dinitrobenzamide prodrugs (Johansson *et al.* 2003). In this study it was proposed that the prodrug binds the two active sites in different binding orientations allowing equal amounts of 2- and 4-hydroxylamine to be produced for CB1954. However our group is sceptical of these structures, and consider it likely that the crystals actually contain acetate (from crystallisation buffer) rather than prodrug CB1954 in the active site.

1.4.4.2 Active Site

The active sites of *NfsB* NTR are constructed from residues from both monomers and FMN cofactors. The FMN cofactor forms a tight non-covalent bond, and is able to form hydrogen bonds to one monomer and hydrophobic contacts with both monomers (Parkinson *et al.* 2000 and Lovering *et al.* 2001). Figure 1.18 shows the crystal structure of *NfsB* NTR.

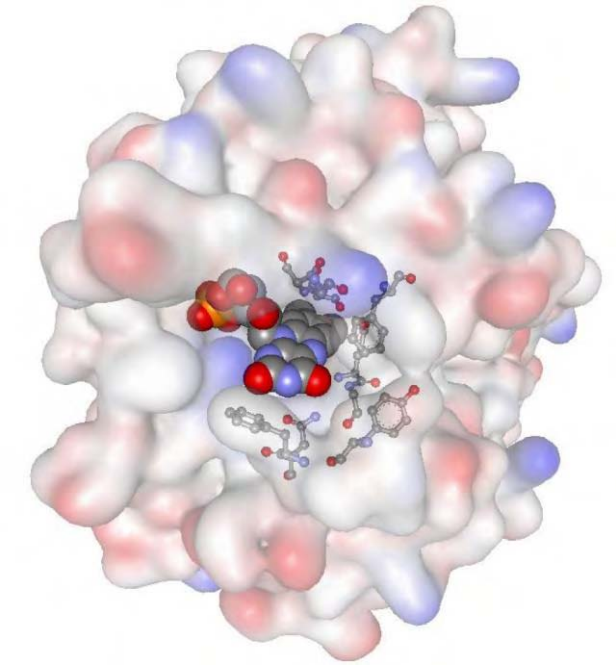

Figure 1.18 Crystal Structure of *NfsB* NTR
Showing the active site with bound FMN cofactor (Lovering *et al.* 2001)

1.4.5 Clinical Trials

Two phase I/II clinical trials using the NTR/CB1954 system have been trialled here in Birmingham. These trials used a replication defective adenovirus CTL102 encoding *NfsB* NTR in conjunction with systemic prodrug CB1954, for the treatment of either resectable liver cancer (Palmer *et al.* 2004) or localised prostate cancer (Patel *et al.* 2009).

The liver trial was the first phase I clinical trial for this system investigating feasibility, safety and determining levels of transgene expression. For this trial each patient with resectable primary or secondary liver cancer received a single dose of CTL102 delivered intratumorally (dose range $1 \times 10^8 - 5 \times 10^{11}$ virus particles) followed by surgical resection 3-8 days later. The vector was tolerated well with no dose limiting toxicity and nitroreductase expression was measured by immunohistochemical staining (see Figure 1.19) (Palmer *et al.* 2004).

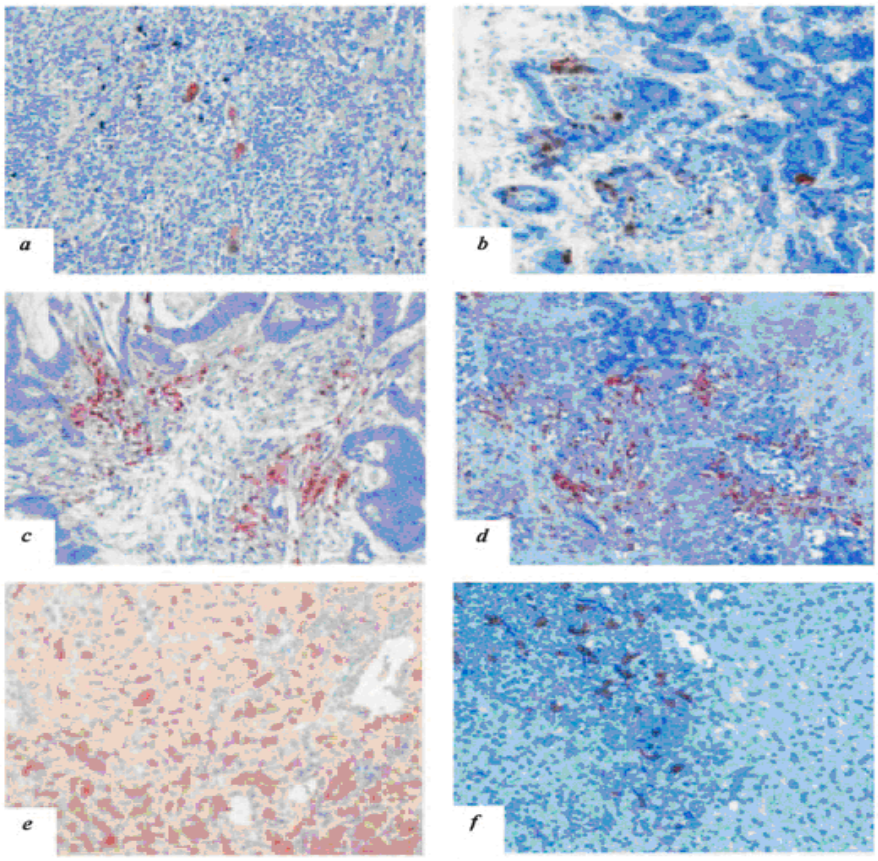

Figure 1.19 Immunohistochemical staining of tumour sections with anti-nitroreductase antibody
a) 1 x 10^8 virus particles, b) 1 x 10^9 virus particles, c) 1 x 10^{10} virus particles, d) 1 x 10^{11} virus particles, e) 1 x 10^{11} virus particles f) 5 x 10^{11} virus particles x200 magnification. Nitroreductase expressing cells restain red (Palmer *et al.* 2004)

The prostate trial was a phase I/II clinical trial. Patients underwent TRUS-guided intraprostatic injection of virus in escalating doses (5 x 10^{10} - 1 x 10^{12} virus particles) with subsequent prostatectomy (gene expression group) or intravenous CB1954 24 mg/m^2 (therapeutic group) 48-72 hours post injection. Primary endpoints for this trial were safety and tolerability in both groups, with secondary endpoints of gene expression (gene expression group) and efficacy of TRUS, repeat biopsies and PSA (therapeutic group). The vector was well tolerated with minimal side effects. Immunohistochemical staining of resected prostate showed NTR staining at all dose levels (see Figure 1.20) (Patel *et al.* 2009).

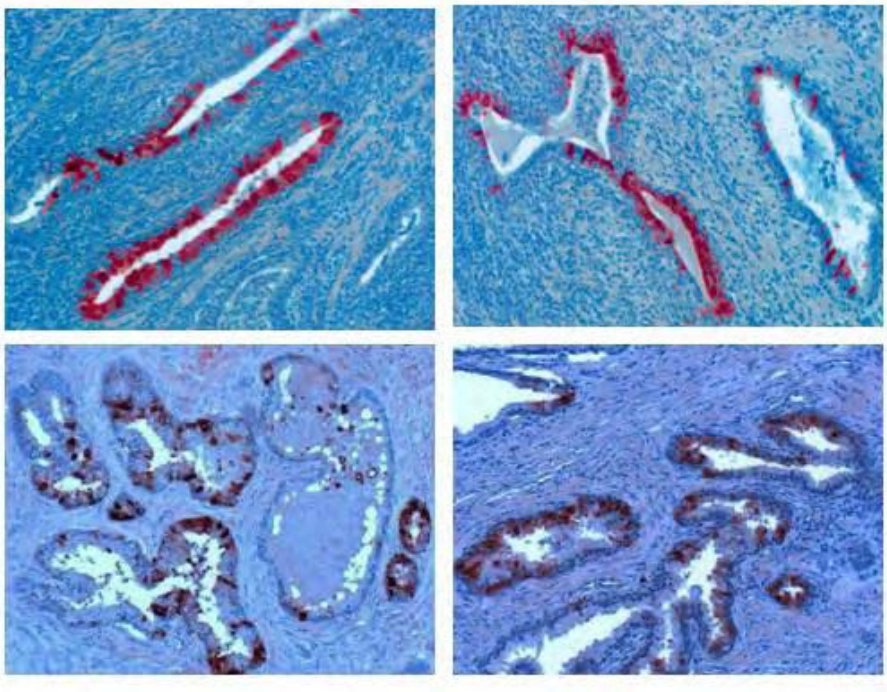

Figure 1.20 Immunohistochemical staining of tumour sections with polyclonal sheep anti-nitroreductase (NTR) antibody and counter stained with Mayer's haematoxylin
(Patel *et al.* 2009)

19 patients received virus plus prodrug, minimal toxicity was observed, with preliminary evidence of efficacy indicated by a drop in PSA level (see Figure 1.21). 4 out of 19 showed a 10-50 percent reduction, and 2 out of 19 showed greater than 50 percent reduction in PSA 6 months after treatment (Patel *et al.* 2009).

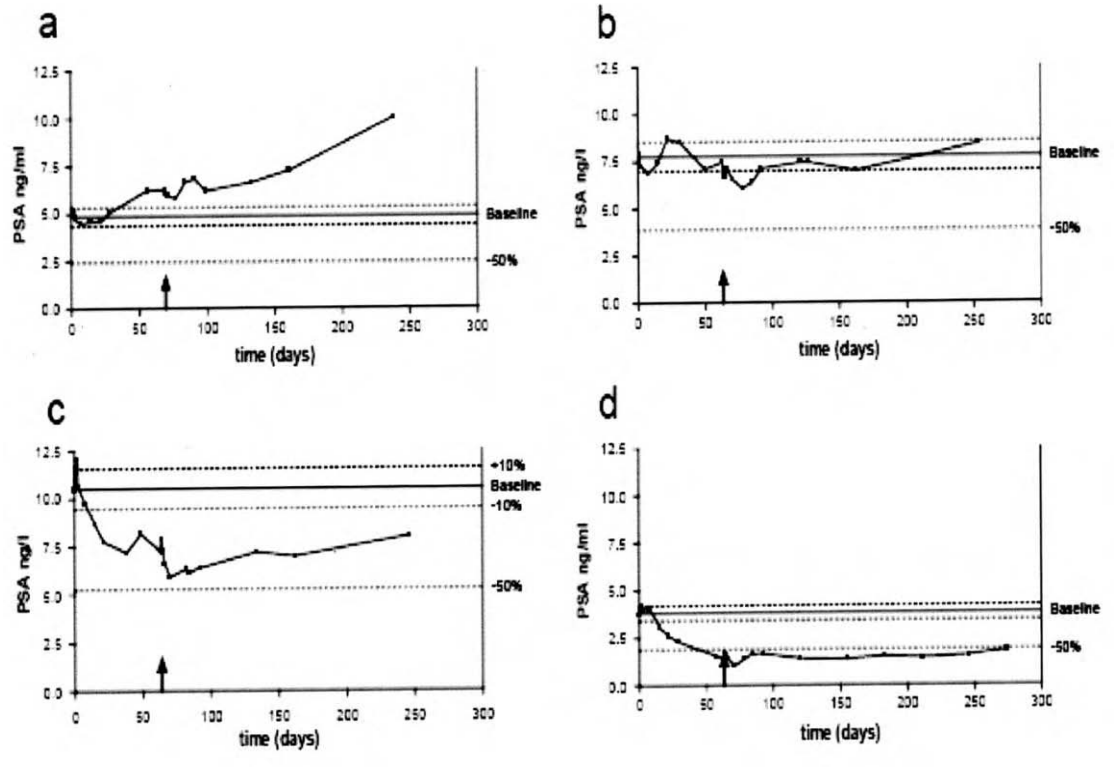

Figure 1.21 PSA kinetics
Examples of PSA kinetics in patients classified at 6 months showing a) progressive disease, b) stable disease, c) partial response and d) good response (Patel *et al.* 2009)

1.4.6 Improving the NTR system

As stated previously the prodrug CB1954 is not an optimum substrate for NTR. At a clinical achievable dose of CB1954, the peak serum concentration is 5-10 µM (Chung-Faye *et al.* 2001a). However kinetic analysis has shown that the K_m of NTR is approximately 100-fold greater than this (Anlezark *et al.* 1992 and Jarrom *et al.* 2009). Therefore the amount of CB1954 that can be activated is limited. Several ways for improving clinical efficacy will be discussed below.

1.4.6.1 Alternative Enzymes

The search for enzymes able to efficiently reduce CB1954-HAs mainly focussed on prokaryotes. Many nitroreductases species have been studies, however only three alternative enzymes have showed potential relative to *Escherichia coli NfsB.*

1.4.6.1.1 *Bacillus amyloliquefaciens YwrO*

The *Bacillus amyloliquefaciens YwrO* nitroreductase is capable of reducing CB1954 using NADPH as electron donor. This NTR produces only the 4-hydroxylamine product. Kinetic parameters for CB1954 showed that both the k_{cat} and K_m are similar to *NfsB* NTR with a k_{cat} 618 µM and K_m 8.2 µM (Anlezark *et al.* 2002).

1.4.6.1.2 *Escherichia coli YieF*

YieF a chromate reductase from *Escherichia coli* also shows CB1954 reducing activity. Mutation in the *YieF* enzyme for enhanced chromate reduction has also enhanced the CB1954 reductase capacity of the enzyme with ~ 5-fold improvement in efficiency at killing HeLa cells than the wildtype *YieF* enzyme and NTR enzyme *NfsA* (Barak *et al.* 2006).

1.4.6.1.3 *Escherichia coli NfsA*

NfsA nitroreductase from *Escherichia coli* is considered as the major nitroreductase and is NADPH specific for electron donation (Zenno *et al.* 1996a). *NfsA* has a k_{cat} of 20.9 µM and K_m of 140 µM for CB1954 using NADPH as the electron donor. This gives a k_{cat}/K_m of 0.15 µM which is ~25-fold higher than that of *NfsB* (Vass *et al.* 2009).

NfsA shares approximately 7 percent of its sequence with *NfsB*, but has similar overall folds. Many structural features are shared. Both enzymes are homodimers with a α/β fold and two active sites at the dimer interface. The biggest difference between *NfsA* and *NfsB* NTR is the active site. *NfsA* has a more open structure with a lack of residues at positions corresponding to *NfsB* Phe 123 and Phe 124 (Kobori *et al.* 2001).

1.4.6.2 Alternative Prodrugs

In addition to CB1954 two other classes of compounds have been used as prodrugs for NTR: dinitrobenzamide mustards and nitroaromatic phosphoramides.

1.4.6.2.1 Dinitrobenzamide mustards

Dinitrobenzamide mustards are analogues of CB1954, where the aziridine ring has been replaced by nitrogen mustard. SN23862 is the most well known dinitrobenzamide mustard, which was first used as a prodrug for targeting tumour hypoxia. Anlezark later used SN23862 with NTR (Anlezark *et al.* 1995). Reduction of SN23862 by NTR produces only the highly toxic 2-hydroxylamine product and is also more lipophilic than CB1954, giving a better bystander effect. Kinetic parameters for SN23862 with *NfsB* NTR as substrate showed a K_m of 2.5 mM and a k_{cat} of 26.4 mM (Anlezark *et al.* 1995) (see Figure 1.22).

Figure 1.22 Nitroreduction of SN23862 Dinitrobenzamide mustard by NTR
Production of 2-hydoxylamine

1.4.6.2.2 Nitroaromatic phosphoramides

The most well known nitroaromatic phosphoramide, cyclophosphamide has been successfully used as an anticancer agent for many years. Like CB1954 cyclophosphamide is toxic towards both dividing and non-dividing cells. Cyclophosphamide is metabolised in hepatic cells by cytochrome P450 enzymes, releasing acrolein and phosphoramide mustard. Cyclophosphamide is effective for the treatment of slow growing tumours. The by product acrolein however can lead to life threatening haemorrhagic cystitis.

Nitroaromatic phosphoramide prodrugs have been designed to allow activation of the phosphoramide mustard in the tumour rather than in hepatic cells. The nitroaromatic phosphoramide prodrug LH7 (an acyclic 4-nitrobenzyl phosphoramide mustard) contains a nitro group, allowing NTR reduction to release phosphoramide mustard (see Figure 1.23). Kinetic analysis of LH7 shows it to be a better substrate for NTR than CB1954 with a K_m of 195 µM and k_{cat} of 14 µM. Giving a k_{cat}/K_m 19 times better than CB1954 (Hu *et al.* 2003).

Figure 1.23 Nitroreduction of LH7 nitroaromatic phosphoramide by NTR
Production of phosphoramide mustard

1.4.7 Improving Nitroreductase Efficiency

In view of the fairly modest improvements obtained by using alternative prodrugs, or alternative enzymes for activation of CB1954, a third strategy adapted by our group was to attempt to improve the efficiency of CB1954 activation, through molecular engineering of nitroreductase. Based on the crystal structure (Lovering *et al*. 2001), nine residues around the active site were identified as targets for mutagenesis (see Figure 1.24) (Grove *et al.* 2003).

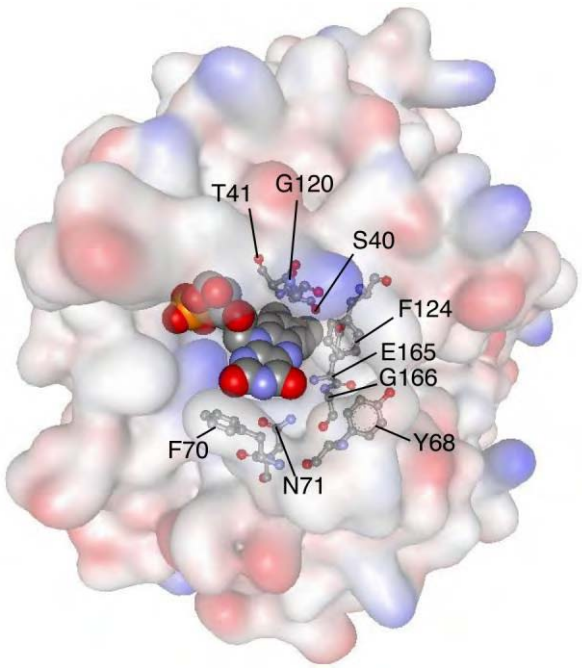

Figure 1.24 Crystal Structure of *NfsB* NTR with mutated residues highlighted
Showing the active site with bound FMN cofactor and residues S40, T41, Y68, F70, N71, G120, F124, E165 and G166 (Lovering *et al.* 2001 and Grove *et al.* 2003)

For each targeted residue a pool of all possible codon variants was generated and cloned into bacteriophage lambda vector JG3J1. The resulting libraries of NTR mutants were used to generate *E. coli* bacterial lysogens and screened for increased sensitivity to CB1954 by plating out on agar plates containing a range of CB1954 concentrations. Mutants with improved NTR enzyme activity were expected to cause increased sensitivity to CB1954.

50 amino acid substitutions were identified across the nine residues that gave greater sensitivity that wild-type NTR (see Figure 1.25). The best mutants achieved gave 2-6 fold improvement over WT when sensitising *E. coli* to CB1954 (Grove *et al.* 2003). Mutations at F124 gave the greatest increase in activity when compared to wild-type. 15 amino acid changes at this position gave rise to improved mutants. The F124K mutant was inserted into an adenovirus vector, and shown to confer ~5-fold greater sensitivity to SKOV3 ovarian carcinoma cells than WT *NfsB* NTR.

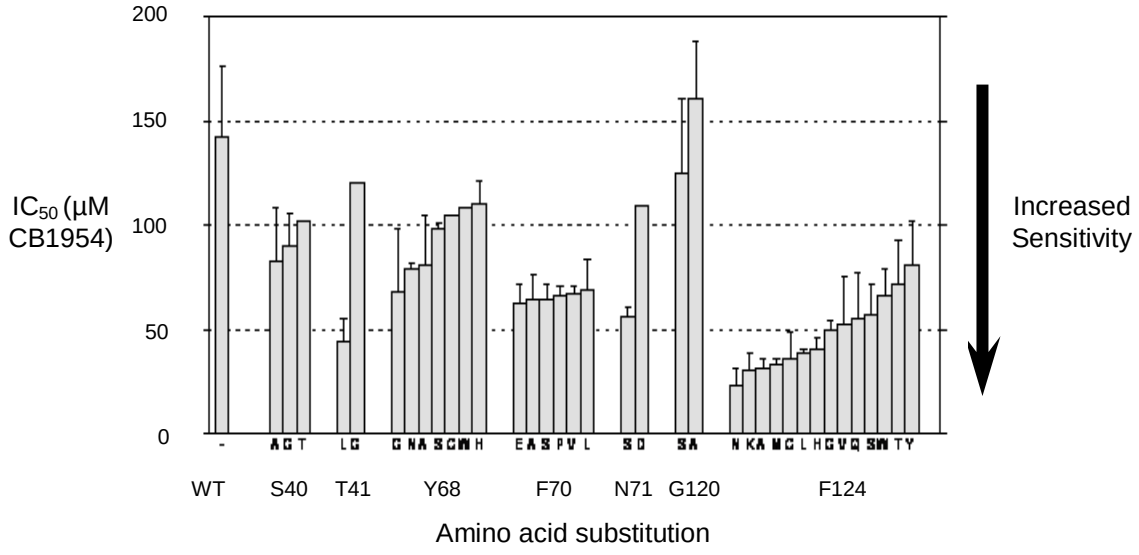

Figure 1.25 CB1954 prodrug sensitivity of NTR mutants
Comparing WT NTR with mutant NTR encoding any amino acid at S40, T41, Y68, F70, N71, G120, and F124 (Grove *et al.* 2003)

Following on from these improvements a second generation of *NfsB* NTR mutants was generated by combining beneficial single mutants (S40A or G, T41L, Y68G, F70A or V, N71S, and F124H, K, M, N, Q, S or W) giving a total of 53 double mutants. All mutants were again screened for increased sensitivity to CB1954. Six double mutants showed the most improvement: S40A F124K, S40A F124M, S40A F124N, T41L N71S, N71S F124K and N71S F124N.

The double mutant T41L N71S gave the most improvement with an IC_{50} for CB1954 of 12 µM in *E. coli* 12.5-fold better than WT. When tested in human carcinoma cells, an IC_{50} for CB1954 of 0.9 µM was determined giving a 14-fold reduction in IC_{50} relative to WT enzyme. These results show significant improvement over the two single mutants T41L and N71S. Kinetic analysis has shown that the k_{cat}/K_m for T41L N71S is 100-fold greater than the k_{cat}/K_m for WT (Jaberipour *et al.* 2010).

Both Grove and Jaberipour screened clones for improved sensitivity by replica plating. This method is both labour intensive and laborious. However there is greater potential for further improvement using a direct positive selection strategy allowing the study of multiple residue combinations. One such strategy was designed by the Gene Therapy group here in Birmingham which uses bacteriophage lambda and the SOS response (Guise *et al.* 2007). Before this strategy is discussed a brief overview of bacteriophage lambda, its life cycle and the SOS response will be given for clarity.

1.4.7.1 Bacteriophage Lambda

Bacteriophage lambda was first discovered by Ester Lederberg in 1951 as a prophage in *Escherichia coli* K12 (Court *et al.* 2007). Lambda has since become a model system for the study of molecular biology (Murray and Gann 2007). Lambda phage contains a linear double-stranded DNA genome of 48.5 kb, a capsid and a tail (see Figure 1.26). The finished capsid is an icosahedron shape approximately 0.05 µ in diameter, whereas the tail is a thin flexible tube that ends in a small conical part and a single fibre approximately 0.15 µ long. Lambda phage particles consist of half protein and half double-stranded DNA (Hershey and Dove 1971 and Arber 1983).

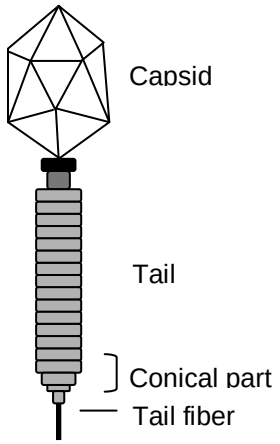

Figure 1.26 Structure of lambda bacteriophage
This image demonstrates the capsid, tail and fibre of the bacteriophage

1.4.7.1.1 Lambda life cycle

Bacteriophage lambda is a temperate bacteriophage, allowing reproduction and development in a lytic or lysogenic state (Oppenheim *et al.* 2005 and Court *et al.* 2007). Early stages of infection are the same whichever pathway is eventually followed.

A phage identifies a host bacterium by binding or adsorbing to a specific structure on the surface of the cell. Lambda binds to an outer membrane protein called LamB via a protein that resides at the tip of the tail called the J protein (Arber 1983). Lambda DNA is then injected by the phage and taken up by the bacterium. Lambda gains entry to the cytoplasm by using an inner membrane protein PstM (Arber 1983). Once inside the cytoplasm the lambda DNA circularises via *cos* sites situated at each end of the DNA, to prevent degradation by exonucleases.

The lambda genome contains six major promoters known as P_L for promoter leftward, P_R for promoter rightward, P_{RE} promoter for repressor establishment, P_{RM} promoter for repressor maintenance, P_I promoter for integration and $P_{R'}$ for secondary rightward promoter. Transcription begins from the P_L and P_R promoters, transcribing and translating a series of genes which are known as early genes. The protein products of these genes are required for phage development see Figure 1.27 showing protein products produced from the P_L and P_R promoters.

The decision between lysogeny and lysis depends on the relative amounts of CI and Cro and their promoter binding, both bind to the same promoter known as O_R (Oppenheim *et al.* 2005). The O_R is comprised of three parts O_{R1}, O_{R2} and O_{R3}.

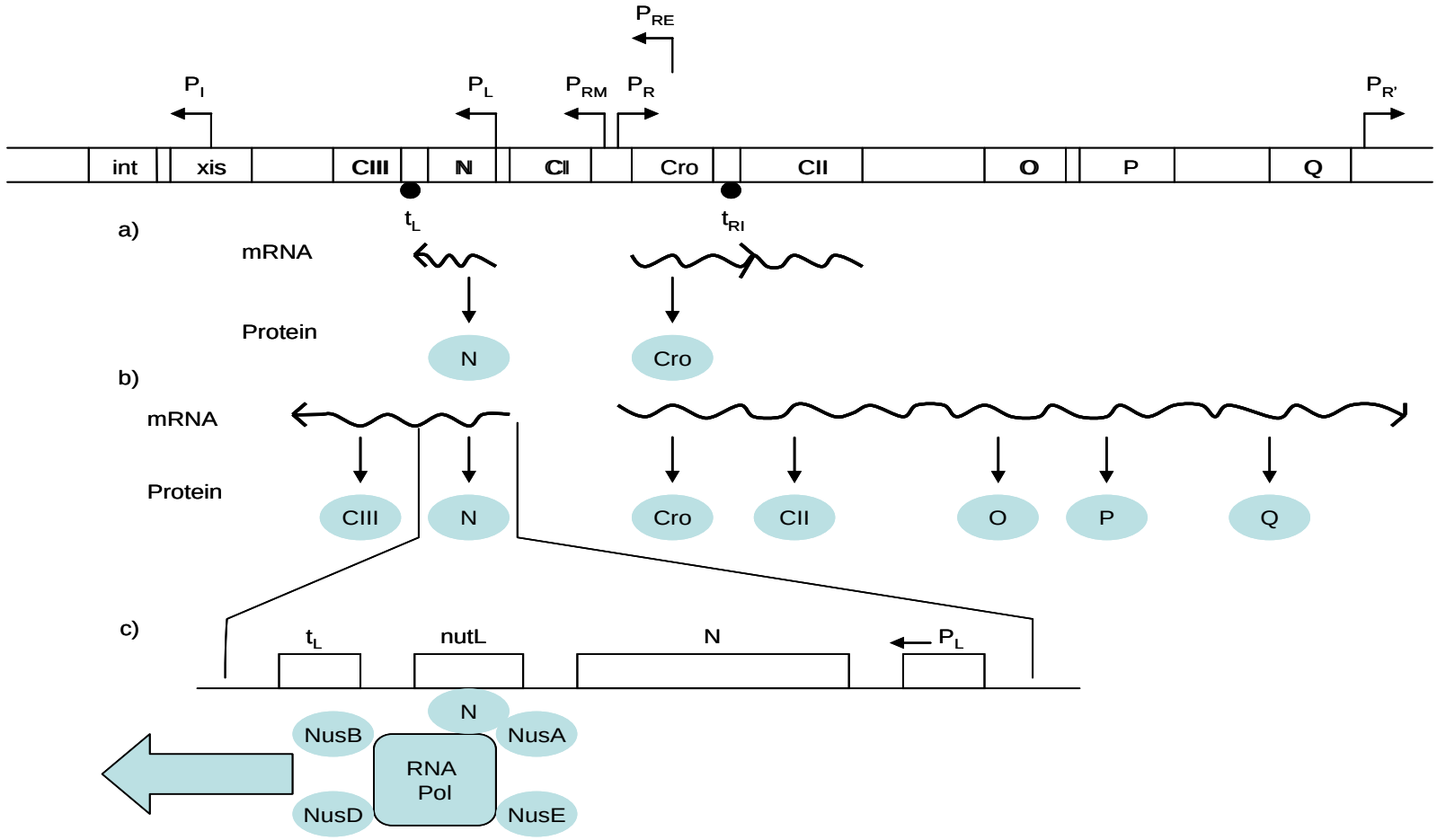

Figure 1.27 Initial transcription and translation events that take place on the lambda genome after infection
a) Transcription from P_L leads to the production of N protein and transcription from P_R leads to Cro protein, b) Protein N is an anti-terminator which allows RNA polymerase to read through t_L and t_{R1} terminators. This allows the transcription of CIII protein from $P_{L'}$ and CII, O, P, and Q protein from $P_{R'}$, c) N binds to the *nutL* site on the DNA. In conjunction with four bacterial proteins, NusA, NusB, NusD, and NusE, N allows RNA polymerase to read through the terminator t_L.

Protein CI binds to O_{R1} with high affinity; as CI concentration increases it binds to O_{R2} and then O_{R3}. This inhibits the P_R promoter preventing Cro production, and the phage enter lysogeny. Alternatively protein Cro binds to O_{R3} with high affinity; as Cro concentration increases it binds to O_{R2} and then O_{R1}. This inhibits the P_{RM} promoter preventing CI production leading to lytic growth (Oppenheim *et al.* 2005).

1.4.7.1.1.1 Lysogeny

A continuous supply of CI from the P_{RM} promoter represses transcription from both P_R and P_L, and leads to the activation of the P_I promoter, which produces integrase protein. This protein facilitates recombination of lambda DNA into the bacterial chromosome. Recombination occurs between *attP* on the lambda and *attB* on the bacterial chromosome. Once in the chromosome the DNA is bound at hybrid *att* sites known as *attL* and *attR*. The lambda DNA can now replicate when the bacterial chromosome is replicated allowing stable transmission to daughter cells. Once a lysogen is established it is stable, with the prophage remaining dormant almost indefinitely, and only approximately one cell per thousand cell generations will spontaneously revert to phage production. However if the cell is threatened, this state can easily be reversed, switching into lytic cycle by a process known as induction.

1.4.7.1.1.2 Lysis

Continuous expression from P_R promoter allows Q protein to accumulate in the cell. This leads to the activation of the $P_{R'}$ promoter. $P_{R'}$ transcribes late genes that are essential for lytic infection eg: the production of head, tail and lysis proteins. Phage replication proceeds using O and P proteins. Initial replication uses theta replication which is later changed to rolling circle replication (Furth and Wickner 1983).

Construction of phage particles proceeds first with the assembly of the phage capsid using ten phage encoded proteins and the host proteins GroEL and GroES (Georgopoulos *et al.* 1983). The capsid consists of eight proteins E, D, B, W, FII, B*, X1 and X2. Addition of the major coat protein results in the formation of the phage head, into which DNA is inserted. The phage head is stabilised by the addition of two further proteins, which also allows connection of the tail. The completed phage tail is composed of twelve genes Z, U, V, G, T, H, 208, M, L, K, I and J (Katsura 1983). Once the phage particles have been generated the next step is to get out of the bacterial cell into the environment. Two proteins R and S are required for this. S is a 15K protein used to form a hole in the inner membrane allowing protein R endolysin a 17K protein access to the cell wall for degradation of the bacterial peptidoglycan (Friedman and Gottesman 1983). This entire lytic cycle takes approximately 35 minutes and approximately 100 intact phage particles are released. Figure 1.28 demonstrates lytic replication of lambda.

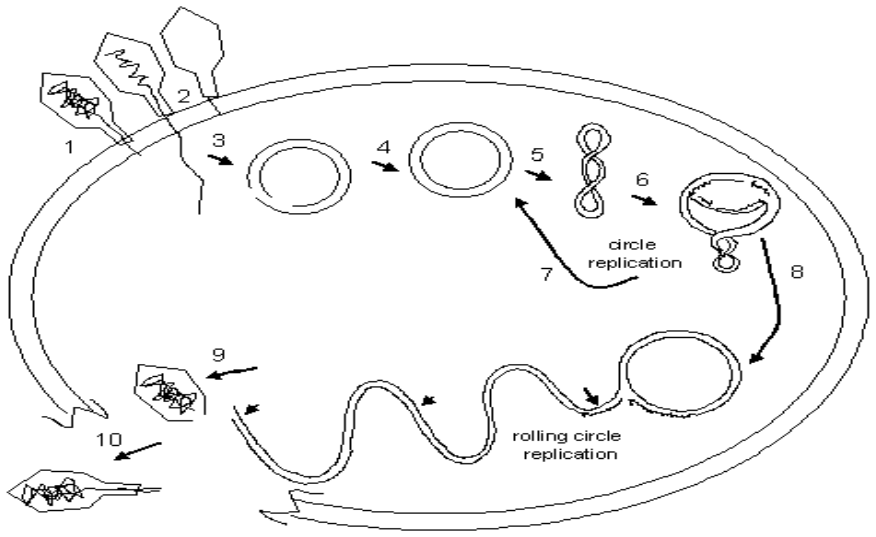

Figure 1.28 DNA replication cycle for bacteriophage lambda
(1) Phage particle attaches to the host cell, (2) Injection of linear duplex DNA molecule, (3) DNA circularises by base pairing of complementary single stranded ends, (4) Nicked circle closed by DNA ligase, (5) Supercoils are introduced by DNA gyrase, (6) DNA replication initiates on supercoiled circle, (7) termination of a round of replication yields two daughter circles, (8) At later point replication proceeds by rolling circle replication, cut at cos sites (arrows), (9) packaged into phage heads, (10) Addition of a tail completes maturation of phage particles (Adapted from Firth and Wickner 1983).

1.4.7.2 SOS response

The exposure of *E. coli* to agents that can damage DNA or interfere with DNA replication eg: ultraviolet light (UV) or mitomycin can induce a diverse set of physiological responses that have been termed as SOS responses. Single-stranded DNA in the bacterial cell binds to the protein RecA with assistance from RecFOR and RecBC proteins (Michel 2005). RecA in turn becomes activated and binds to another protein LexA. Proteolytic cleavage of LexA by autocleavage allows activation of approximately 30 DNA damage genes (Matic *et al.* 2000). It is believed that RecA acts in an indirect stimulatory role to help facilitate LexA autocleavage (Walker 1984). These DNA damage genes play several roles such as delaying cell division until the damage is repaired or allowing the cell to replicate past the DNA damage (Snyder and Champness 2003).

The regulation of the SOS response through cleavage of the LexA repressor is very similar to the induction of lambda. The activated RecA also initiates autocleavage of lambda CI protein at a rate ten times slower than the cleavage of LexA (Walker 1984, Matic *et al.* 2000 and Janion 2001). This switches lambda from lysogeny to lytic reproduction, by de-repressing transcription from the P_R and P_L promoters, ensuring lambda survival from a bacterial cell that's under stress.

1.4.7.3 Selection Strategy

A direct positive selection strategy using bacteriophage lambda and the SOS response has been developed. In order to use this system the lambda genome has been modified for the expression of NTR from an inducible Ptac promoter (see Figure 1.29).

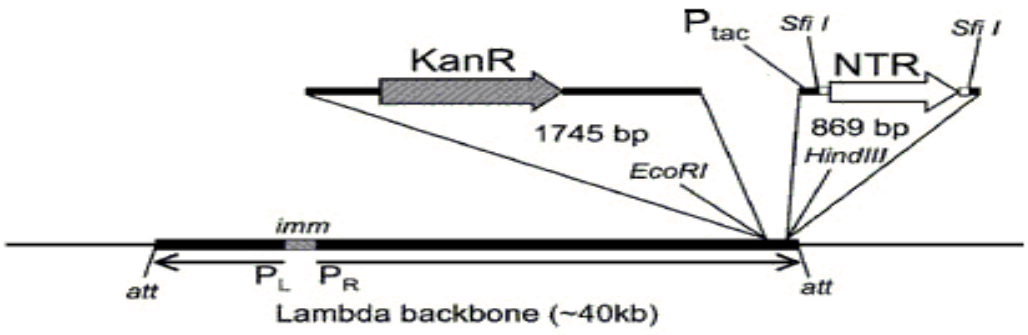

Figure 1.29 Schematic of lambda vector JG16C2 integrated to the *E. coli* chromosome by its att sites
PL, PR, lytic cycle promoters. The cI repressor encoded in immunity (imm) region. NTR is inserted between *Sfi* I sites downstream of the IPTG-inducible Ptac promoter. KanR indicates a Kanamycin resistance gene for lysogen selection (Adapted from Guise *et al.* 2007)

This strategy utilizes lambda's ability to switch between a lytic (lysis) and latent (lysogenic) state. In a lysogenic state the lambda's genome integrates into the bacterial *E. coli* host DNA and is stably transmitted to daughter cells. The bacterial SOS response is used, to trigger NTR expressing lambda lysogens to enter the lytic cycle. The SOS response is triggered when CB1954 activation leads to DNA cross linking. Therefore phages that encode NTR, which more readily activates CB1954, will enter the lytic cycle at low prodrug concentration. This allows preferential enrichment of phage encoding improved NTR (Guise *et al.* 2007).

A phage library containing mutant *NfsB* NTR with randomised codons encoding for F124, F70 or N71, and S40 or T41 was generated, giving greater than 1 x 10^6 possible nucleotide combinations. 6.8 x 10^5 independent clones were then put through multiple rounds of selection. The most active mutant identified was the triple mutant T41Q N71S F124T, which was found to have an IC_{50} of 3 µM CB1954 in *E. coli*, 50-fold lower than wild type (Guise *et al.* 2007). However, it may be possible to further improve *NfsB* NTRs ability to sensitise cells to CB1954.

1.5 AIM OF THESIS

ULTIMATE AIM:

To improve the efficacy of VDEPT using NTR and CB1954 by improving our knowledge of the contribution of different active site residues of *NfsB* NTR to the efficacy of CB1954 activation, and using this understanding, together with the direct positive selection method to select NTR mutants with greater efficiency of CB1954 activation.

OBJECTIVES:

1. To investigate the contribution of specific active site amino acid residues, or combinations of residues, via construction and selection of small libraries.

2. To design and select a large library of NTR mutants containing mutations at multiple sites, to obtain one or more improved enzymes.

3. To purify and kinetically characterise the *NfsB* NTR mutants of greatest interest, and to compare with WT and other previously purified mutant *NfsB* NTR enzymes.

4. To construct adenoviral vectors expressing the most promising *NfsB* NTR mutants and assess their ability to sensitise tumour cells to CB1954.

CHAPTER 2: MATERIALS AND METHODS

2.1 INTRODUCTION

Molecular biology techniques were derived from Current Protocols in Molecular Biology (Wiley), and Molecular Cloning: a Laboratory Manual (Sambrook *et al.* 1989).

2.2 MOLECULAR BIOLOGY

2.2.1 Oligonucleotide Primers

The following Oligonucleotide primers were used during this study:

PS1013A	GCTTCAGCCAGACATCCGTCC
PS1013B	GTTGCCAAATCCGCTGCCG
JG2A	TGGCGGAAAGGTATGCATGC
JG2B	CAGAGCATTAGCGCAAGGTG
JG138A	GCACGCTAGCAAGCTTCCACCATGGATATCATTTCTGTCGCC
JG138B	GCACAAGCTTGCTAGCTCATTACACTTCGGTTAAGGTGATG
SH1A	GCCAGCAAAAAACTTACCCCG
SH1B	CCGGGGTAAGTTTTTTGCTGGCATCAAATGCNNNAGTGGAATGACGCTTTAAGGC
JG126A	CCCAGCCGTGGCATTTTATTGTTG
CG4041	CAACAATAAAATGCCACGGCTGGGAGTTNNNNNNGG
JG122A	TTGACGCCGCCATCCTCGATGCAG
CG165166	CTGCATCGAGGATGGCGGCGTCAAANNNNNNGATGG
SH33A	ATGCACCGTAAAGATCTGCATGATG
SH33B	CATCATGCAGATCTTTACGGTGCATATCSNNSNNSNNCTTSNNACCTTTATCGTTCGCGGCTT TCGC S = C or G
PS1296F	CTGCGATTAATGCATTCTGC

2.2.2 Growth Media

Luria Broth (LB): 20 g LB (Sigma) per litre.

Tris buffered Luria Broth (TBLB): 20 g LB (Sigma) and 62.5 ml Tris (1 M pH 7.5) per litre.

SOB Broth: 20 g Bacto-tryptone (Difco), 5 g yeast extract (Difco) and 2 ml NaCl (5 M), 10 ml $MgSO_4$ (1 M), 10 ml $MgCl_2$ (1 M) and 2.5 ml KCl (1 M) per litre.

SOB Agar: 20 g Bacto-tryptone (Difco), 5 g yeast extract (Difco), 2 ml NaCl (5 M), 10 ml $MgSO_4$ (1 M), 10 ml $MgCl_2$ (1 M), 2.5 ml KCl (1 M) and 7.5 g Bacto Agar (sigma) per litre.

SOC Broth: 20 g Bacto-tryptone (Difco), 5 g yeast extract (Difco) and 2 ml NaCl (5 M), 10 ml $MgSO_4$ (1 M), 10 ml $MgCl_2$ (1 M), 2.5 ml KCl (1 M) and 20 ml glucose (1 M) per litre.

SM Buffer: 5.8 g NaCl, 8 g $MgSO_4$, 2.5 ml Gelatin (2% W/V) and 50 ml Tris (1 M pH 7.5) per litre.

NZYCM Broth: 10 g NZ Amide (Sigma), 5 g NaCl, 5 g yeast extract (Difco) 1 g Casamino acids (Sigma), 2 g $MgSO_4$. The pH was adjusted to 7 using NaOH.

NZYCM Top Agar: 10 g NZ Amide (Sigma), 5 g NaCl, 5 g yeast extract (Difco), 1 g Casamino acids (Sigma), 2 g $MgSO_4$, 7 g Agarose (Sigma). The pH was adjusted to 7 using NaOH.

NZYCM Agar: 10 g NZ Amide (Sigma), 5 g NaCl, 5 g yeast extract (Difco), 1 g Casamino acids (Sigma), 2 g $MgSO_4$ and 7.5 g Bacto Agar (Sigma). The pH was adjusted to 7 using NaOH.

2.2.3 Bacterial Strains

Table 2.1 provides a summary of the bacterial strains used in this study

E. coli strain	Genotype of strain
UT5600	F^- ara-14 leu B6 azi-6 lacY1 proC14 tsx-67 Δ (omp T- fep C) 266 ent A403 gln V44 (AS) λ^- trp E38 rfb D1 rps L109 (str R) xyl A5 mtl-1 thi-1
C600	BNN93 hflA150: Tn10 (Tet^r)
XL-2 Blue	recA1 endA1 gyrA96 thi-1 hsdR17 supE44 relA1 lac (F'proAB $lacI^qZ\Delta M15$ Tn10 (Tet^r) Amy Cam^r)[a]
BL21 λDE3	PhysS trc tac λPL araD T7 Ion^- $ompT^-$

Table 2.1 *Escherichia coli* strains used in this study

2.2.4 Polymerase Chain Reaction (PCR)

Polymerase chain reaction (PCR) was used for the amplification of DNA. Standard Taq DNA polymerase (Roche Applied Sciences, Germany) was used for phage library preparation. Two PCR reactions were used. An initial PCR was performed using 5 µl of DNA encoding WT or mutant NTR as template. The PCR was performed using 5 µl 10x buffer, 5 µl dNTP's (2 mM), 1 µl primer 1 (25 µM), 1 µl primer 2 (25 µM), 0.5 µl Taq polymerase and 32.5 µl water. A second combined PCR also using Taq Polymerase was used to join PCR fragments together making full length NTR (encoding mutations at specific residues). This PCR was performed using 5 µl 10 x buffer, 5 µl dNTP's (2 mM), 1 µl primer 1 (25 µM), 1 µl primer 2 (25 µM), 50 ng PCR fragment 1, 50 ng PCR fragment 2, 0.5 µl Taq polymerase and water to 50 µl.

KOD DNA polymerase (Novagen, USA) was used for cloning purposes, allowing the amplification of specific NTR's for subsequent cloning into plasmids. KOD polymerase increases fidelity when amplifying and ensures blunt ends for cloning. These PCR's were performed using 5 µl of DNA template, 5 µl 10x buffer, 5 µl dNTP's, 3 µl $MgSO_4$, 1 µl primer 1 (25 µM), 1 µl primer 2 (25 µM), 0.5 µl KOD Polymerase and 29.5 µl water.

Routinely, PCR reactions were run as a total volume of 50 µl in a thermalcycler (PE Biosystems) under the following conditions:

Initial denaturation	95 °C	5 minutes	
Denaturation	95 °C	50 seconds	x 25 cycles
Annealing	55 °C	50 seconds	
Extension	72 °C	60 seconds	
Final Extension	72 °C	7 minutes	
Hold	4 °C		

2.2.5 Agarose Gel Electrophoresis

Analytical gels were used to visualise DNA products eg: PCR fragments or restriction enzyme digests of DNA. Agarose gels (0.6% to 1% agarose) were prepared in 1x TAE running buffer (diluted from 50x TAE stock solution: 242 g of Tris HCl, 57.1 ml of glacial acetic acid, 18.2 g of disodium EDTA in 1 litre H_2O). Gels were placed in a gel tank containing 1x TAE. DNA was mixed with glycerol loading buffer and loaded into appropriate lanes. DNA marker was loaded into the first lane, and the gel run at 100 volts for approximately 2 hours dependent on the clarity and separation of bands required. Gels were stained in water containing 0.5 µg/ml ethidium bromide and visualised under UV illumination using a Kodak DC290 camera in combination with a Spectroline TVC312A UV transilluminator.

2.2.6 DNA Purification

2.2.6.1 Gel Purification with QIAquick gel extraction kit

Specific DNA fragments (70 bp to 10 kb in size) were separated on preparative agarose gels made using SeaKem GTG agarose (Cambrex Bio Science Wokingham, Ltd). The DNA sample was mixed 1:1 with Ficoll loading buffer plus the addition of 2 µl per 100 µl of sample of SYBR Gold before loading. (Molecular Probes, Inc). After electrophoresis, the desired fragment was visualised on a blue light transilluminator and cut from the gel using a sterile scalpel. Appropriate size excised bands were purified using QIAquick gel extraction Kit (Qiagen). Extraction and purification followed the manufacturer's recommendations.

2.2.6.2 Phenol/chloroform extraction

Phenol/chloroform extraction was performed to remove enzymes and other contaminating proteins from DNA samples. An equal volume of phenol/chloroform was added to the DNA sample and mixed thoroughly to form an emulsion. The sample was centrifuged at 13,000 rpm for 1 minute to separate phases, and the lower organic phase removed. An equal volume of chloroform was added, and the process was repeated. The aqueous phase was carefully removed and transferred to a clean tube.

2.2.6.3 PCR purification with Roche High Pure Purification kit

To remove primers, DNA polymerase, unincorporated nucleotides and other components following a PCR reaction High Pure PCR Product Purification Kit (Roche Applied Science, Germany) was used. Methods followed manufacturer's instructions.

2.2.7 DNA Precipitation

NaCl was added to the solution containing DNA, to a final concentration of 0.1 M, diluted from a 5 M stock solution. DNA was precipitated by the addition of 2 volumes of absolute Ethanol. Samples were incubated at -20 °C for 30 minutes to aid precipitation. DNA was recovered by centrifugation at 13,000 rpm for 10 minutes in a bench top microcentrifuge. The supernatant was aspirated and the pellet dried at room temperature. DNA was resuspended in a convenient volume of $T_{10}E_1$ (10 mM Tris, 1 mM EDTA, pH 7.5).

2.2.8 DNA quantitation

DNA was quantified using the DNA binding reagent PicoGreen (Molecular Probes, USA). Sample DNA and diluted standard DNA (phage λ DNA, supplied with kit) were diluted in $T_{10}E_1$ (10 mM Tris, 1 mM EDTA, pH 7.5). 100 µl sample DNA was loaded in triplicate on a 96 well plate. DNA standards were prepared containing 0, 20, 40, 60, 80 and 100 ng of DNA per 100 µl. 100 µl PicoGreen reagent diluted 1 to 200 in $T_{10}E_1$ was added to each well and samples were mixed by pipetting. Following 2 minute incubation in the dark, fluorescence at 485/535 nm was determined using a Wallac victor 1420 plate reader (Perkin Elmer, Italy). DNA concentration was calculated from a standard curve of the known diluted DNA standards.

2.2.9 Restriction Endonuclease Digestion

DNA restriction enzymes from New England Biolabs (Hitchin, Herts) or Roche (Roche Diagnostics) were used. These were used in accordance with the reaction conditions described in the manufacturer's instructions using the appropriate buffers, supplied with the enzymes. Restriction enzymes used during this study can be seen in Table 2.2

Restriction Enzyme	Temperature (°C)	BSA	Buffer	Heat Inactivation
Bam HI	37	Yes	NEB 3	No
Bgl II	37	No	NEB 3	No
Cla I	37	Yes	NEB 4	Yes
Eco RV	37	Yes	NEB 3	No
Hind III	37	No	Roche B	Yes
Hpa I	37	No	Roche A	Yes
Nco I	37	No	Roche H	Yes
Nde I	37	No	NEB 4	Yes
Pac I	37	Yes	NEB 1	Yes
Sfi I	50	Yes	NEB 4	No
Swa I	25	Yes	NEB 3	Yes

Table 2.2 Restriction Enzymes used and the conditions required

Typically, for diagnostic DNA digestions, 0.5 μg of DNA was cut in a total volume of 20 μl, with 2 μl of appropriate 10x enzyme buffer and 1 unit of restriction endonuclease. This was incubated at 37 °C unless otherwise stated for at least four hours. For digestion of larger quantities of DNA, (e.g. for fragment purification) restriction endonuclease digestion was scaled up accordingly.

2.2.10 Dephosphorylation

The removal of 5 prime phosphate groups from the ends of linear DNA was achieved using calf alkaline phosphatase (CAP) and incubated at 37 °C for one hour with 1x concentration of supplied buffer. The enzyme was then heat inactivated at 75 °C for 10 minutes before cleaning the DNA by phenol/chloroform extraction and ethanol precipitation. This prevents plasmid vectors re circularising themselves without insert.

2.2.11 Ligation

T4 DNA ligase (Roche Diagnostics) was used for the construction of recombinant DNA products (phage λ, plasmids and viral vectors). Usually a 3:1 molar excess of insert to vector was used in sticky end ligation and a 10:1 excess for blunt ended ligation. Ligation reactions were incubated overnight at 14 °C. After overnight incubation, DNA was cleaned by phenol/chloroform extraction and ethanol precipitation. The resulting pellet was then resuspended in 10 μl T_{10} E_1.

2.2.12 Preparation of competent cells

Competent *E. coli* cells for the transformation of plasmid DNA were prepared based on a method by Hanahan (Hanahan 1983). Competent XL-2 and BL21λDE3 cells were used for this study. *E. coli* cells taken from a frozen stock were streaked onto a fresh SOB agar plate and incubated overnight (approximately 16 hours) at 37 °C. A single isolated colony was transferred into 1 ml SOB with 20 mM $MgSO_4$, and the bacteria dispersed by vortexing. This was then added to 100 ml SOB containing 20 mM $MgSO_4$. The cells were shaken at 37 °C for 4-6 hours until the OD_{600} had reached 0.5.

The cells were then transferred into sterile, ice cold 50 ml tubes and stored on ice for 10 minutes, before being centrifuged for 10 minutes at 4,000 rpm in a Beckman GSR6 table top centrifuge using GH-38 rotor at 4 ^{o}C. The pellet was resuspended in 20 ml ice cold FSB transforming buffer per 50 ml tube (10 mM Potassium acetate (pH 7.5), 45 mM $MnCl_2$, 10 mM $CaCl_2$, 100 mM KCl, 3 mM hexamine cobalt chloride, and 10% v /v glycerol, pH 6.4), and again stored on ice for 10 minutes before centrifugation for 10 minutes at 4,000 rpm.

The pellets were resuspended in 4 ml FSB per 50 ml tube prior to mixing with 140 μl DMSO and incubating on ice for 15 minutes. An additional 140 μl DMSO was added and the cells were quickly dispensed into 300 μl aliquots in sterile eppendorf tubes and immediately snap frozen in liquid nitrogen. The aliquoted competent bacteria were stored at -80 °C until required.

2.2.13 Bacterial Transformation

For bacterial transformation 100 μl of competent *E. coli* cell suspension was mixed with approximately 10 ng of recombinant plasmid DNA or ligation mixture in an eppendorf and stored on ice for 45 minutes. Cells were then heat shocked at 42 °C for 2 minutes. 900 μl of room temperature SOC was then added, mixed thoroughly by inverting several times and incubated at 37 °C for 1 hour with gentle agitation. Cells were then plated on SOB agar plates (containing either 100 μg/ml Ampicillin or 30 μg/ml Kanamycin antibiotic) and incubated overnight at 37 °C.

2.2.14 Plasmid Mini Preparation

Bacterial colonies were picked into 5 ml of SOB medium (Difco Laboratories, UK) containing the appropriate antibiotic and grown overnight at 37 °C. The bacterial culture was pelleted by centrifugation at 5,000 rpm for 5 minutes in Sorvall SM24 rotor. The supernatant was discarded and the pellet was thoroughly resuspended in 100 μl of ice-cold solution I (50 mM glucose, 10 mM EDTA pH 7.5, 25 mM Tris HCl pH 8.0).

To this solution, 200 µl of freshly prepared solution II (0.2 M NaOH, 1% w/v SDS) was added to lyse the bacteria, and the tube inverted five times, before leaving the contents for 5 minutes on ice. 150 µl of ice-cold solution III (5 M acetate and 3 M potassium, pH 4.8-5.0) was added, and the tube mixed by inversion before leaving on ice for 5 minutes. Samples were centrifuged at 13,000 rpm for 5 minutes and the clear supernatants were transferred to clean tubes before DNA recovery was carried out via phenol/chloroform extraction and ethanol precipitation. DNA pellets were washed with 70% ethanol and resuspended in 50 µl 10 mM Tris. Cl (pH8.5) containing 50 µg/ml heat treated RNase A. DNA was checked by digestion of 5-10 µl of the DNA with appropriate restriction enzymes, before analysis by agarose gel electrophoresis.

2.2.15 Plasmid Bulk Preparation

Bacterial colonies containing the desired plasmid were inoculated into 200 ml of SOB medium supplemented with an appropriate antibiotic and grown overnight at 37 °C in a shaking incubator. The bacterial culture was centrifuged for 5 minutes at 5,000 rpm in a Sorvall GSA rotor at 4 °C. The supernatant was discarded and the bacterial pellet thoroughly suspended in 4 ml ice-cold solution I (50 mM glucose, 10 mM EDTA pH 7.5, 25 mM Tris HCl pH 8.0). 1 ml of freshly prepared 10 mg/ml lysozyme (in solution I) was added and the suspension left on ice for 10 minutes. Complete lysis proceeded by the addition of 10 ml of solution II (0.2 M NaOH, 1% w / v SDS). The pot was gently inverted a few times to ensure complete mixing before being left on ice for a further 10 minutes. 7.5 ml of solution III (5 M acetate and 3 M potassium, pH 4.8-5.0) was added and the pot was vortexed to ensure thorough mixing. After storage on ice for a further 10 minutes, bacterial debris was pelleted by centrifugation at 8,000 rpm for 15 minutes at 4 °C in a Sorvall GSA rotor.

Plasmid containing supernatant was carefully removed into a fresh 250 ml centrifuge bottle and all nucleic acids were precipitated by the addition of 22.5 ml of propan-2-ol. Precipitation was assisted by incubation at -20 °C for 30 minutes. The centrifuge bottle was then centrifuged at 8,000 rpm for 20 minutes at 4 °C. Pellets were allowed to drain before being dissolved overnight at room temperature in 2.5 ml of $T_{50}E_{10}$ (50mM Tris HCl and 10 mM EDTA). 3.03 g of caesium chloride (CsCl) was added to the plasmid solution. The liquid weight of the plasmid solution was made up to 2.75 ml by the addition of $T_{50}E_{10}$, and 275 µl of ethidium bromide solution (10 mg/ml) before storing on ice for 10 minutes. The plasmid solution was then centrifuged at 9,000 rpm for 10 minutes in a Sorvall SM24 rotor to precipitate contaminating RNA. The plasmid preparation was then transferred into 3.9 ml Beckman Quick-Seal centrifuge tubes, with any gap between the liquid and neck of tube filled with isopycnic CsCl solution (1 g CsCl:1ml $T_{50}E_{10}$). Tubes were heat sealed and ultra centrifuged at 100,000 rpm for 4 hours followed by a 95,000 rpm spin for 2 hours, followed by a 65,000 rpm gradient relaxation step for 30 minutes in a Beckman Optima TLX bench top ultracentrifuge using a TLN-100 near vertical tube rotor. The plasmid band was carefully removed by puncturing the side of the tubes with a 21 gauge needle and 2 ml syringe. DNA was diluted with 3 volumes of $T_{10}E_1N_{100}$ and the ethidium bromide was removed by two phenol/chloroform extractions. One volume of propan-2-ol was added to precipitate the DNA followed by centrifugation at 9,000 rpm for 10 minutes in a Sorvall SM24 rotor at 4 °C to pellet it. The DNA pellet was suspended in 500 µl of $T_{10}E_1N_{100}$ and transferred to a clean eppendorf tube before precipitation with 2 volumes of absolute ethanol. The pellet was finally suspended in a suitable volume of $T_{10}E_1$ and the concentration of the plasmid DNA was determined.

2.2.16 Sequencing

PCR based sequencing reactions were performed with an appropriate primer in a 20 μl reaction volume using ABI Prism Big Dye Terminator cycle sequencing ready reaction kits (PE Biosystems), according to the manufacturer's protocol. The reaction solution consisted of 4 μl of 5x buffer, template DNA, 2 μl of 2.5 μM sequencing primer, 1 μl terminator mix, and the appropriate volume of water. The reaction was run in a thermal cycler under the following condition: 94 °C for 2 seconds followed by 25 cycles: 96 °C for 10 seconds, 50 °C for 5 seconds and 60 °C for 4 minutes

Following the above reaction, the extension products were transferred to eppendorf tubes and precipitated by addition of 80 μl 75% propan-2-ol. The mixtures were well mixed, left at room temperature for 10 minutes before centrifuging at 13,000 rpm for 8 minutes. Each resultant pellet was washed with 180 μl 70% ethanol, followed by centrifugation at 13,000 rpm for 4 minutes. The final DNA pellets were left to air dry for 15 minutes and stored at -20 °C for subsequent sequencing.

Immediately prior to loading the sequencing, the pellets were resuspended in 10 μl of loading dye (5:1 mixture of de ionised formamide and 50 mg/ml dextran blue in 25 mM EDTA, pH 8), vortexed and spun down briefly. The samples were heated at 90 °C for 2 minutes in a heat block. 10 μl of each sample was loaded onto a 96 well plate and analysed on a Prism DNA sequencer, using a base calling algorithm ABI100.

2.3 PHAGE LAMBDA

2.3.1 Plating cells

E. coli plating cells UT5600 and C600 were required for phage lambda work. *E. coli* cells taken from a frozen stock were streaked onto a fresh LB plate and incubated overnight (approximately 16 hours) at 37 ^{o}C. A single isolated colony was transferred into 50 ml LB; the cultures were shaken at 37 ^{o}C for 4-6 hours until the OD_{600} had reached 0.5. The cells were then transferred into a sterile, 50 ml tube and centrifuged for 5 minutes at 1,500 rpm at 4 ^{o}C. The pellet was resuspended in 25 ml ice cold 10 mM $MgS0_4$. Plating cells can be stored at 4 ^{o}C and can be used for approximately 1 week.

2.3.2 Phage Purification

10 ml of C600 plating cells were infected with λJG3J1 and λSV054 (5×10^5 - 1×10^7 pfu) and incubated at 37 ^{o}C for 30 minutes, before adding to 250 ml of pre-warmed NZYCM in a 1 litre flask. The culture was incubated at 37 ^{o}C shaking until clear lysis was observed. The OD_{600} of the culture was monitored every 15 minutes. Once clear lysis had been observed 5 ml of chloroform was added and the culture shaken for a further 10 minutes to ensure complete lysis.

2.3.2.1 Qiagen Lambda Maxi Kit

Bacterial debris was removed from the culture by centrifuging for 20 minutes at 9,000 rpm in a Sorvall GSA rotor at 4 °C. Purification proceeded according to the manufacturer's instructions.

2.3.2.2 Sambrook PEG and CsCl gradient centrifugation

The lysed culture was cooled to room temperature and DNase I and RNase A were added at a concentration of 1 µg/µl, before swirling for 30 minutes at room temperature. NaCl was added to 1M and the culture incubated on ice for 1 hour. Bacterial debris was removed by centrifuging for 20 minutes at 9,000 rpm in a Sorvall GSA rotor at 4 °C. PEG 6000 at 10% w/v was added to the supernatant and dissolved slowly on a magnetic stirrer. The culture was then cooled on ice before precipitating overnight at 4 ^{o}C. Precipitated phage was retrieved by centrifugation for 20 minutes at 9,000 rpm in a Sorvall GSA rotor at 4 °C. The supernatant was discarded and the phage pellet thoroughly resuspended in 4 ml SM buffer by slow shaking in a desktop shaker. 4 ml of chloroform was added to extract PEG and cell debris from the phage suspension. The solution was mixed thoroughly before centrifugation at 4,500 rpm for 20 minutes. The aqueous phase containing the phage was recovered. This was repeated four times to ensure thorough PEG extraction. 0.75 g of caesium chloride (CsCl) was added per ml of phage preparation and dissolved by inverting several times. The phage preparation was then transferred into 3.9 ml Beckman Quick-Seal centrifuge tubes, with any gap between liquid and neck of tube filled with isopycnic CsCl solution. Tubes were heat sealed and ultra centrifuged at 100,000 rpm for 4 hours, followed by 60,000 rpm for 4 hours in a Beckman Optima TLX bench top ultracentrifuge using a TLN-100 near vertical tube rotor. The phage band was carefully removed by puncturing the side of the tubes with a 21 gauge needle and a 2 ml syringe. The phage DNA was transferred to 1.5 ml eppendorfs and 50 µl of 1 x SET (1% SDS, 1 mM EDTA, 10 mM Tris pH 8) and 0.5 µl Proteinase K (20 mg/ml) were added per 500 µl of DNA before incubating at 50 ^{o}C for 1 hour. The DNA was cooled to room temperature and diluted with 3 volumes of $T_{10}E_1N_{100}$.

Phenol/chloroform extraction was used to remove protein debris. 2 volumes of absolute ethanol were added to precipitate the DNA followed by centrifugation at 13,000 rpm for 20 minutes in a Sorvall SM24 rotor at 4 ^{o}C. The pellet was finally suspended in 150 µl of $T_{10}E_1$ and concentration of the phage DNA was determined.

2.3.3 Packaging into phage particles

Recombinant lambda phages were generated using Giga Pack Gold III packaging extract (Stratagene, USA). Ligation reactions using digested λJG3J1 and λSV054 DNA and insert were packaged according to the manufacturer's instructions.

2.3.4 Phage titre

Serial, ten fold dilutions of phage were made in SM buffer. 100 µl of each phage dilution was added to 3.5 ml of NZYCM top agar (heated in microwave and cooled to 45 ^{o}C) and inverted several times before pouring out onto LB plates. The plates are then rocked to ensure an even layer is produced. The plates were allowed to set before incubated upside down at 37 ^{o}C overnight. The resulting plaques were counted and phage titres determined.

2.3.5 Phage Amplification

2.3.5.1 Plate Lysate

100 µl of plating cell bacteria UT5600 was mixed with between 1 x 10^4 to 1 x 10^6 pfu of phage in SM buffer. The plating cell/phage mix was added to 3.5 ml of NZYCM top agar (heated in microwave and cooled to 45 ^{o}C) and inverted several times before pouring out onto LB plates. The plates are then rocked to ensure an even layer is produced.

The plates were allowed to set before incubation upside down at 37 ^{o}C overnight until the phages have spread out over the plate. 5 ml SM buffer was added to plate and incubated at 37 ^{o}C for several hours with intermittent swirling. The SM buffer now containing diffused bacteriophage was removed and filter sterilised with a 0.45 µm Acrodisc (Pall, UK).

2.3.5.2 Liquid Culture

10 µl of plating cell bacteria C600 was added to 20 ml NZYCM and allowed to grow at 37 ^{o}C to an OD_{600} of 0.5. 300 µl of the bacterial culture was added to 1 x 10^{6} pfu of pre-warmed bacteriophage library and incubated at 37 ^{o}C for 30 minutes to allow phage binding. The bacteria/phage mix was then added to 2.7 ml of NZYCM and incubated at 37 ^{o}C shaking until lysis. Large bacterial debris was pelleted by centrifugation at 5,000 rpm for 5 minutes in Sorvall SM24 rotor. The supernatant was filter-sterilised with a 0.45 µm Acrodisc (Pall, UK).

2.3.6 Selection

200 µl of plating cell bacteria UT5600 was mixed with 10^{8} pfu of unselected phage library and grown at room temperature with shaking in LB/kanamycin, to an OD_{600} of 0.1. IPTG was then added to a final concentration of 0.1 mM to induce NTR expression. At OD_{600} 0.5, 1 ml of the culture was added to 4 ml of pre-warmed LB/kanamycin containing 0.1 mM IPTG, 62.5 mM Tris pH 7.5 and CB1954 at final concentrations of 100, 200 and 300 µM. After shaking for 15 minutes at 37 ^{o}C, 5 ml of each culture was added to 45 ml fresh, pre-warmed LB to dilute out CB1954. The 50 ml culture was centrifuged at 2,500 rpm for 5 minutes at room temperature to pellet bacteria.

The pellet was resuspended in 5 ml LB and incubated for 1 hour, to allow lysogens induced by the prodrug exposure to enter lysis. Remaining bacteria and debris were removed by centrifugation, followed by filter sterilisation through a 0.45 µm Acrodisc (Pall, UK), to recover the released bacteriophage in the flow through.

2.3.7 Lysogen Generation

200 µl of the plating cell bacteria was mixed with 10^8 pfu phage stock and grown overnight at room temperature with shaking in LB/kanamycin. At OD_{600} 0.5, the culture was diluted 10,000 fold and 100 µl spread onto LB agar plates containing 50 mM Tris pH 7.5 and 30 µg/ml kanamycin. Plates were incubated overnight at 37 ^{o}C for colony growth. Each colony represents an individual lysogen.

2.3.8 Replica Plating

Individual lysogens were grown in 96 well plates for 24 hours at 37 ^{o}C in LB/kanamycin. Resulting clones were replica-plated using a 48-pin metal plate onto freshly prepared LB/kanamycin agar plates containing 50 mM Tris (pH 7.5), 0.1 mM IPTG and a range of CB1954 concentrations. The plates were incubated at 37 ^{o}C; the growth of each clone was examined and photographed.

2.3.9 Colony Forming and IC_{50} Assays

Either representative phages after selection (mixed with 200 µl plating cells) or individual lysogens were grown to OD_{600} of 0.1. NTR expression was then induced by adding IPTG to a final concentration of 0.1 mM. The culture was allowed to grow to OD_{600} of 0.5 and diluted 10,000 fold. CB1954 sensitivity was determined by plating out 100 µl of culture onto freshly prepared LB/kanamycin agar plates containing 50 mM Tris (pH 7.5), 0.1 mM IPTG and a range of CB1954 concentrations. The plates were incubated at 37 ^{o}C overnight, and the numbers of colonies on each plate counted. The plating efficiency at each prodrug concentration was calculated as a percentage of the number of colonies obtained in the absence of prodrug. IC_{50} of individual lysogens (prodrug concentration required for 50% reduction in colony number) were estimated by interpolation.

2.4 PROTEIN ANALYSIS

2.4.1 Bradford Assay

Bradford assays in Chapters 6 were performed using Biorad Bradford reagent (Biorad, UK). The Bradford reagent was diluted 1 in 5 with deionised water and filtered with an Acrodisc with a 0.45 µm pore size (Pall, UK). 180 µl was added to wells in a 96 well Falcon flat bottomed plate containing 20 µl of 0-20 µg dilutions of 1 mg/ml bovine serum albumin (BSA) diluted in the same buffer as the protein being measured. The plate was incubated for 10 minutes at room temperature and then the absorbance at 595 nm was determined using a Wallac Victor 1420 plate reader (Perkin Elmer, Italy (Formerly Wallac, Finland)). Protein concentration was calculated from a standard curve of the known diluted BSA standards (Bradford 1976).

Bradford Assays in Chapter 5 were performed using Sigma Bradford Reagent (Sigma-Aldrich, UK). Standard curves were prepared from a BSA stock 1 mg/ml using a range from 0-10 µg. Each standard and sample was made up in 500 µl deionised water, to this 500 µl of Bradford reagent was added. The samples/standards were thoroughly mixed and left for 10 minutes before reading at 595 nm on a Uvikon 923 spectrophotometer (Kontron).

2.4.2 SDS PAGE Gel Electrophoresis

SDS PAGE polyacrylamide gels usually consisted of a 12% resolving gel and a 5% stacking gel. Gels were all made fresh in the Biorad apparatus (Biorad, UK), with 30% acrylamide mix (37.5:1 acrylamide/bisacrylamide ratio), 10% Ammonium persulphate (0.1g in 1 ml) made fresh and TEMED which was always added last. See Table 2.3 for details. The resolving gel was poured; a thin layer of butanol/water was overlayed and the gel was then left to set for approximately 10 minutes. The layer of butanol/water was removed and the stacking gel poured and a comb for the wells added. The gel was left to set for approximately 1 hour.

Solution components	12% resolving gel (10 ml)	5% stacking gel (4 ml)
H_20	3.3 ml	2.7 ml
30% acrylamide mix	4 ml	670 µl
1.5 M Tris (pH 8.8)	2.5 ml	-
1.0 M Tris (pH 6.8)	-	500 µl
10% SDS	100 µl	40 µl
10% APS	100 µl	40 µl
TEMED	10 µl	6 µl

Table 2.3 Reagents of an SDS PAGE gel

2.4.3 Western Blotting

Proteins were transferred from a polyacrylamide gel to a nitrocellulose membrane (Biotrace, UK) by means of a semi-dry blotting tank (Biometra, USA) running at 100 volts for 1-2 hours. Following transfer, membranes were blocked in 5% non-fat milk protein (made up in PBS-Tween (0.1% Tween 20 in PBS) for 1 hour with agitation. Primary antibody was diluted according to the manufacturer's guidelines in 10 ml of 5% milk protein and sealed in a 50 ml screw cap tube (Sartstedt Limited, UK) with the nitrocellulose membrane. The tube was incubated at room temperature on a 3D rotary shaker for 2 hour after which time the membrane was removed and washed 3 times over 30 minutes in PBS-Tween. The secondary antibody was diluted and used as for the primary antibody.

Immobilon Western Detection Reagents were used for detection. This was carried out according to the manufacturer's protocol (Millipore Corporation, USA). Kodak X-OMAT AR 8 x 10 inch film was cut to size and exposed for times between 10 seconds and 1 minute. Exposed radiographs were developed in a Kodak X-O-graph developer.

2.5 TISSUE CULTURE

2.5.1 Cell lines

The cell lines used throughout this thesis are shown in Table 2.4

Cell Line	Origin	Reference
SKOV3	Ovarian carcinoma	(Fogh *et al.* 1977)
HEK 293	Human embryonic kidney expressing Ad5 E1	(Graham *et al.* 1977)
HER 911	Human embryonic retinoblast	(Fallaux *et al.* 1998)

Table 2.4 Human cell Lines used for this study

2.5.2 Routine tissue culture

Cells were grown in a Galaxy R humidified incubator (RS Biotech, UK) at 37 °C with 5% CO_2. All cell lines were maintained in Dulbecco's Modified Eagles Medium (DMEM) (Gibco, UK), containing 10% Foetal Bovine Serum (FBS), 2 mM Glutamine, and 20 mM HEPES. Cell lines were routinely grown in 75 cm^2 tissue culture flasks (Iwaki, Japan) containing 20 ml medium.

Cells were passaged before reaching confluence by removing medium, washing cells in 5 ml Dulbecco's phosphate buffered saline (without Ca^+ or Mg^+), and incubated in 2 ml trypsin EDTA (1 mM) until cells detached. Cells were collected in 10 ml medium containing 10% FBS to inhibit trypsin, counted, and either diluted 1:10 for maintenance of live cells or used for experimental purposes.

2.5.3 Cell counting

10 µl of cell suspension was mixed with 10 µl of Trypan blue (5 mg/ml). 10 µl of this was pipetted into a chamber of a Hycor KOVA Glasstic® Slide 10 with grid cell counter (Hycor Biomedical Inc, USA). Individual cells were counted on the grid. The cell concentration was calculated using the following formula:

$$number\ of\ cells\ \ per\ ml = number\ of\ cells\ in\ 10\ small\ grid\ squares\ \text{x}\ 9000$$

2.5.4 Cryogenic storage of cell lines

To freeze cells for long term storage, cells were grown to approximately 75% confluence, trypsinised as usual, and re suspended in 10 ml medium. Cells were transferred to a 15 ml Falcon tube and centrifuged at 1,000 rpm for 5 minutes (Beckman GS-6R bench top centrifuge). The supernatant was decanted, and the pellet resuspended in 1 ml ice cold FBS containing 10% (v/v) DMSO. Cells were transferred into cryovials (Nunc), and frozen to -80 °C at 1 °C per hour overnight in an isopropanol containing Cryofreezing Container (Nalgene, UK). Cells were then transferred to the vapour phase of liquid nitrogen storage tank.

Cells revived from long term storage were quickly defrosted in a 37 °C water bath, followed by the drop wise addition of 10 ml pre warmed medium. Cells were then centrifuged at 1,000 rpm for 5 minutes, medium decanted, and cells were resuspended in fresh medium and transferred to tissue culture flasks.

2.6 MICROSCOPY

A Zeiss Axiovert 25 inverted microscope was used for all phase-contrast and fluorescence microscopy using 5x, 10x, 20x, and 40x objectives with 21x, 42x, 84x, and 168x overall magnification. Pictures were taken using a Spot camera and processed using Spot Advanced software (Diagnostic Instruments, USA).

CHAPTER 3: GENERATION AND CB1954 PRODRUG SELECTION OF THREE SMALL LIBRARIES OF NTR MUTANTS

3.1 INTRODUCTION

The aim of this chapter is to determine whether mutations at several residues around the active site improve the efficiency of CB1954 activation. Two small libraries will be constructed with mutations at adjacent sites S40/T41 and E165/G166 and a third library with mutations at a single site K14. All possible nucleotide conditions will be incorporated at each targeted codon in the libraries, allowing any amino acid to be incorporated, this will be denoted as * throughout this chapter.

3.1.1 Library S40*/T41* ± N71S

S40 and T41 are residues which lie deep within the active site cavity. These residues have previously been mutated individually; mutations at either residue gave improvements over WT. At residue S40 alanine, glycine and threonine showed improvement and at T41, leucine and glycine. T41L N71S has been generated as a double mutant which is 12-fold better than WT. This library will allow comparison of the remaining T41 amino acid combinations with N71S and examine S40 and T41 combinations alone and in the context of N71S.

3.1.2 Library E165*/G166* ± N71S

Residues E165 and G166 have previously been mutated individually. No single mutations at either E165 or G166 were recovered with activity close to or better than WT. Glutamate is a large residue close to the FMN at the active site, while glycine has no side chain. It was considered possible that varying both residues simultaneously might allow improved combinations of amino acid residues to be discovered.

3.1.3 Library K14*

K14-HAs never previously been mutated and gives two hydrogen bonds to FMN. The rationale behind mutating this residue is that other residues that interact with FMN such as N71S give good mutants and therefore it is possible that mutations at K14 could also improve catalysis.

A PDB image showing each residue selected for mutation in these libraries is shown in Figure 3.1.

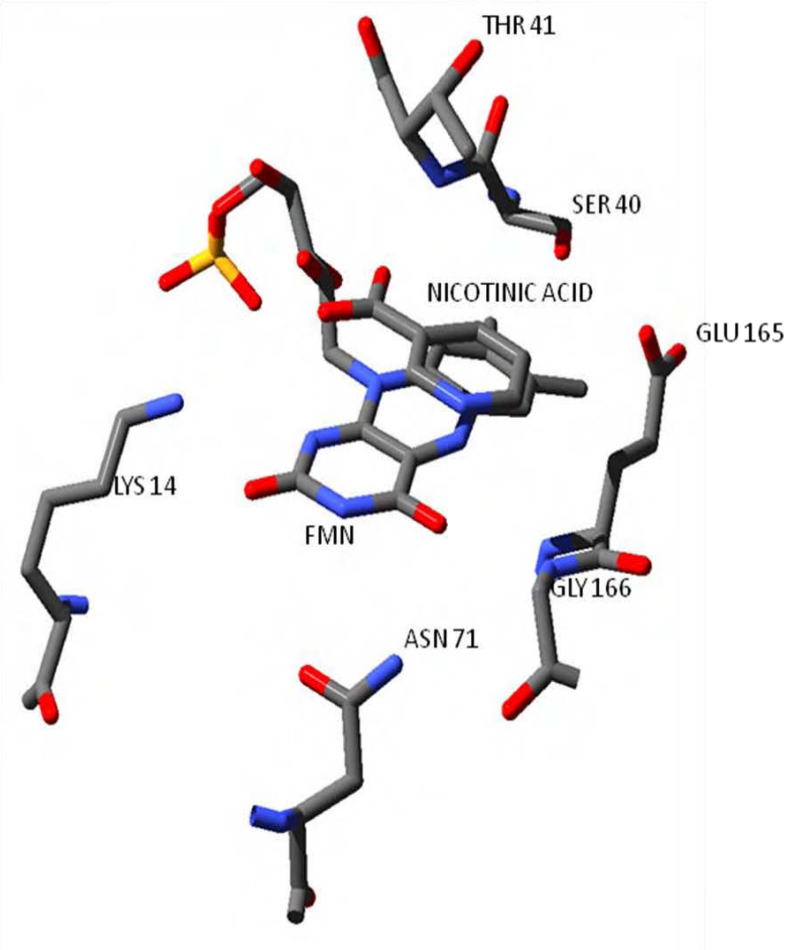

Figure 3.1 Relative positions of residues K14, S40, T41, N71, E165 and G166 in the active site cavity of WT NTR enzyme
The structures shown are of the NTR/nicotinic acid complex. The FMN cofactor, nicotinic acid ligand and selected residues are represented in stick form. This image was created from the 1ICR crystal structure using SWISS PDB Viewer 4.0.1 and rendered in Pov-Ray V3.6.

These libraries will be put through a powerful selection system to quickly select best variants (Guise *et al.* 2007). The three libraries are relatively small, so would expect efficient selection within a small number of cycles. Three cycles of selection were chosen.

3.2 MATERIALS AND METHODS

3.2.1 Library Construction

3.2.1.1 PCR mutagenesis

Two templates were used for PCR to give limited diversity at residue N71. λ lysogens encoding WT *NfsB* NTR and mutant N71S were streaked onto LB plates containing a fresh lawn of *E. coli* UT5600. Resulting lysis areas were picked with a tip and used as templates for PCR mutagenesis using Taq DNA polymerase.

Mutations were introduced using PCR primers that amplify overlapping left and right ends of the NTR gene. Randomisations at residues of interest were achieved using degenerate PCR primers CG4041, CG165166 and SH1B (see section 2.2.1). Resulting PCR products were resolved by agarose gel electrophoresis to confirm DNA fragments of the correct size were amplified. PCR products of the correct size were purified using Roche High Pure PCR Product Purification Kit. Left and right ends were subsequently combined in a second PCR reaction using flanking primers (see Figures 3.2-3.4). A total of 50 ng of template DNA was used at a 1:1 molar ratio of left and right ends. Full length PCR products were resolved by agarose gel electrophoresis to confirm DNA fragments of the correct size were amplified and purified using Qiagen QIA-Quick Gel Extraction Kit.

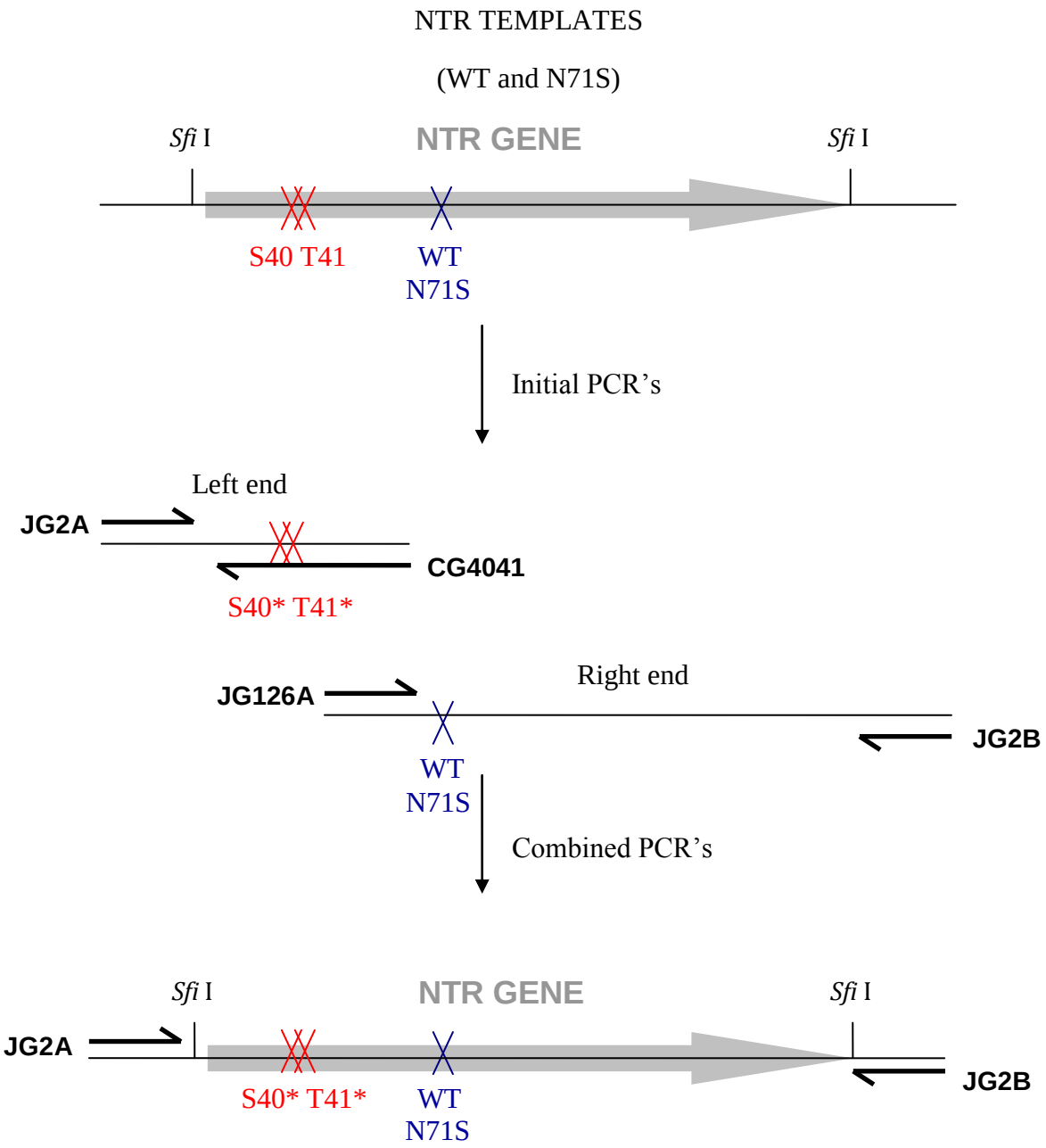

Figure 3.2 S40*/T41* ± N71S Library - schematic of degenerate PCR's making left and right ends of NTR gene and joining together by combined PCR's
Degenerate primer CG4041 was used to randomise residues S40 and T41. Left end fragment made using primers JG2A and CG4041 gave a fragment size of 392 bp and the right hand fragment made using primers JG126A and JG2B gave a fragment size of 715 bp. Primers CG4041 and JG126A overlap by 24 nucleotides, allowing the left and right fragments to be joined in a second PCR step using the flanking primers JG2A and JG2B. Note this schematic is not to scale

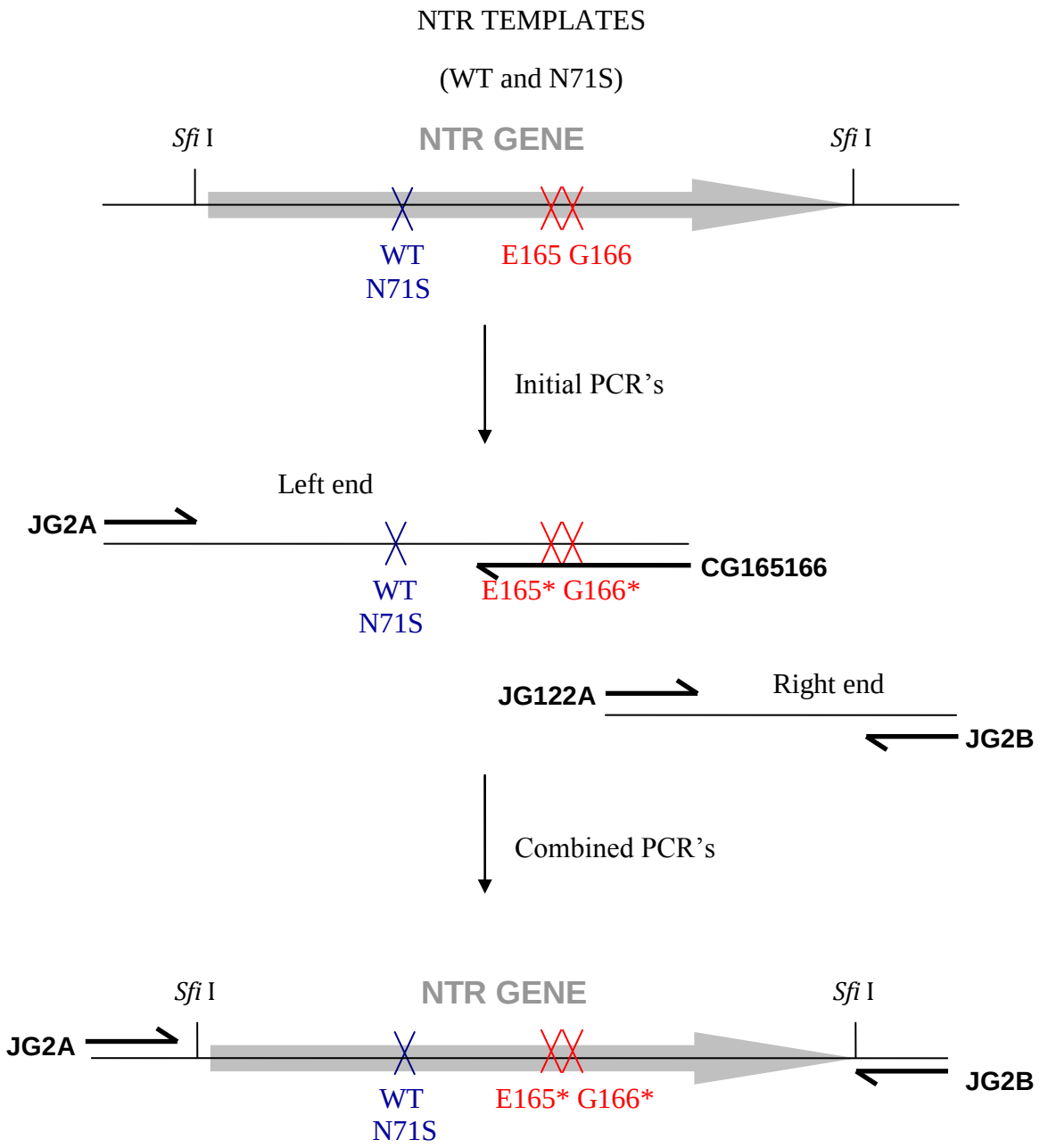

Figure 3.3 E165*/G166* ± N71S Library - schematic of degenerate PCR's making left and right ends of NTR gene and joining together by combined PCR's
Degenerate primer CG165166 was used to randomise residues E165 and G166. Left end fragment made using primers JG2A and CG165166 gave a fragment size of 774 bp and the right hand fragment made using primers JG122A and JG2B gave a fragment size of 342 bp. Primers CG165166 and JG122A overlap by 24 nucleotides, allowing the left and right fragments to be joined in a second PCR step using the flanking primers JG2A and JG2B. Note this schematic is not to scale

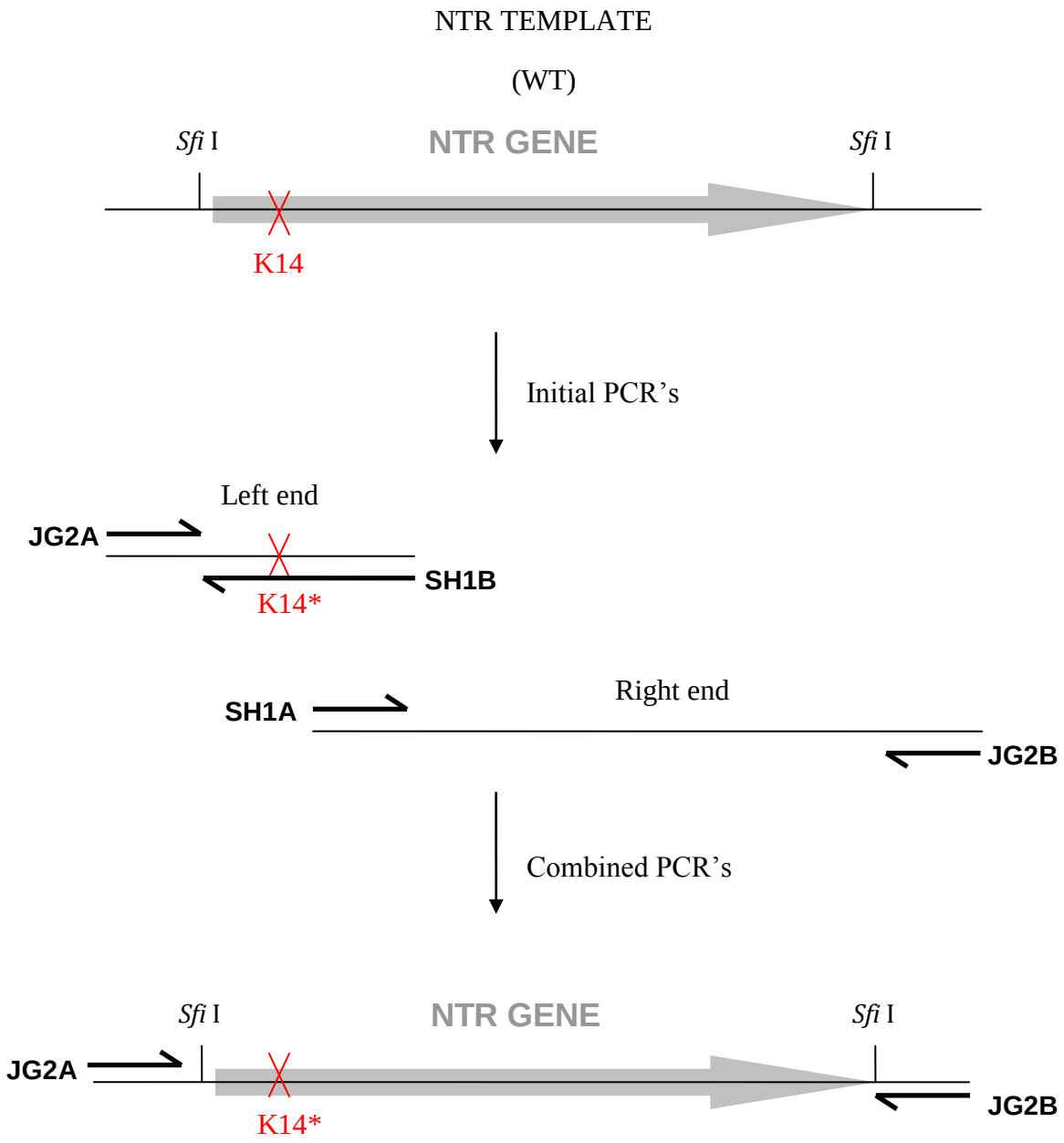

Figure 3.4 K14* Library - schematic of degenerate PCR's making left and right ends of NTR gene and joining together by combined PCR's
Degenerate primer SH1B was used to randomise residue K14. Left end fragment made using primers JG2A and SH1B gave a fragment size of 324 bp and the right hand fragment made using primers SH1A and JG2B gave a fragment size of 790 bp. Primers SH1B and SH1A overlap by 21 nucleotides allowing the left and right fragments to be joined in a second PCR step using the flanking primers JG2A and JG2B. Note this schematic is not to scale

3.2.1.2 Insertion of NTR PCR products into lambda vector

PCR fragments for each small library, encoding full length mutant NTR genes were digested with *Sfi* I restriction enzyme and the digestion products resolved by agarose gel electrophoresis. NTR genes of 751 bp were excised from preparative agarose gels and purified using Qiagen QIA-Quick Gel Extraction Kit. The DNA concentrations for each library of digested PCR's were measured using PicoGreen.

The three libraries (S40* T41*, E165* G166* and K14*) were prepared by ligating 67.5 ng of NTR with 1.5 µg λ DNA vector (λJG3J1 stock was grown, purified and digested with *Sfi* I and *Pac* I by Dr Chris Guise and given as a generous gift for this work). See Figure 3.5 for a schematic of λJG3J1 vector. The ligation reaction was cleaned and concentrated by ethanol precipitation and resuspended in 2 µl $T_{10}E_1$. Resulting ligation products were packaged into phage particles using Stratagene Giga pack III gold packaging extract and plaque titres determined by plating out onto an *E. coli* UT5600 lawn.

3.2.1.3 Library Amplification

100 µl of each phage library stock was amplified by plate lysate and 4 ml of amplified stock was retrieved for each library.

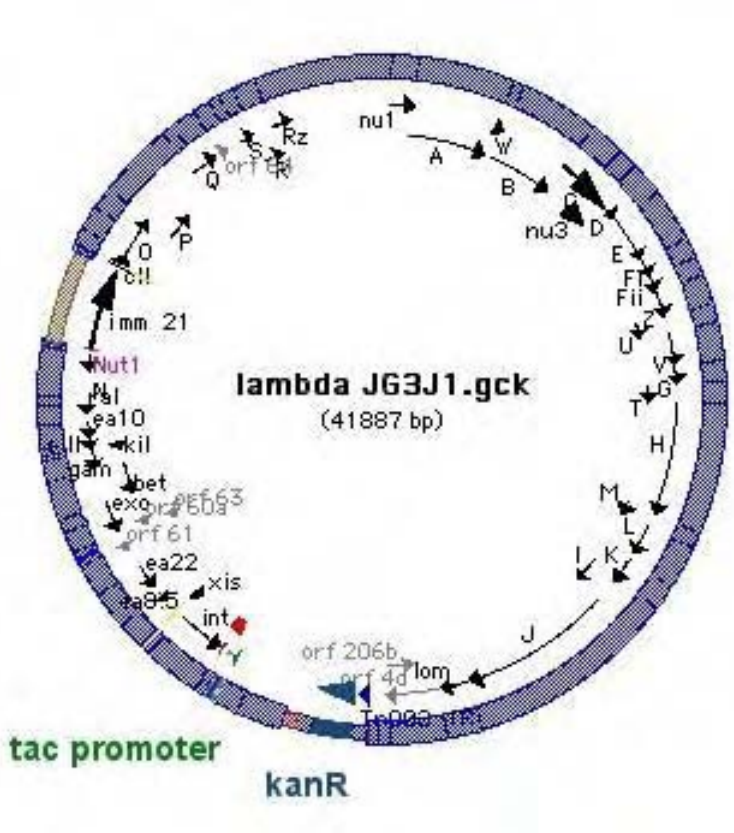

Figure 3.5 Schematic diagram of λ phage construct λJG3J1
Showing *Sfi* I and *Pac* I sites. The two *Sfi* I sites have non-matching 3 base pair sticky ends, thus ensuring that the inserts are in the correct orientation. A *Pac* I site sits between the two *Sfi* I sites and can be used as a failsafe. Any vector not digested with *Sfi* I will be *Pac* I digested preventing carryover of empty vector

3.3 RESULTS

3.3.1 Validation of PCR mutagenesis

For each library PCR fragments were determined by agarose gel electrophoresis (see Figure 3.6). Bands of the correct size were the major products of each PCR reaction and were purified by gel purification.

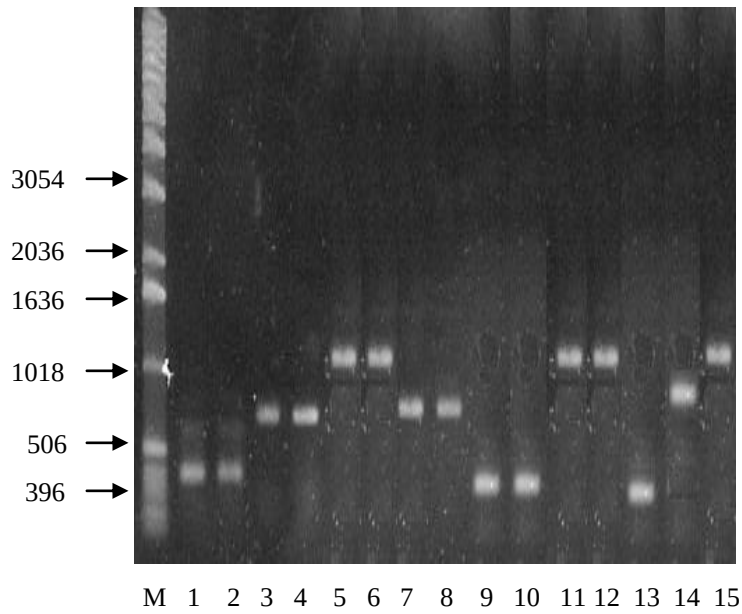

Figure 3.6 Agarose gel for PCR products from initial right and left end NTR PCR products and combined PCR's
Total PCR products amplified from NTR. PCR products were run on a 0.7% agarose gel. M = Marker 1 kb plus ladder, Lanes 1-2 library S40/T41 left end PCR using alternative templates WT and N71S respectively (392 bp), Lane 3-4 library S40/T41 right end PCR using alternative templates WT and N71S respectively (715 bp) Lanes 5-6 combined PCR for library S40/T41 WT and N71S respectively (1093 bp). Lane 7-8 library E165/G166 left end PCR using alternative templates WT and N71S respectively (774 bp), Lane 9-10 library E165/G166 right end PCR using alternative templates WT and N71S respectively (342 bp) Lanes 11-12 combined PCR for library E165/G166 WT and N71S respectively (1093 bp). Lanes 13 library K14 left end PCR (324 bp), Lane 14 library K14 right end PCR (790 bp) and Lane 15 combined PCR for library K14 (1093 bp)

3.3.2 Preparation of PCR product for inserting in lambda vector

The PCR fragments encoding libraries of full length mutant NTR genes were digested with *Sfi* I and the digestion products were resolved by agarose gel electrophoresis (see Figure 3.7).

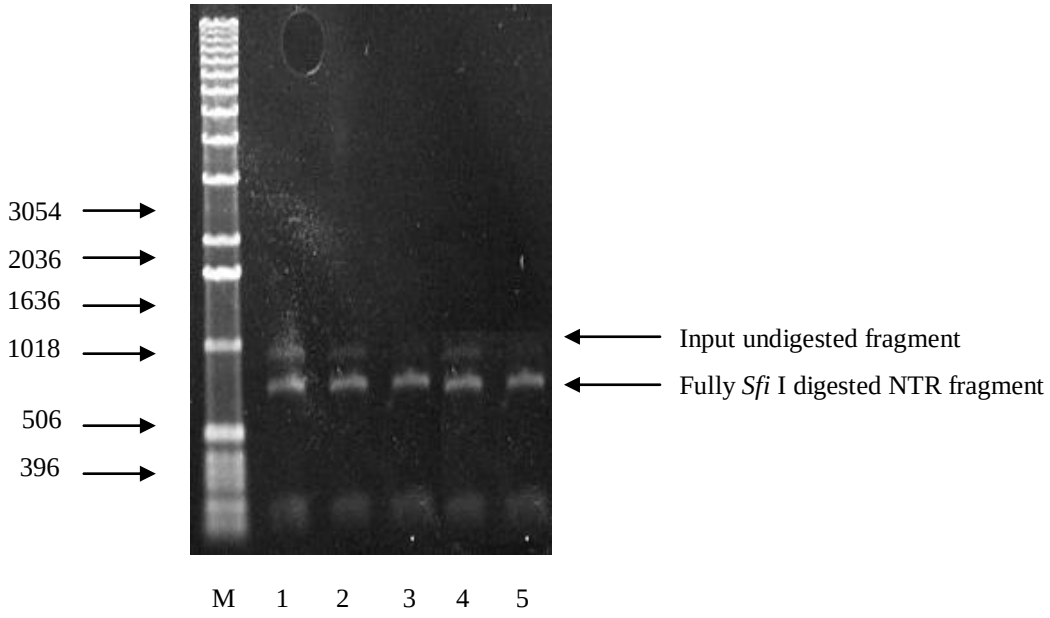

Figure 3.7 Agarose gel of *Sfi* I digested NTR PCR products
PCR products were run on a 0.7% agarose gel. M = Marker 1 kb plus ladder, Lanes 1-2 *Sfi* I digested S40/T41 WT and N71S fragments. Lane 3-4 *Sfi* I digested E165/G166 WT and N71S fragments. Lanes 5 *Sfi* I digested K14 fragment. Two *Sfi* I sites cut for each fragment. Bands of the expected size were excised from a preparative gel. Digestion failed to go to completion as shown on the above gel, therefore the major 751 bp band containing NTR was purified prior to ligation into a lambda vector

3.3.3 Insertion of PCR products into lambda vector

The DNA concentration for each digested PCR was measured and 67.5 ng of each was ligated with 1.5 µg of λJG3J1 λ DNA vector (λJG3J1 stock was grown, purified and digested with *Sfi* I and *Pac* I by Dr Chris Guise and given as a generous gift for this work). See Figure 3.5 for a schematic of λJG3J1 vector. The resulting ligation reaction was cleaned by ethanol precipitation and resuspended in 2 µl $T_{10}E_1$.

3.3.4 Phage production and amplification

The resulting ligation products were packaged into phage particles and plaque titres for each library were determined by plating out a series of 10-fold dilutions onto *E. coli* UT5600 cells. Phage yields were between $1.1 \times 10^5 – 3.5 \times 10^5$ (see Table 3.1). These yields range from 13-5469 times greater than calculated numbers of possible nucleotide variants. Therefore each of the three small libraries should contain the majority of variants. However the process of generating bacterial lysogens from lambda phage, as required for selection method, is only 1% efficient (the remainder of infected cells enter the lytic cycle. Therefore, in order to maintain maximum diversity when selecting from lysogens each library was amplified by plate lysate (100 µl of each phage library stock was amplified by making a plate lysate and 4 ml of amplified stock retrieved), giving $8.4 \times 10^8 – 7.2 \times 10^9$ phage particles as shown in Table 3.1.

Template	Initial phage yield of independent clones (pfu total)	Number of possible nucleotide variants	Phage yield after amplification (pfu total)
S40/T41	1.2×10^5	8.2×10^3	8.4×10^8
E165/G166	1.1×10^5	8.2×10^3	7.2×10^9
K14	3.5×10^5	6.4×10^1	1.7×10^9

Table 3.1 Initial phage yield of independent clones, number of possible nucleotide variants and phage yield after amplification by plate lysate

PCR was used to check NTR presence, 5 phage plaques from each small library were analysed, using primers JG2A and JG2B. NTR presence is indicated by a band of 1093 bp and empty vector a band of 385 bp (see Figure 3.8).

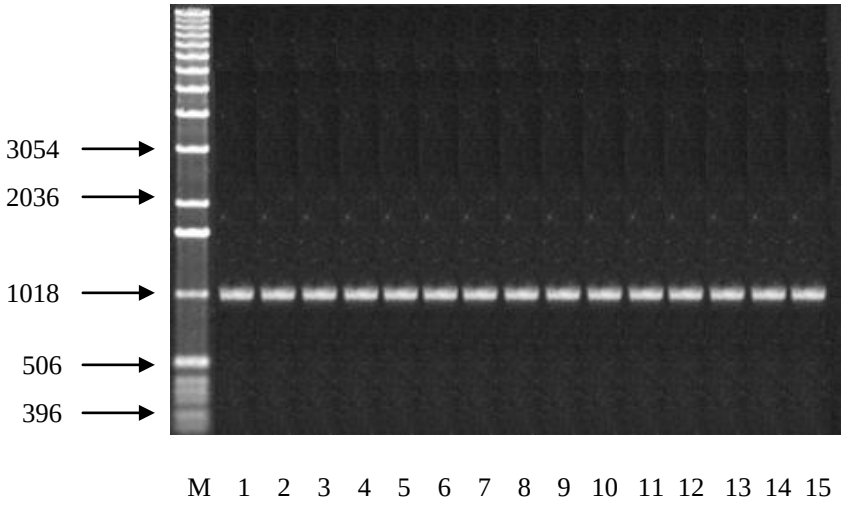

Figure 3.8 Agarose gel of PCR products, for confirmation of NTR presence in individual clones from the three libraries
Primers JG2A and JG2B were used for each PCR, the PCR products were run on 0.7% agarose gel. M = Marker 1 kb plus ladder, Lanes 1-5 S40/T41, Lanes 6-10 E165/G166 and Lanes 11-15 K14. NTR insert PCR's a band at 1093 bp and no NTR insert (empty vector) a band at 385 bp

3.3.5 Selection

1 x 10^8 pfu of phage were infected into 2 x 10^8 UT5600 cells to generate lysogens for selection. Kanamycin was used to select for lysogens. Aliquots of mid log culture were exposed to CB1954 for 15 minutes, diluted and pelleted before being resuspended in prodrug free media as described in Materials and Methods. Phage released after 1 hour were separated from lysogens by 0.2 µm filtration. See Figure 3.9 for a flow diagram of selection.

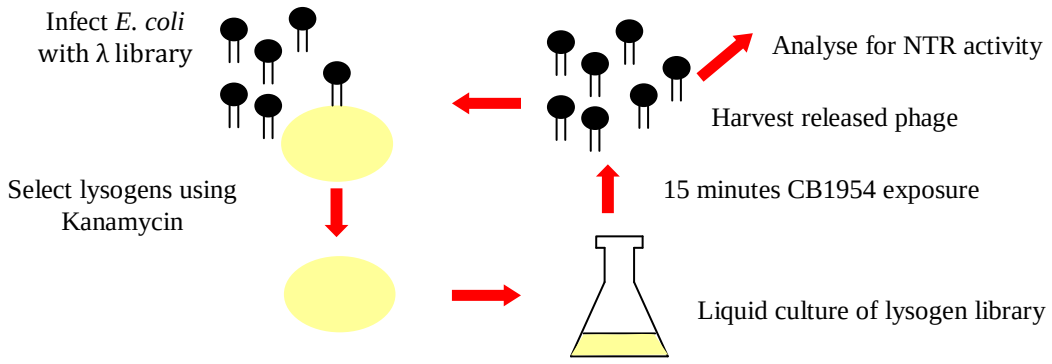

Figure 3.9 Flow diagram representing stages of selection
Diagram adapted from Guise *et al.* 2007

The concentration of CB1954 prodrug required for effective selection of each library was hard to predict. Guise *et al.* 2007 examined the prodrug dose required to activate lysogens into lytic cycle. It was found that too low a concentration of prodrug gave no selection. However if too high a concentration was used the most improved mutants were not selected. See Figure 2b Guise *et al.* 2007 for further details. Several concentrations of CB1954 prodrug were used in parallel for selection in order to allow comparison of the effect of selection at different prodrug concentrations. The best conditions for each library after three rounds of selection were examined further by testing individual clones for CB1954 sensitivity. Clones with the most sensitivity were sequenced and IC_{50} assays used to determine the concentration of CB1954 required for 50% reduction in plating efficiency. Results for each library are discussed below.

3.3.6 Library S40*/T41* ± N71S

3.3.6.1 Monitoring population sensitivity of the library under selection

The effect of selection was monitored using lysogen colony forming assays. Mid log lysogenic cultures were split into four parallel aliquots and exposed to 0, 100, 200 and 300 μM CB1954. After three rounds of selection with no CB1954 almost all of the lysogens were resistant when plated out on agar plates containing CB1954 up to a concentration of 200 μM. Therefore the vast majority of lysogens were less sensitive than wild type; with wild type NTR having an IC_{50} of 150 μM.

After three rounds of selection using 100 µM CB1954, colony forming efficiency was just below 50% at 25 µM CB1954, dropping further to approximately 30% at 150-200 µM. This shows enrichment of improved prodrug sensitive clones to about 50% of the selected library, while the remainder were relatively insensitive. After selection with 200 µM and 300 µM CB1954, a reduction in colony forming efficiency was seen relative to the library selected with no CB1954, but to a lesser extent than selection at 100 µM CB1954 (see Figure 3.10).

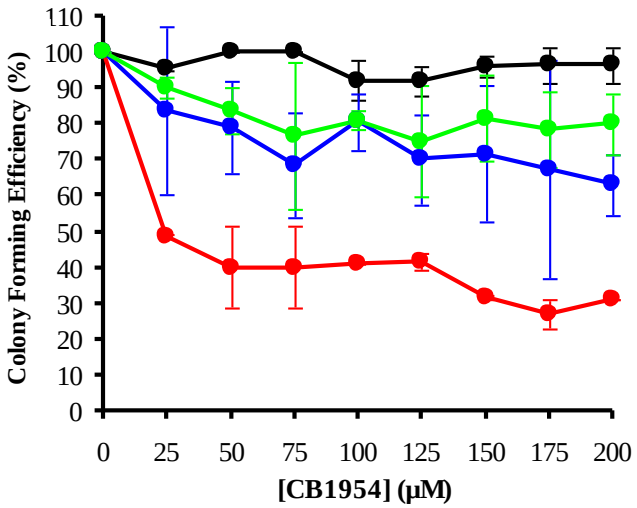

Figure 3.10 Dose Response curves for colony forming assay for S40*/T41* ± N71S library in *E. coli* UT5600
After three rounds of selection with 0, 100, 200 and 300 µM CB1954, mid log lysogenic cultures of the whole library were plated out onto agar plates containing a range of CB1954 concentrations. The colonies were counted after overnight growth and the number compared to colony growth on plates with no prodrug. No CB1954 selection (black), 100 µM CB1954 selection (red), 200 µM selection (blue) and 300 µM selection (green)

3.3.6.2 Screening CB1954 sensitivity of individual clones from selected library

180 individual lysogen colonies were picked from the library following selection with 100 μM CB1954. Individual cultures were grow overnight in 96 well plates and replica plated onto agar plates containing a range of CB1954 concentrations up to 200 μM. All lambda lysogens showed strong growth in the absence of CB1954. Two lysogens disappeared at 25 μM showing sensitivity to this concentration, thirty one at 35 μM, twelve at 50 μM, fourteen at 100 μM and a further eight at 200 μM. The remaining lysogens were not sensitive to the highest CB1954 concentration (see Figure 3.11).

The NTR genes from sixty seven lysogens that were unable to grow at low CB1954 concentrations were sequenced. Seventeen different amino acid changes were observed as well as many silent mutations. Table 3.2 shows these amino acid changes and details of their codon usage. Fifty two of the sequenced NTR genes had amino acid substitutions only at targeted residues, leaving fifteen NTR genes with one or more amino acid substitutions at non-targeted residues.

IC_{50} assays were used to determine the concentration of CB1954 required for 50% reduction in plating efficiency. This assay is more stringent than replica plating, showing the survival of individual bacteria. IC_{50} assays are quantitative with individual colonies being counted as opposed to just scoring the presence or absence of bacterial growth for a mass of bacterial cells. A single IC_{50} assay was performed for a single representive clone for each of the thirteen amino acid sequences. Low IC_{50} values indicate a greater sensitivity to CB1954 due to either more efficient catalysis of CB1954 activation or higher levels of NTR enzyme expression.

N71S and WT were the starting points for this library; these have IC_{50} values of 62 μM and 150 μM CB1954 respectively. Nine mutants had IC_{50} values less than 25 μM. The most sensitive mutant was T41G N71S (IC_{50} value 8 μM) followed by T41L N71S (IC_{50} value 14 μM) (see Figure 3.12 and Table 3.2).

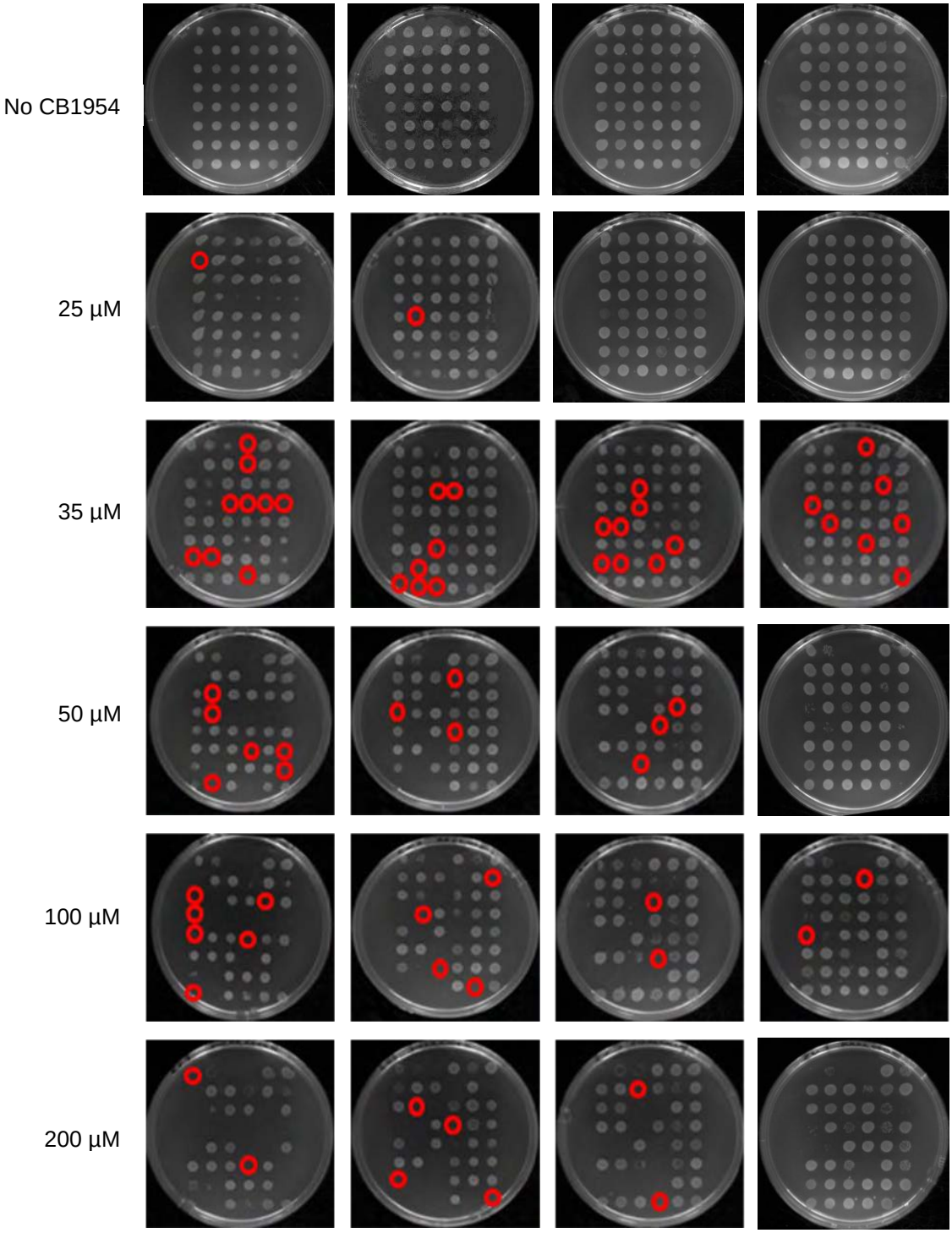

Figure 3.11 Replica plating of individual lysogens after three rounds of selection using 100 µM CB1954 for the S40*/T41* ± N71S library

Individual lysogen colonies were picked and grown overnight in 96 well plates and replica plated onto agar plates containing a range of CB1954 concentrations. Following overnight growth each mass of bacterial cells were scored as present or absent at each CB1954 concentration. CB1954 concentrations of 0 µM, 25 µM, 35 µM, 50 µM, 100 µM and 200 µM concentrations were used. The first three lysogens on top left of each plate are controls WT, F124N and T41L N71S respectively. Red circles indicate the lowest concentration at which growth was absent

Amino acid substitution	Codon Usage	Number of mutants	Replica Plating Prodrug susceptibility (μM CB1954)	IC_{50} Prodrug susceptibility (μM CB1954)
T41L N71S	L = CTT (22) L = TTA (3) L = CTC (1)	26	35-50	14
N71S	S = AGT	14	100	62
T41G N71S	G = GGA (1) G = GGT (2)	3	25	8
S40T T41L N71S	T = ACG L = CTA (1) T = ACC L = CTT (2)	3	35	17
T41I N71S	I = ATT (1) I = ATA (2)	3	50	24
T41N N71S	N = AAT (1) N = AAC (1)	2	35	14
T41N N71S E197K	N = AAT K = AAA	2	35-50	18
N71S F124L	L = CTC	2	35	24
T41Q V69A N71S	Q = CAA A = GCA	2	35-50	16
S43A N71S	A = GCC	2	100	54
N71S K119E	E = GAA	2	100	65
T41L S43A N71S	L = CTT A = GCC	1	35	14
T41Q N71S	Q = CAG	1	35	21
T41H S43A N71S	H = CAC A = GCC	1	50	38
S40T T41L V69L N71S	T = ACA L = CTC L = CTG	1	100	45
K9N N71S	N = AAC	1	100	-
E55V N71S V93I	V = GTA I = ATC	1	100	-

Table 3.2 Summary of NTR mutants isolated for the S40*/T41* ± N71S library
Shown are the amino acid substitution in each NTR clone, the codon usage, the number of mutants that had each mutation, prodrug susceptibility based on replica plating indicating the lowest concentration of CB1954 required to prevent growth of an individual clone and IC_{50} assay indicating the lowest concentration of CB1954 required for a 50% reduction in colony growth. All sequenced NTR's had AGT at residue N71 which corresponds with the original start template. Targeted amino acid substitutions are shown in black and non-targeted amino acid substitutions in blue

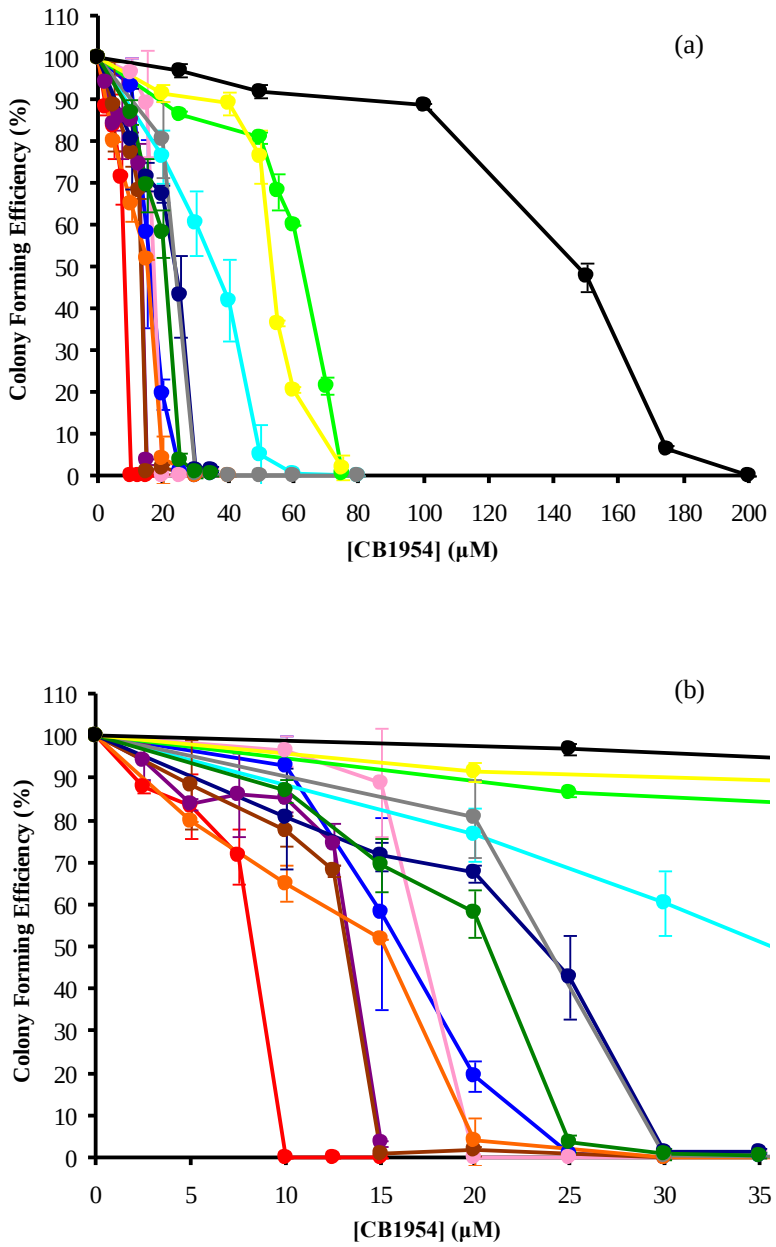

Figure 3.12 CB1954 IC_{50} assays of selected lysogens from S40*/T41* ± N71S library in UT5600 cells

Lysogenic cultures of individual clones were spread onto agar plates containing a range of CB1954 concentrations. The number of colonies were counted after overnight growth and compared to colony growth on plates with no prodrug. T41G N71S (red), T41L N71S (purple), T41N N71S (brown), T41Q V96A N71S (orange), S40T T41L N71S (blue), T41N N71S E197K (pink), T41Q N71S (dark green), T41I N71S (grey), N71S F124L (dark blue), T41H S43A N71S (cyan), S43A N71S (yellow), N71S (green), WT (black) (a) shows detail T41H S43A N7S, N71S, S43A N71S and WT (b) shows detail T41G N71S, T41L N71S, T41N N71S, T41Q V96A N71S, S40T T41L N71S, T41N N71S E197K, T41Q N71S, T41I N71S, N71S F124L

3.3.7 Library E165*/G166* ± N71S

3.3.7.1 Monitoring population sensitivity of the library under selection

As with the previous library the effect of selection was monitored using lysogen colony forming assays. Three rounds of selection were performed using 100 µM, 200 µM and 300 µM CB1954 and with no CB1954 as a control. After three rounds of selection with no CB1954 almost all of the lysogens were resistant when plated out on agar plates containing CB1954 up to a concentration of 200 µM.

After three rounds of selection with 100 µM CB1954 25% of the lysogenic library were sensitive to 125 µM CB1954, showing some enrichment for active NTR's. After selection with 200 µM CB1954 10% of the library was sensitive to 125 µM CB1954 showing an intermediate level of enrichment. Selection with 300 µM CB1954 showed no enrichment of the library with most lysogens still resistant to 200 µM CB1954 (see Figure 3.1).

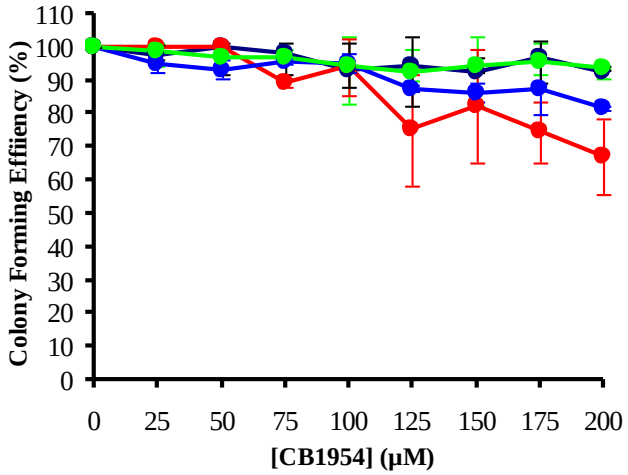

Figure 3.13 Dose Response curves for colony forming assay for E165*/G166* ± N71S library in UT5600 cells
After three rounds of selection with 0, 100, 200 and 300 µM CB1954, mid log lysogenic cultures of the whole library were plated out onto agar plates containing a range of CB1954 concentrations. The number of colonies were counted after overnight growth and compared to colony growth on plates with no prodrug. No CB1954 selection (black), 100 µM CB1954 selection (red), 200 µM selection (blue) and 300 µM selection (green)

3.3.7.2 Screening CB1954 sensitivity of individual clones from selected library

180 individual lysogen colonies were picked from the library after three rounds of selection with 100 μM CB1954. Individual cultures were grown overnight in 96 well plates and replica plated onto agar plates containing a range of CB1954 concentrations up to 200 μM. All the lambda lysogens tested showed strong growth in the absence of CB1954 and at CB1954 concentrations of 25 μM and 35 μM. One lysogen disappeared at 50 μM showing sensitivity to this concentration, twelve at 100 μM and forty six at 200 μM. The remaining lysogens were not sensitive to the highest CB1954 concentration (see Figure 3.14).

The NTR genes from fifty nine lysogens that failed to grow between 50-200 μM CB1954 were sequenced. No mutations were seen at either residue 165 or 166. The vast majority of NTR genes had either no mutation (being WT) or a single mutation at N71 to serine which was the starting templates. Seven other random mutants were observed, only one of these N71S A125T showed any improvement relative to N71S and WT (see Table 3.3).

An IC_{50} assay was performed for mutant N71S A125T. WT and N71S are also demonstrated for comparison (see Figure 3.15 and Table 3.3).

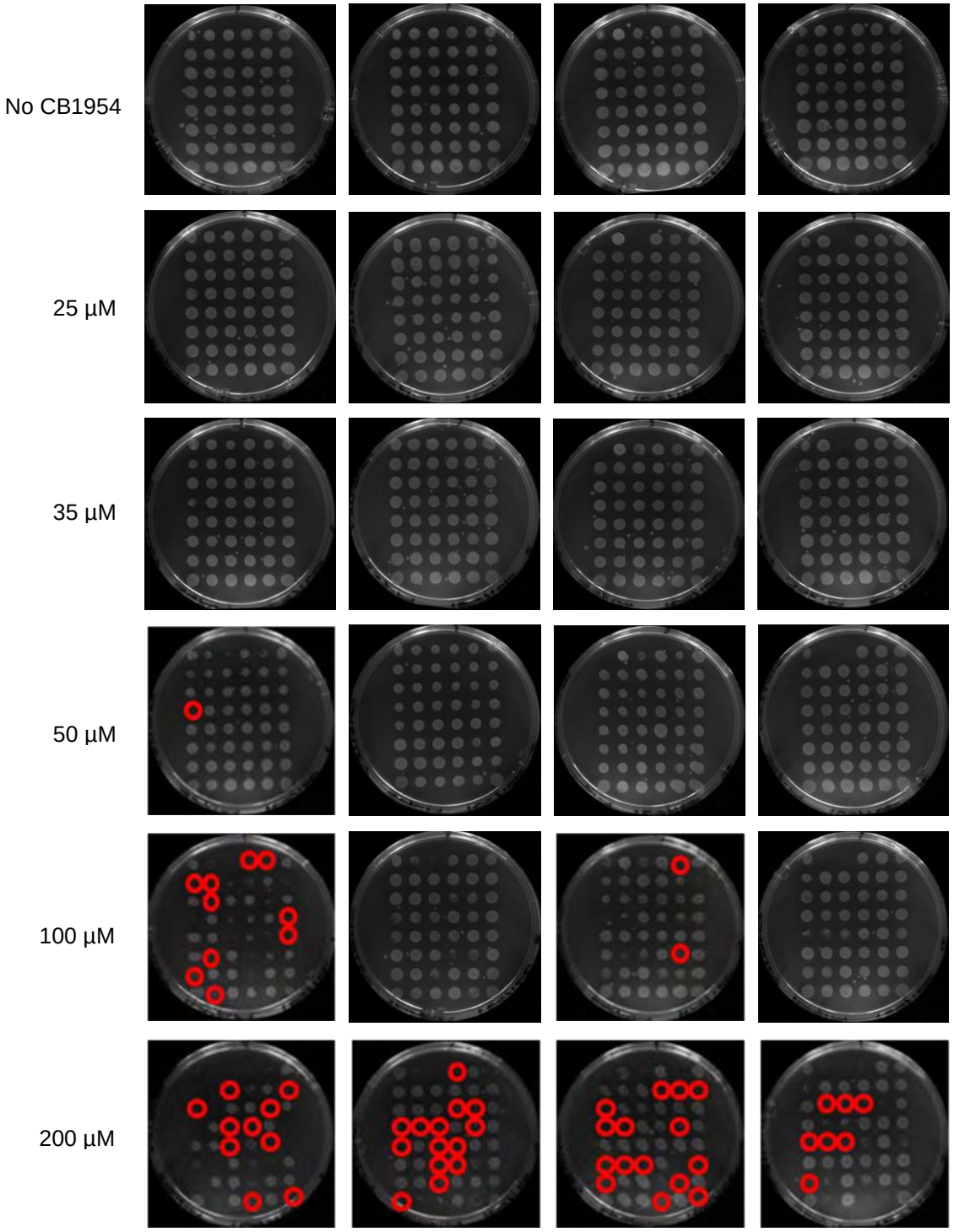

Figure 3.14 Replica plating of individual lysogens after three rounds of selection using 100 µM CB1954 for E165*/G166* ± N71S library

Individual lysogen colonies were picked and grown overnight in 96 well plates and replica plated onto agar plates containing a range of CB1954 concentrations. Following overnight growth each mass of bacterial cells were scored as present or absent at each CB1954 concentration. CB1954 concentrations of 0 µM, 25 µM, 35 µM, 50 µM, 100 µM and 200 µM concentrations were used. The first three lysogens on top left of each plate are controls WT, F124N and T41L N71S respectively. Red circles indicate the lowest concentration at which growth was absent

Amino acid substitution	Codon Usage	Number of mutants	Replica Plating Prodrug susceptibility (μM CB1954)	IC_{50} Prodrug susceptibility (μM CB1954)
WT	-	31	200	150
N71S	S = AGT	20	100	62
T13A	A = GCT	2	100	-
N71S A125T	T = ACT	1	50	18
P111S	S = TCG	1	100	-
H194R	R = CGC	1	100	-
Y69H	H = CAC	1	200	-
F70S N71S	R = CGC S = TCC	1	200	-
K21R	R = AGA	1	200	-

Table 3.3 Summary of NTR mutants isolated for E165*/G166* ± N71S library
Shown are the amino acid substitution in each NTR clone, the codon usage, the number of mutants that had each mutation, prodrug susceptibility by replica plating indicating the lowest concentration of CB1954 required to prevent growth of an individual clone and IC_{50} assay indicating the lowest concentration of CB1954 required for a 50% reduction in colony growth. Targeted amino acid substitutions are shown in black and non-targeted amino acid substitutions in blue

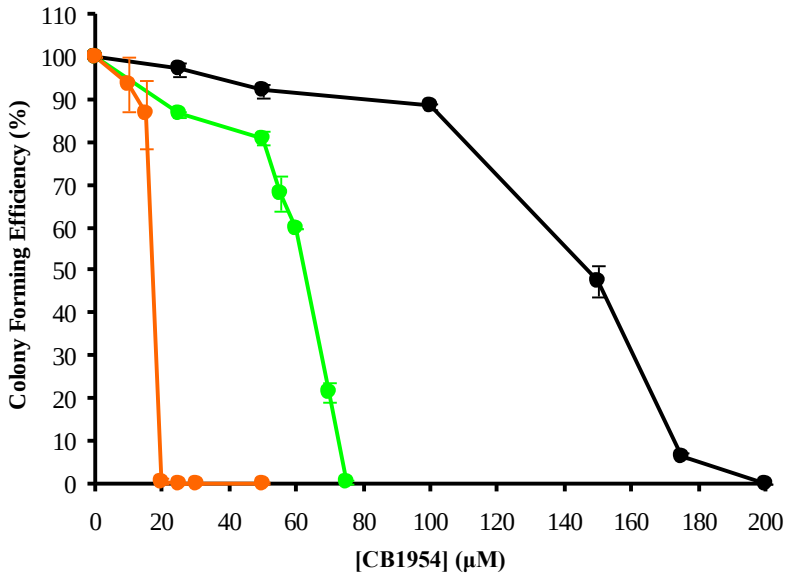

Figure 3.15 CB1954 IC_{50} assays of selected lysogens from E165*/G166* ± N71S library in UT5600 cells
Lysogenic cultures of individual clones were spread onto agar plates containing a range of CB1954 concentrations. The number of colonies were counted after overnight growth and compared to colony growth on plates with no prodrug. N71S A125T (orange), N71S (green) and WT (black)

3.3.8 Library K14*

3.3.8.1 Monitoring population sensitivity of the library under selection

The K14* library was also monitored using lysogen colony forming assays. Following three rounds of selection with no CB1954 almost all of the lysogens were resistant when plated out on agar plates containing CB1954 up to a concentration of 200 µM.

After three rounds of selection with 100 µM CB1954 no enrichment of the library was observed with most lysogens resistant to 200 µM CB1954. However after selection with 200 µM CB1954 25% of the library was sensitive to 175 µM CB1954 and with 300 µM CB1954 15% of the library was sensitive to 175 µM (see Figure 3.16).

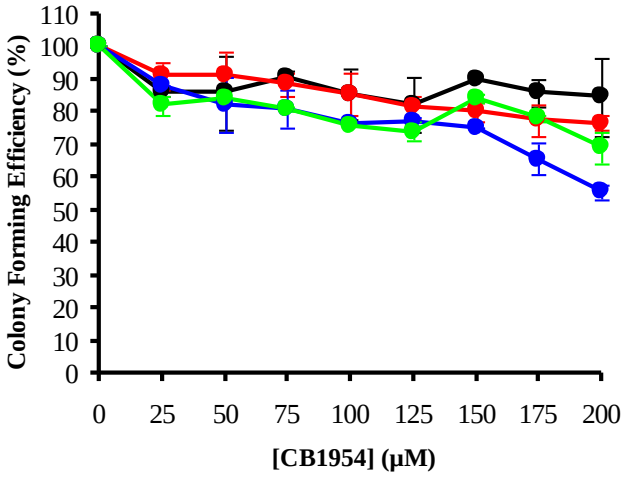

Figure 3.16 Dose Response curves for colony forming assay for K14* library in UT5600 cells
After three rounds of selection with 0, 100, 200 and 300 µM CB1954, mid log lysogenic cultures of the whole library were plated out onto agar plates containing a range of CB1954 concentrations. The number of colonies were counted after overnight growth and compared to colony growth on plates with no prodrug. No CB1954 selection (black), 100 µM CB1954 selection (red), 200 µM selection (blue) and 300 µM selection (green)

3.3.8.2 Screening CB1954 sensitivity of individual clones from selected library

180 individual lysogen colonies were picked from the library after three rounds of selection with 200 µM CB1954. Individual cultures were grow overnight in 96 well plates and replica plated onto agar plates containing a range of CB1954 concentrations up to 200 µM. All lambda lysogens showed strong growth in the absence of CB1954 and at CB1954 concentrations of 25 µM, 35 µM and 50 µM. One lysogen disappeared at 100 µM showing sensitivity to this concentration and twenty eight at 200 µM. The remaining lysogens were not sensitive to the highest CB1954 concentration tested (see Figure 3.17).

The NTR genes from twenty eight lysogens that failed to grow between 100-200 μM CB1954 were sequenced. Seven mutants showed substitutions at residue K14. Two were stop codons and five had additions at a residue downstream resulting in a frame-shift. Many silent mutations were seen, along with a few other random mutations. None of the mutations sequenced gave any distinctive advantage over WT (see Table 3.4).

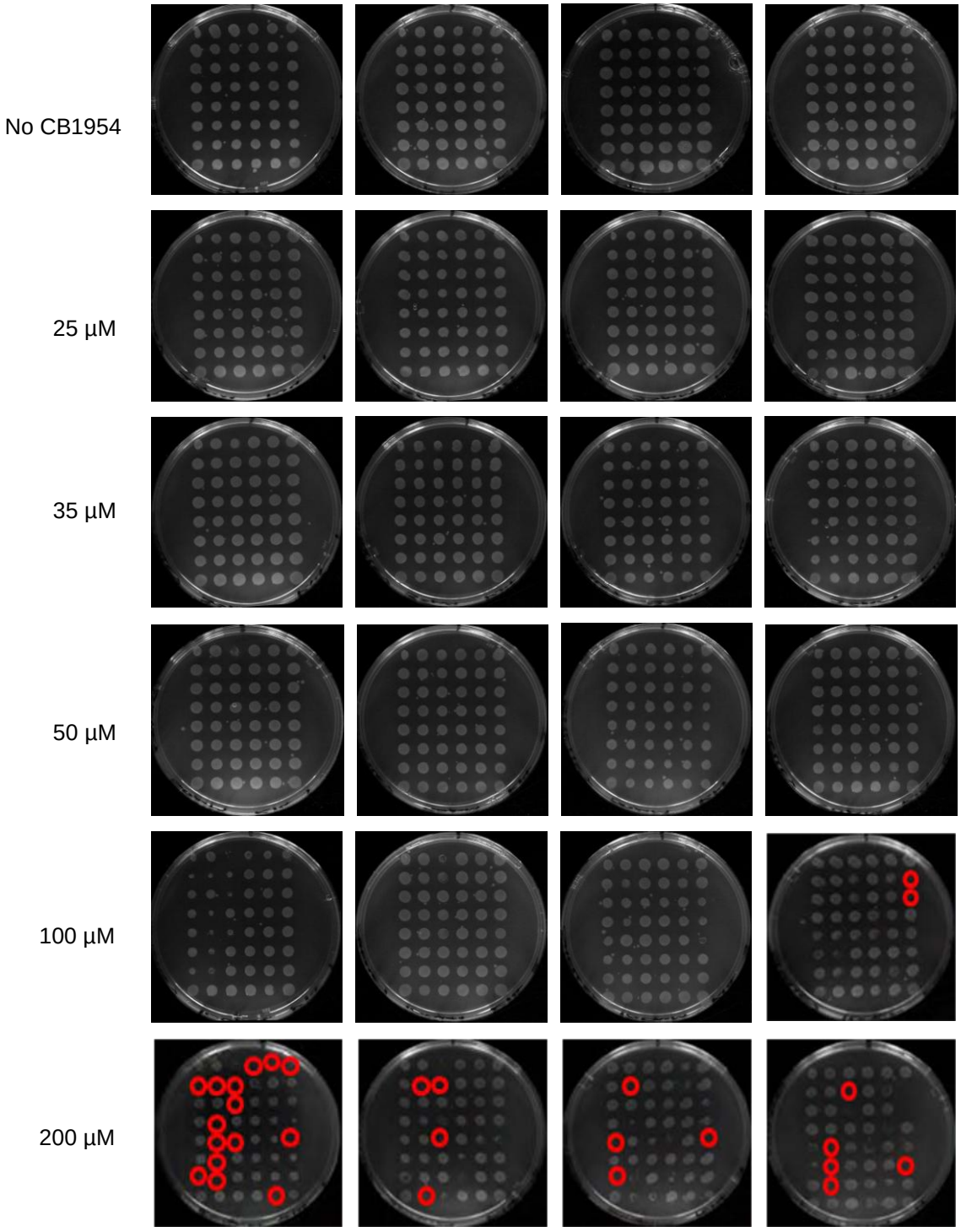

Figure 3.17 Replica plating of individual lysogens after three rounds of selection using 200 µM CB1954 for K14* library

Individual lysogen colonies were picked and grow overnight in 96 well plates and replica plated onto agar plates containing a range of CB1954 concentrations. Following overnight growth each mass of bacterial cells were scored as present or absent at each CB1954 concentration. CB1954 concentration 0 µM, 25 µM, 35 µM, 50 µM, 100 µM and 200 µM concentrations were used. The first three lysogens on top left of each plate are controls WT, F124N and T41L N71S respectively. Red circles indicate the lowest concentration at which growth was absent

Amino acid substitution	Codon Usage	Number of mutants	Replica Plating Prodrug susceptibility (μM CB1954)
K14 A86	K = AAA A = GCG	13	200
K14 STOP	STOP = TAA	2	200
K14R ADDITION AT P24	R = CGG	3	200
K14 A65T	K = AAA T = ACC	3	100-200
A86	A = GCG	2	200
K14R ADDITION AT P24 A64	R = CGG A = GCC	2	200
V6 A7R K14 A86	V = GTG R = CGC K = AAA A = GCG	1	200
K14 A15P A86	K = AAA P = CCA A = GCG	1	200
WT	-	1	200

Table 3.4 Summary of NTR mutants isolated for K14* library
Shown are the amino acid substitution in each NTR clone, the codon usage, the number of mutants that had each mutation and prodrug susceptibility by replica plating indicating the lowest concentration of CB1954 required to prevent growth of an individual clone. Targeted amino acids are shown in black, single frame-shift additions in red, stop codons in pink and non-targeted amino acids in blue

3.4 DISCUSSION

The basis for this chapter was to generate NTR mutants with improved catalysis for the prodrug CB1954. A PCR based method was utilised for the generation of three small libraries of NTR mutants, where NNN was inserted at each codon targeted for mutation. This allowed complete randomisation, giving all possible codon changes. The PCR products were then cloned into lambda vectors and put through three rounds of selection at three different CB1954 concentrations. Individual clones from the selected phage libraries were analysed for their sensitivity to CB1954, and sequenced to determine any changes in the encoded amino acid.

3.4.1 Library S40*/ T41* ± N71S

This library was cloned and put through three rounds of selection. Colony forming assays showed that selection with 100 μM CB1954 gave best enrichment of this library. 180 lysogens were replica plated onto agar plates containing a range of CB1954 concentrations. The best sixty seven lysogens were sequenced. Seventeen amino acid changes were determined and there codon usages shown. Only four of the lysogens analysed had amino acid substitutions at residue S40. In all four the lysogen serine was changed conservatively to threonine, and all the S40T substitutions also had mutations at T41. At residue T41, forty five lysogens had amino acid substitutions. By far the most abundant was T41L N71S with twenty six mutants giving this amino acid combination. Several clones were N71S alone with no mutations at residues S40 or T41. A few random mutations at other residues were also observed.

The codon usage for each residue was examined. As previously discussed only four lysogens had mutation at residue S40. All four encoded S40T. There are four codons for threonine; three were seen (ACG, ACA and ACC). A further thirteen lysogens sequenced had silent mutations at residue S40. There are six codons for serine four of which were seen (TCA, TCT, TCC and AGT).

Forty six lysogens sequenced had mutations at T41. Three lysogens had silent mutations, one for each of the other three threonine encoding residues (ACA, ACG and ACT). Twenty nine had leucine at this residue. Six codons encode leucine, four of which were observed (CTA, CTT, CTC and TTA). By far the most frequent leucine codon seen was CTT which accounted for twenty two out of the twenty nine lysogens. Four mutants encoded asparagine; both codons were observed (AAC and AAT). A further three encoded glutamine; again both codons were observed (CAA and CAG). Three had glycine; two of the four codons were seen (GGA and GGT). A further three encoded isoleucine; two of the three codons were present (ATT and ATA). Finally one encoded histidine (CAC). The diversity of synonymous codons recovered helps confirm the sequence diversity of the starting library. However the strong preference for the leucine codon CTT could indicate a non-random library. Research by Maloy *et al* has shown that *E. coli* bacteria has a preference for the leucine codon CTG with 55% of residues being this codon, as opposed to CTT with 10% of residues using this codon (Maloy *et al.* 1996). CTG was not shown by any of the sequenced lysogens at residue T41. Codon preference clearly fails to account for CTT being most abundant.

Several mutants recovered had mutations at non-planned residues. In all but one case a single base substitution resulted in the change in amino acid. These would have been introduced by error-prone PCR, due to the use of Taq DNA polymerase. It has been possible to determine the location of unexpected residues relative to the active site by examining NTR's 3D crystal structure. Table 3.5 shows some of the unexpected residues, what affect each specific mutations has on CB1954 activation and there location with NTR's 3D crystal structure. Two residues were of particular interest F124 and S43. Residue F124-HAs previously been extensively examined (Grove *et al.* 2003) with 15 amino acid changes showing improvement relative to phenylalanine. This residue is located within the active site. Phenylalanine is a bulky amino acid that obstructs the active site making it more difficult for CB1954 to bind. Changing phenylalanine to a smaller amino acid such as leucine opens up the space allowing easier binding of the substrate. Residue S43 is also located within the active site. Although serine is a small residue alanine is even smaller being the smallest amino acid possible. This slight shift in amino acid size, could allowing better access for the prodrug CB1954. However when the residue T41 has also been mutated alanine mutation at S43 no longer has an effect. It appears that a mutation at T41 allows optimum confirmation in this region, with neither mutations at residues S40 nor an S43A mutation having a positive effect.

Unexpected mutation	Context	Deduced consequence of untargeted mutation	Comment
E197K	T41N N71S E197K	1.3 fold increase in IC_{50}	Surface residue not expected to improve CB1954 binding
K119E	N71S K199E	1.0 fold increase in IC_{50}	Surface residue not expected to improve CB1954 binding
S43A	S43A N71S T41L S43A N71S	1.2 fold decrease in IC_{50} No difference	Residue S43 is located within the active site. Serine is a small amino acid, however alanine is even smaller. This slight shift in size may allow better access for the prodrug CB1954. However when the residue T41 has also been mutated a mutation to S43A no longer has an effect
V69A/L	T41Q V69A N71S S40T T41L V69L N71S	1.3 fold decrease in IC_{50} 2.7 fold increase in IC_{50}	Surface residue not expected to improve CB1954 binding
F124L	N71S F124L	2.6 fold decrease in IC_{50}	Residue F124 is located within the active site. Phenylalanine is a bulky amino acid; smaller amino acids such as leucine allows more binding space

Table 3.5 Summary of unexpected mutations seen for S40*/T41* library
Shown are unexpected mutations, the context they were seen in, what consequence was deduced from examining the untargeted mutations and any comments. A decrease in IC_{50} indicates increased CB1954 activation; where as an increase in IC_{50} indicates decreased CB1954 activation

IC_{50} values were determined for each mutant; with T41G N71S being the best mutant isolated having an IC_{50} of 8 μM. The most abundant mutation seen was T41L N71S; this mutant has been seen in previous studies and has an IC_{50} of 14 μM. T41N N71S was also a good mutant with an IC_{50} virtually identical to T41L N71S. S40T T41L N71S had an IC_{50} of 17 μM; this indicates that the mutation of residue S40 to threonine was slightly detrimental with the IC_{50} increasing by 3 μM.

Mutations to E197K, K119E and V69L were also detrimental with T41N N71S E197K having an IC_{50} of 18 μM, 4 μM higher than T41N N71S. N71S K119E had an IC_{50} of 65 μM, 3 μM higher than N71S and S40T T41L V69L N71S having an IC_{50} of 45 μM, 28 μM higher than S40T T41L N71S. Alternatively a mutation at residue V96 to alanine gave an improvement in combination with T41 and N71S, with T41Q V69A N71S having an IC_{50} of 16 μM and T41Q N71S having an IC_{50} of 21 μM. This is also the case with S43A N71S improving the IC_{50} by 8 μM compared to N71S alone. However when in combination with T41L and N71S no improvement was seen with the IC_{50} remaining at 14 μM. T41H S43A N71S is also found within this library however it is not possible to determine what effect S43A has on this mutant as T41H N71S wasn't observed. Finally the mutant N71S F124L has an IC_{50} of 24 μM which is lower than N71S at 62 μM and F124L at 40 μM (Grove *et al.* 2003).

In conclusion most mutants analysed did not have mutations at both targeted S40 and T41 positions. Therefore it is possible to conclude that S40 and T41 mutations do not tend to work well together when in combination with N71S. There was a good distribution of mutants with a number of improved mutations achieved at residue T41. T41G N71S was the best mutant determined from this library and is a very promising new mutant, which will be tested further in chapters 5 and 6.

3.4.2 Library E165* /G166* ± N71S

This library was cloned and put through three rounds of selection. Colony forming assays showed that selection at 100 μM CB1954 gave greatest enrichment of this library. 180 lysogens were replica plated onto agar plates containing a range of CB1954 concentrations. The best fifty nine lysogens were sequenced. Only WT and N71S mutants were found as well as a few random mutations. An IC_{50} assay was performed for lysogen N71S A125T and an IC_{50} value of 18 μM determined.

Previous work indicated that all single amino acid substitutions at E165 or G166 were detrimental to CB1954 activation and this work indicates that no combination of substitutions at these two sites can allow efficient CB1954 activation. One random mutation at a non-targeted site was obtained (A125T in the mutant N71S A125T), which appeared improved relative to N71S. N71S A125T is an intriguing mutant, which will be tested further in chapters 5 and 6.

3.4.3 Library K14*

This library was cloned and put through three rounds of selection. Colony forming assays showed that selection at 200 μM CB1954 gave greatest enrichment. 180 lysogens were replica plated onto agar plates containing a range of CB1954 concentrations. The best twenty nine lysogens were sequenced. Only silent mutations were found at residue K14. No IC_{50} assays were performed as no improved mutants were observed.

It is possible to conclude that all single amino acid substitutions at residue K14 were detrimental to CB1954 activation. This correlates with the observation that lysine FMN contact is highly conserved in many FMN flavoproteins. The mutation of some lysine residues in FMN-containing flavoproteins has greatly diminished FMN binding (Watanabe *et al.* 1998).

CHAPTER 4: GENERATION AND CB1954 PRODRUG SELECTION OF A LARGE LIBRARY OF NTR MUTANTS

4.1 INTRODUCTION

Previous work has indicated that the efficiency of CB1954 activation by NTR can be progressively improved by specific changes at 1, 2 and 3 amino acid residues surrounding the active site (Grove *et al.* 2003, Guise *et al.* 2007, Jaberipour *et al.* 2010 and chapter 3 from this thesis). The selection method developed by Guise *et al* and used in chapter 3 potentially allows the isolation of rare improved mutants from even larger libraries (Guise *et al.* 2007). The aim of this chapter was to apply the selection method to a library containing mutations at six residues around the active site and to determine whether still further optimised NTR mutants could be isolated.

A single large library was constructed by a PCR based method combining mutations at T41, N71, R121, F123, F124 and A125. Limited amino acid diversity was incorporated at T41 and N71 with complete randomisation of amino acids at residues R121, F123, F124 and A125. Throughout this chapter * denotes any codon which has been mutated to encode any amino acid (eg: F124*). Residues T41, N71 and F124 have previously been found to be important for the catalytic improvement of NTR. T41L N71S, T41N N71S, T41Q N71S and T41G N71S double mutants were highly beneficial for the reduction of CB1954 therefore these have been used as starting points for this library as well as WT and N71S. Many amino acid changes at F124 have been shown to greatly improve NTR catalysis by allowing greater accessibility to the active site. Inspection of the structure suggests changes to residues around F124 could further improve CB1954 catalysis. A precedent has already been set by a mutation at A125, which showed good improvement over WT when combined with N71S. See Figure 3.15 for IC_{50} curves comparing N71S A125T with N71S and WT NTR.

A PDB image showing each residue for mutation is shown in Figure 4.1

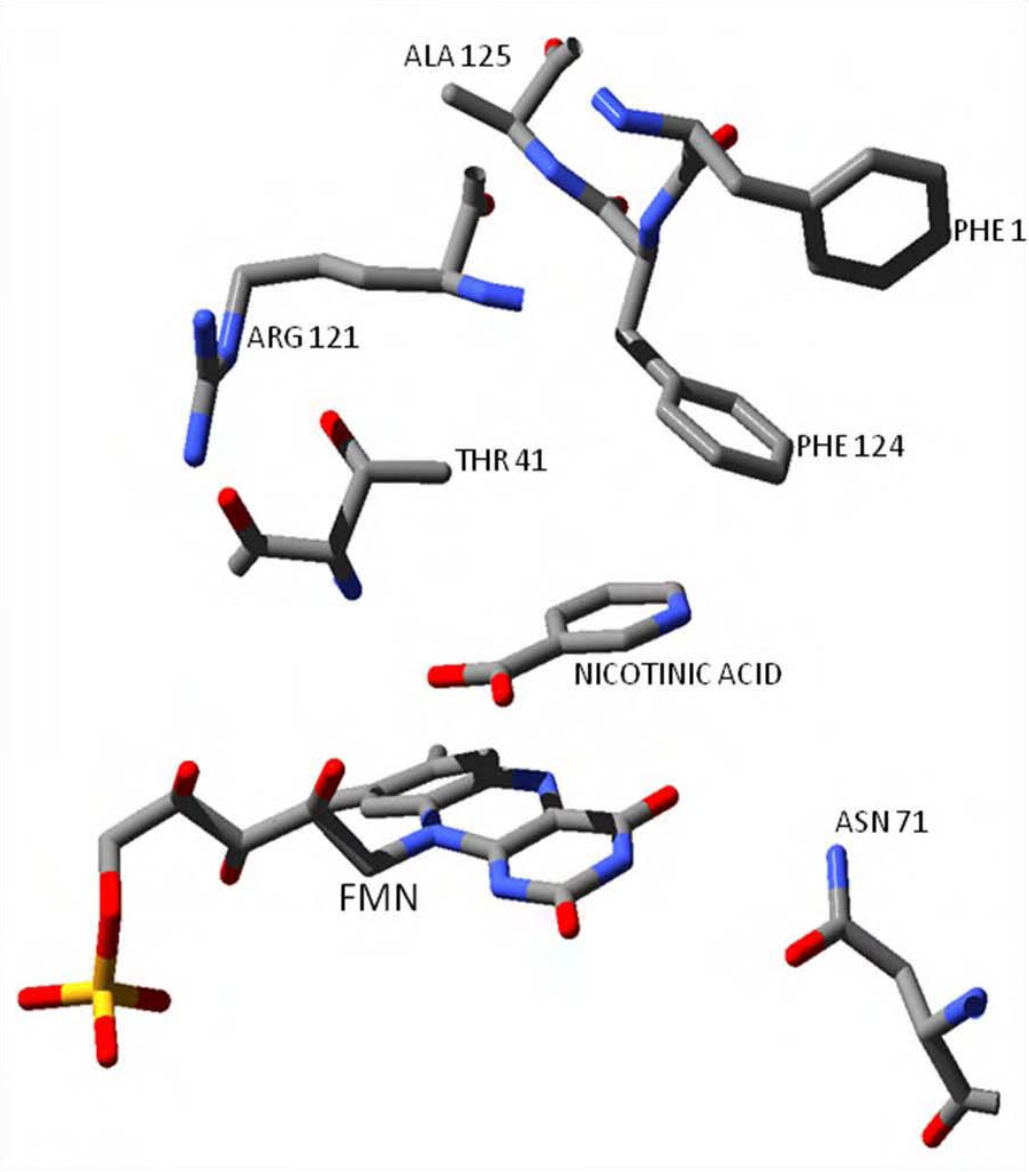

Figure 4.1 Relative positions of residues T41, N71, R121, F123, F124 and A125 in the active site cavity of WT NTR enzyme
The structures shown are of the NTR/nicotinic acid complex. The FMN cofactor, nicotinic acid ligand and selected residues are represented in stick form. This image was created from the 1ICR crystal structure using SWISS PDB Viewer 4.0.1 and rendered in Pov-Ray V3.6.

The three small libraries used in chapter 3 contained a theoretical maximum diversity of 6.4 x 10^1 (64 alternatives at K14), 8.2 x 10^3 ([2 alternative start templates] x [64 alternatives at S40] x [64 alternatives at T41]) and 8.2 x 10^3 ([2 alternative start templates] x [64 alternatives at E165] x [64 alternatives at G166]) different nucleotide sequences including stop codons. The large library selected by Guise *et al* contained a theoretical maximum diversity of 1.1 x 10^6 ([64 alternatives at T41] x [64 alternatives at N71] x [64 alternatives at F124]) + ([64 alternatives at T41] x [64 alternatives at F70] x [64 alternatives at F124]) + ([64 alternatives at S40] x [64 alternatives at N71] x [64 alternatives at F124]) + ([64 alternatives at S40] x [64 alternatives at F70] x [64 alternatives at F124]) disregarding any possible additional random mutations that may arise from the error prone PCR process. However the library generated was somewhat smaller than this, with just 6.8 x 10^5 independent clones (Guise *et al.* 2007). In these previous libraries NNN was incorporated at completely randomised codons however due to the redundancy of the genetic code all possible amino acids can be represented by mutant oligos containing NNS with S being either a C or G. This allowed the reduction of codons from 64 to 32, allowing more residues to be analysed without a big increase to the overall size of the library. Theoretically the large library for this chapter had a maximum diversity of 6.3 x 10^6 possible nucleotide combinations ([6 alternatives start templates] x [32 alternatives at R121] x [32 alternatives at F123] x [32 alternatives at F124] x [32 alternatives at A125]. This equates to 9.6 x 10^5 amino acid combinations and 5.5 x 10^5 full length encoding proteins.

It previously took three rounds to successfully select the S40/T41 ± N71S small library (see chapter 3). Guise *et al* found that with his large library the best mutants were progressively enriched through ten cycles of selection (Guise *et al.* 2007). It was therefore anticipated that 10-20 cycles of selection might be required for this library.

4.2 MATERIALS AND METHODS

4.2.1 Library Construction

4.2.1.1 PCR mutagenesis

The limited diversity at residues T41 and N71 was achieved by using six different templates for PCR, containing WT NTR and the mutants N71S, T41N N71S, T41L N71S, T41G N71S and T41Q N71S. λ lysogens for each were streaked onto LB plates containing a fresh lawn of *E. coli* UT5600. Resulting lysis areas were picked with a tip and used as templates for PCR mutagenesis using Taq DNA polymerase.

As before, mutations were introduced via PCR primers used to amplify overlapping left and right ends of the NTR gene. Randomisation at residues R121, F123, F124 and A125 was achieved using the degenerate PCR primer SH33B (see Figure 4.2). Resulting PCR products were resolved by agarose gel electrophoresis to ensure DNA fragments of the correct size were amplified. PCR products of the correct size were purified using Roche High Pure PCR Product Purification Kit.

Left and right ends were subsequently combined in a second PCR reaction using flanking primers (see Figure 4.3). A total of 50 ng of DNA was used at a 1:1 molar ratio of left and right ends. Full length PCR products were resolved by agarose gel electrophoresis to ensure DNA fragments of the correct size were amplified and purified using Qiagen QIA-Quick Gel Extraction Kit.

10 µl of each PCR product was sequenced to check the diversity of nucleotides at targeted codons.

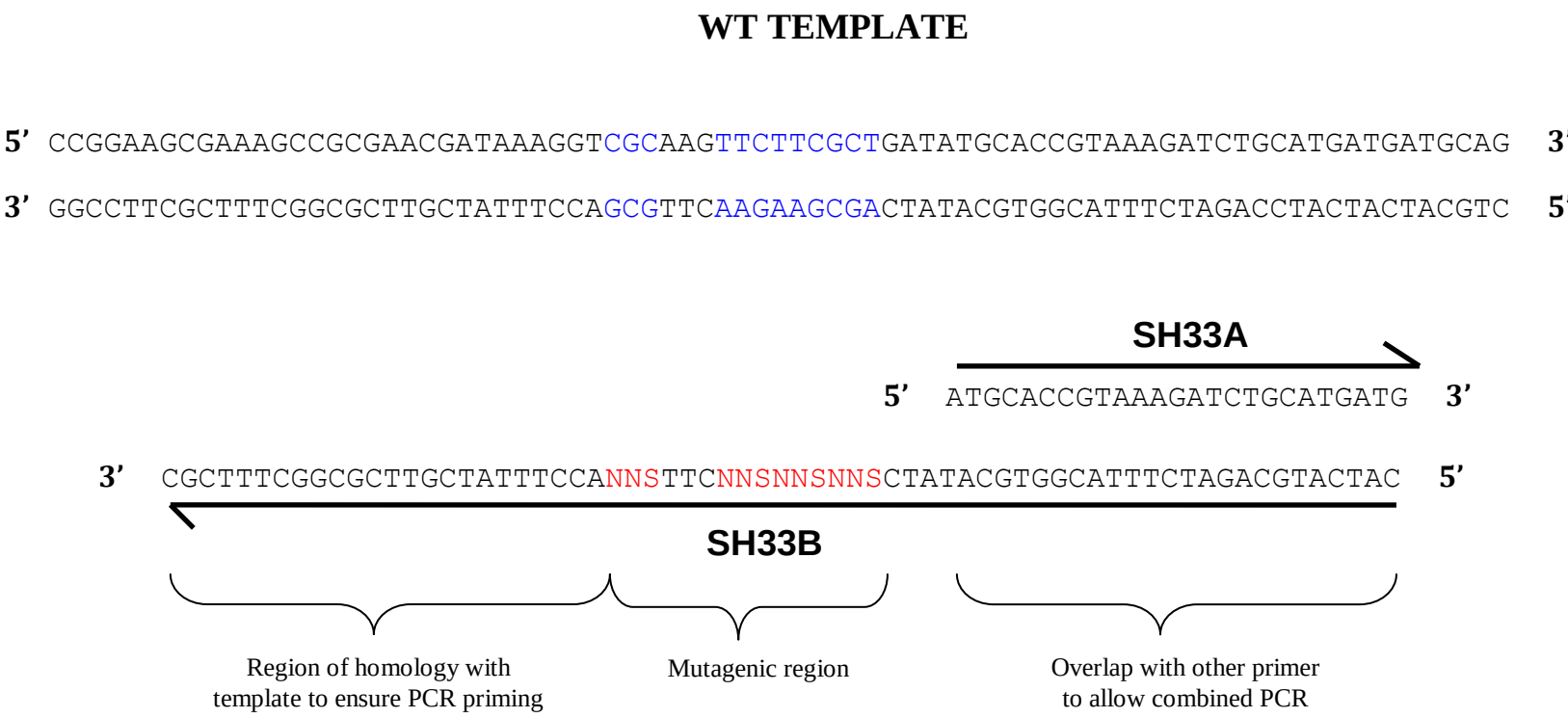

Figure 4.2 Schematic of primers SH33B and SH33A
Degenerate primer SH33B was used to randomise residues R121, F123, F124 and A125. Primer SH33A overlaps with SH33B allowing the joining of resulting PCR fragments. Residue to be mutated are highlighted in blue on WT template and mutagenic residues are highlighted in red on the SH33B degenerate primer

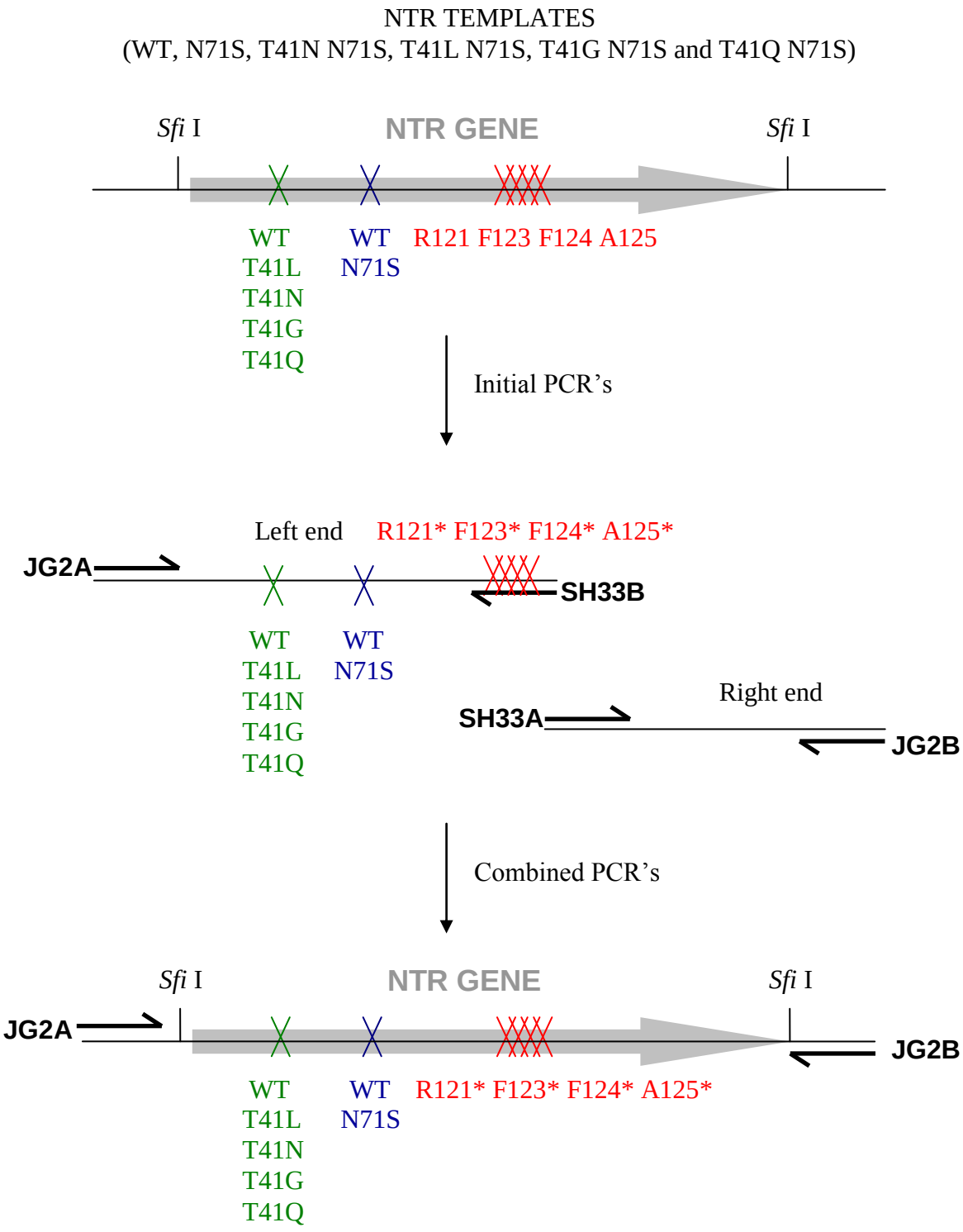

Figure 4.3 Schematic of degenerate PCR's making left and right ends of NTR gene and joining together by combined PCR's

Degenerate primer SH33B was used to randomise residues R121, F123, F124 and A125. Left end fragment made using primers JG2A and SH33B gave a fragment size of 654 bp and the right hand fragment made using primers SH33A and JG2B gave a fragment size of 463 bp. Primers SH33A and SH33B overlap by 25 non-degenerate nucleotides, allowing the left and right fragments to be joined in a second PCR step using the flanking JG2A and JG2B. Note this schematic is not to scale

4.2.1.2 Insertion of NTR PCR products into lambda vector

PCR fragments encoding libraries of full length mutant NTR genes were digested with *Sfi* I restriction enzyme and the digestion products were resolved by agarose gel electrophoresis. NTR genes of 751 bp were excised from a preparative agarose gel and purified using Qiagen QIA-Quick Gel Extraction Kit. The DNA concentration for each digested PCR was measured using PicoGreen.

Fresh stocks of λJG3J1 and λSV054 DNA vectors were grown and purified using PEG precipitation to separate λ phage from the bacterial culture, followed by CsCl density gradient centrifugation. This was based on Sambrook method (Sambrook 1989). Resulting λ DNA preparations were digested with restriction enzyme *Sfi* I before being treated with Calf Alkaline Phosphatase to prevent self ligation.

Initial small test sub-libraries were prepared by ligating the NTR fragment library with λ DNA and packaged into phage particles. Individual plaques were analysed by PCR to determine the proportion containing NTR insert, to original template ratios.

Once optimised each template sub-library (starting from the templates WT, N71S, T41L N71S, T41G N71S, T41N N71S and T41Q N71S) was prepared by ligating 28 ng of NTR sub-library with 1400 ng λ DNA. The ligation reaction was cleaned and concentrated by ethanol precipitation and resuspended in 2 µl $T_{10}E_1$. Resulting ligation products were packaged into phage particles using Stratagene Giga pack III gold packaging extract. Plaque titres were determined by plating out onto an *E. coli* UT5600 lawn.

4.2.1.3 Library Amplification

3×10^6 - 5×10^6 pfu of phage stock for each sub-library was amplified by liquid culture or plate lysate. In some experiments, the UT5600 used for amplification had been previously transformed with pET 24b, to increase the level of the *Lac* I repressor in the cells. 4-7 ml of amplified stock was retrieved. Plaque titres after amplification for each sub-library were determined by plating out onto an *E. coli* UT5600 lawn.

4.2.1.4 Experiments to test the effects of *Lac* I over-expression on CB1954 sensitivity of lysogens

E. coli bacteria C600 and UT5600, were transformed with the *Lac* I expressing plasmids pET 15b and pET 21b (see Figures 4.4 and 4.5). Lysogens generated using C600 and UT5600 *Lac* I over-expressing strains were constructed as described in Chapter 2 Materials and Methods. *Lac* I and NTR expression for each bacterial cell line was determined by western blotting. Amplification of a mixed population of phage was used to determine if *Lac* I over-expression could reduce preferential growth of empty vector phage. The sensitivity of F124N lysogens were determined by colony forming efficiency and phage release when exposed to a range of concentrations of CB1954.

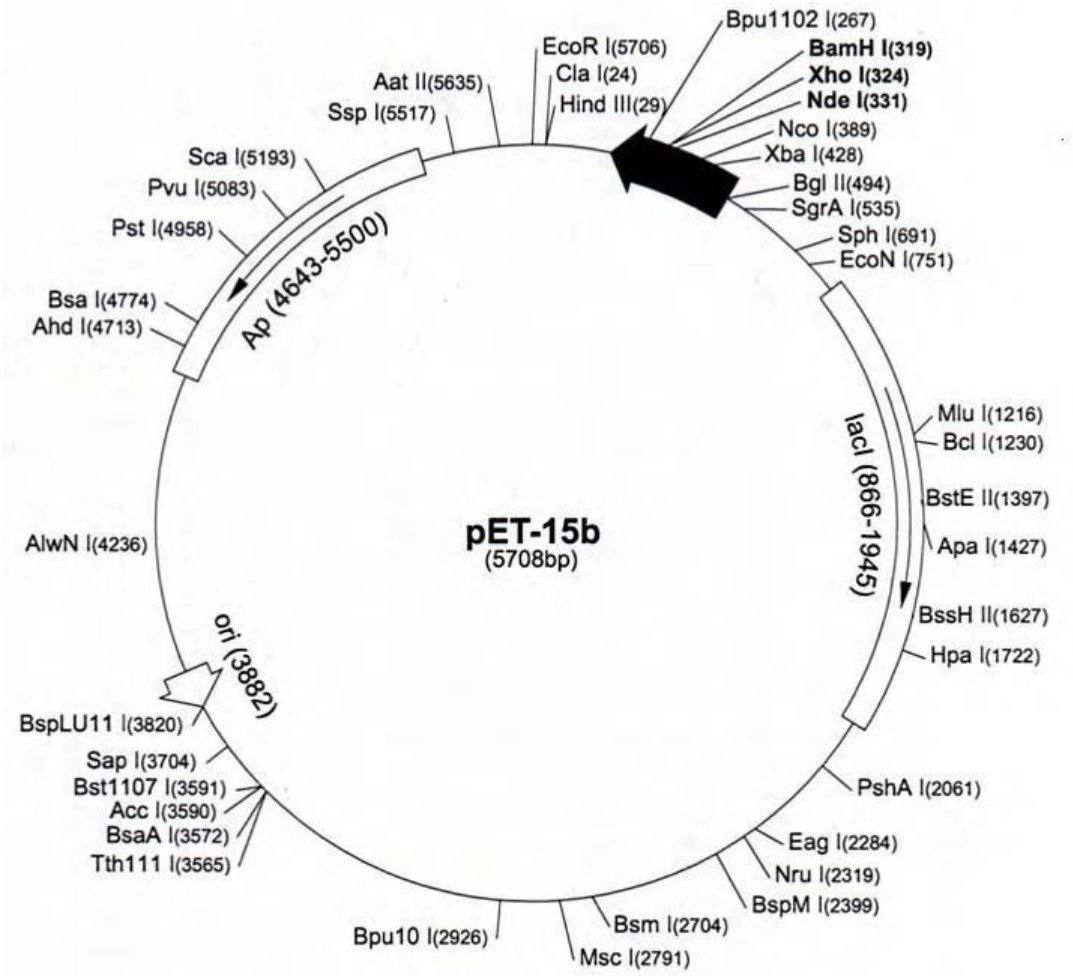

Figure 4.4 Schematic of plasmid vector pET 15b map encoding *lac* I gene from Novagen

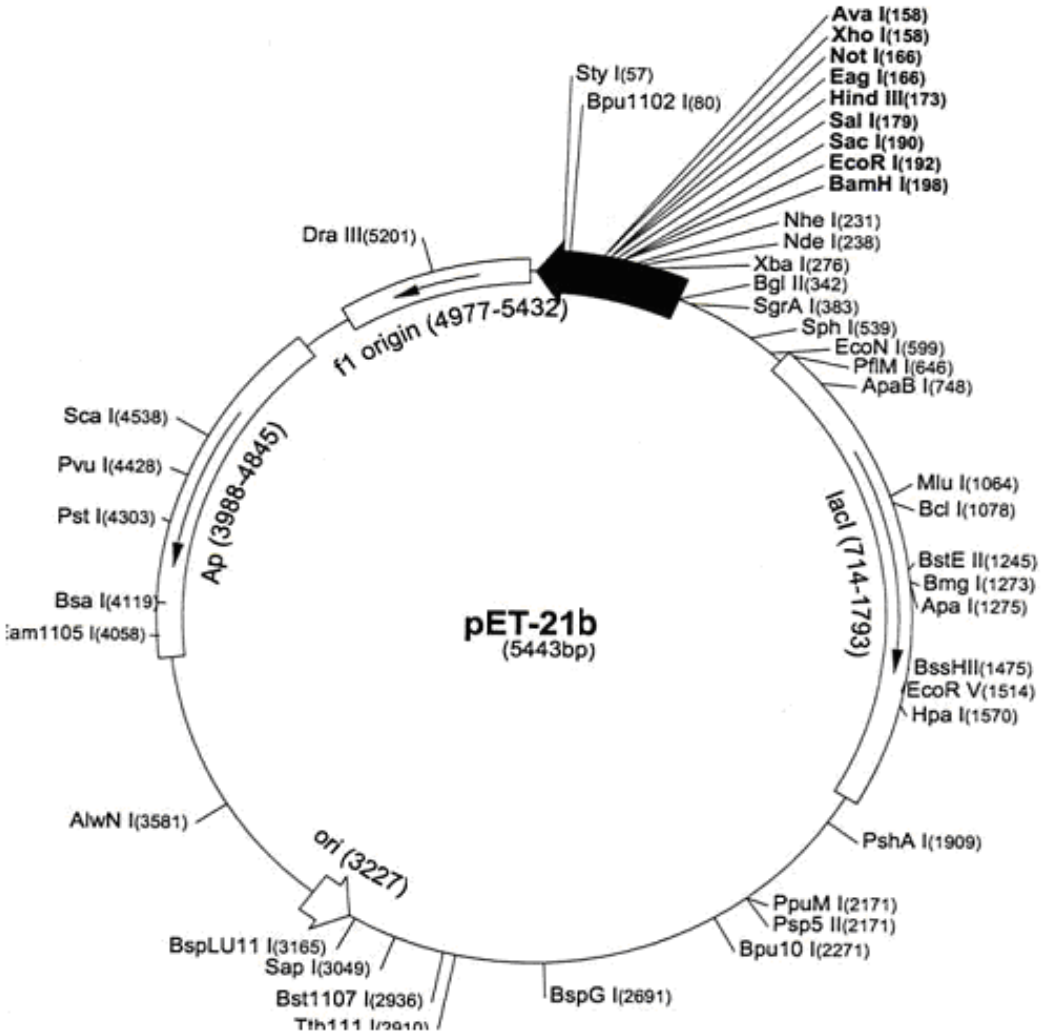

Figure 4.5 Schematic of plasmid vector pET 21b map encoding *lac* I gene from Novagen

4.3 RESULTS

4.3.1 Validation of PCR mutagenesis

Agarose gel electrophoresis was used to ensure DNA fragments of the correct size were amplified. Bands of the correct size were the major products of each PCR reaction, although additional bands were present in the unpurified reactions (see Figure 4.6a). All the additional bands were effectively removed by the gel purification (see Figure 4.6b).

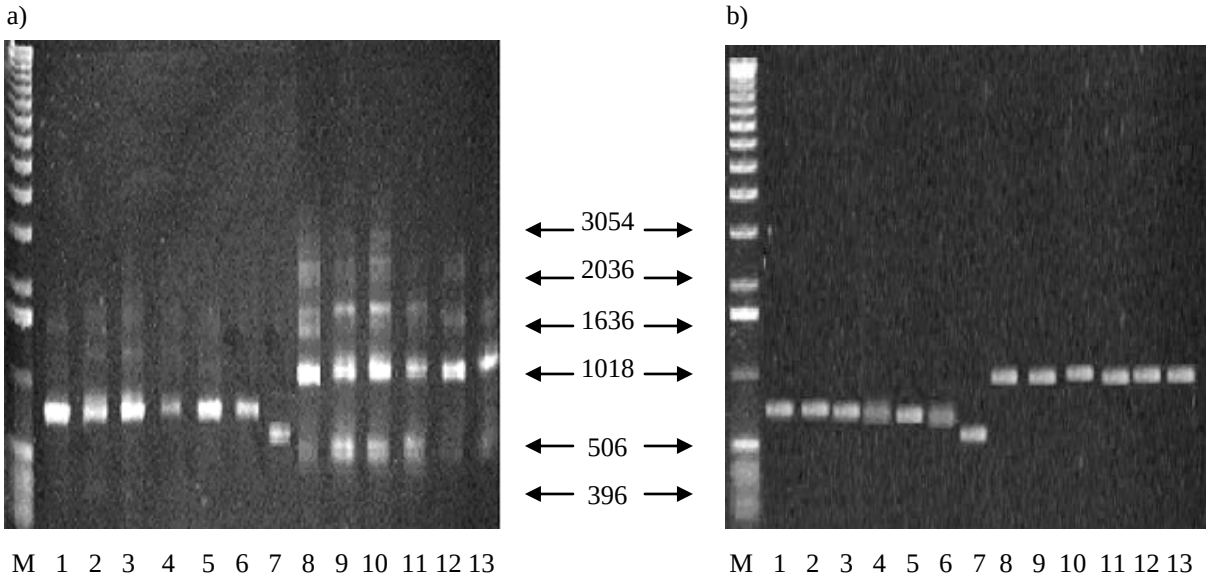

Figure 4.6 Agarose gel for PCR products from initial right and left end NTR PCR products and combined PCR's
a) Example of total PCR products from NTR PCR, b) Examples of PCR products after clean up by gel extraction. PCR products were run on a 0.7% agarose gel. M = Marker 1 kb plus ladder, Lanes 1-6 Left End PCR's using the alternate templates WT, N71S, T41L N71S, T41N N71S, T41G N71S and T41Q N71S respectively (654 bp), Lane 7 Right End (463 bp), Lanes 8-13 combined PCR's WT, N71S, T41L N71S, T41N N71S, T41G N71S and T41Q N71S respectively (1093 bp)

After the second PCR step to combine left and right end into full length NTR, resulting PCR fragments were sequenced to check the diversity of nucleotides at targeted codons. At residues not targeted for mutagenesis single strong predominant peaks corresponding with expected nucleotides, were observed as demonstrated by K122 (see Figure 4.7). In contrast, at targeted nucleotides, there are clear peaks for all four bases (C, G, A, T) at positions corresponding to "N" in the mutagenic primer and two bases (C and G) at positions corresponding to "S". In some cases the height of the peaks are similar but it others the T peak is substantially higher. This suggests that there is not perfectly equal representation of all the variants, nevertheless mutations were clearly present therefore high diversity is expected in this library.

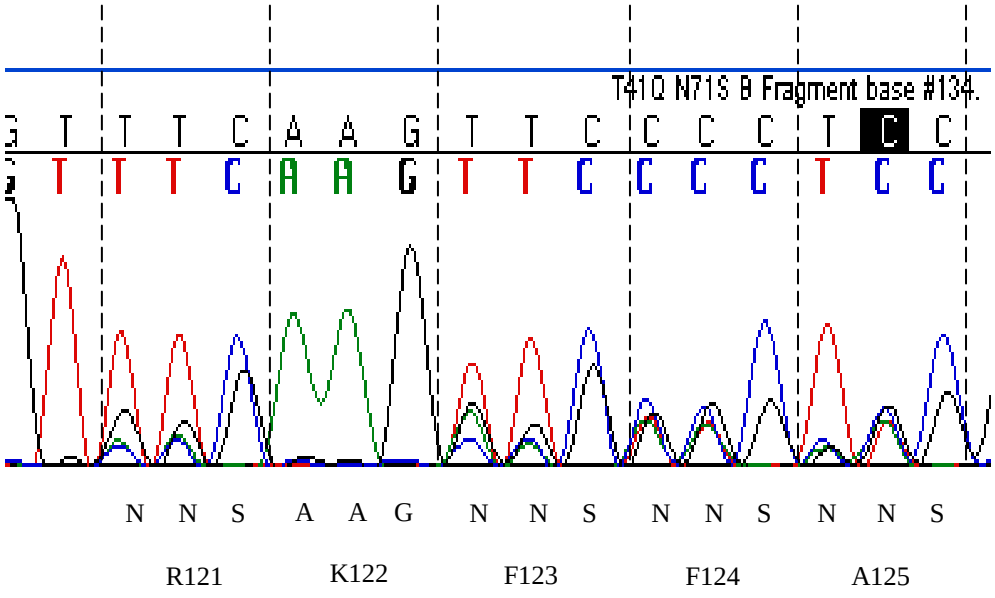

Figure 4.7 Extract from sequencing plot for residues R121-A125 NTR following degenerate primer mutagenesis
As expected either four or two peaks can be seen for each nucleotide of residues R121, F123, F124 and A125. A single peak for each nucleotide can also clearly be seen for residue K122

4.3.2 Preparation of PCR product for inserting in lambda vector

Following digested with *Sfi* I PCR fragments encoding libraries of full length mutant NTR genes were resolved by agarose gel electrophoresis (see Figure 4.8).

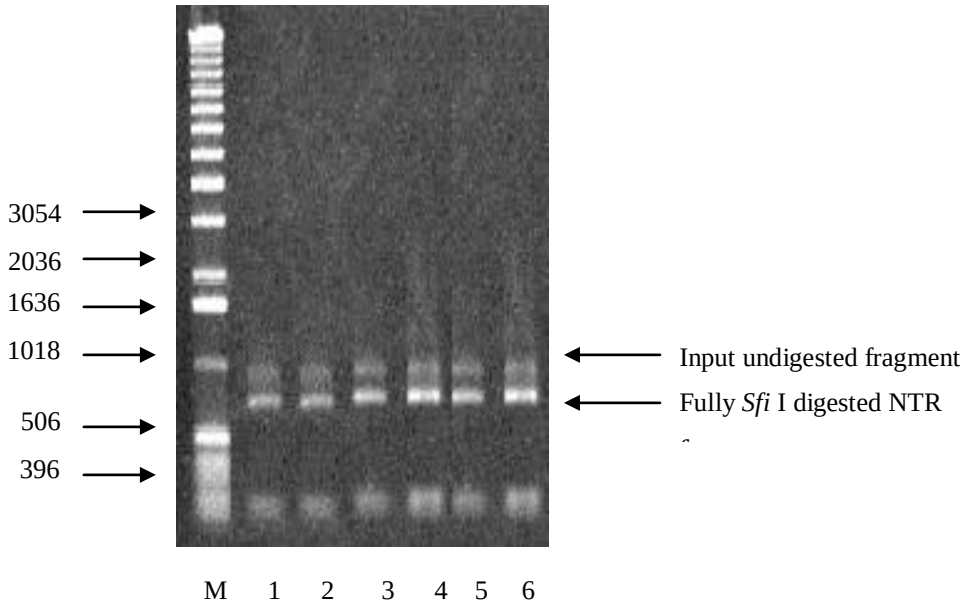

Figure 4.8 Agarose gel of digested PCR products
PCR products were run on a 0.7% agarose gel. M = Marker 1 kb plus ladder, Lanes 1-6 *Sfi* I digested WT, N71S, T41L N71S, T41N N71S, T41G N71S and T41Q N71S fragments. Two *Sfi* I sites were cut and the bands of expected size were excised from a preparative gel. As indicated on this gel, the digestion did not go to completion, and the major 751 bp band containing NTR was purified on a further preparative gel, prior to ligation into the lambda vector

4.3.3 Optimisation of lambda growth, purification and digestion

4.3.3.1 Lambda growth

The production of λJG3J1 vector has previously been problematic both with achieving good yield, purification and *Sfi* I digestion. Phage were grown following standard protocols by infecting C600 bacteria in the early stages of culture growth with a low inoculum of phage, expecting the phage to go through several cycles of lytic growth as the bacterial culture grew up, and expecting to obtain lysis of most remaining bacteria at a high culture density.

However, although the culture OD_{600} increased with bacterial growth, the amount of lysis was minimal, giving low yields of poor quality phage DNA. Initial experiments increasing the phage inoculum did not improve the result. In retrospect, it appears likely that most bacteria in the culture lysed early on, and the bacteria that grew were actually lysogenised, and so the levels of lambda repressor in the cells would inhibit the lytic cycle. An experiment was conducted to test whether lower amounts of phage inoculum would lead to better lysis. Approximately 1 x 10^9 C600 cells were used for each culture.

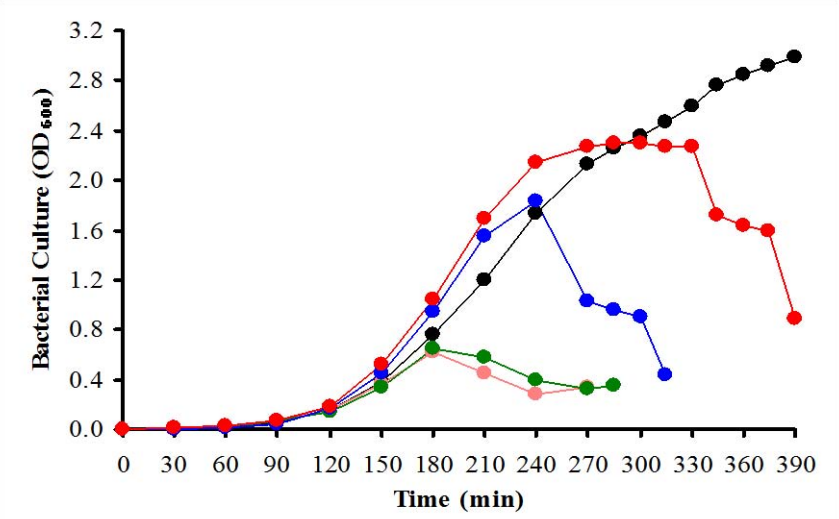

Figure 4.9 Growth curves measuring OD_{600} of *E. coli* C600 cells with a range of phage titres
Growth was measured at an OD^{600} from 0 to 390 minutes after infection at 30 minute intervals. Four different phage titres were used along with an uninfected control. No phage (Black), 5 x 10^5 pfu (Red), 1 x 10^6 pfu (Blue), 5 x 10^6 pfu (Green) and 1 x 10^7 pfu (Pink)

As shown in Figure 4.9 the uninfected culture (black) shows good growth right up to 390 minutes. After infection with 5 x 10^6 pfu (green) and 1 x 10^7 pfu (pink) growth of the cultures remained good up to 180 minutes. A small drop in OD_{600} from 0.8 to 0.4 was observed before culture growth started to increase again. After infection with 1x 10^6 pfu (blue) the culture grew well until 240 minutes, following which a large drop in OD_{600} from 2 to 0.4 was observed.

After infection with 5 x 10^5 pfu (red) the culture grew well until 270 minutes where it began to plateau before a large drop in OD_{600} from 2.4 to 0.8. Optimal growth and lysis was observed when using 5 x 10^5 – 1 x 10^6 pfu of phage to infect the cultures, therefore subsequent phage preparations used parallel cultures using these sizes of phage inoculum.

4.3.3.2 Purification of lambda vector

Two techniques were tested for purifying lambda vector. A method based on PEG precipitation of phage from culture supernatant, followed by CsCl density gradient centrifugation (Sambrook 1989) and a Qiagen lambda maxi kit method which used ion exchange column to purify the PEG precipitated phage. Optimum purification was achieved using the PEG and CsCl (see Figure 4.10).

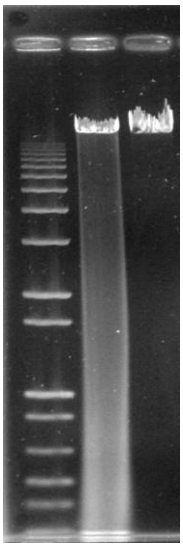

M 1 2

Figure 4.10 Agarose gel of purified lambda DNA
Two purification techniques tested for the purifying of lambda DNA. Lane 1 Qiagen Maxi kit, Lane 2 PEG and CsCl

Poor purification with either degradation of lambda DNA or carryover of bacterial DNA was observed when using the Qiagen kit. However a clean single band of phage DNA was observed when using PEG and CsCl.

4.3.3.3 *Sfi* I digestion of lambda vector

As with chapter 3 initial attempts to generate this large library used λJG3J1 vector. This vector contains two *Sfi* I sites, 21 bp apart downstream of a tac promoter, used for directional insertion of mutant NTR gene as an *Sfi* I fragment (see Figure 3.7). It is essential to achieve complete *Sfi* I digestion, in order to minimise the occurrence of empty vector (original vector) phage within the library. Significant problems with digestion were encountered as can be seen from Figure 4.11 where partial digestion was observed.

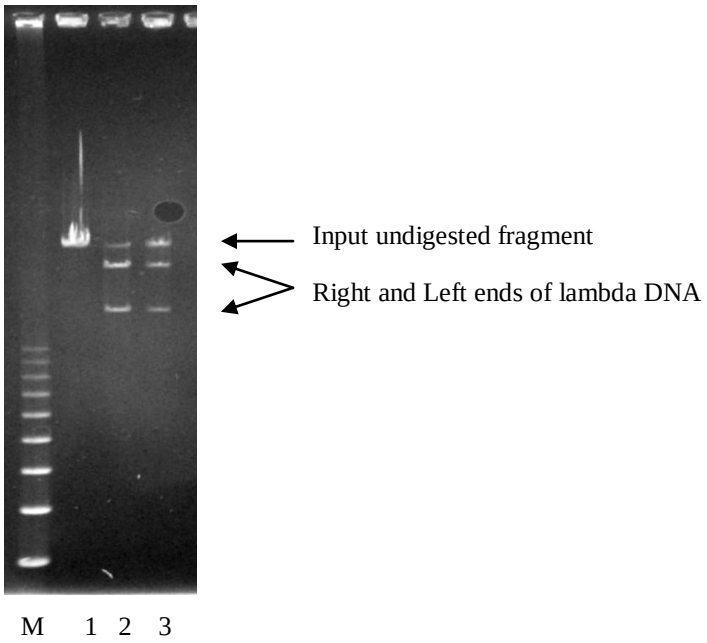

Figure 4.11 Agarose gel of *Sfi* I digested λJG3J1 DNA
M = Marker 1 kb plus ladder, Lane 1 Undigested λJG3J1 DNA. Lane 2-3 *Sfi* I digested DNA. Two *Sfi* I sites were cut. As indicated on this gel, the digestion did not go to completion.

Whereas most restriction enzymes can cut efficiently at a single site, *Sfi* I must bind simultaneously to two recognition sequences (GGCC*nnnn*↓*n*GGCC) in order for the enzyme to cut and the addition of excess enzyme inhibits the reaction (Nobbs *et al.* 1998, Wentzell *et al* 1998, Embleton *et al.* 1999, Watson et al.2000 and Embleton *et al.* 2004).

Optimisation of DNA preparation resulted in improvement in *Sfi* I digestion, however still long digestion times and several rounds of digestion were required. Small pilot libraries using these preparations showed that at least 15-20% of the clones lacked NTR insert despite improvements in digestion. An example test library PCR result can be seen in Figure 4.12, in this case three out of the twenty plaques lacked NTR insert.

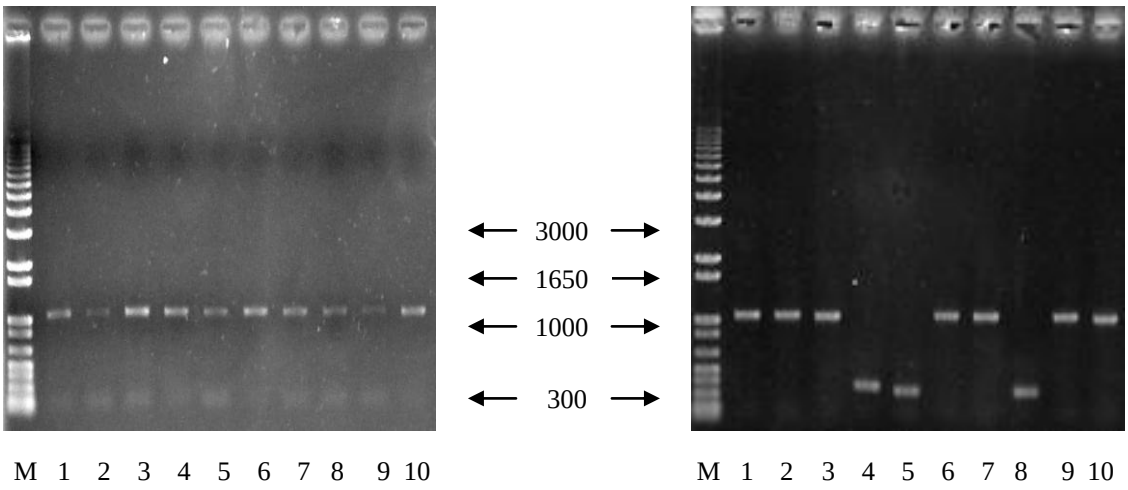

Figure 4.12 Agarose gel for PCR products using flanking primers JG2A and JG2B
Twenty plaques were analysed. The PCR products were run on a 0.7% agarose gel. M = Marker 1 kb plus ladder, Lanes 1-10 PCR products. NTR presence was indicated by a band of 1093 bp and empty vector by a band of 385 bp

Two alternative methods were considered to overcome digestion problems, the first was to gel purify the correct, fully *Sfi* I digested fragments. However, lambda DNA is large at approximately 40 kb in size; purification of large fragments from a gel was too inefficient for this strategy to be used effectively.

An alternative approach was to exploit the unique *Pac* I restriction enzyme site, included between the two *Sfi* I sites of the vector (see Figure 3.7). Following *Sfi* I, further digestion with *Pac* I would cut any undigested vector. Alkaline phosphatase treatment would then be used to prevent self ligation. Despite *Pac* I digestion small pilot libraries showed that at least 5-10% of the clones analysed showed no NTR insert. An example test library PCR result can be seen in Figure 4.13, in this case one out of the twenty plaques lacked NTR insert.

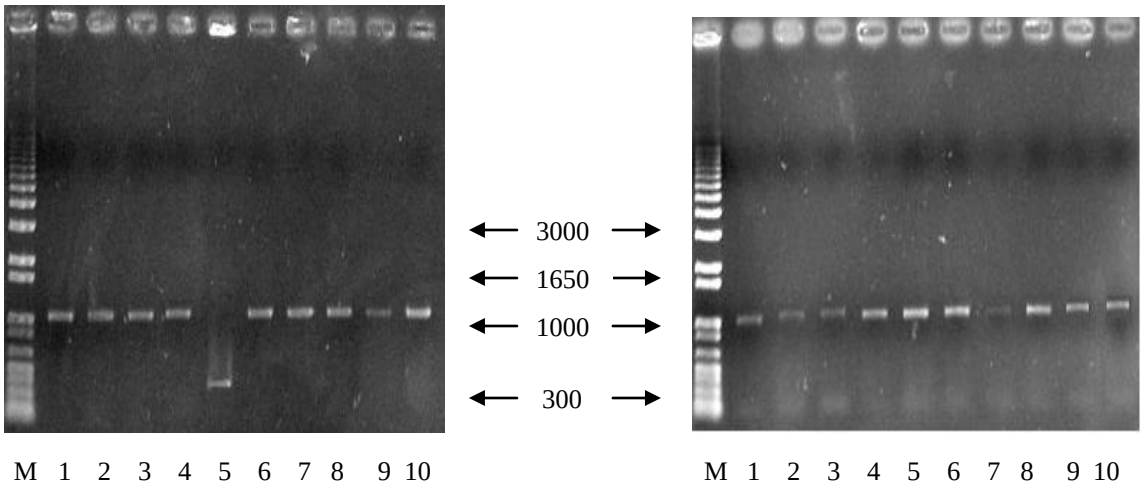

Figure 4.13 Agarose gel for PCR products using flanking primers JG2A and JG2B
Twenty primary plaques were analysed. The PCR products were run on a 0.7% agarose gel. M = Marker 1 kb plus ladder, Lanes 1-10 PCR products. NTR presence was indicated by a band of 1093 bp and empty vector by a band of 385 bp

A single round of phage amplification further increased the proportion of the libraries with no NTR insert to as much as 30-50%, as shown in Figure 4.14, in this case ten out of the twenty plaques lacked NTR insert.

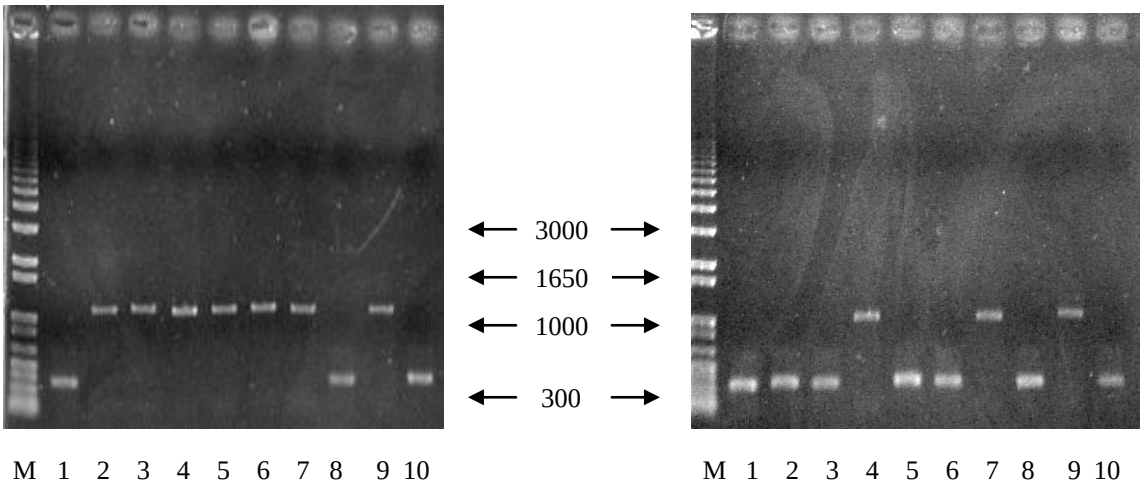

Figure 4.14 Agarose gel for PCR products using flanking primers JG2A and JG2B
Twenty plaques from an amplified test library were analysed. The PCR products were run on a 0.7% agarose gel. M = Marker 1 kb plus ladder, Lanes 1-10 PCR products. NTR presence was indicated by a band of 1093 bp and empty vector by a band of 385 bp

The ten clones lacking NTR insert from Figure 4.14 were then test digested with *Pac* I. Four of the ten PCR products were digested by the *Pac* I enzyme (see Figure 4.15).

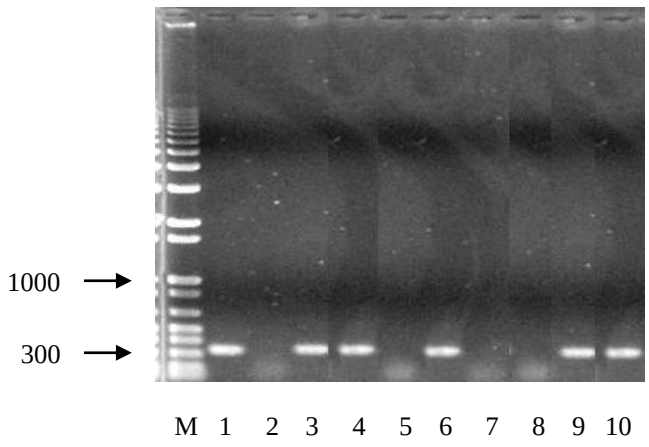

Figure 4.15 Agarose gel of *Pac* I digested empty vector PCR products
M = Marker 1 kb plus ladder, Lane 1-10 Pac I digested PCR's

The remaining six clones which failed to digest were sequenced. Only one of the plaques was identical to the original starting vector, the remaining five phage clones had small deletions within the region of the *Sfi* I and *Pac* I sites as shown in Figure 4.16.

Original start vector

```
ATCTAGGGCCTGCGAGGCCTTAATTAAGGCCTCCCGGGCCTCTAGAGTCG
TAGATCCCGGACGCTCCGGAATTAATTCCGGAGGGCCCGGAGATCTCAGC
```

Sequenced plaque

```
ATCTAGGGCCT:::::::::::::::::::::::::::::CTAGAGTCG
TAGATCCCGGA:::::::::::::::::::::::::::::GATCTCAGC
```

Figure 4.16 Deletion found in 5/6 clones lacking NTR inserts, from library testing the efficiency of *Pac* I digestion
Individual clones lacking NTR inserts as indicated by PCR with flanking primers, were sequenced following *Pac* I digestion. Red sequence represents *Sfi* I sites and green represents *Pac* I site location

The lambda DNA ends may have become nibbled during *Sfi* I digestion allowing blunt end ligation. This is especially likely to happen during the prolonged exposure time required for adequate digestion, and it may therefore be difficult to further reduce the proportion of phage lacking inserts by these approaches.

As mentioned previously, *Sfi* I enzyme requires two target sequences in order to cut. The two *Sfi* I sites in λJG3J1 vector are separated by 21 bp. As shown by Embleton *et al* the optimal separation for *Sfi* I sites is 211-1023 bp. The rate becomes increasingly inefficient as the sites get closer together. Separations shorter than 100 bp showed very slowest rates. However intermediate lengths showed oscillating rates, due to *Sfi* I reactions yielding helical repeat of about 11.5 bp per turn (Wentzell *et al* 1998).

Therefore it was decided to try using a derivative of λJG3J1 with a DNA insert between the *Sfi* I sites. λSV054 contains an inserted *NfsA* gene, with the sites separated by 784 bp. This greater separation of *Sfi* I sites is predicted to improve the efficiency of *Sfi* I digestion. However, an obvious potential problem would be how to prevent *NfsA* from re-ligating into the vector. Calf alkaline phosphatase treatment will be used after *Sfi* I digestion to remedy this problem. *NfsA* can also easily be distinguished from *NfsB* NTR by PCR, so the presence of *NfsA* in the resulting library can easily be monitored. It is also possible to predict that phage with *NfsA* may have more similar growth properties to phage with *NfsB* genes, than empty vector.

This phage was grown and purified using the same method as the λJG3J1 vector. Digestion of this vector with *Sfi* I still required three rounds of digestion but with four hour incubations rather than overnight (see Figure 4.17). This should reduce nibbling and was therefore used for subsequent library construction.

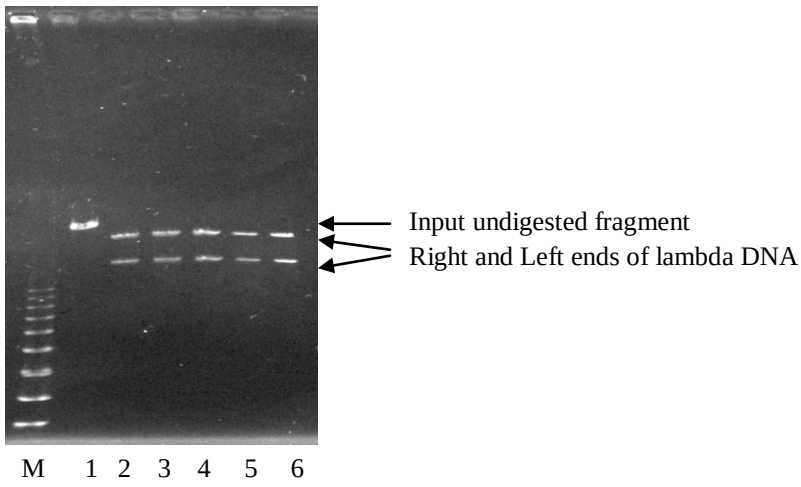

Figure 4.17 Agarose gel of *Sfi* I digested λSV054 DNA
M = Marker 1 kb plus ladder, Lane 1 Undigested λSV054 DNA. Lane 2-6 *Sfi* I digested DNA. Two *Sfi* I sites were cut. As indicated on this gel, the digestion appears to have gone to completion with clear distinct bands

4.3.4 Over-expression of the lac repressor, to reduce background NTR expression and reduce growth-advantage of empty vector

Observation on the propagation of lysogens with or without NTR inserts indicated that those with NTR genes grew more slowly (Guise *et al.* unpublished). When analysing phage plaques in this study it was also noted that empty vector plaques were larger than NTR-containing counterparts also demonstrating this growth advantage.

One of the possible reasons for this growth advantage is the leaky expression of NTR, which is slightly detrimental to the bacterial lysogen. NTR expression is under the control of a tac promoter, which is a hybrid derived from both trp and lac. Expression from tac is more efficient than either promoter alone. The lac repressor *Lac* I controls expression, by normally binding to the lac operator sites and inhibiting transcription. In the presence of inducers such as IPTG, the lac repressor dissociates from the DNA, allowing transcription to proceed.

The addition of excess *Lac* I will hopefully completely shut off NTR expression while amplifying the library therefore NTR encoding phage should be able to grow more quickly, removing the growth advantage of empty vector.

Two closely related plasmids containing *Lac* I gene were available, their efficiency for *Lac* I expression and shut off of NTR expression were therefore compared. The two plasmids pET 15b and pET 21b were transformed into C600 and UT5600 bacterial cell lines (see Figure 4.4-4.5). *Lac* I and NTR expression were comparing by western blotting for each bacterial cell line (see Figure 4.18).

a)

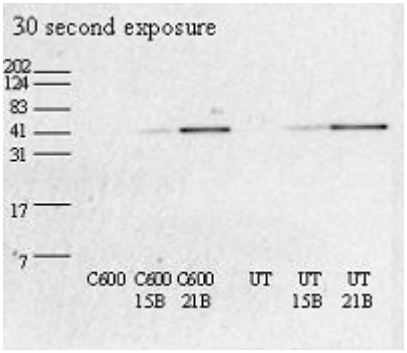

b)

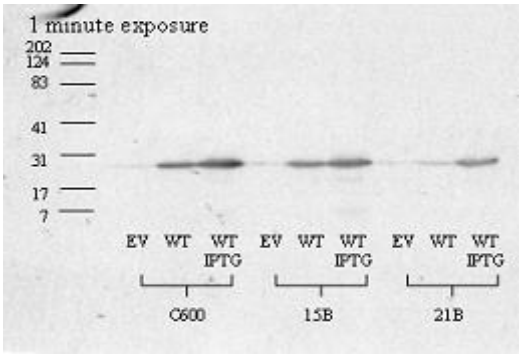

Figure 4.18 Western Blotting of C600 and UT5600 bacterial cells
a) Western blotting for *Lac* I expression comparing C600, C600 pET 15B, C600 pET 21B, UT5600, UT5600 pET 15B and UT5600 pET 21B cell lines. b) NTR expression comparing empty vector (EV), wild type NTR (WT) and wild type NTR that has been induced by IPTG (WT IPTG) in C600, C600 pET 15B and C600 pET 21B

No *Lac* I expression was detected in C600 and UT5600 cells alone confirming that endogenous expression is low. Both cell lines with plasmid pET 15b showed *Lac* I expression and both cell lines with pET 21b showed even higher expression of *Lac* I (see Figure 4.18a).

Clear reduction in *NfsB* NTR expression can be seen in C600 cells with both plasmid pET 15b and pET 21b when compared with C600 cells alone (see Figure 4.18b). However the greatest reduction in NTR expression can be seen with pET 21b. NTR expression can still be induced with IPTG however lower expression was seen with pET 15b and pET 21b plasmids. This correlates well with the results seen for *Lac* I expression.

To determine whether over-expression of *Lac* I was able to overcome the preferential growth of empty vector phage, a mixed population of 1 x 10^6 phage, containing 50% NTR and 50% empty vector was used to infect C600, C600 pET 15b and C600 pET 21b bacterial cells. This method modelled the procedure used for amplification of phage libraries. The original input phages were checked by PCR to ensure the correct proportions of NTR and EV were used. The resulting PCR bands indicate 50% NTR and 50% EV (see Figure 4.19a). When C600 cells were used for amplification the proportion of empty vector increased to 90% (see Figure 4.19b). The expression of pET 15b in the C600 cells had no effect on amplification; the proportion of empty vector increased to 90% (see Figure 4.19c). However the expression of pET 21b in the C600 cells reduced the preferential growth with only 60% of the phage encoding empty vector (see Figure 4.20d). Therefore pET 21b could be advantageous when amplifying phage libraries.

a) Control – No Amplification

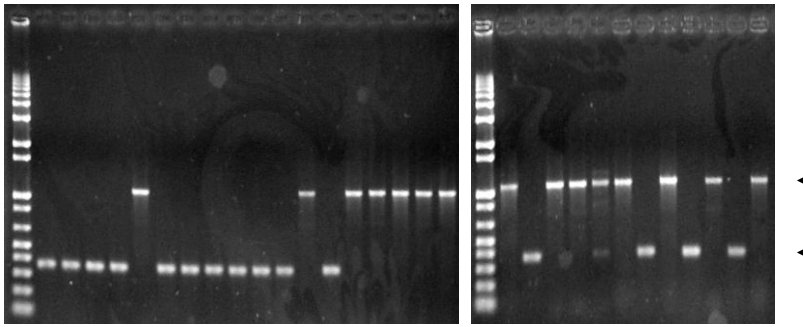

15 plaques NTR 50%
15 plaques EV 50%

b) C600 cells

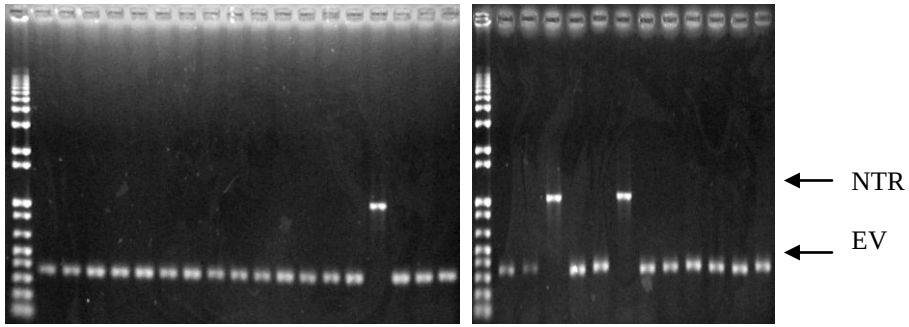

3 plaques NTR 10%
27 plaques EV 90%

c) C600 15b cells

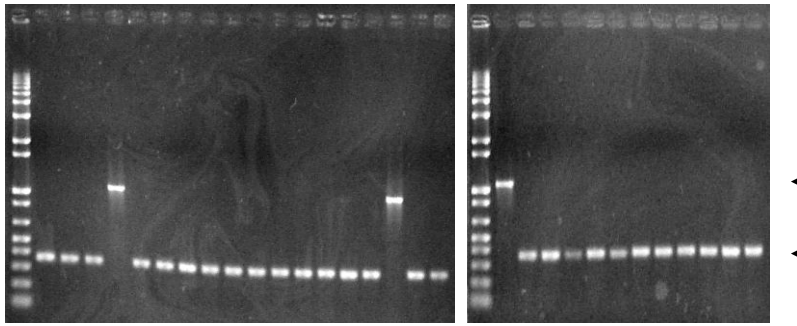

3 plaques NTR 10%
27 plaques EV 90%

d) C600 21b cells

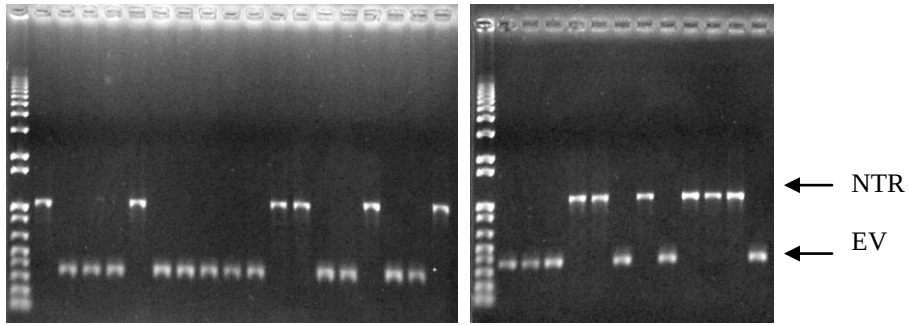

12 plaques NTR 40%
18 plaques EV 60%

Figure 4.19 Testing the ability of *Lac* I over-expression to reduce preferential amplification of empty vector phage
Gels showing PCR products from individual plaques comparing input phage with phage amplified in C600, C600 pET 15b and pET 21b cell line. a) Input phage (before amplification), b) Liquid culture amplification in C600 cells, c) Liquid culture amplification in C600 pET 15b and d) Liquid culture amplification in C600 pET 21b. 1 x 10^6 phage was used for each with 50% NTR and 50% EV phage used. NTR presence was indicated by a band of 1093 bp and empty vector by a band of 385 bp

However western blotting showed that high levels of *Lac* I reduced the amount of NTR expression upon induction with IPTG. This could potentially reduce the sensitivity of lysogens to CB1954, so an experiment was designed to test this by exposing lysogenic cultures to a range of CB1954 concentrations. The sensitivity of the lysogens to the different CB1954 concentrations was tested by plating efficiency and the amount of phage release measured. The cultures were exposed to CB1954 as a 15 minute pulse. F124N mutant phage were used for this experiment comparing UT5600, UT5600 pET 15b and UT5600 pET 21b bacterial cells. F124N was used because this mutant produces a clear peak in phage release at approximately 100 µM CB1954 allowing any shift to be easily compared (Guise *et al.* 2007).

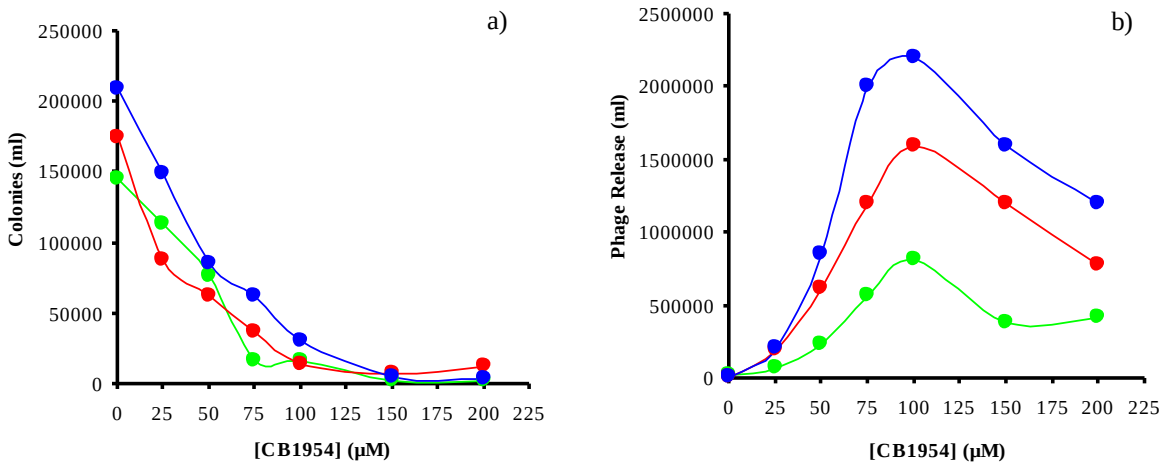

Figure 4.20 Colony Forming Efficiency for UT5600, UT5600 pET 15b and UT5600 pET 21b bacteria and Plaque Forming Units for F124N phage when exposed to a range of concentrations of CB1954
a) Colony forming efficiency at CB1954 concentrations ranging from 0-225 µM CB1954 of F124N in UT5600, UT5600 pET 15b and UT5600 pET 21b b) F124N phage release at CB1954 concentrations ranging from 0-225 µM CB1954. UT5600 cells alone **(**blue), UT5600 pET15b (red) and UT5600 pET21b (green)

As shown in Figure 4.20a expression of *Lac* I had little effect on the dose-response for cytotoxicity of CB1954 to the bacterial lysogens. The titres of phage released were reduced by approximately 30% and 60% by expression of *Lac* I from pET15b and pET 21b respectively in Figure 4.20b. However there was minimal increase in the concentration of CB1954 giving optimum phage release.

4.3.5 Phage production and amplification

Having optimised the stages of lambda vector production, *Sfi* I digestion, choice of vector, and decided on the use of *Lac* I, it was possible to proceed on to generate, amplify and characterise the large library of NTR mutants. The ligation products were packaged into phage particles and plaque titres for each sub-library were determined; the phage yields were between $8.1 \times 10^6 - 1.9 \times 10^7$ (see Table 4.1). These yields range from 8-14 times greater than calculated numbers of possible nucleotide variants, and so the sub-libraries should contain the majority of these variants. However the selection process (using CB1954 to enrich for mutants better able to activate the prodrug) uses bacterial lysogens and the efficiency of generating lysogens is only 1%. In order to maintain the maximum diversity in the lysogens, it was necessary to amplify the phage library prior to the generation of lysogens. This was done by amplification with liquid culture, giving between $2.7 \times 10^{10} - 8.0 \times 10^{10}$ independent phages as shown in Table 4.1.

Template	Initial phage yield of independent clones (pfu total)	Number of possible nucleotide variants	Phage yield after amplification (pfu total)
WT	1.2×10^7	1.05×10^6	7.6×10^{10}
N71S	1.9×10^7	1.05×10^6	5.2×10^{10}
T41L N71S	1.3×10^7	1.05×10^6	8.0×10^{10}
T41N N71S	1.4×10^7	1.05×10^6	4.4×10^{10}
T41G N71S	8.1×10^6	1.05×10^6	2.7×10^{10}
T41Q N71S	9.8×10^6	1.05×10^6	3.2×10^{10}

Table 4.1 Initial phage yield of independent clones, number of possible nucleotide variants and phage yield after amplification by liquid culture

PCR was used to check NTR presence, 30 phage plaques from each sub-library were analysed. Two sets of primers were used in order to distinguish between *NfsA* and *NfsB* NTR and empty vector. All the PCR's contained *NfsB* insert; no *NfsA* or empty vector was seen (see Appendix Figure 8.1).

4.3.6 Selection 1

6.0×10^9 pfu of phage were infected into 1.5×10^{10} UT5600 pET 21b cells, using kanamycin to select for lysogens. Aliquots of mid log culture were exposed to CB1954 for 15 minutes, diluted and pelleted before being resuspended in prodrug free media as described in Materials and Methods. Phage released after 1 hour were separated from lysogens by 0.2 µm filtration (see Figure 3.9). The library was taken through eight rounds of selection at 10 µM, 25 µM, 50 µM or 100 µM in parallel (see Figure 4.21). Phage release at each round of selection was measured (see Figure 4.22).

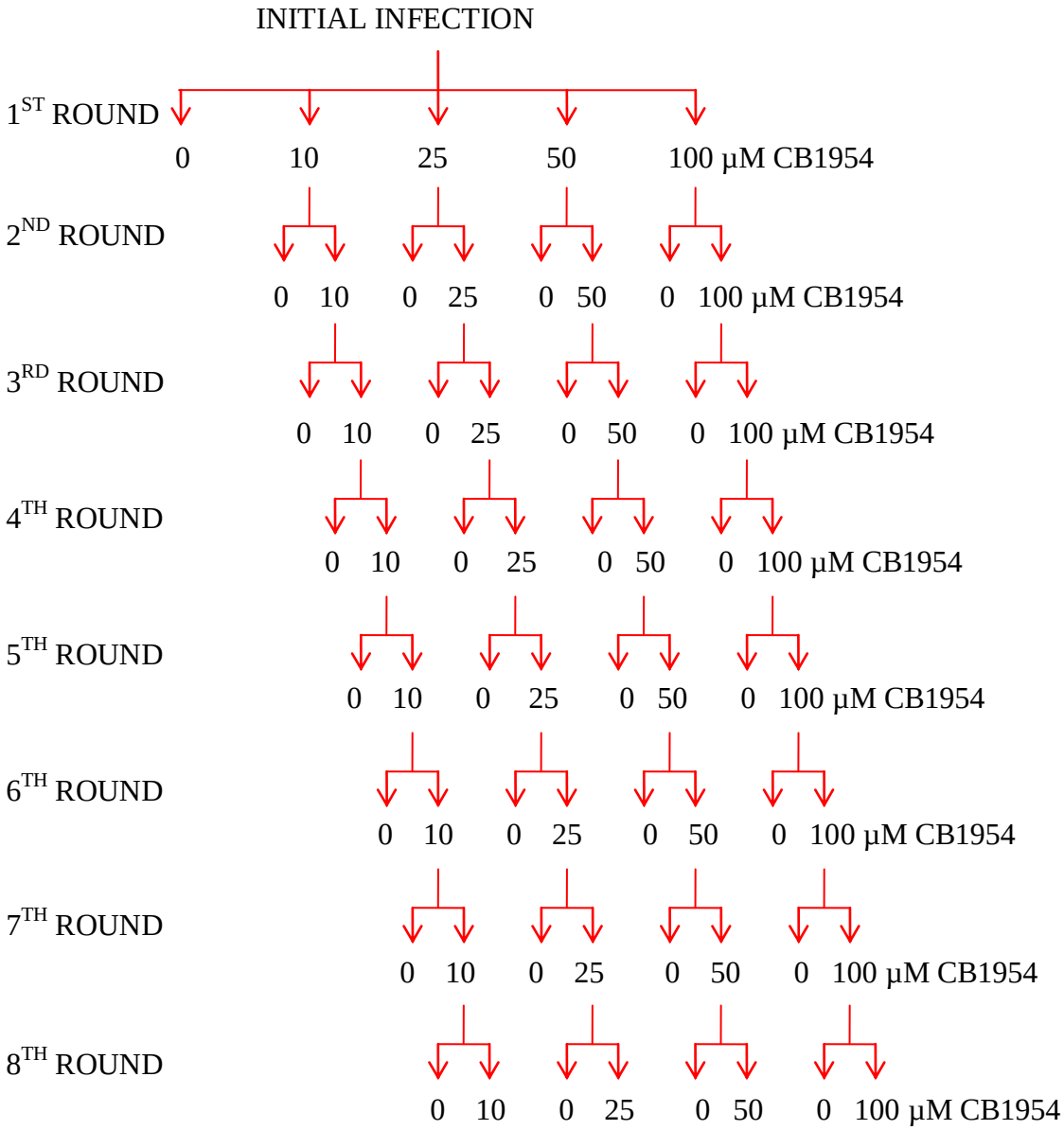

Figure 4.21 Flow chart showing culture lineages from initial infection through to the eighth round of selection

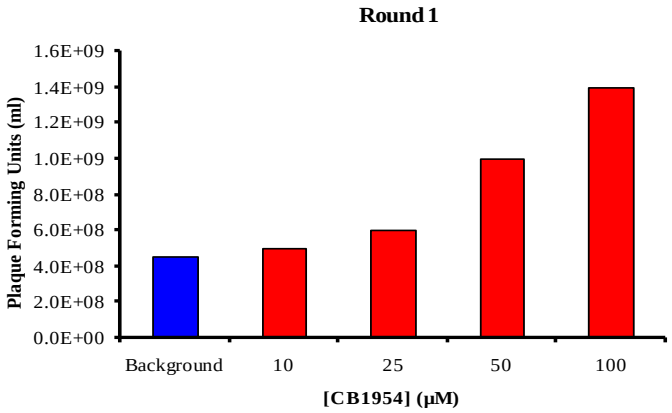
Round 1
Plaque Forming Units (ml)
1.6E+09
1.4E+09
1.2E+09
1.0E+09
8.0E+08
6.0E+08
4.0E+08
2.0E+08
0.0E+00
Background
10
25
50
100
[CB1954] (µM)

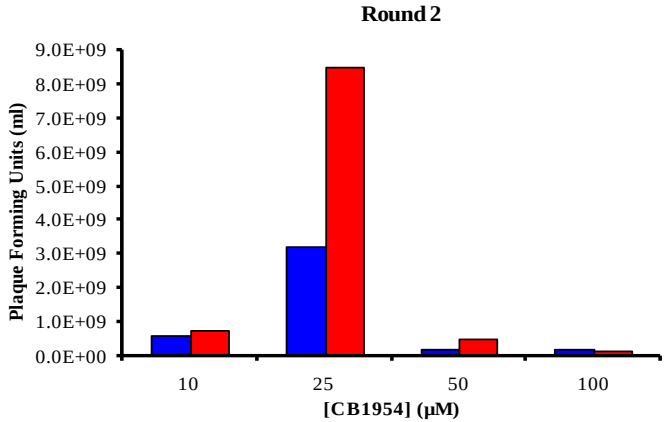
Round 2
Plaque Forming Units (ml)
9.0E+09
8.0E+09
7.0E+09
6.0E+09
5.0E+09
4.0E+09
3.0E+09
2.0E+09
1.0E+09
0.0E+00
10
25
50
100
[CB1954] (µM)

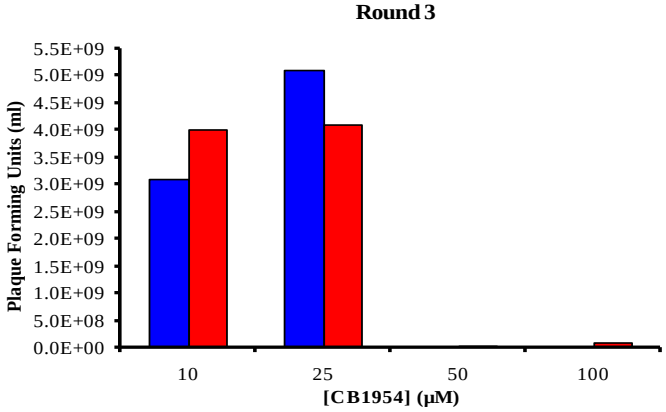
Round 3
Plaque Forming Units (ml)
5.5E+09
5.0E+09
4.5E+09
4.0E+09
3.5E+09
3.0E+09
2.5E+09
2.0E+09
1.5E+09
1.0E+09
5.0E+08
0.0E+00
10
25
50
100
[CB1954] (µM)

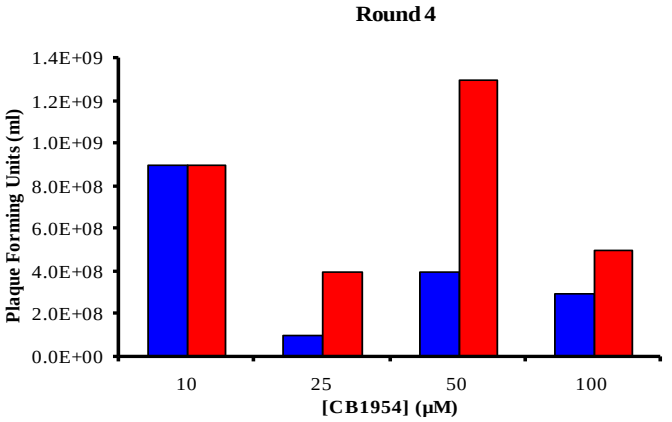
Round 4
Plaque Forming Units (ml)
1.4E+09
1.2E+09
1.0E+09
8.0E+08
6.0E+08
4.0E+08
2.0E+08
0.0E+00
10
25
50
100
[CB1954] (µM)

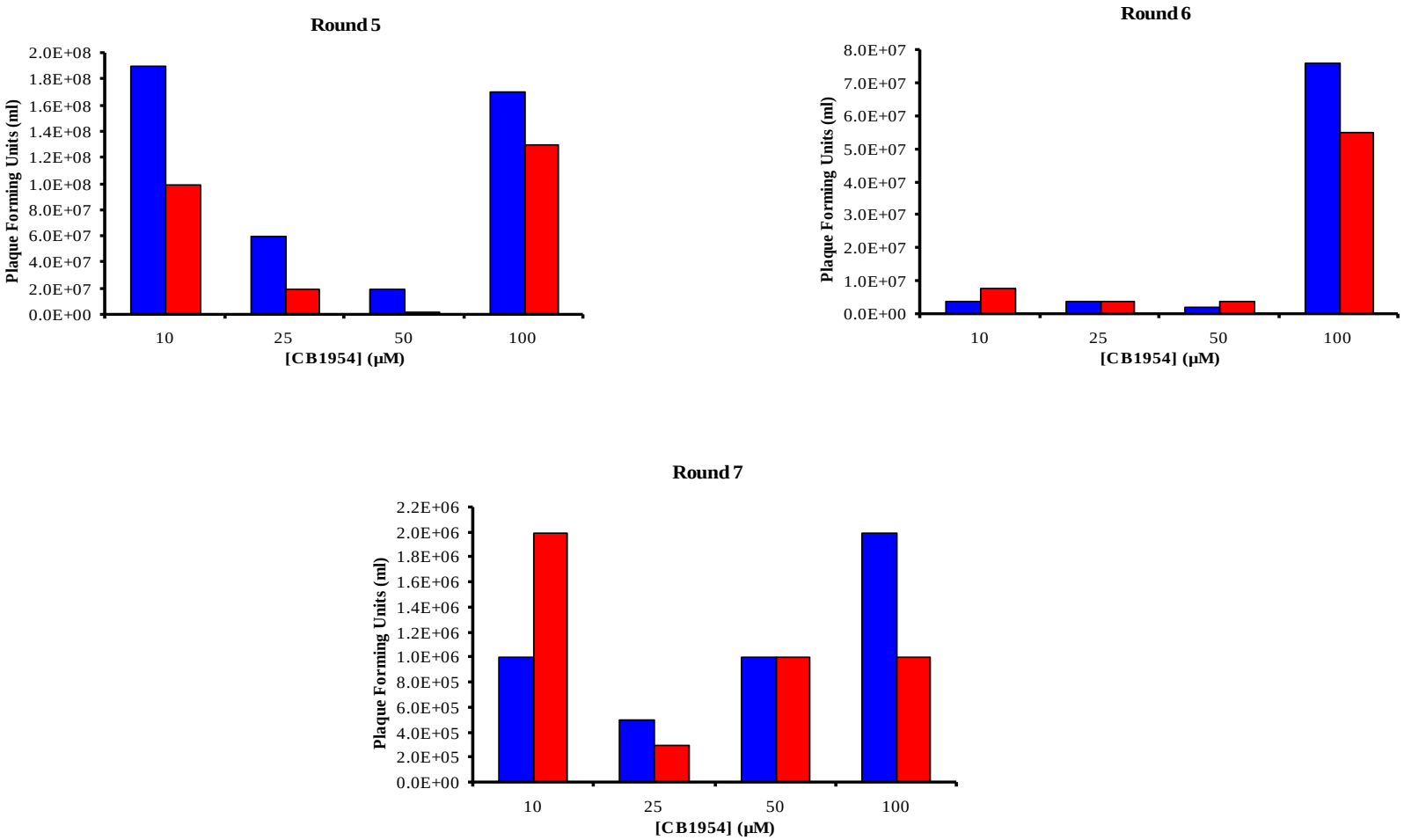

Figure 4.22 Phage release for rounds 1-7 of selection with 10 µM, 25 µM, 50 µM and 100 µM CB1954
Background phage release (blue) and CB1954 induced phage release (red)

Background release of phage was determined by exposing the culture to no CB1954. After 1 round of selection with CB1954, phage release was as expected with increased release of phage induced by increasing concentrations of CB1954. For subsequent rounds of selection, the background had to be determined separately for each lineage. Phage release was again expected to increase when induced by increasing concentration of CB1954. Theoretically in later rounds as selection enriches improved mutants low CB1954 concentrations may induce increased phage release.

After 2 rounds of selection higher titres of phage were observed after induction with 25 μM than with 10 μM CB1954. However lower phage release was observed after induction with 50 μM and 100 μM. At 100 μM induction phage release was particularly low and background levels appeared to be slightly higher than the induced culture. Varying levels of background phage release was observed for each culture. From round 3 onwards no obvious pattern of phage release was observed, relative to the CB1954 concentration used for induction.

4.3.6.1 Monitoring population sensitivity of the library under selection

The effect of selection was also monitored using a lysogen colony forming assay for each selection lineage, after three and seven rounds of selection. The unselected library showed that almost all of the lysogens were resistant to 200 μM. After three rounds of selection a small improvement was seen compared to unselected. Most improvement was seen after induction with 10 μM and 25 μM CB1954 (see Figure 4.23a). After seven rounds of selection little difference was seen compared to three rounds of selection (see Figure 4.23b). By seven rounds of selection better enrichment of this library would be expected.

a) b)

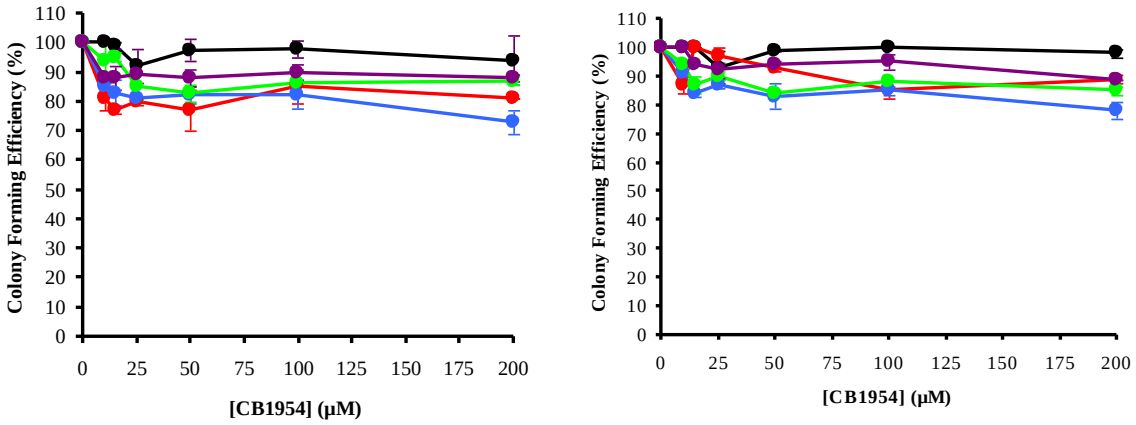

Figure 4.23 Dose Response curves for colony forming assay in UT5600 cells
a) Three rounds of selection, b) Seven rounds of selection. Unselected (black), 10 µM CB1954 induction (red), 25 µM CB1954 induction (blue), 50 µM CB1954 induction (green) and 100 µM CB1954 induction (purple)

4.3.6.2 Screening CB1954 sensitivity of individual clones from selected library

460 individual lysogen colonies were picked from each of the lineages selected with 10 µM and 25 µM CB1954. Cultures were grown overnight in 96 well plates and replica plated onto plates containing no CB1954 and 35 µM CB1954. All the lambda lysogens showed strong growth in the absence of CB1954. All lysogens selected at 10 µM, which gave good growth in the absence of CB1954 also grew well at 35 µM (see Figure 4.24). Three lysogens selected at 25 µM, disappeared at 35 µM and were therefore sensitive to this concentration of CB1954 (see Figure 4.25). The remaining 457 lysogenic colonies were not sensitive to 35 µM.

The NTR genes from the three lysogens that failed to grow at 35 µM were sequenced. All three NTR genes had the same amino acid changes N71S A113 R121V F123N F124V A125C K179R referred to as clone 282 for this thesis. IC_{50} assays were performed for clone 282 (see Figure 4.26). WT and N71S have also been shown for comparison.

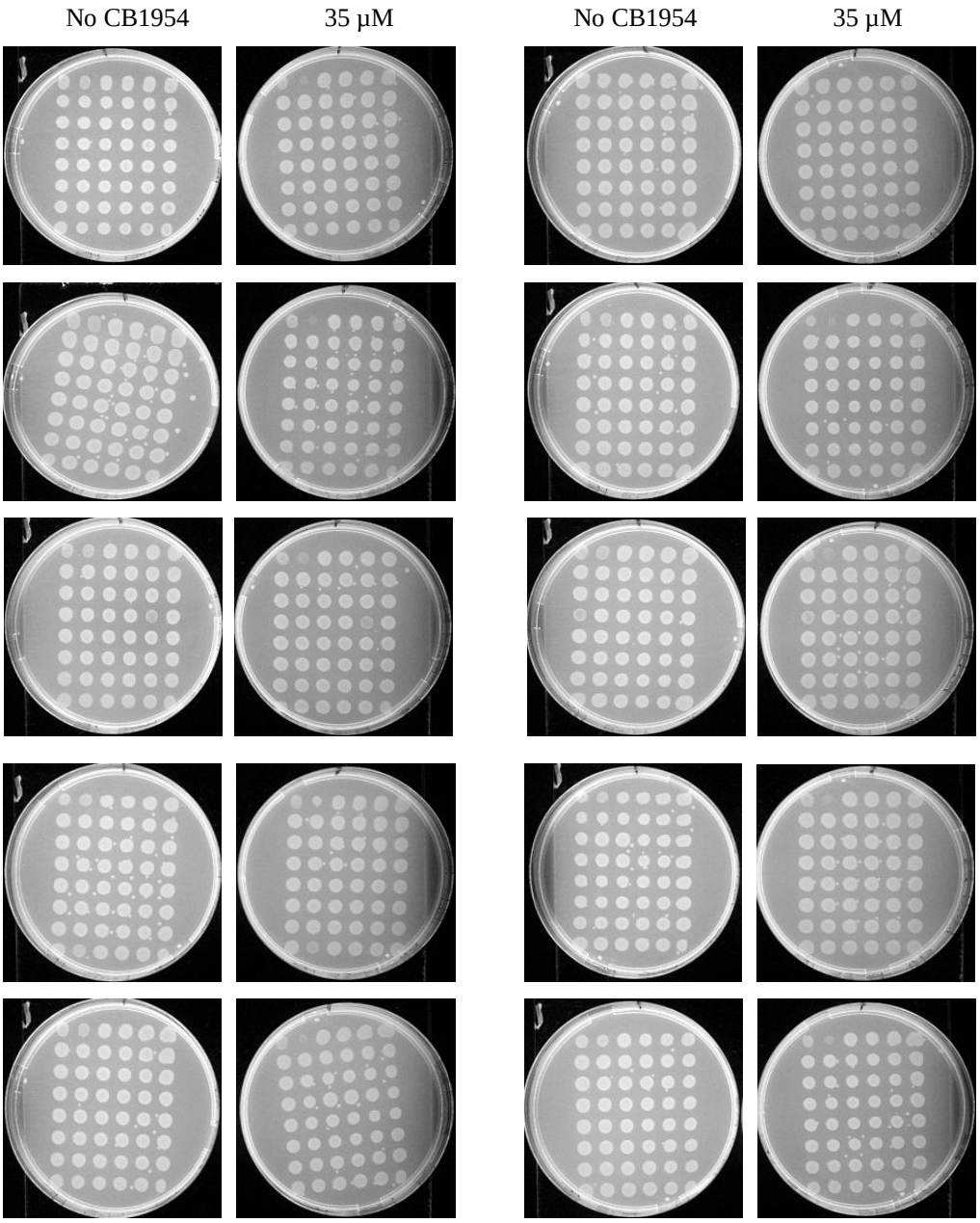

Figure 4.24 Replica plating of individual lysogens after seven rounds of selection using 10 µM CB1954

No CB1954 and 35 µM CB1954 was used for replica plating. The first two lysogens on the top left of each plate are controls WT and T41G N71S respectively.

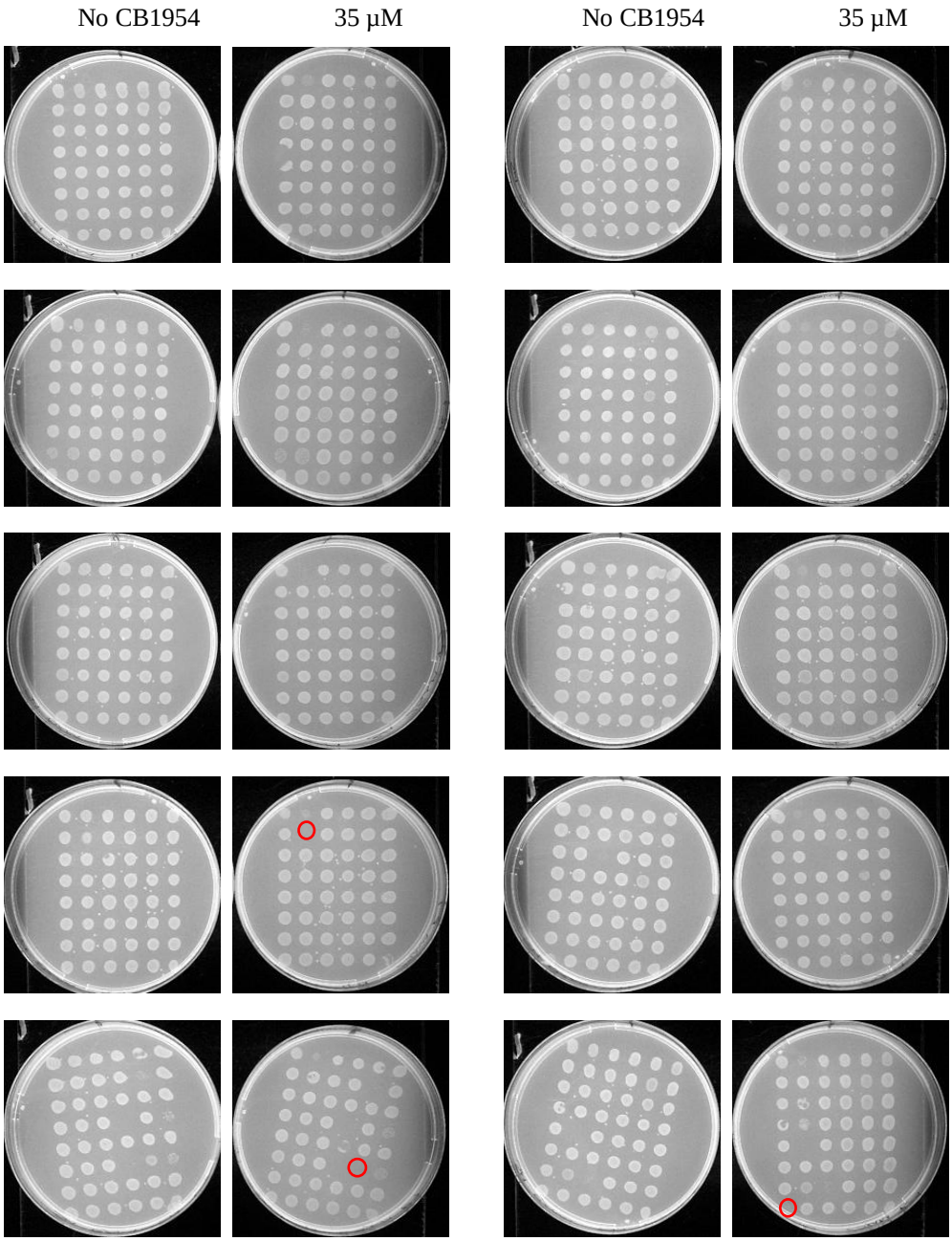

Figure 4.25 Replica plating of individual lysogens after seven rounds of selection using 25 µM CB1954
No CB1954 and 35 µM CB1954 was used for replica plating. The first two lysogens on the top left of each plate are controls WT and T41G N71S respectively. The red circles indicate where lysogens have disappeared

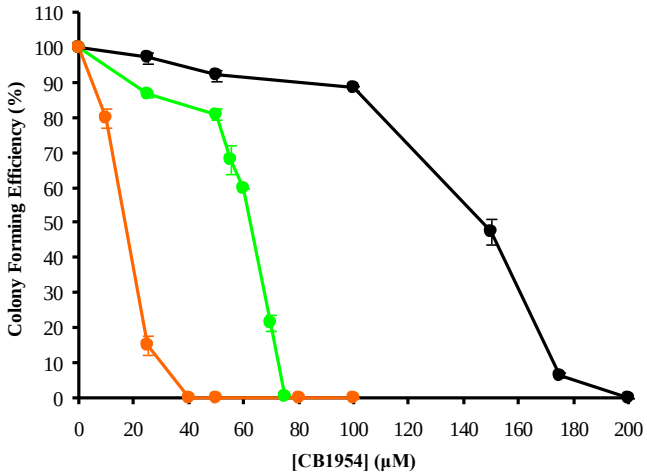

Figure 4.26 CB1954 IC_{50} Assay of selected lysogen N71S A113V R121V F123N F124V A125C K179R (clone 282)
Lysogenic cultures were spread onto plates containing a range of CB1954 concentrations, and the number of colonies on each plate counted after overnight growth. The numbers of colonies were compared to plates with no prodrug. Clone 282 (orange), N71S (green) and WT (black)

4.3.6.3 Sequencing of random clones from selected and unselected library to check representation

Due to the limited increase in CB1954 sensitivity of the library it was decided to test random clones after selection to check mutant representation. Twenty plaques were screened by PCR to detect NTR insert. All twenty plaques were found to have inserted NTR (*NfsB*) genes. The NTR genes for each was then sequenced (see Table 4.2). Fifteen different mutants were observed. Eight mutants had single nucleotide deletions resulting in a frame-shift. Deletions were observed at residues R121, F123, A125 and M127.

The high incidence of frame-shift mutations following selection was surprising. Therefore twenty four clones from the unselected library (four from each of the amplified sub-libraries) were also sequenced (see Table 4.3). Twenty one of the twenty four gave clear sequences. However only nine encoded full length NTR, seven have frame-shift single nucleotide deletions, which were seen at residues P110, F123, F124, A125, D126 and M127. Two mutants had deletions at more than one residue. The remaining five mutants had at least one stop codon. Furthermore four NTR sequences were seen more than once, this was highly unlikely to happen by chance, either each sub-library failed to contain the diversity that was expected or only a small proportion of each sub-library was retrieved following amplification. Therefore twenty four clones from the unselected library prior to amplification (four from each of the un-amplified sub-libraries) were then sequenced (see Table 4.4). Twenty two of the twenty four clones encoded full length NTR, with the remaining two having stop codons at either R121 or A125. No two NTR sequences were the same, therefore good diversity was seen for each initial sub-library and amplification must have only expanded a small proportion of each sub-library.

Amino Acid substitutions	Number of mutants	Codon Usage
T41Q N71S F123V F124A A125S M127 deletion D135G	4	V = GTG A = GCC S = TCG G = GGT (4)
T41Q N71S R121 deletion F123L F124S A125H	1	L = TTG S = AGC H = CAG
T41Q N71S A113V R121F F124D A125C G177G	1	V = GTG F = TTC D = GAC C = TGC G = GGC
T41Q N71S F123 deletion F124G A125 deletion D126R D135G	1	G = GGC R = CGG G = GGT
T41Q N71S R121V F123V F124T A125Y	1	V = GTC V = GTG T = AAC Y = TAC
T41N N71S F123V F124A A125S M127 deletion D135G	1	V = GTG A = GCC S = TCG G = GGT
T41L N71S R121Y F124G A125L	1	Y = TAC G = GGC L = CTG
E25G T41L N71S A113V R121V F123L F124P	1	G = GGA V = GTG V = GTC L = TTG P = CCG
T41G N71S	1	-
N71S R121L F123S F124S A125W V143A	2	L = CTC S = TCC S = TCC W = TGG A = GCT (2)
N71S R121A F123L F124G A125Q	1	A = GCG L = CTC G = GGC Q = CAG
A113V R121L F123I F124T A125S	1	V = GTG L = CTC I = ATC T = ACG S = TCG
R121A F123N F124S A125E K141E	1	A = GCC N = AAC S = AGC E = GAG E = GAA
R121Y F123 STOP F124Y A125 deletion V191E	1	Y = TAC STOP = TAG Y = TAC E = GAA
R121C F123I F124S A125F	1	C = TGC I = ATC S = AGC F = TTC
F124N	1	N = AAC

Table 4.2 Summary of sequenced NTR mutants following eight rounds of selection at 25 μM
Targeted amino acid substitutions are shown in black, single residue frame-shift deletions in red and non-targeted mutations in blue

Amino Acid substitutions	Number of mutants	Codon Usage
R121W F123I F124S A125 STOP	2	TGG = W ATC = I AGC = S TAG = STOP
R121V F123Y F124Y A125Q	1	GCT = V TAC = Y TAC =Y CAG = Q
SEQUENCE FAILED	1	-
N71S REST OF SEQUENCE FAILED	2	-
N71S K87R R121C F123T F124K A125L	1	AGA = R TGC = C TCG = T AAG = K CTG = L
N71S A113V D118N R121F F123L F124H A125 STOP	1	GTG = V AAT = N TTC = F CTC = L CAC = H TAG = STOP
T41L N71S P110 - D126 several deletions	1	-
T41L N71S R121I F123F F124K A125F	1	ATC = I TTC = F AAG = K TCC = F
T41L N71S R121F F123V F124S A125S W138R	1	TTC = F GTC = V AGC = S TCT = S CGG = R
T41L N71S R121F F123L F124 STOP A125Y P206L	1	TTC = F TTG = L TAG = STOP TAC = Y CTG = L
I4T T41N N71S R121D F123N F124 STOP A125S	2	ACT = T GAC = D AAC = N AGC = STOP TCG = S
T41N N71S	1	-
T41N N71S R121Y F123V F124H A125C	1	TAC = Y GTC = V CAC = H TGC = C
T41Q N71S R121R F123V F124A A125S M127 deletion D135G	2	AGG = R GTG = V CCC = A TCG = S G = GGT
T41Q N71S R121H F123V F124N A125Y	1	CAC = H GTC = V AAC = N TAC = Y
T41Q N71S R121S F123V F124 - D126 deletion	1	TCG = S GTC = V
T41G N71S R121I F123A F124 deletion A125 deletion I164T	2	ATC = I GCC = A ACC = T
T41G N71S R121F F123F F124E A125S	1	TTC = F TTC = F GAG = E TCC = S
T41G N71S R121I F123 deletion F124R A125 deletion	1	ATC = I CGG = R

Table 4.3 Summary of sequenced NTR mutants, with four from each sub-library following liquid culture amplification
Targeted amino acid substitutions are shown in black, single residue frame-shift deletions in red and non-targeted mutations in blue

Amino Acid substitutions	Number of mutants	Codon Usage
A113V R121G F124N A125Y	1	GTG = V GGG = G AAC = N TAC = Y
S5P R121 STOP F123M A125V	1	CCT = P TAG = STOP ATG = M GTG = V
R121F F124L F124G A125N	1	TTC = F TTG = L GGC = G AAC = N
R121R F123L F124P A125G	1	CGG = R TTG = L CCC = P GGC = G
N71S R121F F123S F124T A125C	1	TTC = F AGC = S ACC = T TGC = C
N71S A113V R121F F123S F124I A125R	1	GTG = V TTC = F TCC = S ATC = I CGC = R
N71S A113V K119T R121Y F123D F124A A125C	1	GTG = V ACA = T TAC = Y GAC = D GCC = A TGC = C
N71S A113V F123M F124Y A125Y	1	GTG = V ATG = M TAC = Y TAC = Y
T41L N71S R121Y F123W F124G A125 STOP	1	TAC = Y TGG = W GGC = G TAG = STOP
T41L N71S R121M F123C F124M A125L	1	ATG = M TGC = C ATG = M TTG = L
T41L N71S H80Y R121Y F123M F124R A125S	1	TAC = Y TAC = Y ATG = M CGC = R TCC = S
T41L N71S R121E F123L F124S A125L	1	GAG = E TTG = L AGC = S CTC = L
T41N N71S R121V F123I F124S A125F	1	GTC = V ATC = I AGC = S TTC = F
T41N N71S R121S F123L F124A A125Y	1	TCC = S TTG = L GCG = A TAC = Y
T41N N71S R121P F123V F124P A125S	1	CCC = P GTG = V CCC = P TCG = S
M1V T41N N71S R121Y F123T F124E A125C	1	GTG = V GAC = Y ACC = T GAG = E TGC = C GAC = D
T41Q N71S R121V F123V F124S A125P	1	GTC = V GTG = V TCC = S CCC = P
T41Q N71S A113V R121C F123L F124G A125S	1	GTG = V TGC = C CTC = L GGC = G TCC = S
T41Q N71S T109S R121V F124T A125C	1	TCG = S GTG = V ACC = T TGC = C
Q6R T41Q N71S R121Y F123M F124R A125S	1	CGG = R TAC = Y ATG = M CGC = R TCC = S
T41G V50A N71S R121G F124G A125A	1	GCT = A GGC = G GGG = G GCG = A
T41G N71S R121L F123L F124S A125Y	1	TTG = L CTC = L TCC = S TAC = Y
T41G N71S R121I F123C F124Y A125C	1	ATC = I TGC = C TAC = Y TGC = C
T41G N71S R121F F123L F124D A125W	1	TTC = F CTG = L GAC = D TCG = W

Table 4.4 Summary of sequenced NTR mutants, with four from each start sub-library prior to liquid culture amplification
Targeted amino acid substitutions are shown in black and non-targeted mutations in blue

4.3.6.4 Validation of library amplified by plate lysate

Amplification by liquid culture failed to maintain diversity within the library. An alternative approach which has been used previously (Chapter 3) used amplification by plate lysate. Phage plaques spread out across the agar plates, ensuring no loss in diversity. 3×10^6 pfu of phage stock for each sub-library was amplified using 1×10^6 pfu to infect bacteria spread as a lawn in top agar on each of three 10 cm plates. A total of 7 ml of amplified stock was retrieved from each sub-library. Plaque yields before and after amplification are shown in Table 4.5

Template	Initial phage yield of independent clones (pfu total)	Number of possible nucleotide variants	Phage yield after amplification (pfu total)
WT	7.0×10^6	1.05×10^6	2.7×10^9
N71S	1.4×10^7	1.05×10^6	1.1×10^9
T41L N71S	8.0×10^6	1.05×10^6	1.4×10^9
T41N N71S	9.0×10^6	1.05×10^6	1.3×10^9
T41G N71S	3.1×10^6	1.05×10^6	3.9×10^9
T41Q N71S	4.8×10^6	1.05×10^6	1.8×10^9

Table 4.5 Initial phage yield of independent clones, number of possible nucleotide variants and phage yield after amplification by plate lysate

Four individual plaques from each amplified sub-library were sequenced (see Table 4.6). Twenty out of the twenty four plaques encoded full length NTR. Two had stop codons at either R121 or A125 and a further two had frame-shift deletions. Although there were two frame-shift deletions this is substantially lower than previously seen, and no duplicate sequences were seen. These plate lysate amplification stocks were therefore used for a further attempt at library selection.

Amino Acid substitutions	Number of mutants	Codon Usage
R121A F123L F124Q A125S	1	GCG = A CTC = L CAG = Q TCC = S
R121L F123L F124R A125 STOP	1	TTG = L CTG = L CGC = R TAG = STOP
R121I F123 STOP F124T A125Y F199S	1	ATC = I TAG = STOP ACC = T TAC =Y TCT = S
R121N F123 - A125 deletions	1	AAC = N
N71S R121L F123C F124C A125W	1	CTG = L TGC = C TGC = C TGG = W
N71S K74R R121F F123L F124I A125Q	1	AGA = R TTC = F CTG = L ATC = I CAG = Q
N71S R121L F123C F124Q A125C	1	CTC = L TGC = C CAA = Q TGT = C
N71S R121L F123S F124C A125W	1	CTG = L AGC = S TGC = C TGG = W
T41L N71S R121L F123L F124Y A125 deletion	1	TTG = L TTG = L TAC = Y
S5P T41L N71S R121V F123V F124N A125C Q142R	2	CCT = P GTC = V GTG = V AAC = N TGC = C CGG = R
A7V T41L N71S R121T F123L F124R A125S	1	GTC = V ACC = T CTC = L CGG = R TCC = S
T41N N71S R121L F123C F124T A125C	1	TTG = L TGC = C ACG = T TGC = C
T41N N71S R121P A125Y	1	TTC = P TAC = Y
T41N N71S R121I F123L F124L A125W	1	ATC = I TTG = L CTG = L TGG = W
T41N N71S R121F F123L F124K A125F	1	TTC = F TTG = L AAG = K TTC = F
T41Q N71S A113V R121L F123L F124N A125H	1	GTG = V TTG = L CTG = L AAC = N CAC = H
T41Q N71S R121L A125R	1	CTC = L CGG = R
T41Q N71S R121D F123A F124T A125S	1	GAC = D GCG = A ACC = T TCC = S
T41Q N71S A113V R121L F123E F124P A125Y M139V	1	GTG = V TTG = L GAG = E CCG = P TAC = Y GTG = V
T41G N71S R121V F123S F124R A125F	1	GTC = V TCC = S CGG = R TCC = F
T41G N71S R121P F123P F124H A125Y P209L	1	CCC = P CCC = P CAC = H TAC = Y CTG = L
T41G N71S A113V R121 STOP F123H F124S A125L	1	GTG = V TAG = STOP CAC = H TCG = S CTG = L
T41G N71S R121F F123W F124P A125 STOP K181R	1	TTC = F TGG = W CCC = P TAG = STOP AGA = R

Table 4.6 Summary of sequenced NTR mutants, with four from each sub-library amplified by plate lysate
Targeted amino acid substitutions are shown in black, single residue frame-shift deletions in red and non-targeted mutations in blue

4.3.7 Selection 2

6.0 x 10^9 pfu of phage were infected into 1.5 x 10^{10} UT5600 cells to generate lysogens for selection (containing 1.0 x 10^9 pfu of phage from each sub-library). Selection followed as Figure 3.9. The library was taken through twenty rounds of selection at 25 µM, 50 µM, 75 µM or 100 µM in parallel. Phage release at each round of selection was measured (see Figure 4.27).

As previously in this chapter background release of phage was determined by exposing the culture to no CB1954. After 1 round of selection with CB1954, phage release was as expected with increased release of phage induced by increasing concentrations of CB1954 up to 75 µM. This wasn't observed with 100 µM CB1954 which gave the lowest release of phage. For subsequent rounds of selection, background phage release was determined separately for each lineage. Phage release was expected to increase when induced by increasing concentration of CB1954.

After 2 rounds of selection higher titres of phage were observed after induction with 25 µM and 50 µM. However lower phage release was observed for 75 and 100 µM. For each CB1954 concentration greater phage release was observed relative to background. Varying levels of background phage release was observed for each culture.

From round 3 onwards no obvious pattern of phage release was observed, relative to the CB1954 concentration used for induction.

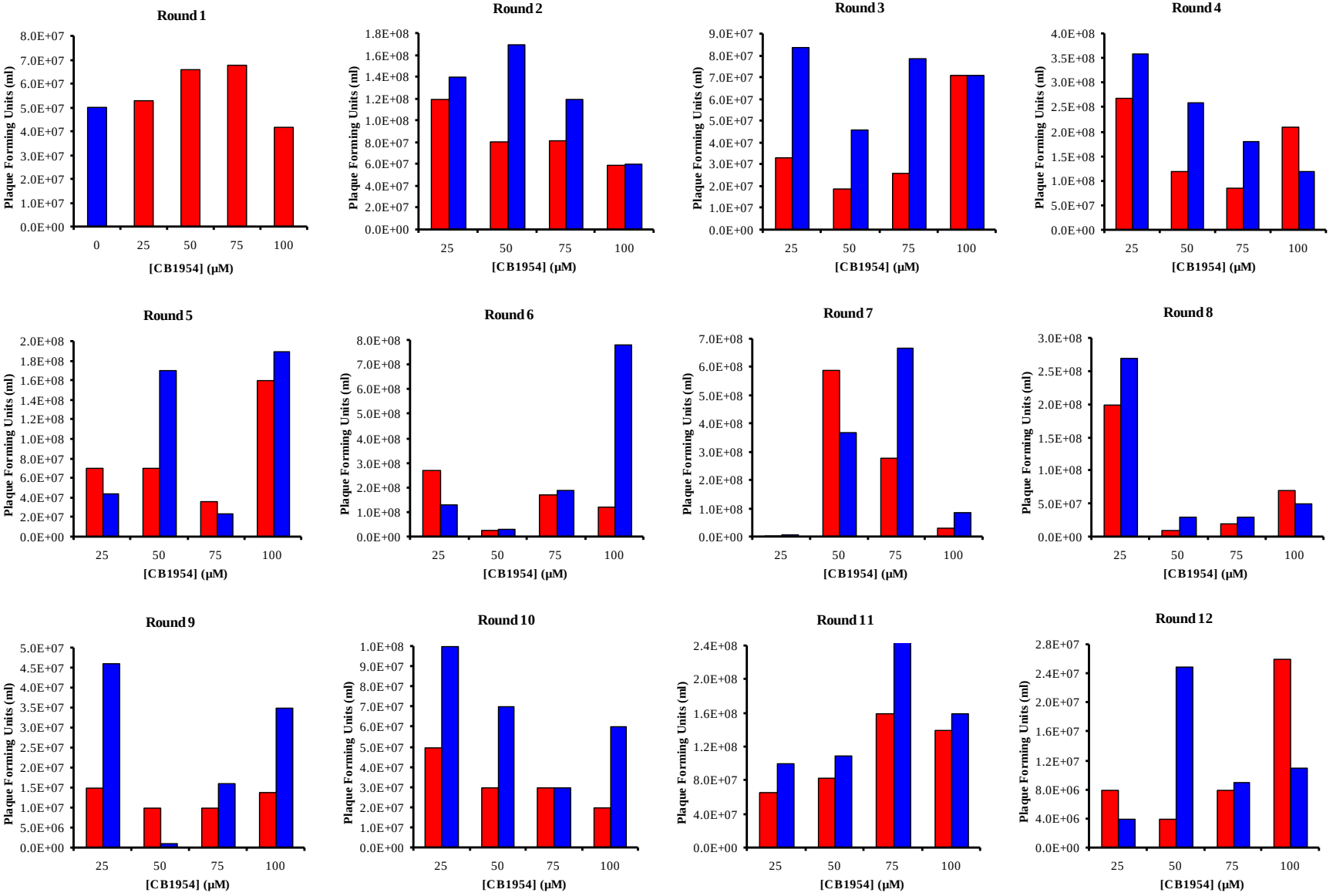
Round 1
Plaque Forming Units (ml)
8.0E+07
7.0E+07
6.0E+07
5.0E+07
4.0E+07
3.0E+07
2.0E+07
1.0E+07
0.0E+00
0
25
50
75
100
[CB1954] (µM)
Round 2
Plaque Forming Units (ml)
1.8E+08
1.6E+08
1.4E+08
1.2E+08
1.0E+08
8.0E+07
6.0E+07
4.0E+07
2.0E+07
0.0E+00
25
50
75
100
[CB1954] (µM)
Round 3
Plaque Forming Units (ml)
9.0E+07
8.0E+07
7.0E+07
6.0E+07
5.0E+07
4.0E+07
3.0E+07
2.0E+07
1.0E+07
0.0E+00
25
50
75
100
[CB1954] (µM)
Round 4
Plaque Forming Units (ml)
4.0E+08
3.5E+08
3.0E+08
2.5E+08
2.0E+08
1.5E+08
1.0E+08
5.0E+07
0.0E+00
25
50
75
100
[CB1954] (µM)
Round 5
Plaque Forming Units (ml)
2.0E+08
1.8E+08
1.6E+08
1.4E+08
1.2E+08
1.0E+08
8.0E+07
6.0E+07
4.0E+07
2.0E+07
0.0E+00
25
50
75
100
[CB1954] (µM)
Round 6
Plaque Forming Units (ml)
8.0E+08
7.0E+08
6.0E+08
5.0E+08
4.0E+08
3.0E+08
2.0E+08
1.0E+08
0.0E+00
25
50
75
100
[CB1954] (µM)
Round 7
Plaque Forming Units (ml)
7.0E+08
6.0E+08
5.0E+08
4.0E+08
3.0E+08
2.0E+08
1.0E+08
0.0E+00
25
50
75
100
[CB1954] (µM)
Round 8
Plaque Forming Units (ml)
3.0E+08
2.5E+08
2.0E+08
1.5E+08
1.0E+08
5.0E+07
0.0E+00
25
50
75
100
[CB1954] (µM)
Round 9
Plaque Forming Units (ml)
5.0E+07
4.5E+07
4.0E+07
3.5E+07
3.0E+07
2.5E+07
2.0E+07
1.5E+07
1.0E+07
5.0E+06
0.0E+00
25
50
75
100
[CB1954] (µM)
Round 10
Plaque Forming Units (ml)
1.0E+08
9.0E+07
8.0E+07
7.0E+07
6.0E+07
5.0E+07
4.0E+07
3.0E+07
2.0E+07
1.0E+07
0.0E+00
25
50
75
100
[CB1954] (µM)
Round 11
Plaque Forming Units (ml)
2.4E+08
2.0E+08
1.6E+08
1.2E+08
8.0E+07
4.0E+07
0.0E+00
25
50
75
100
[CB1954] (µM)
Round 12
Plaque Forming Units (ml)
2.8E+07
2.4E+07
2.0E+07
1.6E+07
1.2E+07
8.0E+06
4.0E+06
0.0E+00
25
50
75
100
[CB1954] (µM)

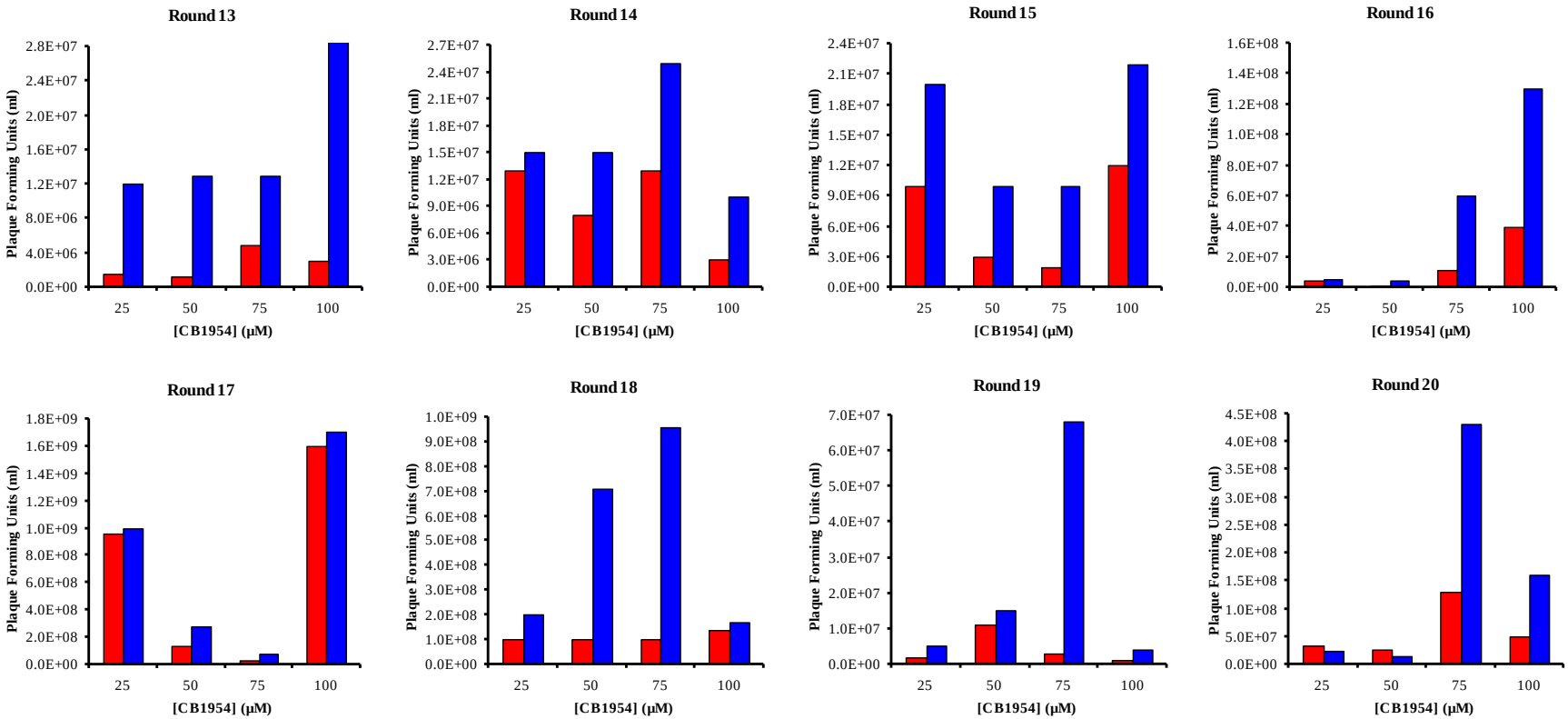

Figure 4.27 Phage release after 1-20 rounds of selection with 0 μM, 25 μM, 50 μM, 75 μM and 100 μM CB1954
Red columns indicate background phage release and blue columns indicate CB1954 induced phage release

4.3.7.1 Monitoring population sensitivity of the library under selection

The effect of selection was also monitored using a lysogen colony forming assay for each selection lineage, after three, seven, fourteen and twenty-one rounds of selection. The unselected library showed that almost all the lysogens were resistant to 200 μM CB1954. After three rounds of selection a small improvement was seen compared to the unselected library. Most improvement was seen with lysogens selected with 75 μM however 70% of the lysogens were still resistant to 200 μM CB1954 (see Figure 4.28a). After seven rounds of selection little difference was seen relative to three rounds (see Figure 4.28b). By fourteen rounds 60% of the lysogens selected with 75 μM were still resistant to 200 μM (see Figure 4.28c). No further improvement was seen after twenty-one rounds (see Figure 4.28d). Further selection is unlikely to improve the library further.

4.3.7.2 Screening CB1954 sensitivity of individual clones from selected library

230 individual lysogen colonies were picked from each of the lineages selected with 25 μM, 50 μM, 75 μM and 100 μM CB1954. Cultures were grown overnight in 96 well plates and replica plated onto agar plates containing no CB1954, 5 μM, 12 μM and 25 μM CB1954. All lambda lysogens showed strong growth in the absence of CB1954. None of the clones demonstrated any susceptibility to CB1954 within this range (see Appendix Figures 8.2-8.5).

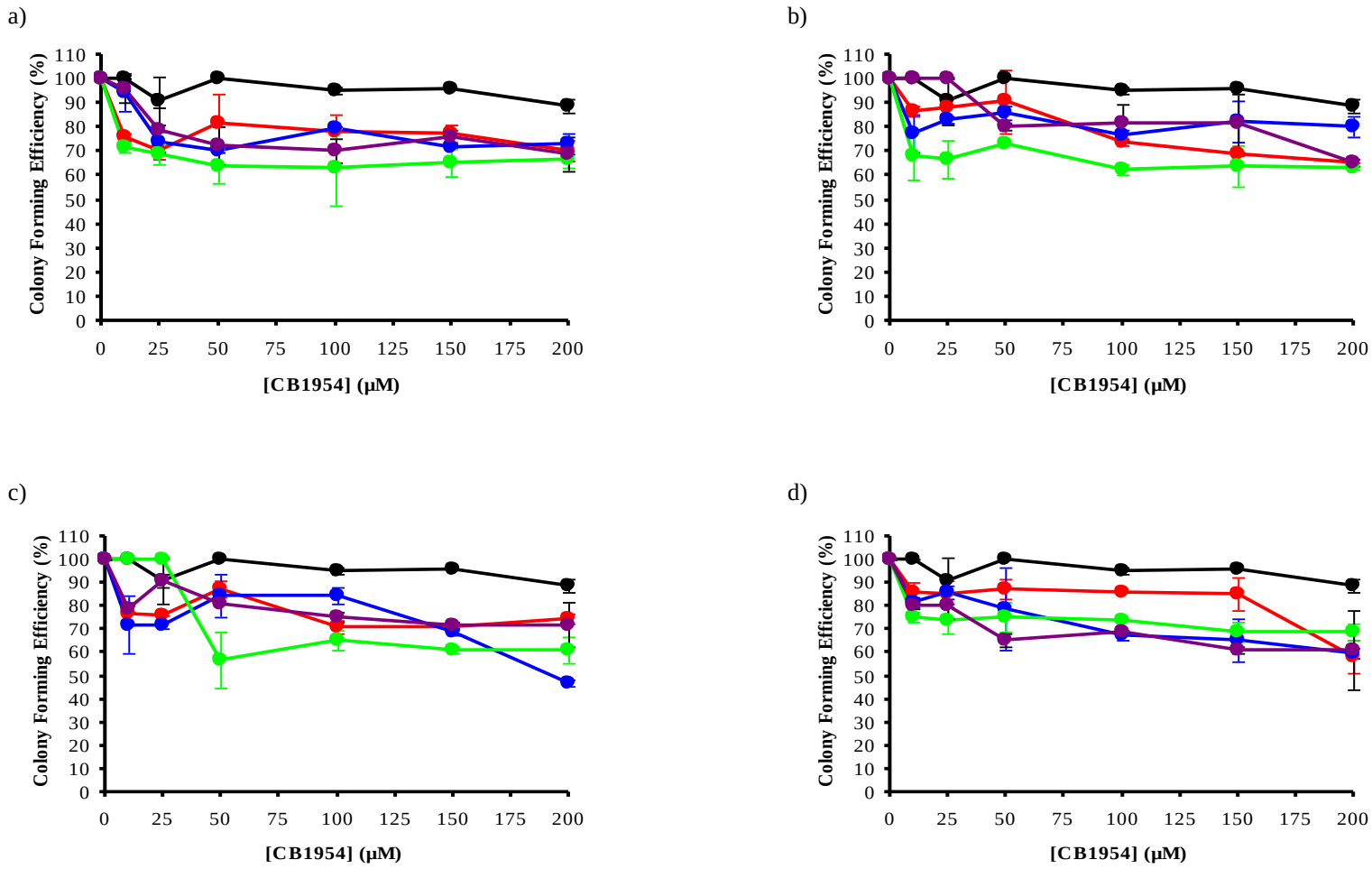

Figure 4.28 Dose Response curves for colony forming assay in UT5600 cells
a) Three rounds of selection, b) Seven rounds of selection, c) Fourteen rounds of selection, d) Twenty-one rounds of selection. Unselected (black), 25 µM CB1954 induction (red), 50 µM CB1954 induction (blue), 75 µM CB1954 induction (green) and 100 µM CB1954 induction (purple)

4.4 DISCUSSION

This chapter aimed at determining whether six residues around the active site were able to improve the efficiency of CB1954 activation. Mutant generation involved PCR using a degenerate primer, incorporating NNS at four out of five adjacent residues. Prior to cloning, the incorporated sequence diversity was checked by sequencing the PCR product. A good diversity of mutations were seen at each residue. However considerable difficulties were encountered at several steps in the generation of the library.

4.4.1 Phage lambda vector

4.4.1.1 Lambda growth

Initially phage λJG3J1 vector was grown following standard protocols by infecting C600 bacteria in the early stages of culture growth with a low innoculum of phage. The phages were expecting to go through several cycles of lytic growth, while the bacterial culture multiplied. By high culture density it was hoped that a large proportion of the bacteria would be lysed by the phage. However the amount of lysis was minimal, giving low yields of poor quality phage DNA. This was remedied by reducing the amount of lambda added to the culture, allowing the bacteria more time to multiply before being lysed. The optimum quantities of phage to bacterial cells were determined with 1×10^9 C600 cells being infected with $5 \times 10^5 - 1 \times 10^6$ pfu of phage.

4.4.1.2 Purification of lambda vector

Two techniques were tested for the purification of the lambda vector. Firstly a Qiagen lambda maxi kit method, which used ion exchange column to purify the PEG precipitated phage and secondly a more successful PEG precipitation and CsCl density gradient centrifugation method (Sambrook 1989). A clean single band of phage DNA was observed when using PEG and CsCl.

4.4.1.3 *Sfi* I digestion of lambda vector

The lambda vector was cut using *Sfi* I enzyme. It was essential to achieve complete *Sfi* I digestion, in order to minimise the amount of empty vector (original vector) phage carrying over into the library. However problems with partial digestion were encountered. This led to the use of two alternative methods as an attempt to overcome digestion problems: the first was to gel purify the correct, fully *Sfi* I digested fragments, and secondly to exploit the unique *Pac* I restriction enzyme site, included between the two *Sfi* I sites of the vector. However neither of these methods totally prevented carryover of empty vector.

4.4.1.4 Alternative vector

An alternative vector λSV054 that is a derivative of λJG3J1, which contains a DNA insert (*NfsA* gene) between the *Sfi* I sites was grown and digested, in the hope that it would *Sfi* I digest more efficiently than λJG3J1. Greater separation of *Sfi* I sites did improve the efficiency of *Sfi* I digestion, allowing libraries with no empty vector to be constructed.

4.4.1.5 *Lac* I expression

The effect of over-expression of *Lac* I repressor was examined, for the prevention of background leaky NTR expression. Two pET vectors expressing *Lac* I were compared in several bacterial cell lines. Western blot analysis showed that pET 21b was most efficient at reducing NTR expression and that IPTG was still able to induce NTR expression. Further experiments showed that over-expression of *Lac* I was able to reduce preferential growth of empty vector, without having a major effect on the dose-response with CB1954.

4.4.2 Selection

Two attempts at selection were undertaken with eight and twenty-one rounds performed. After every round of selection phage release was measured, initially increased release of phage was seen after induction by increasing concentrations of CB1954. However as selection proceeded no obvious phage release patterns were observed.

4.4.2.1 Population sensitivity

Population sensitivity was analysed by examining lysogen colony forming efficiency; this showed very little improvement relative to the starting library. Individual clones were screened for their sensitivity to CB1954. Only three clones showed any sensitivity; all three had the following amino acid changes N71S A113 R121V F123N F124V A125C K179R. IC_{50} assays showed that this clone has an IC_{50} of 20 µM. It is very unlikely that this mutant was the only good mutant in the starting library. The library should at least have contained several of the previously known good mutants such as T41L N71S, T41G N71S and T41Q N71S F124T.

Construction for this library was different from that in Guise *et al* 2007. Guise *et al* used multiple PCR reactions with several degenerate primers, before joining fragments together with flanking primers. However in this library a single large and intricate degenerate primer was used, making miss-priming and deletions in the mutagenic region more likely. In an attempt to prevent primer errors SH033A and SH033B were specially purified. Sequencing appeared to indicate that these primers had worked well with clear sequencing seen within mutagenic regions; however a large number of deletion frame shift mutation were seen when analysing individual clones. All these frame shift deletions were observed in primer regions.

Selection is not entirely clean, with some spontaneous phage release. If the frequency of beneficial mutants was low it is possible that the recovered phage were largely random. However it was expected that after multiple cycles of selection, the relative abundance of good mutants would increase. It is possible that uncontrolled spontaneous phage release interfered with the selection process.

The library generated in this chapter consisted of maximum diversity of 6.3×10^6 possible nucleotide combinations relative to 6.8×10^5 possible combinations for Guise *et al.* 2007. It is possible that this library was too large for successful selection. In hind sight it may have been wiser to have performed selection separately for each sub-library, with each having a maximum diversity of 1.05×10^6. This was not possible for this thesis due to time constraints, but should be considered for future work when dealing with very large libraries.

CHAPTER 5: KINETIC STUDIES OF WT AND MUTANT NTR

5.1 INTRODUCTION

Nitroreductase is a flavoenzyme with tightly bound FMN cofactor. The enzyme's action is by a substituted, "ping-pong", mechanism, where the enzyme bound FMN is first reduced by NAD(P)H to $FMNH_2$ and the $NAD(P)^+$ product dissociates. A number of different substrates can then bind to the enzyme and be reduced by $FMNH_2$. NTR is highly soluble and stable and can easily be over expressed and purified from bacteria (Anlezark *et al.* 1992 and Lovering *et al.* 2001). Steady state kinetic assays have determined the Michaelis constants of WT NTR with a range of substrates (Anlezark *et al.* 1992, Race *et al.* 2003 and Zenno *et al.* 1996b). Several NTR mutants have also been kinetically analysed (Jaberipour 2005, Race *et al.* 2007 and Jarrom 2008).

During this study, a number of improved NTR mutants have been generated and tested in bacterial cells, see Chapters 3 and 4. The aim of the work in this chapter was to purify and kinetically characterise the two double mutants T41G N71S and T41L F70A and the multiple mutant N71S A113V R121V F123N F124V A125C K179R (clone 282). It should be noted mutant T41L F70A was generated by Mansooreh Jaberipour (Jaberipour 2005). This mutant showed promise in tissue culture assays and therefore kinetic characterisation was considered useful. The three mutants were compared to WT NTR, the single mutant F124N, the double mutant T41L N71S and the triple mutant T41Q N71S F124T which had previously been characterised. Kinetic parameters were determined with CB1954, nitrofurazone and menadione as substrates.

5.2 MATERIAL AND METHODS

5.2.1 NTR expression

5.2.1.1 Plasmid construction

λ lysogens encoding desired NTR mutants were streaked onto LB plates containing a fresh lawn of *E. coli* UT5600. The resulting lysis area was picked and used to provide a template for a PCR reaction, using Kod polymerase with primers JG2A and JG2B (see Section 2.2.1) to generate NTR PCR fragments. PCR products were resolved by agarose gel electrophoresis to confirm that DNA fragments of the correct size had been amplified, and purified using Roche High Pure PCR Product Purification Kit (Roche Applied Sciences, Germany).

A plasmid vector pET 24c was digested with *Nde* I and *Bam* HI and the appropriate size fragment was extracted using Qiagen QIA-Quick Gel Extraction Kit (Qiagen, West Sussex). The NTR PCR products were sequentially digested with *Nde* I and *Bam* HI before ligation with the digested pET 24c (0.2 pico moles of PCR insert with 200 ng plasmid vector) and transformed into competent *E. coli* XL-2 blue cells. Individual colonies were picked and grown in 10 ml of LB Broth containing kanamycin. Mini Prep plasmid purification was performed on the bacterial cultures and the resulting plasmids were digested with *Nde* I, *Eco* RV and *Bgl* II and analysed by agarose gel electrophoresis (see section 2.2.14). Plasmids with correct digestion patterns were taken on to large-scale 300 ml cultures. Bulk Prep purification was performed on the bacterial cultures (see section 2.2.15) and aliquots of the resulting plasmid preps were again digested with *Nde* I, *Eco* RV and *Bgl* II. Plasmids with correct digestion patterns were linearised with *Hind* III and the inserted NTR gene sequenced with primers PS1013A and PS1013B (see section 2.2.1).

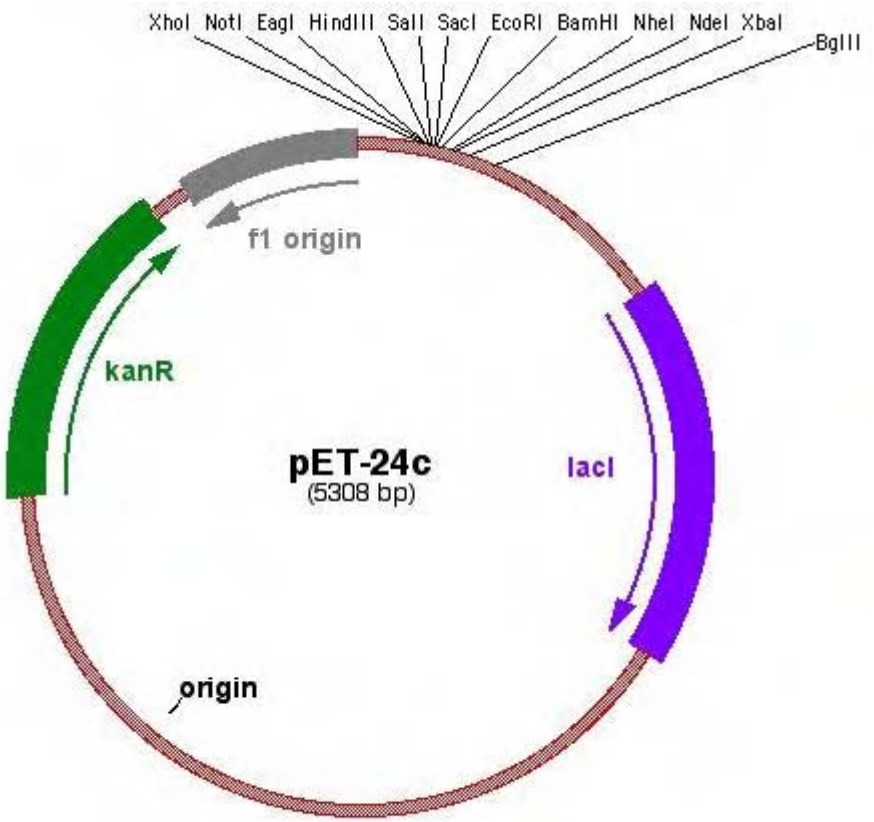

Figure 5.1 Schematic diagram of plasmid pET 24c vector
Plasmid pET 24c is a high level vector that contains a bacteriophage T7 promoter and terminator, allowing large amounts of protein to be generated. This plasmid was designed for the expression of open reading frames from multiple cloning sites, in this case insertion of NTR between *Nde* I and *Bam* HI sites

5.2.1.2 Bacterial growth and protein Induction

1 µl (200 ng) of undigested plasmid DNA construct pET 24c encoding mutant NTR was transformed into *E. coli* BL21 λDE3. These cells allow over-expression of mutant NTR as the λDE3 encodes T7 RNA Polymerase (RNAP). A single colony was picked for each mutant and grown at 37 ^{o}C overnight in 50 ml LB Broth containing kanamycin as a starter culture. 10 ml of this initial culture was used to inoculate 1 litre of LB kanamycin and left to shake at 37 ^{o}C until an OD_{600} of approximately 0.6 was reached. Absorbance readings were taken on an Eppendorf Biophotometer. Expression of NTR was induced by the addition of IPTG to a final concentration of 1 mM. Subsequently, the cells were grown for a further 4 hours and harvested by centrifugation at 8000x g for 20 minutes. Pelleted cells were frozen at -20 ^{o}C to facilitate cell wall weakening and aid lysis.

5.2.2 Preparation of crude extract

The cells and all cell suspensions were incubated on ice during the preparation of the extract. 4 ml of lysis buffer (20 mM sodium phosphate pH 7.0, 10 µg/ml DNase I, 10 µg/ml RNase A, 10 µg/ml PMSF and 20 µM FMN) was added per gram of cells. The cells were gently resuspended using a rubber teat on the end of a glass rod, and were broken open by sonication for approximately 2.5 minutes using 4 cycles of 20 seconds pulse, 20 seconds pause. The lysed cells were then centrifuged at 8000x g for 20 minutes (MSE Europa) and the supernatant collected. Ammonium sulphate was added to the supernatant to a final concentration of 0.5 M. A distinct gold colour was observed. This was followed by a further centrifugation step at 8000x g for 20 minutes (MSE Europa). The resultant gold supernatant was then filtered through a 0.45 µm filter.

5.2.3 Purification of crude extract

5.2.3.1 Phenyl sepharose column (Hydrophobic interaction column)

Phenyl sepharose columns bind NTR at high ionic strength allowing the removal of the majority of contaminating proteins before elution from the column at low ionic strength. The phenyl sepharose column (50 ml in volume) was pre-equilibrated with 20 mM sodium phosphate (pH 7.0), 0.5 M ammonium sulphate and 50 µM FMN. The cell extract (~51 ml from 1 litre) was applied onto the column at room temperature and washed with the same buffer containing 10 µg/ml of PMSF (flow rate of ~31.2 ml/hr). The absorbance of each fraction was measured at 280 nm (this monitors the protein content). Once the absorbance of the fractions approached zero, the bound protein was eluted with 10 mM Tris (pH 7.0), 50 µM FMN and 10 µg/ml PMSF. Fractions containing NTR were identified by absorbance (280 nm) and activity (550 nm). Peak fractions containing NTR were pooled.

5.2.3.2 Q-sepharose column (Ion Exchange column)

Q-sepharose is an ion exchange column that uses a linear NaCl gradient. The Q-Sepharose column (50 ml in volume) was pre-equilibrated with 20 mM Tris HCl (pH 7.0), 50 µM FMN and 10 µg/ml PMSF. The pooled fractions from the Phenyl Sepharose column were diluted with the above buffer (final volume of ~75 ml) to reduce the conductivity to 4.5. The sample was loaded onto the column (flow rate of ~36 ml/hr). The column was eluted with a gradient of 0.1 M NaCl buffer to 0.3 M NaCl buffer 80 ml and 15 minute fractions collected. Absorbance at 280 nm and activity at 550 nm were measured for each fraction as well as the conductivity.

Conductivity of gradient buffers at 4 ^{o}C:

0.1 M NaCl / 20 mM Tris/20 µM FMN/ PMSF = 4.5

0.5 M NaCl / 20 mM Tris/20 µM FMN/ PMSF = 12

1 M NaCl / 20 mM Tris/20 µM FMN/ PMSF = 32

5.2.4 Concentration of NTR protein

NTR pools were concentrated using an Amicon series 8000 50 ml or 3 ml capacity stirred ultrafiltration cell (Millipore, UK). YM10 membrane was used and each protein was concentrated to a final concentration of approximately 2.5 mg/ml.

5.2.5 Determination of protein concentration

NTR protein concentrations were estimated from the absorbance at 280 nm using an extinction coefficient of 43,000 M^{-1} cm^{-1} (Race *et al.* 2005), which was determined by calculation of amino acid composition and flavin content, or by Bradford Assay using UV absorbance at 595 nm. Standard curves were prepared from a BSA stock 1 mg/ml using a range from 0-10 µg. (Bradford 1976).

5.2.6 SDS PAGE

Gels were prepared using Biorad apparatus (Biorad, Hemel Hempstead), see section 2.4.2. Samples were diluted 1:1 with Laemmli loading buffer (4% SDS, 20% glycerol, 10% β-mercaptoethanol, 0.0004% bromophenol blue and 0.125 M Tris HCl) and run alongside Biorad Broad range molecular weight markers to verify molecular weights (Laemmli 1970). The gels were run at 100 volts for approximately 2 hours. SDS Page gels were stained in Coomassie Blue R-250 (2.5 g in 1L 50% Methanol, 10% Glacial Acetic Acid) for 2 hours and then destained overnight (in 10% Glacial Acetic Acid, 40% Methanol and 50% Water) to remove excess stain. Several changes of destain were required. The fully destained gels were dried between sheets of cellulose for 2 hours using a gel dryer.

5.2.7 NTR activity and specific activity

The activity of NTR was determined using assays with 100 µM NADH (in 10 mM Tris pH 8.0) and 200 µM Menadione (in DMSO) as enzyme substrates in the presence of 100 µM cytochrome c and 10 mM Tris HCl buffer (pH 7.0). The reaction was initiated by the addition of a small volume of purified NTR and activity determined by measuring reduction of cytochrome c at 550 nm (on Kontron Uvikon 923 spectrophotometer) for 3 minutes at 25 ^{o}C. Each $2e^{-}$ electron reduction of Menadione leads to two single-electron reductions of cytochrome c.

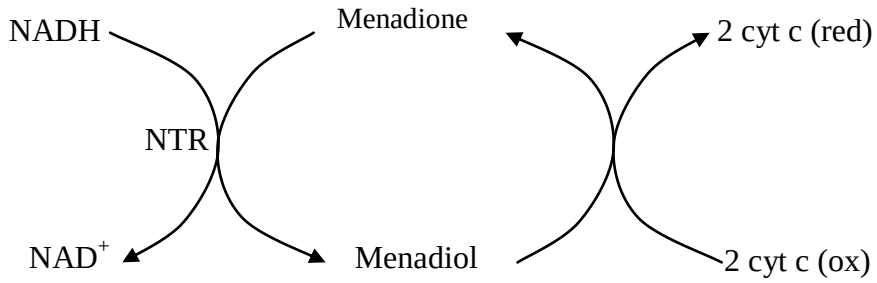

The specific activity of NTR was calculated using the cytochrome c extinction coefficient of 27,000 M^{-1} cm^{-1}.

$$Specific\ Activity = \frac{Change\ OD_{550}}{(\varepsilon\ cyt\ c)\,\mathrm{x}\,[protein]\,\mathrm{x}\,\mu l\ NTR\ used}\,\mathrm{x}\,1000\,(s^{-1})$$

5.2.8 Preparation of dialysis tubing

All dialysis tubing was prepared by boiling for 10 minutes in a litre of water containing 0.1 mM EDTA, 0.1% v/v β-mercaptoethanol and 10-20 mg of sodium bicarbonate. Boiled tubing was rinsed with sterile water and stored at 4 ^{o}C.

5.2.9 Kinetic assays

Initial velocity studies of WT and mutant NTR were performed using a series of spectrophotometric assays (using Kontron Uvikon 923 spectrophotometer) for substrates CB1954, nitrofurazone and menadione, using NADH as cofactor. The menadione assay was coupled with 100 µM cytochrome c. This allows menadione to be recycled preventing substrate inhibition.

Changes Monitored	Substrate	$\lambda_{reaction}$ nm	ε at $\lambda_{reaction}$ M^{-1} cm^{-1}	$\lambda_{[substrate]}$ nm	ε at $\lambda_{[substrate]}$ M^{-1} cm^{-1}
2 and 4 hydroxylamine formation	CB1954	420	1,200	327	12,000
Nitrofurazone reduction	Nitrofurazone	440	880	400 420	12,960 5,590
Cytochrome C reduction	Menadione	550	27,000	340 363 251	2,480 15,100 17,400

Table 5.1 Spectrophotometric changes monitored during enzyme kinetics studies and extinction coefficient used at respective wavelengths
Two different λ values are shown for each substrate. These show the wavelength for the substrate and the product(s) of the reaction

Table 5.1 shows the wavelengths used for the reduction of substrates and the extinction coefficients for determining substrate concentrations and for calculation of rates. Reactions were carried out using 0.5 and 1 cm path length cuvettes. Different path lengths were used to reduce background absorbance when high substrate concentrations were required. All reactions were performed in 10 mM Tris HCl pH 7.0, 5% DMSO at a constant temperature of 25 ^{o}C using a circulating water bath. It has been reported that DMSO concentrations of more than 5% (total volume) can inhibit NTR reactions (Anlezark *et al.* 1992) Reactions were initiated by the addition of 2-4 µl (1-50 nM) of ice cold enzyme. All substrates used were dissolved in 90% DMSO, 10% 100 mM Tris pH 7.0.

Rates of reaction were measured in duplicate over a range of substrate concentrations, ranging from 0.5-5 times K_m or as high as substrate concentration permitted by solubility. Direct linear plots were used to estimate initial K_m of NTR mutants to design experiments.

Rates were measured varying one substrate concentration [A] while keeping the other substrate concentration constant. For example varying NADH while keeping CB1954 constant. The v_i (initial rate) and [A] were then fitted to a simple single-substrate Menten equation where [E] is the enzyme concentration (see Equation 5.1).

$$\frac{v_i}{[\mathrm{E}]} = \frac{k_{catapp}[\mathrm{A}]}{K_{mAapp}+[\mathrm{A}]} \quad \textbf{Equation 5.1}$$

The parameter to fit this equation estimates the k_{catapp} (the number of cycles a single enzyme molecule undergoes per unit of time), and the K_{mAapp} (the concentration of substrate A at which the initial rate is half of its possible maximum).

When looking at a "ping pong" mechanism however, these values are dependent on the concentration and kinetic parameters of the fixed substrate B (see Equations 5.2 and 5.3).

$$K_{mAapp} = \frac{K_{mA}[\mathrm{B}]}{K_{mB} + [\mathrm{B}]} \quad \textbf{Equation 5.2} \quad \text{and} \quad k_{catapp} = \frac{k_{cat}[\mathrm{B}]}{K_{mB} + [\mathrm{B}]} \quad \textbf{Equation 5.3}$$

This is why they are described as apparent k_{cat} and K_m (K_{catapp} and K_{mapp}). However for this mechanism, k_{cat}/K_m remains constant at various concentrations of substrate B (Engel 1981).

When apparent k_{cat} or K_m cannot be correctly estimated the k_{cat}/K_m can be determined by fitting to a modified Equation 5.4

$$\frac{v_i}{[\mathrm{E}]} = \frac{k_{catapp}[\mathrm{A}]}{\left(\frac{k_{cat}}{k_{cat}/K_{mA}}\right) + [\mathrm{A}]} \quad \textbf{Equation 5.4}$$

When several plots have been determined at a range of substrate concentrations, it is possible to obtain the overall kinetic parameters by means of a global fit which describes the full "ping pong" reaction (see Equation 5.5).

$$\frac{v_i}{[E]} = \frac{k_{cat}[A][B]}{K_{mA}[B] + K_{mB}[A] + [A][B]}$$ **Equation 5.5**

Again it is possible to estimate the k_{cat}/K_m of each substrate independently by fitting k_{cat}/K_m as an independent parameter (see Equation 5.6).

$$\frac{v_i}{[E]} = \frac{k_{cat}[A][B]}{\left(\frac{k_{cat}}{k_{cat}/K_{mA}}\right)[B] + \left(\frac{k_{cat}}{k_{cat}/K_{mB}}\right)[A] + [A][B]}$$ **Equation 5.6**

5.2.10 Determining kinetic parameters

Sigma Plot 11 software package (SPSS, UK) was used to analyse all steady-state kinetic data using non-linear regression to fit to Michaelis Menten equation. Fitted data was analysed statistically by calculating t test and P values for each regression curve, t equals the ratio of the regression coefficient to its standard error, indicating how much the rate of the reaction depends on the K_m or k_{cat}. A large t value indicates that the data fits the equation and that the rate of reaction can be predicted from the parameters. The P value is the probability that the parameters fit the curve by chance, the smaller the P value the less likely it occurred by chance. Ideally P values should be < 0.05, which indicates a reliable fit to the experimental data.

5.2.11 Nuclear Magnetic Resonance

One-dimensional NMR spectra were collected at 500.18 MHz at 298K using a Bruker 500 spectrometer with a TXI cryoprobe. Typically 128 scans were collected with 32k data points, a sweep width of 12 ppm, and a relaxation delay of 1.5 seconds between scans. The H_2O and DMSO signals were reduced using excitation sculpting (Hwang and Shaka 1995).

NAD(P)H (1 mM final concentration) and CB1954 (0.5 mM final concentration, in 10% final DMSO) were mixed in 10 mM sodium phosphate buffer, pH 7.0, containing 10% D_2O. Approximately 0.1 μM of each enzyme was then added and the one-dimensional NMR spectrum taken within 5-10 minutes.

5.3 RESULTS

5.3.1 NTR expression

5.3.1.1 Plasmid construction

The genes of NTR mutants were recloned from λ lysogens into pET 24c using PCR amplification. PCR products were resolved by agarose gel electrophoresis to ensure DNA fragments of the correct size were amplified (see Figure 5.2). Bands of the correct size were the major products of each PCR reaction and were gel purified.

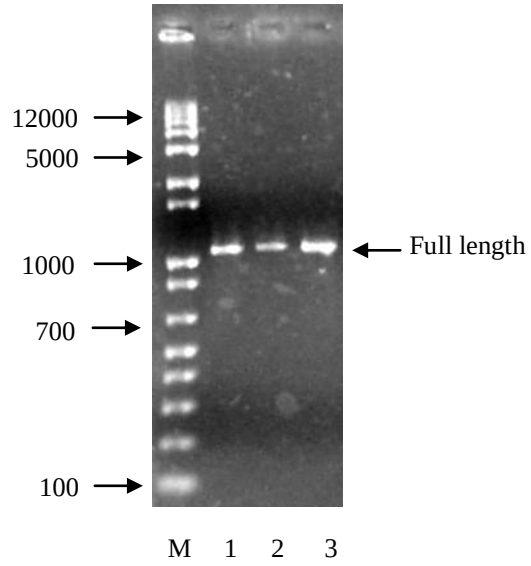

Figure 5.2 Agarose gel of PCR fragments for plasmid construction using primers JG2A and JG2B
Total PCR products amplified from λ phage. PCR products were run on 0.7% agarose gel. M = Marker 1 kb plus ladder, Lanes 1-3 NTR fragments T41G N71S, T41L F70A and 282 respectively. A single fragment of approximately 1000 bp observed for each PCR corresponding to full length gene

The purified PCR products were digested with *Nde* I and *Bam* HI before being ligated with *Nde* I and *Bam* HI digested pET 24c plasmid vector and transformed. Plasmids were isolated from individual colonies, and the resulting plasmid DNA digested with *Nde* I, *Eco* RV and *Bgl* II to check whether the correct plasmids were isolated. Digestion products were resolved by agarose gel electrophoresis (see Figure 5.3).

Plasmids with correct digestion patterns were digested with *Hind* III and sequenced with primers PS1013A and PS1013B to ensure the correct NTR gene was cloned.

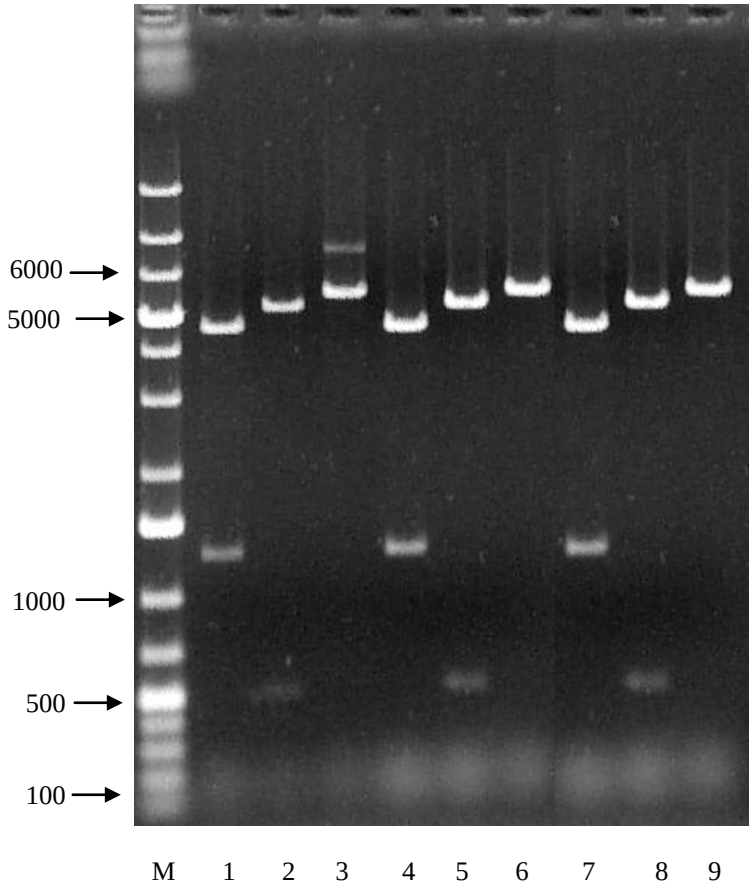

Eco RV	*Bgl* II	*Nde* I
4686	5470	5967
1281	497	

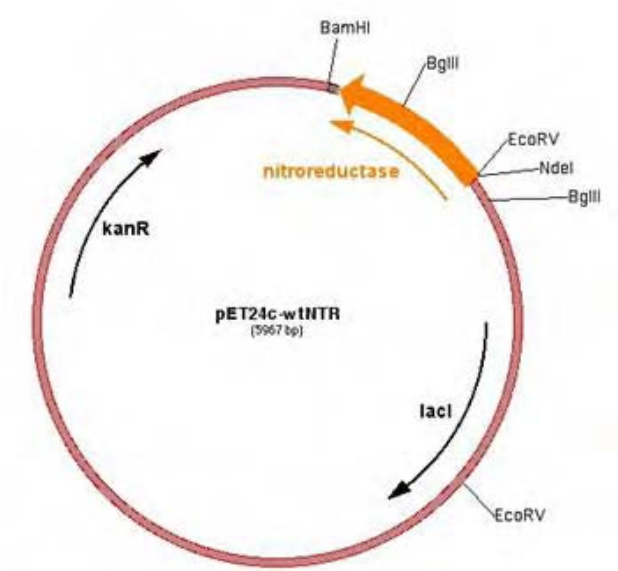

Figure 5.3 Restriction enzyme digests of plasmid bulk preparation DNA
Plasmid digests run on 0.7% agarose gel. M = Marker 1kb plus ladder, Lanes 1-3 pSHT41GN71S24c, Lanes 4-6 pSHT41LF70A24c, Lanes 7-9 pSH28224c. Each set of three showed *Eco* RV, *Bgl* II and *Nde* I digests from left to right. The table on the right shows expected band sizes for each enzyme digestion. The schematic diagram shows the fully constructed plasmid with *Eco* RV, *Bgl* II and *Nde* I restriction sites labelled. Correct digestion patterns were observed for all four plasmids

5.3.2 Purification of T41G N71S NTR

5.3.2.1 Phenyl sepharose Column (Hydrophobic column)

T41G N71S was expressed in BL21 λDE3 cells and crude extracted prepared before being purified on a Phenyl sepharose column. After loading and elution from the column absorbance measurements, activity assays and SDS PAGE gels showed that fractions 34, 35 and 36 contained active NTR with greatest purity (see Figure 5.4). Further NTR was found between fractions 26-33 and 37. It seems that the protein started to lose bonding to the column prior to elution with low NaCl buffer. Two pools were generated: fractions 34-36 and fractions 26-33 and 37. Both pools were concentrated before taking forward to Q-sepharose columns.

5.3.2.2 Q-sepharose Column (Ion Exchange column)

Pool one (fractions 34-36) was loaded onto a Q-sepharose column and eluted using a NaCl gradient. In this case the protein failed to bind to the column. The protein (fractions 4-13) was loaded onto a second column and was eluted between fractions 19-25. See Figure 5.5 for absorbance, activity assays, conductivity and SDS PAGE gels.

Pool two (fractions 26-33 and 37) was loaded on onto a Q-sepharose column and eluted using a NaCl gradient. Conductivity, absorbance, activity assays and SDS PAGE gels were run. The protein bound tightly to the column and eluted between fractions 13-17 (see Figure 5.6).

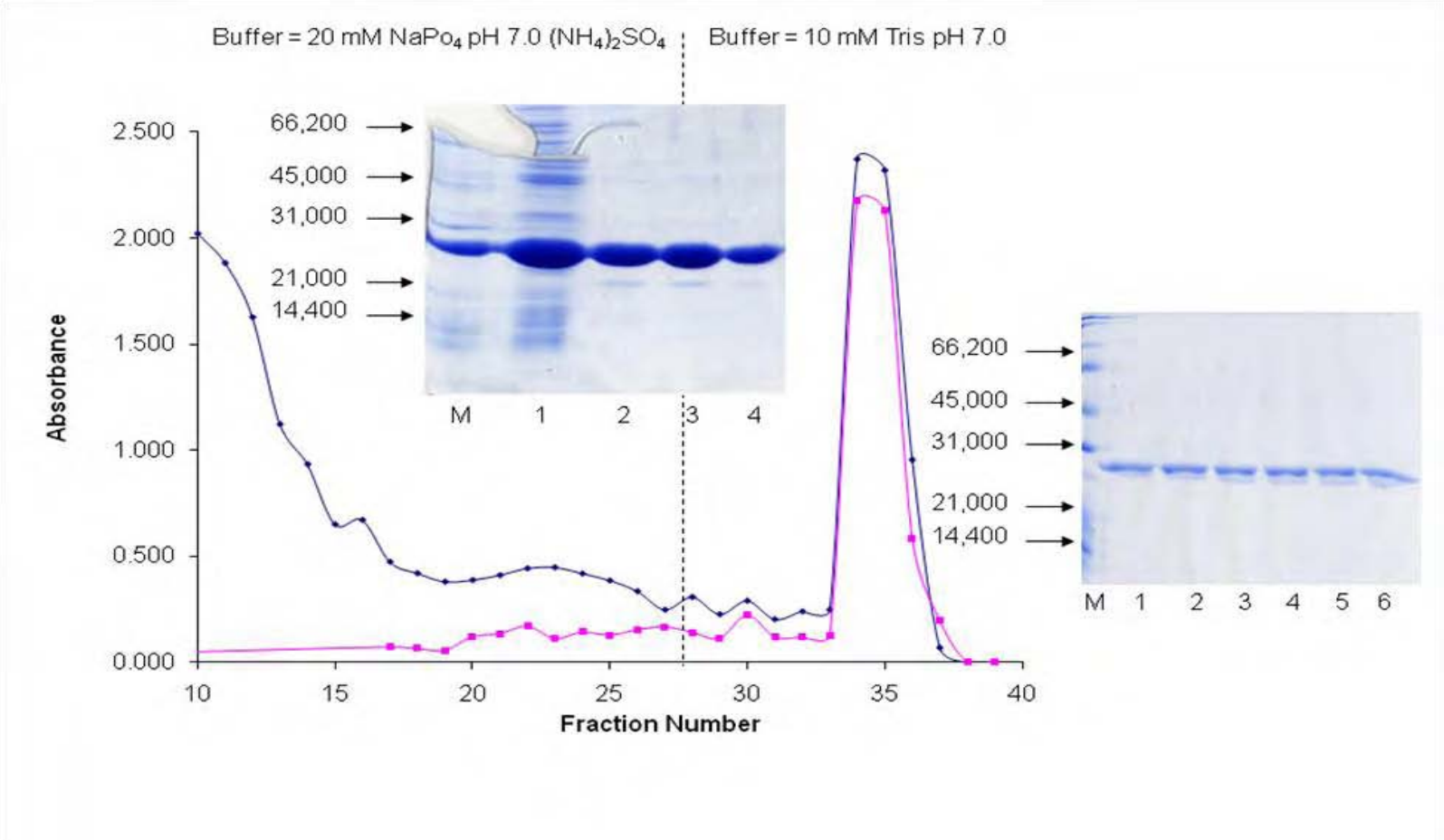

Figure 5.4 Summary of phenyl sepharose column purification T41G N71S
The blue line represents absorbance at 280 nm and the pink line is the activity of each fraction at 550 nm based on activity assays. Each section is labelled with the column buffer, with the vertical dotted line representing the point of buffer change. SDS PAGE gel 1 shows the crude extract put onto the column in lane 1 and peak fractions 34-36 in lanes 2-4. Gel 2 shows fractions 26-32 in lanes 1-6

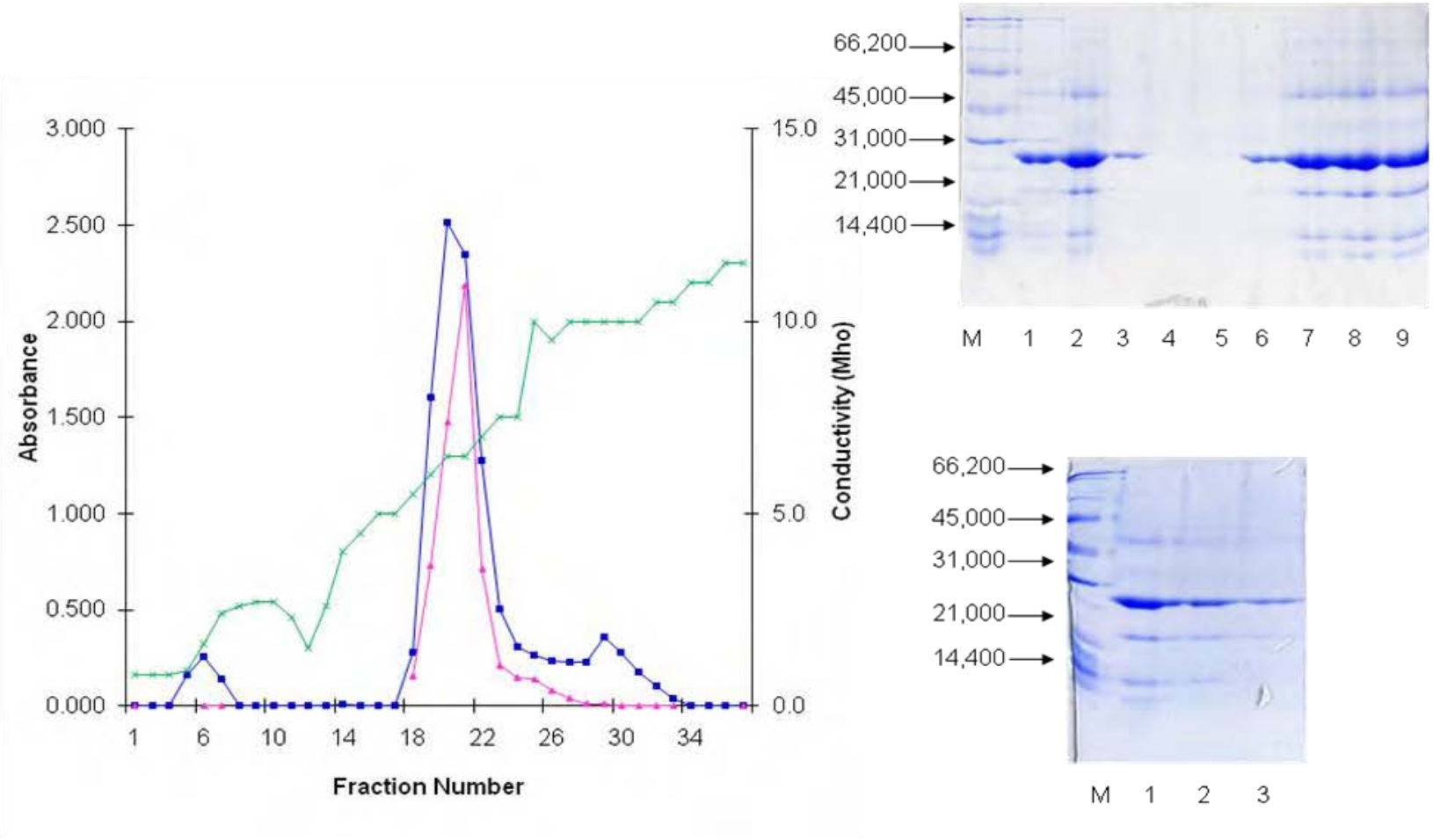

Figure 5.5 Summary of Q-sepharose column purification T41G N71S pool 1
The blue line represents absorbance at 280 nm and the pink line is the activity of each fraction at 550 nm based on activity assays. The green line shows the conductivity of each fraction. SDS PAGE gel 1 shows Q-sepharose pool (fractions 4-13 from first Q-sepharose column), concentrated pool, diluted pool and fractions 6 and 18-22 and gel 2 shows fractions 23-25

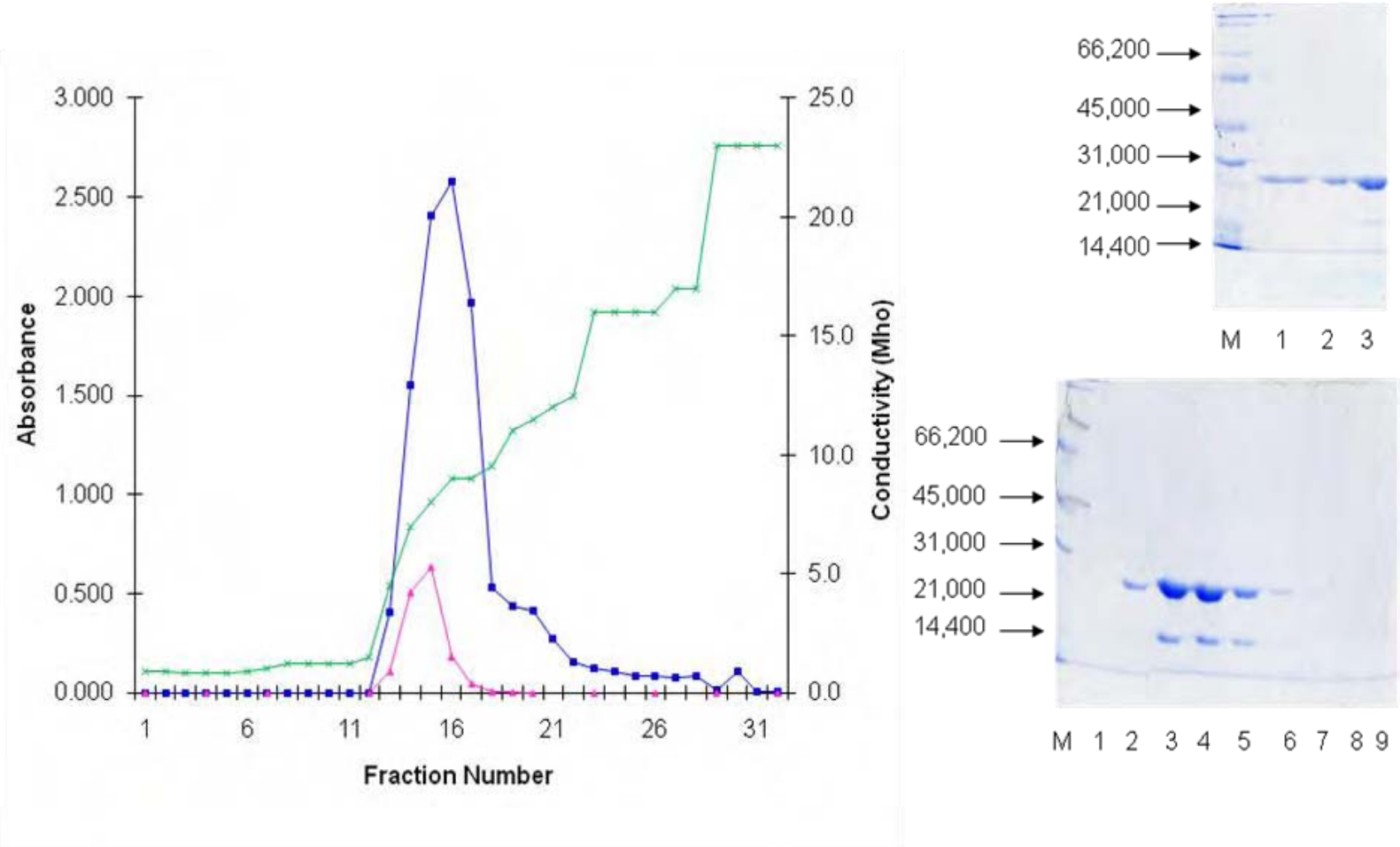

Figure 5.6 Summary of Q-sepharose column purification T41G N71S pool 2
The blue line represents absorbance at 280 nm and the pink line is the activity of each fraction at 550 nm based on activity assays. The green line shows the conductivity of each fraction. SDS PAGE gel 1 showing phenyl sepharose pool (26-33 and 37), dialysed pool and concentrated pool and gel 2 shows fractions 12-20

5.3.3 Purification of T41L F70A NTR

5.3.3.1 Phenyl sepharose Column (Hydrophobic column)

The same method of purification was used for T41L F70A. However absorbance measurements, activity assays and SDS PAGE gels showed that fractions 10-30 contain a large amount of active NTR protein. This indicates that most of the protein didn't bind to the column and washed straight through. A further peak was seen at fractions 38-41 where any tightly bound protein was eluted, as shown in Figure 5.7. The protein which didn't bind to the column was very clean and was therefore pooled, concentrated and stored for later analysis. Fractions 38, 39, 40 and 41 were pooled and concentrated before taking forward to Q-sepharose column.

5.3.3.2 Q-Sepharose Column (Ion Exchange column)

T41L F70A (fractions 38-41) was loaded onto Q-sepharose column and eluted the same as T41G N71S. The protein bound to the column and eluted between fractions 16-22 (see Figure 5.8).

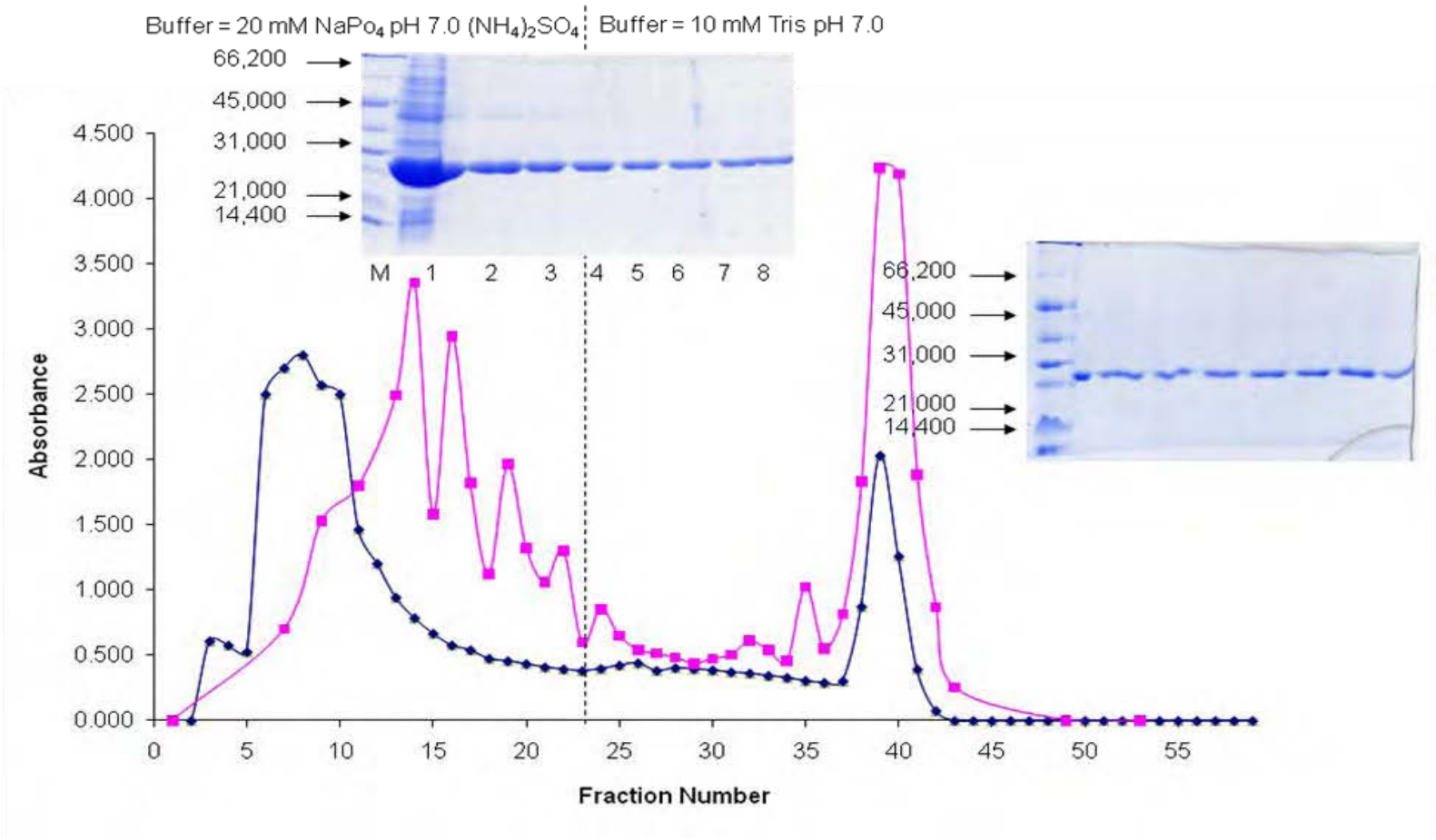

Figure 5.7 Summary of phenyl sepharose column purification T41L F70A
The blue line represents absorbance at 280 nm and the pink is the activity of each fraction at 550 nm based on activity assays. Each section is labelled with the column buffer, with the vertical dotted line representing the point of buffer change. SDS PAGE gel 1 shows the crude extract put onto column in lane 1 and fractions 13, 15, 17, 19, 21, 23 and 25 in lanes 2-8. Gel 2 showing fractions 27, 29, 31, 33, 35, 36, 37 and 42 in lanes 1-8

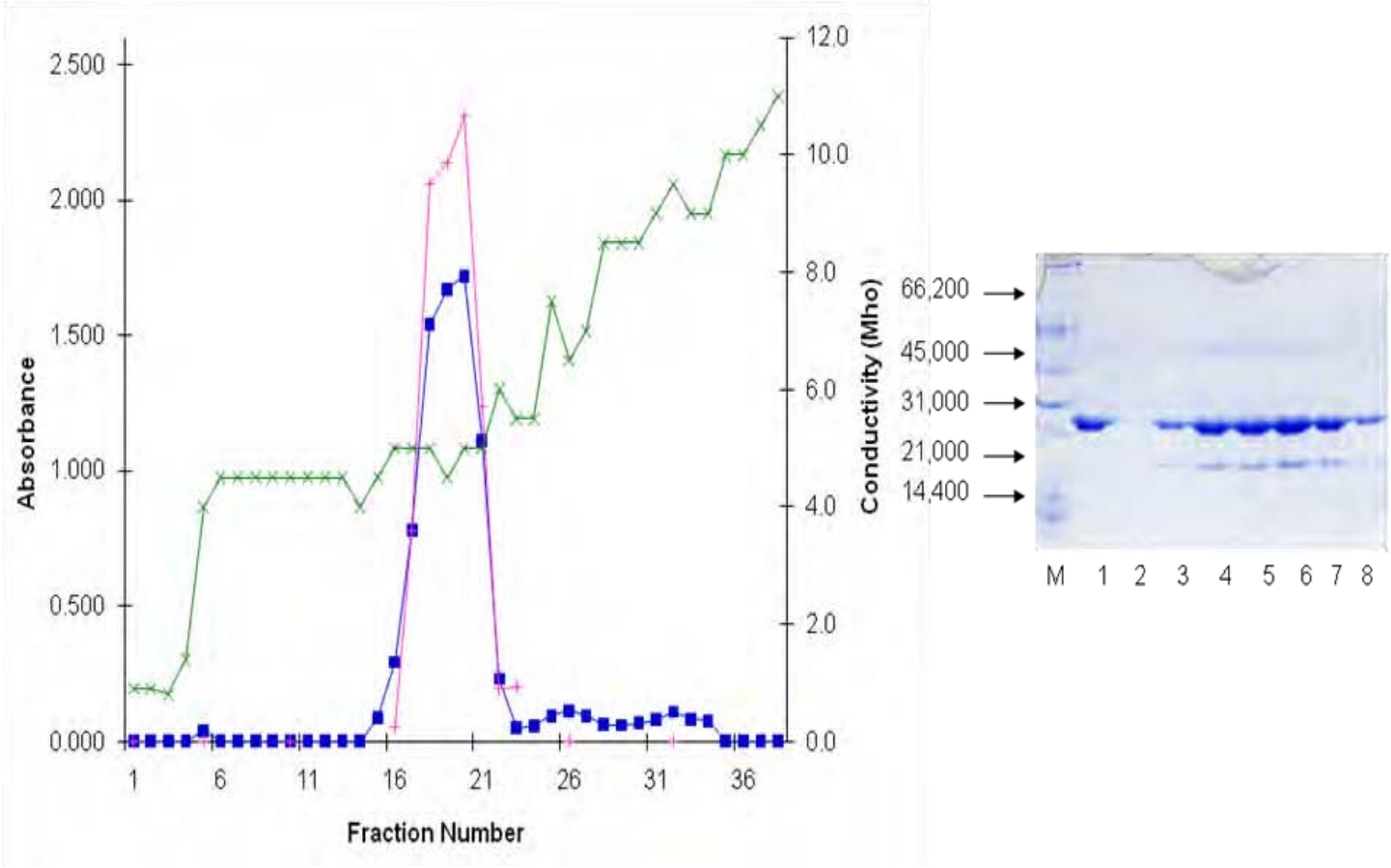

Figure 5.8 Summary of Q-sepharose column purification T41L F70A
The blue line represents absorbance at 280 nm and the pink line activity of each fraction at 550 nm based on activity assays. The green line shows the conductivity of each fraction. The SDS PAGE gel shows diluted onto Q-Sepharose (Phe Seph fractions 38-41) in lane 1 and fractions 16-22 from Q-Sepharose column lanes 2-8

5.3.4 Purification of N71S A113V R121V F123N F124V A125C K179R (282) NTR

5.3.4.1 Phenyl sepharose Column (Hydrophobic column)

The same method of purification was used for N71S A113V R121V F123N F124V A125C K179R. However absorbance measurements were very high for fractions 3-10, indicating most of the protein didn't bind to the column and washed straight through along with any impurities. Fractions 3-14 were pooled and concentrated before loading onto a second phenyl sepharose column under different conditions. The second column was pre-equilibrated with 20 mM Sodium Phosphate (pH 7.0), 1 M ammonium sulphate and 50 µM FMN. The protein was loaded onto the column and washed with 1 M ammonium sulphate, before being eluted first with 0.75 M ammonium sulphate, then 0.5 M ammonium sulphate and finally with Tris (pH 7.0). Fractions containing NTR were identified by absorbance and activity assays. SDS PAGE gels were used to examine the purity of NTR containing fractions (see Figure 5.9). Fractions 39-56 were pooled for loading on Q-Sepharose column.

5.3.4.2 Q-Sepharose Column (Ion Exchange column)

Clone 282 (fractions 39-56) was loaded onto the Q-sepharose column and eluted the same as T41G N71S and T41L F70A. The protein bound to the column and eluted between fractions 21-31 (see Figure 5.10).

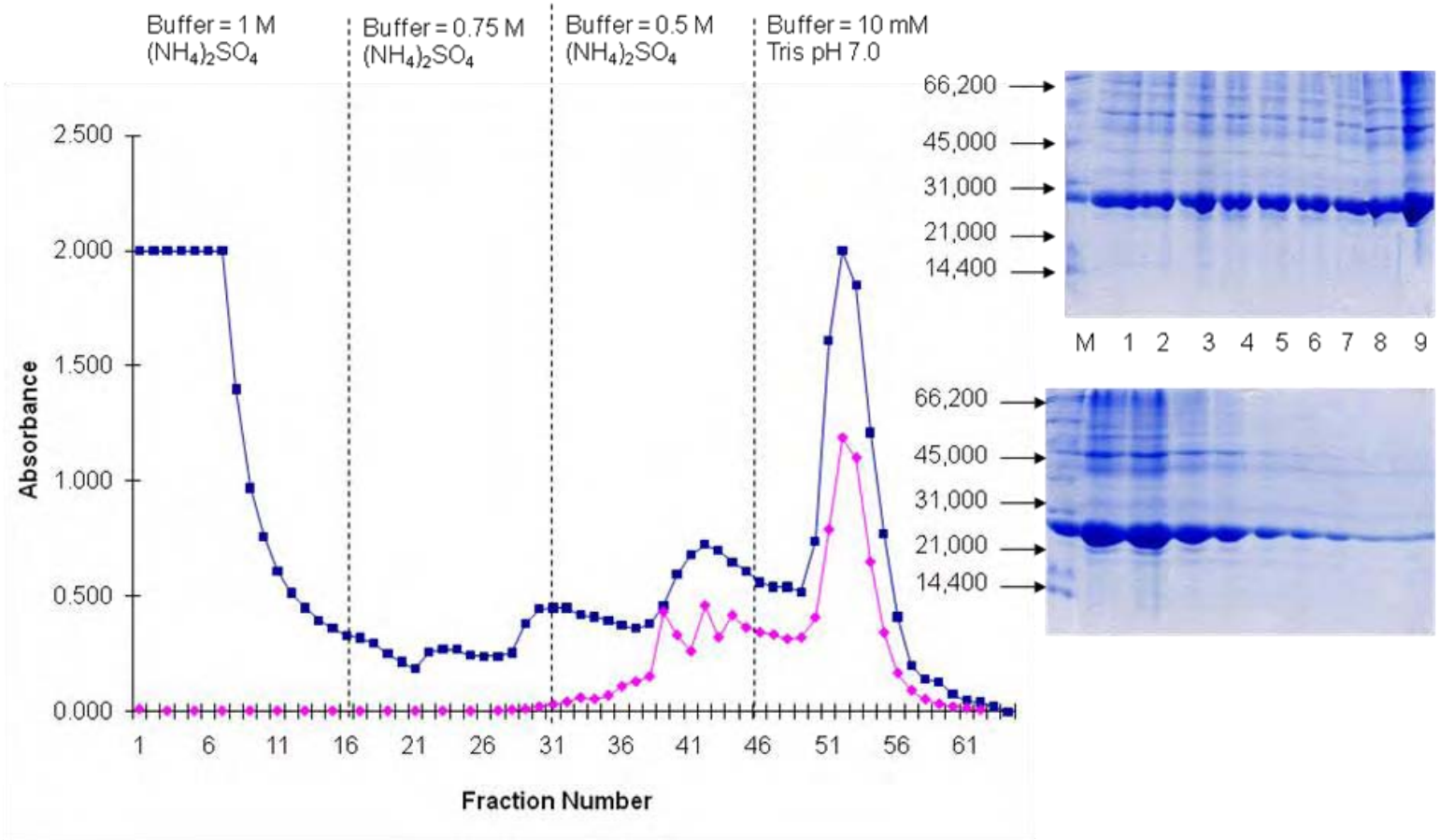

Figure 5.9 Summary of phenyl sepharose column 2 purification 282
The blue line represents absorbance at 280 nm and the pink is the activity of each fraction at 550 nm based on activity assays. Each section is labelled with the column buffer, with the vertical dotted line representing the point of buffer change. SDS PAGE gel 1 shows fractions 44-52 in lanes 1-9. Gel 2 showing fractions 53-61 in lanes 1-9

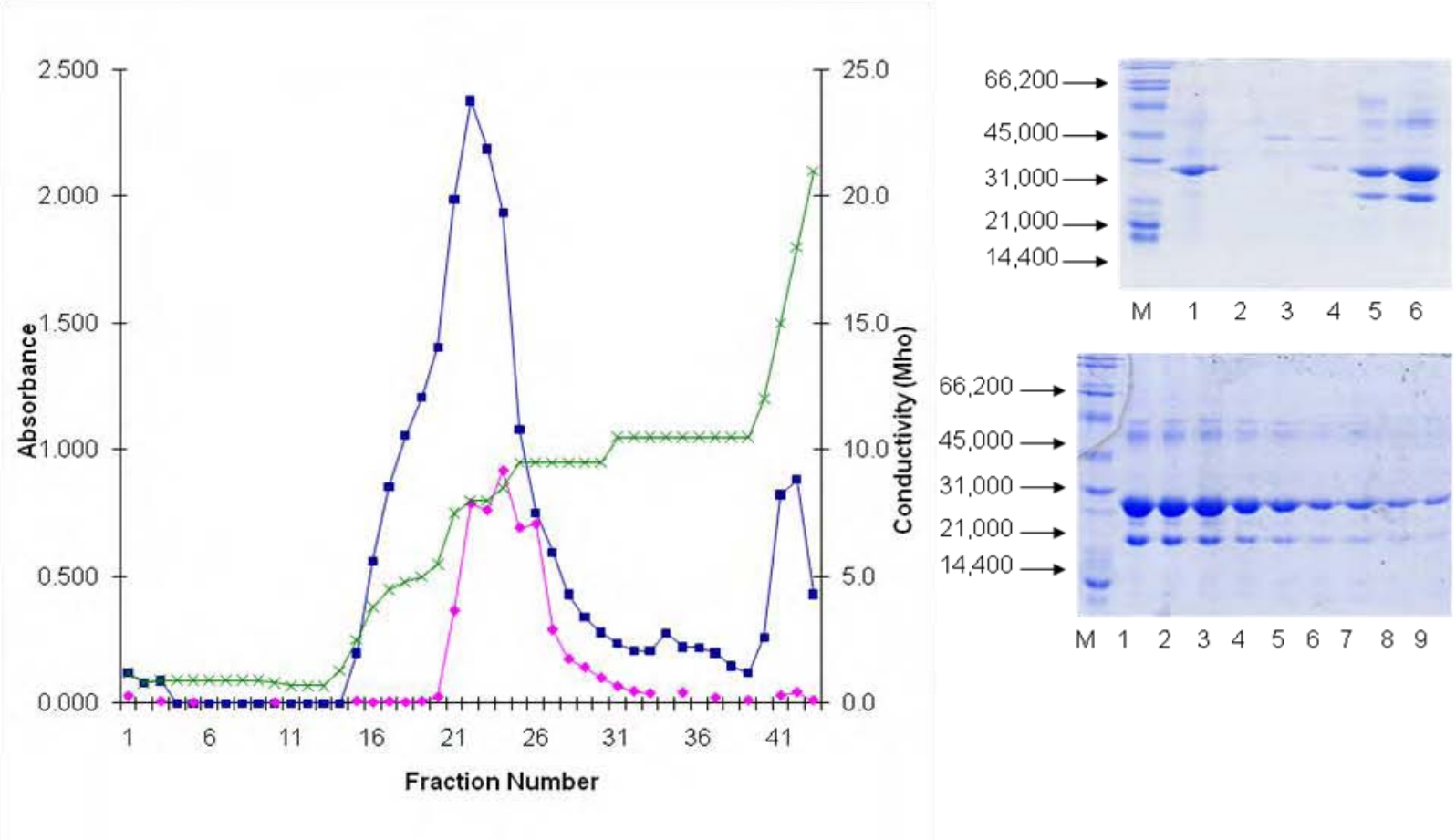

Figure 5.10 Summary of Q-Sepharose column purification 282
The blue line represents absorbance at 280 nm and the pink line activity of each fraction at 550 nm based activity assays. The green line shows the conductivity of each fraction. SDS PAGE gel shows concentrated onto Q-Sepharose (Phe Seph fractions 39-56) in lane 1 and fractions 1, 19-22 lanes 2-6 and gel 2 fractions 23-31 lanes 1-9

5.3.5 Pool and concentration of NTR enzyme stocks

Based on specific activity four pools for T41G N71S, three pools for T41L F70A and three pools for 282 were created. Each pool was dialysed overnight and concentrated (see Table 5.2). UV Spectra (ratio 454/272 nm) was measured for each pool to determine the ratio of bound and free FMN, see Figure 5.11 for an example of NTR UV spectrum.

Enzyme	Pool	Volume (ml)	UV spectra (454/272 nm)	Bradford (µg/µl)	Specific activity (s^{-1})
T41G N71S	Q2 Major	1	0.32	2.1	0.1
	Q2 Minor	1	0.35	1.8	0.1
	Q3	3.5	0.30	2.4	3.7
	Phe	1	0.34	1.1	0.1
T41L F70A	Q	3	0.3	2.3	9.9
	P Major	3	0.25	2.2	9.8
	P Minor	3	0.28	6.8	7.3
282	Q1	4.2	0.24	2.8	1.1
	Q2	2.5	0.22	4.5	1.0
	Q3	2.5	0.20	4.0	0.5

Table 5.2 Final pools for T41G N71S, T41L F70A and 282
Comprising enzyme, pool, volume (ml), UV spectra (454/272 nm), bradford assay (µg/µl) determining the enzyme concentration of each pool and the specific activity of each enzyme pool based on bradford assay. Highlighted in red are the pools to be used for kinetic assays

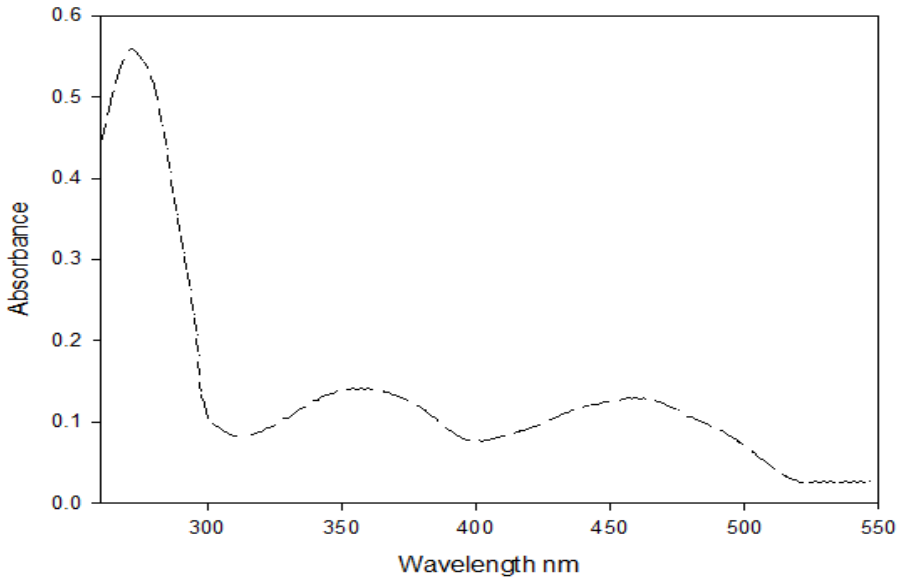

Figure 5.11 UV Spectra
UV spectra of NTR protein containing bound FMN. The ratio of 454/272 nm should be around 0.30 to indicate that most of the FMN present is bound to the enzyme with little free enzyme

Bradford assays were performed for WT, F124N, T41L F70A, T41L N71S, T41G N71S, T41Q N71S F124T and clone 282 to determine protein concentration. This data was used to determine the specific activity (see Table 5.3).

Enzyme	Bradford (µg/µl)	Specific activity (µmol min^{-1})
WT	2.4	2.1
F124N	6.8	3.2
T41L F70A	2.3	9.9
T41L N71S	2.4	4.8
T41G N71S	16.7	3.7
T41Q N71S F124T	12.9	5.2
282	2.5	1.1

Table 5.3 Bradford assay results for purified enzymes
Bradford assays were used to determine µg/µl protein contents for each purified enzymes and the specific activity

30 µg of each enzyme was run on an SDS PAGE gel. This shows the enzyme purity. Enzyme T41L N71S shows fewer impurities than the other enzymes. However good purity was seen for all the enzymes (see Figure 5.12).

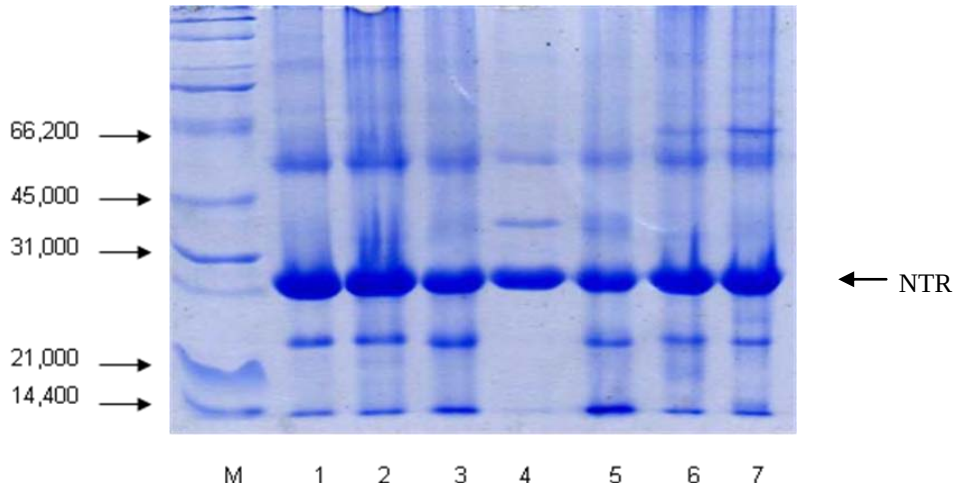

Figure 5.12 Purified enzymes for kinetic studies
This gel shows the purity of each enzyme with 30 µg of NTR protein loaded. Lanes 1 -7 show WT, F124N, T41L F70A, T41L N71S, T41G N71S, T41Q N71S F124T and 282 respectively

5.3.6 Steady-state kinetic assays and substrate specificity

Steady-state kinetic assays were used to determine the kinetic parameters of mutant NTR relative to WT. WT and three of the mutants (T41L N71S, F124N and T41Q N71S F124T) had previously been studied. These were studied by a single assay with each substrate. The three new mutants T41G N71S, T41L F70A and clone 282 were analysed by 8 assays with CB1954 and nitrofurazone substrates and a single menadione assay. For CB1954 global kinetic parameters were determined for the three new mutants. Previous assays were shown for comparative purposes.

5.3.6.1 CB1954 Kinetics

Steady-state rates for the reduction of CB1954 were determined at fixed concentrations of NADH, varying the concentration of CB1954 (see Section 1.4.3.2). These were fitted to Equation 5.1 to give apparent K_m and k_{cat} values for NADH at each CB1954 concentration (see Figures 5.13, 5.15 and 5.17). Rates were also determined at varying concentrations of NADH with fixed concentrations of CB1954. These were also fitted to Equation 5.1 to give apparent K_m and k_{cat} values for CB1954 at each NADH concentration (see Figures 5.14, 5.16 and 5.18). All the curves fitted Michaelis-Menten hyperbolae. The apparent k_{cat} and $K_{m\ CB1954}$ increased with increasing NADH concentration and the apparent k_{cat} and $K_{m\ NADH}$ also increased with increasing CB1954 concentration, as expected for ping pong Menten kinetics.

As with WT NTR and previously purified mutants, the $k_{cat}/K_{m\ CB1954}$ and $k_{cat}/K_{m\ NADH}$ ratios remained constant at each concentration for T41G N71S, T41L F70A and 282 (see Tables 5.4, 5.5 and 5.6). These results indicate that the nitroreduction of CB1954 follows a "ping pong" mechanism as stated in literature (Anlezark *et al.* 1992 and Zenno *et al.* 1996b) and discussed further in Section 1.4.3.

WT, F124N, T41L N71S and T41Q N71S F124T were studied by a single CB1954 assay as these NTR enzymes have already been extensively studied (Jarrom 2008, Jaberipour 2005). The assays were undertaken for comparative purposes. Each enzyme was studied at 500 µM NADH with a range of CB1954 concentrations. Results were fitted to Equation 5.1 and the rate of reaction shown graphically (see Figure 5.19). The rates for T41G N71S, T41L F70A and 282 at the same concentration of NADH have also been added to this graph. This allows all the enzymes to be compared together. The kinetic parameters K_m, k_{cat} and k_{cat}/K_m were determined for each enzyme (see Table 5.7). Again T41G N71S, T41L F70A and 282-HAve also been added for comparison.

Previous data for these enzymes have been compared with the ones obtained in this study. Table 5.8 shows data for WT, F124N, T41L N71S and T41Q N71S F124T (Jarrom 2008). Figure 5.20 shows this comparison in graphical form for each enzyme. A small difference was seen for each enzyme, but most values are within error of fit.

Finally all data from T41G N71S, T41L F70A and 282 have been fitted to Equation 5.5 to give global kinetic parameters for CB1954 and NADH (see Figure 5.21, 5.22, 5.23 and Table 5.9). This allows the determination of the K_m and k_{cat} values, for each substrate. For comparison previous global kinetics data for WT, F124N, T41L N71S and T41Q N71S F124T have been shown in Table 5.10.

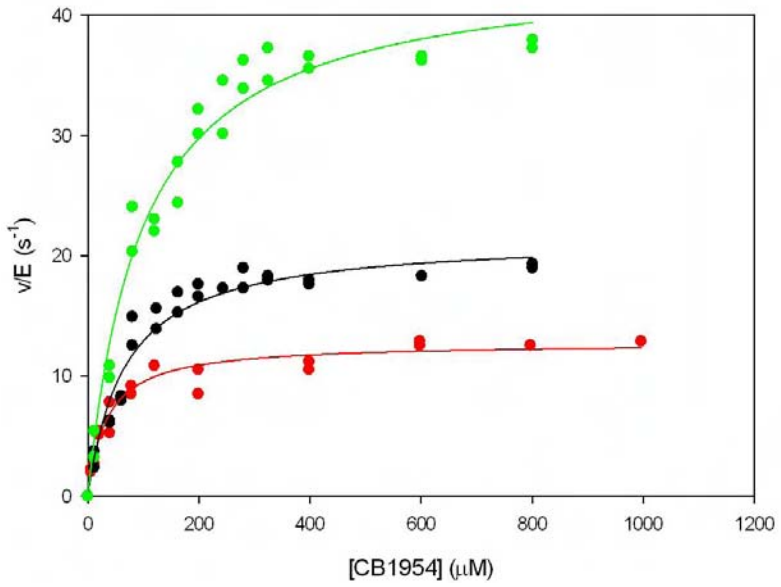

Figure 5.13 Plots of rate of reduction of CB1954 by T41G N71S, versus CB1954 concentration
100 µM NADH (red), 250 µM NADH (black) and 500 µM NADH (green). Lines were fitted to Equation 5.1

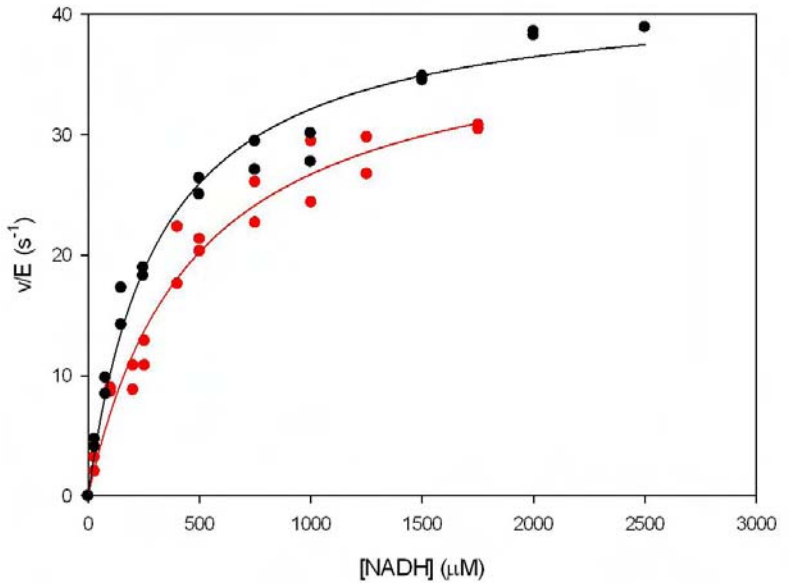

Figure 5.14 Plots of rate of reduction of CB1954 by T41G N71S, versus NADH concentration
400 µM CB1954 (red) and 800 µM CB1954 (black). Lines were fitted to Equation 5.1

[CB1954] (μM)	[NADH] (μM)	$k_{cat\ app\ CB1954}$ (s^{-1})	t test	P	$K_{m\ app\ CB1954}$ (μM)	t test	P	$k_{cat}/K_{M\ CB1954}$ (μM s^{-1})	t test	P
0-1000	100	13 ± 0.3	39.3	<0.0001	34 ± 4	8.8	<0.0001	0.374 ± 0.036	10.3	<0.0001
0-800	250	22 ±0.7	31.6	<0.0001	67 ± 8	8.1	<0.0001	0.322 ± 0.032	10.2	<0.0001
0-800	500	44 ± 1	31.2	<0.0001	97 ± 11	8.9	<0.0001	0.457 ± 0.039	11.8	<0.0001

(A)

[NADH] (μM)	[CB1954] (μM)	$k_{cat\ app\ NADH}$ (s^{-1})	t test	P	$K_{m\ app\ NADH}$ (μM)	t test	P	$k_{cat}/K_{m\ NADH}$ (μM s^{-1})	t test	P
0-1750	400	39 ± 2	18.2	<0.0001	470 ± 66	7.1	<0.0001	0.084 ±0.008	10.9	<0.0001
0-2500	800	42 ± 1	37	<0.0001	312 ± 30	10.3	<0.0001	0.135 ± 0.010	13.3	<0.0001

(B)

Table 5.4 Kinetic Parameters of the reduction of CB1954 by T41G N71S
(A) CB1954 concentration is varied at a range of fixed NADH concentrations (B) NADH concentration is varied at a range of fixed CB1954 concentrations. Parameters for data were fitted to Equation 5.1 for a single substrate Menten equation and analysed statistically by calculating t test and P values for each regression curve, t equals the ratio of the regression coefficient to its standard error, indicating how much the rate of the reaction depends on the K_m and k_{cat}. A large t value indicates that the data fits the equation and that the rate of reaction can be predicted from the parameters. The P value is the probability that the parameters fit the curve by chance, the smaller the P value the less likely it occurred by chance. Ideally P values should be <0.05, which indicates a reliable fit to the experimental data

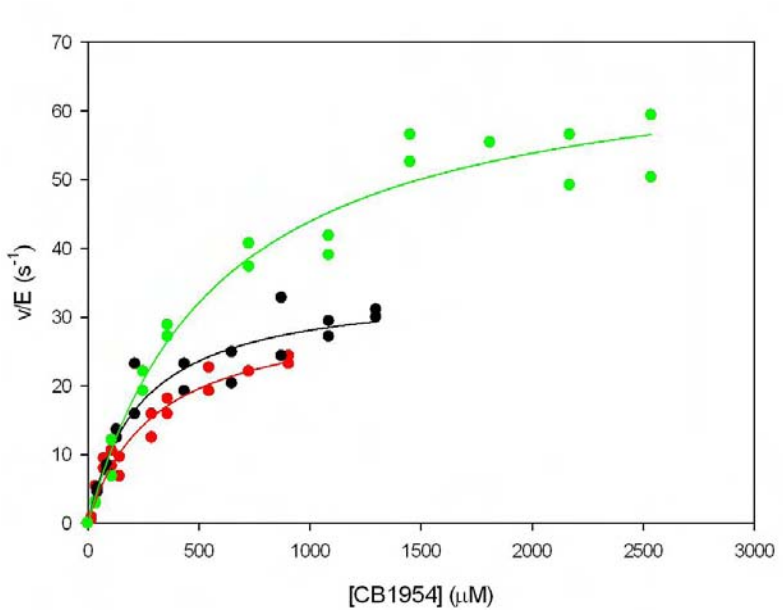

Figure 5.15 Plots of rate of reduction of CB1954 by T41L F70A, versus CB1954 concentration
60 μM NADH (red), 100 μM NADH (black) and 500 μM NADH (green). Lines were fitted to Equation 5.1

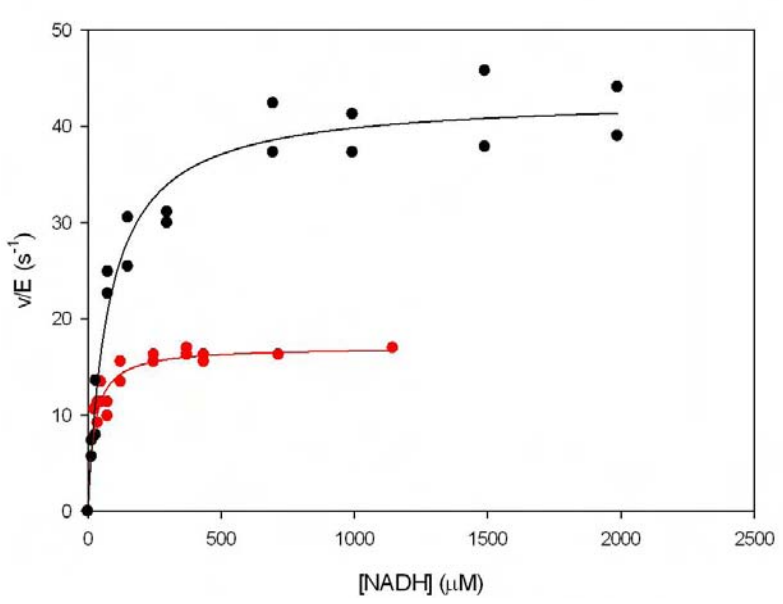

Figure 5.16 Plots of rate of reduction of CB1954 by T41L F70A, versus NADH concentration
400 μM CB1954 (red) and 900 μM CB1954 (black). Lines were fitted to Equation 5.1

[CB1954] (μM)	[NADH] (μM)	$k_{cat\ app\ CB1954}$ (s^{-1})	t test	P	$K_{m\ app\ CB1954}$ (μM)	t test	P	$k_{cat}/K_{m\ CB1954}$ (μM s^{-1})	t test	P
0-900	60	31 ± 2	14.3	<0.0001	295 ± 51	5.8	<0.0001	0.106 ± 0.012	9.1	<0.0001
0-1300	100	35 ± 2	16.1	<0.0001	234 ± 47	5.0	0.0001	0.148 ± 0.022	6.7	<0.0001
0-2500	500	60 ± 3	21.3	<0.0001	584 ±84	7.0	<0.0001	0.103 ± 0.012	9.8	<0.0001

(A)

[NADH] (μM)	[CB1954] (μM)	$k_{cat\ app\ NADH}$ (s^{-1})	t test	P	$K_{m\ app\ NADH}$ (μM)	t test	P	$k_{cat}/K_{m\ NADH}$ (μM s^{-1})	t test	P
0-1150	400	18 ± 0.4	38.7	<0.0001	24 ± 3	7.2	<0.0001	0.699 ± 0.085	8.2	<0.0001
0-2000	900	43 ± 1	34.3	<0.0001	79 ± 11	7.2	<0.0001	0.542 ± 0.065	8.3	<0.0001

(B)

Table 5.5 Kinetic Parameters of the reduction of CB1954 by T41L F70A
(A) CB1954 concentration is varied at a range of fixed NADH concentrations (B) NADH concentration is varied at a range of fixed CB1954 concentrations. Parameters for data were fitted to Equation 5.1 for a single substrate Menten equation and analysed statistically by calculating t test and P values for each regression curve, t equals the ratio of the regression coefficient to its standard error, indicating how much the rate of the reaction depends on the K_m and k_{cat}. A large t value indicates that the data fits the equation and that the rate of reaction can be predicted from the parameters. The P value is the probability that the parameters fit the curve by chance, the smaller the P value the less likely it occurred by chance. Ideally P values should be <0.05, which indicates a reliable fit to the experimental data

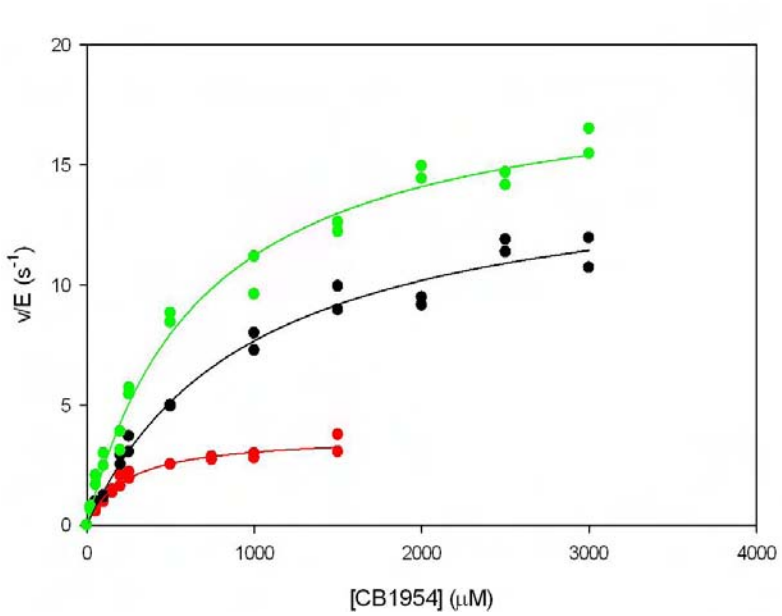

Figure 5.17 Plots of rate of reduction of CB1954 by 282, versus CB1954 concentration
250 µM NADH (red), 500 µM NADH (black) and 1000 µM NADH (green). Lines were fitted to Equation 5.1

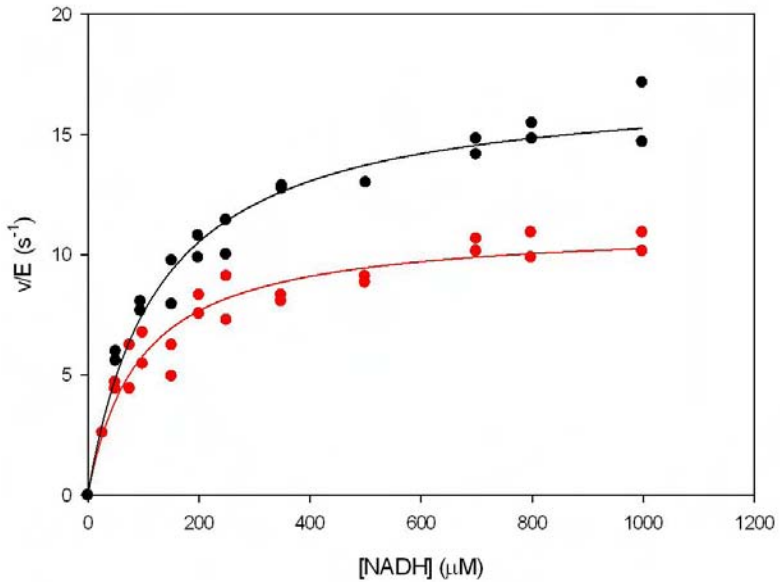

Figure 5.18 Plots of rate of reduction of CB1954 by clone 282, versus NADH concentration
400 µM CB1954 (red) and 800 µM CB1954 (black). Lines were fitted to Equation 5.1

[CB1954] (μM)	[NADH] (μM)	$k_{cat\ app\ CB1954}$ (s^{-1})	t test	P	$K_{m\ app\ CB1954}$ (μM)	t test	P	$k_{cat}/K_{m\ CB1954}$ (μM s^{-1})	t test	P
0-1500	250	4 ± 0.2	24.9	<0.0001	232 ± 28	8.3	<0.0001	0.016 ± 0.001	11.5	<0.0001
0-3000	500	10 ± 0.7	23.3	<0.0001	575 ± 109	8.9	<0.0001	0.017 ± 0.001	13.7	<0.0001
0-3000	1000	19 ± 0.6	30.3	<0.0001	688 ± 67	10.2	<0.0001	0.028 ± 0.002	14.4	<0.0001

(A)

[NADH] (μM)	[CB1954] (μM)	$k_{cat\ app\ NADH}$ (s^{-1})	t test	P	$K_{m\ app\ NADH}$ (μM)	t test	P	$k_{cat}/K_{m\ NADH}$ (μM s^{-1})	t test	P
0-1000	400	11 ± 0.4	28.3	<0.0001	92 ± 12	7.6	<0.0001	0.165 ± 0.012	9.6	<0.0001
0-1000	800	17 ± 0.5	33.5	<0.0001	127 ±14	9.3	<0.0001	0.136 ± 0.011	12.1	<0.0001

(B)

Table 5.6 Kinetic Parameters of the reduction of CB1954 by 282
(A) CB1954 concentration is varied at a range of fixed NADH concentrations (B) NADH concentration is varied at a range of fixed CB1954 concentrations. Parameters for data were fitted to Equation 5.1 for a single substrate Menten equation and analysed statistically by calculating t test and P values for each regression curve, t equals the ratio of the regression coefficient to its standard error, indicating how much the rate of the reaction depends on the K_m and k_{cat}. A large t value indicates that the data fits the equation and that the rate of reaction can be predicted from the parameters. The P value is the probability that the parameters fit the curve by chance, the smaller the P value the less likely it occurred by chance. Ideally P values should be <0.05, which indicates a reliable fit to the experimental data

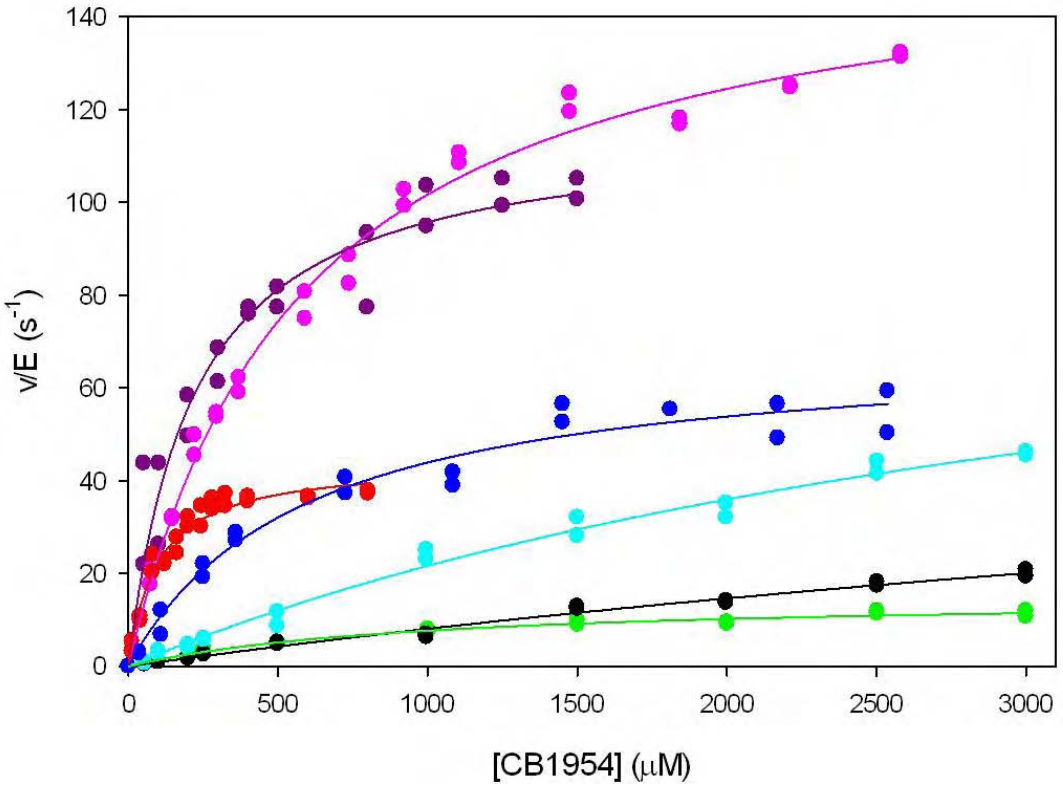

Figure 5.19 Plots of rate of reduction of CB1954, versus CB1954 concentration at 500 μM NADH WT (black), F124N (cyan), T41L N71S (purple), T41Q N71S F124T (pink), T41G N71S (red), T41L F70A (blue) and 282 (green)

NTR	$k_{cat\ app\ CB1954}$ (s^{-1})	t test	P	$K_{m\ app\ CB1954}$ (μM)	t test	P	$k_{cat}/K_{m\ CB1954}$ (μM s^{-1})	t test	P
Wild Type	N.D	-	-	N.D	-	-	0.009 ± 0.0006	15	<0.0001
F124N	106 ±12	9	<0.0001	3917 ± 703	6	<0.0001	0.027 ± 0.002	15	<0.0001
T41L N71S	118 ± 6	23	<0.0001	188 ± 33	7	<0.0001	0.628 ± 0.072	9	<0.0001
T41Q N71S F124T	161 ± 3	55	<0.0001	578 ± 30	20	<0.0001	0.277 ± 0.010	29	<0.0001
T41G N71S	44 ± 1	31	<0.0001	97 ± 11	9	<0.0001	0.457 ± 0.039	12	<0.0001
T41L F70A	60 ± 3	21	<0.0001	584 ± 84	7	<0.0001	0.103 ± 0.012	10	<0.0001
282	10 ± 1	23	<0.0001	975 ± 109	9	<0.0001	0.010 ± 0.001	14	<0.0001

Table 5.7 Kinetic Parameters of WT and six *NfsB* mutants for the reduction of CB1954 at a constant NADH concentration of 500 μM
Parameters for data were fitted to Equation 5.1 for a single substrate Menten equation and analysed statistically by calculating t test and P values for each regression curve, t equals the ratio of the regression coefficient to its standard error, indicating how much the rate of the reaction depends on the K_m and k_{cat}. A large t value indicates that the data fits the equation and that the rate of reaction can be predicted from the parameters. The P value is the probability that the parameters fit the curve by chance, the smaller the P value the less likely it occurred by chance. Ideally P values should be <0.05, which indicates a reliable fit to the experimental data. N.D stands for not determined. It is not possible to determine the k_{cat} apparent and K_m apparent for WT at this concentration. New data highlighted in red

NTR	$k_{cat\ app\ CB1954}$ (s^{-1})	t test	P	$K_{m\ app\ CB1954}$ (μM)	t test	P	$k_{cat}/K_{M\ CB1954}$ (μM s^{-1})	t test	P
Wild Type	N.D	-	-	N.D	-	-	0.006 ± 0.0004	18	<0.0001
F124N	85 ± 2	55	<0.0001	3000 ± 100	27	<0.0001	0.029 ± 0.001	52	<0.0001
T41L N71S	112 ± 3	40	<0.0001	160 ± 20	8	<0.0001	0.700 ± 0.070	10	<0.0001
T41Q N71S F124T	159 ± 4	38	<0.0001	520 ± 40		<0.0001	0.310 ± 0.020	19	<0.0001

Table 5.8 Kinetic Parameters of WT and three *NfsB* mutants for the reduction of CB1954 at a constant NADH concentration of 500 μM
Data from previous studies (Jarrom 2008), which have been included for comparison purposes. N.D stands for not determined

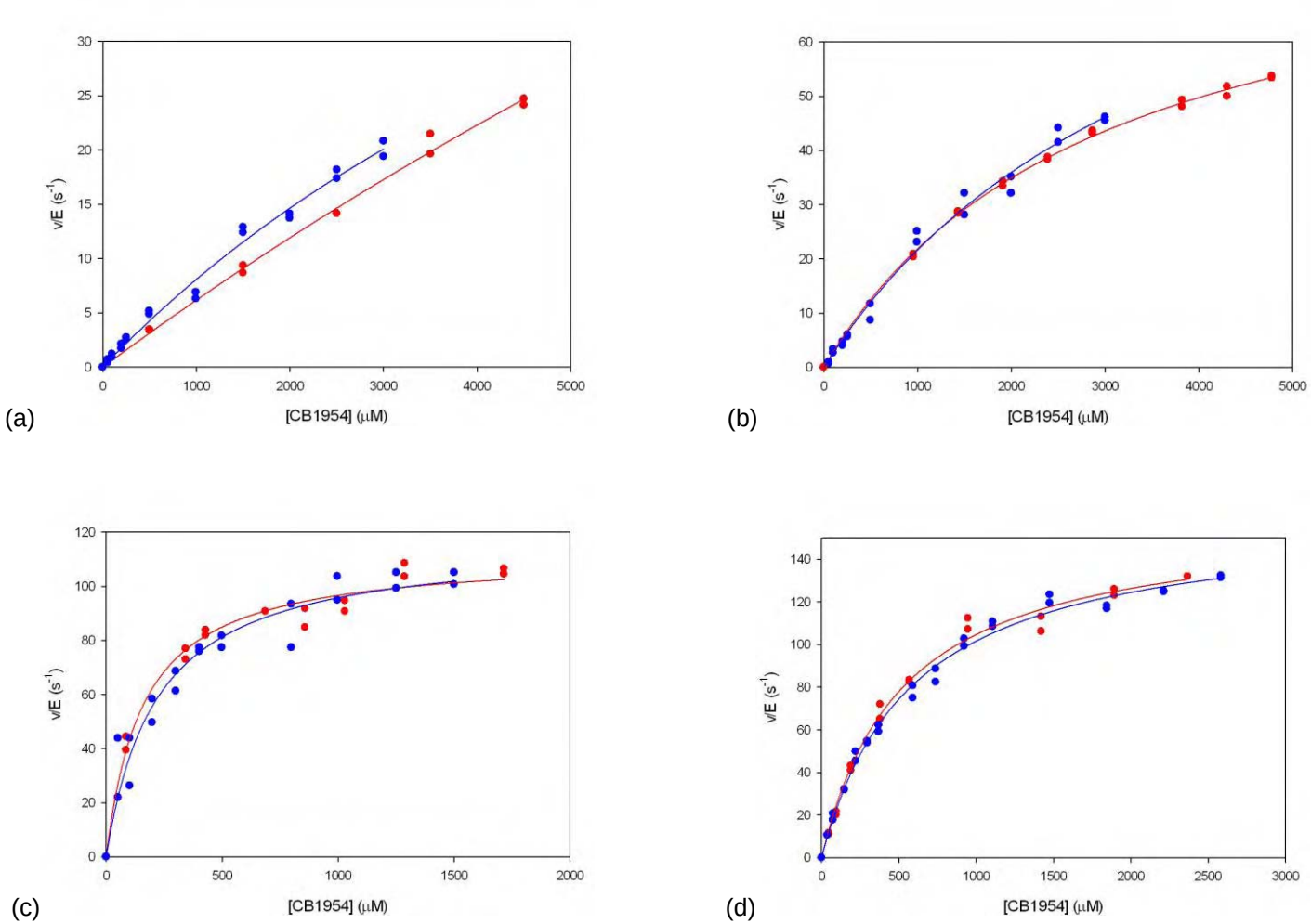

Figure 5.20 Plots of rate of reduction of CB1954, versus CB1954 concentration at 500 μM NADH
Graphical representation with the red lines showing previous data (Jarrom 2008) and the blue lines this study. (a) WT (b) F124N (c) T41L N71S and (d) T41Q N71S F124T

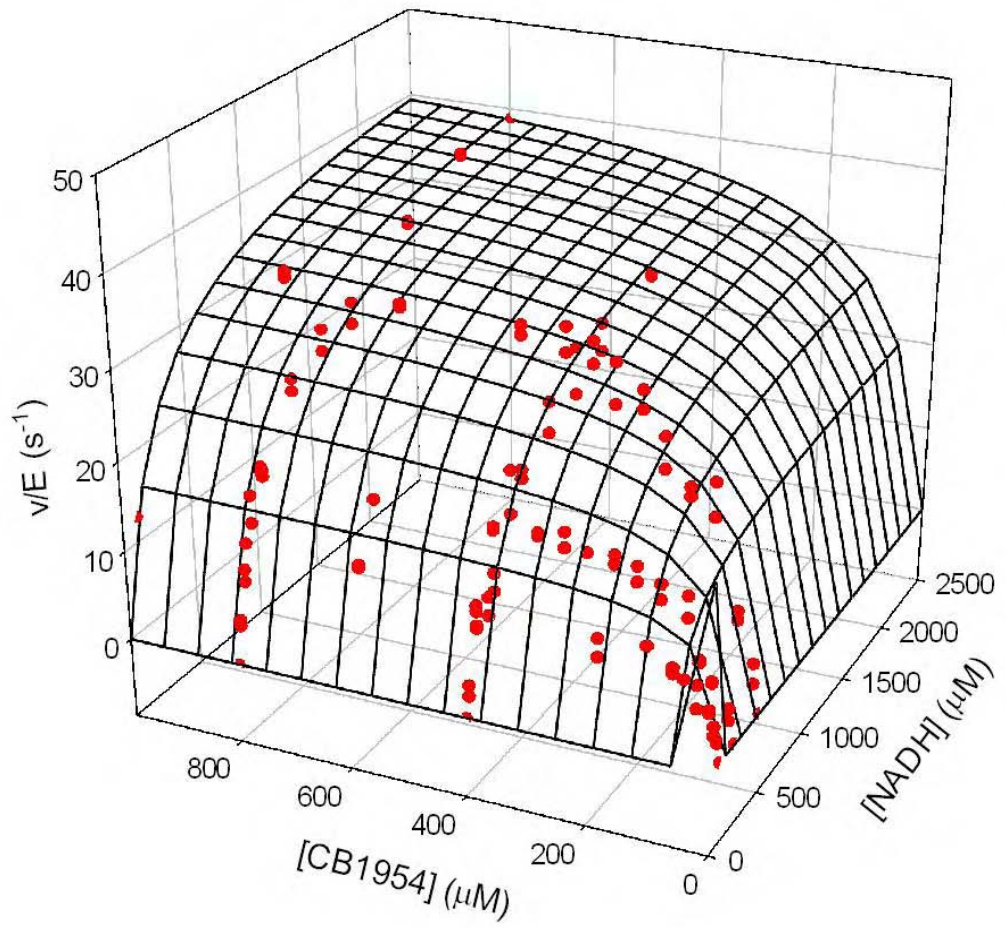

Figure 5.21 Global 3D plot of rate of CB1954 reduction at different NADH and CB1954 concentrations for T41G N71S
Data fitted to Equation 5.5

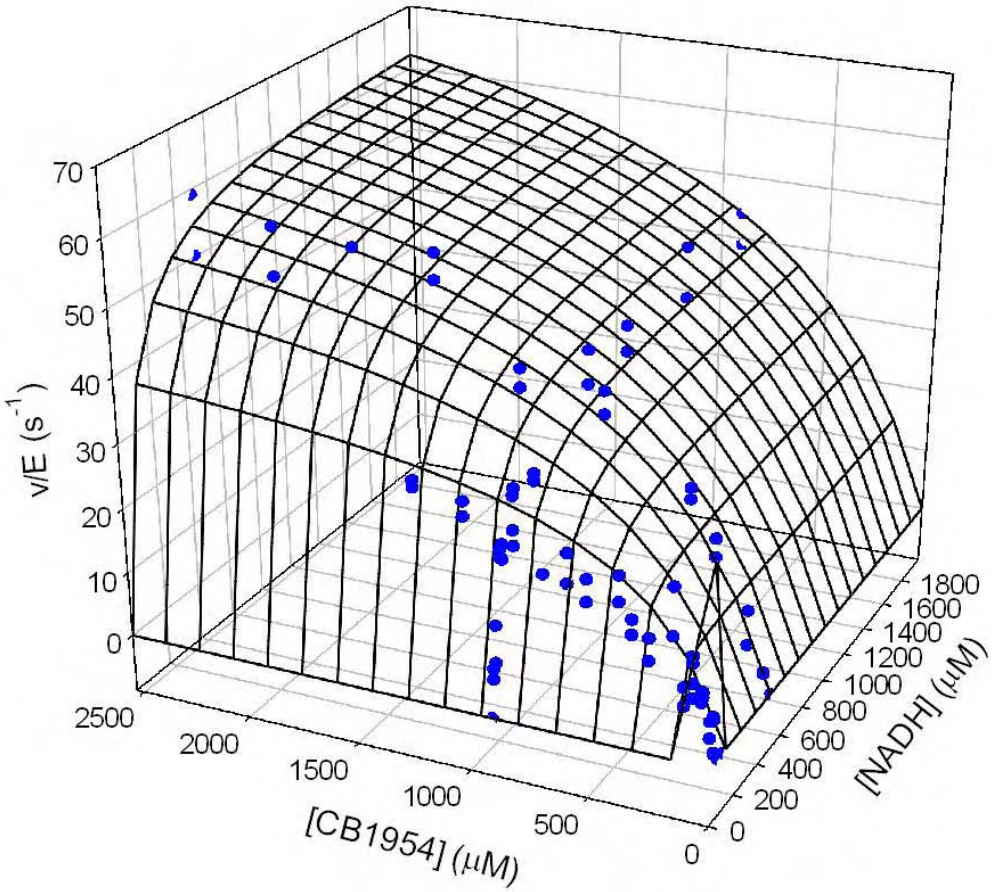

Figure 5.22 Global 3D plot of rate of CB1954 reduction at different NADH and CB1954 concentrations for T41L F70A
Data fitted to Equation 5.5

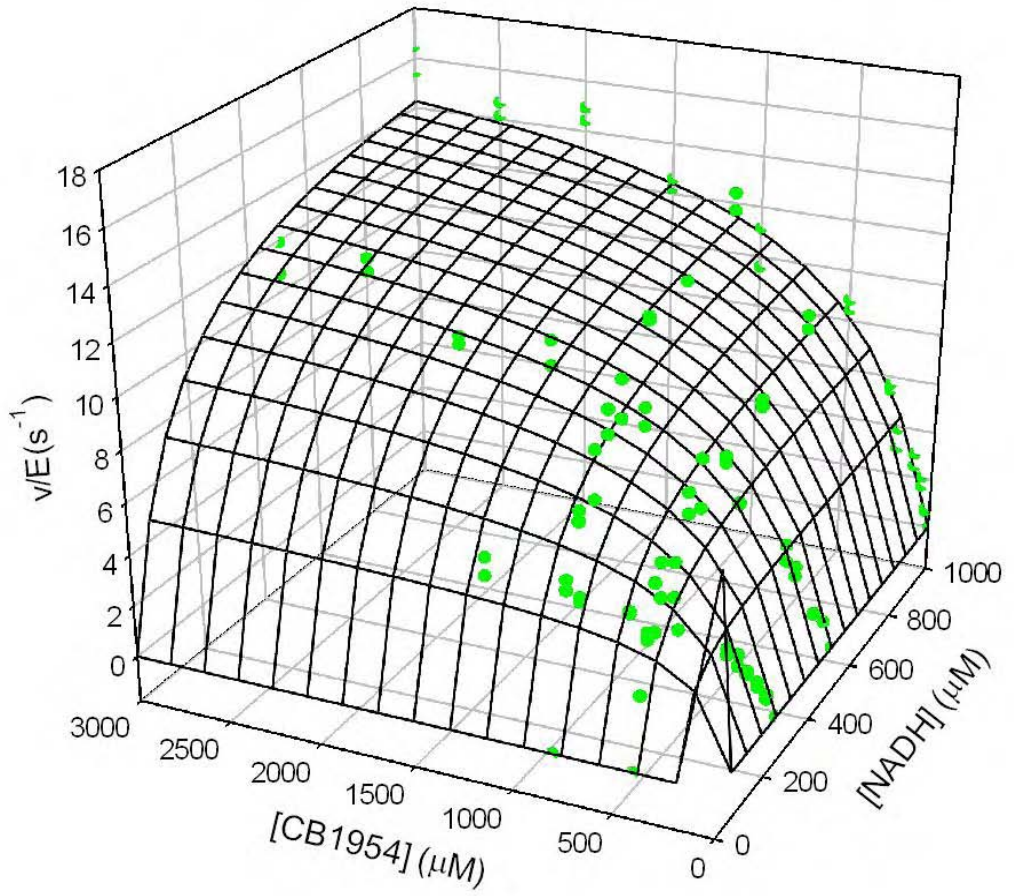

Figure 5.23 Global 3D plot of rate of CB1954 reduction at different NADH and CB1954 concentrations for 282
Data fitted to Equation 5.5

	T41G N71S	t test	P	T41L F70A	t test	P	282	t test	P
k_{cat} s^{-1}	46 ± 3	18.6	<0.0001	86 ± 5	18.8	<0.0001	20 ± 2	9.2	<0.0001
$K_{m\ CB1954}$ µM	88 ± 18	4.7	<0.0001	750 ± 91	8.7	<0.0001	619 ± 135	4.6	<0.0001
$k_{cat}/K_{m\ CB1954}$ µM s^{-1}	0.52 ± 0.1	5.4	<0.0001	0.11 ± 0.01	14.4	<0.0001	0.018 ± 0.01	6.6	<0.0001
$K_{m\ NADH}$ µM	305 ± 38	8.2	<0.0001	125 ± 13	9.7	<0.0001	183 ± 60	3.0	0.0029
$k_{cat}/K_{m\ NADH}$ µM s^{-1}	0.15 ± 0.01	11.6	<0.0001	0.69 ± 0.05	13.1	<0.0001	0.11 ± 0.03	3.9	0.0002

Table 5.9 Global kinetics parameters for the reduction of CB1954
Data for T41G N71S, T41L F70A and 282 were fitted to Equation 5.5 and analysed statistically by calculating t test and P values for each regression curve, t equals the ratio of the regression coefficient to its standard error, indicating how much the rate of the reaction depends on the K_m and k_{cat}. A large t value indicates that the data fits the equation and that the rate of reaction can be predicted from the parameters. The P value is the probability that the parameters fit the curve by chance, the smaller the P value the less likely it occurred by chance. Ideally P values should be <0.05, which indicates a reliable fit to the experimental data

	WT	F124N	T41L N71S	T41Q N71S F124T
k_{cat} s^{-1}	140 ± 12	95 ± 7	135 ± 9	181 ± 7
$K_{m\ CB1954}$ µM	17000 ± 5000	3100 ± 500	150 ± 38	570 ± 45
$k_{cat}/K_{m\ CB1954}$ µM s^{-1}	0.0072 ± 0.0002	0.031 ± 0.03	0.9 ± 0.1	0.32 ± 0.02
$K_{m\ NADH}$ µM	30 ± 16	55 ± 7	180 ± 33	140 ± 12
$k_{cat}/K_{m\ NADH}$ µM s^{-1}	0.83 ± 0.01	1.7 ± 0.2	0.7 ± 0.1	1.33 ± 0.08
Reference	Jarrom, 2008	Jaberipour, 2005	Jarrom, 2008	Jarrom, 2008

Table 5.10 Global kinetics parameters for the reduction of CB1954
WT, F124N, T41L N71S and T41Q N71S F124T NTR from previous studies

5.3.6.2 Nitrofurazone Kinetics

Similar experiments were done for the reduction of nitrofurazone (see Section 1.4.3.2). Figures 5.24, 5.26 and 5.28 give apparent K_m and k_{cat} values for NFZ with fixed concentrations of NADH and Figures 5.25, 5.27 and 5.29 gives apparent K_m and k_{cat} values for NADH with fixed concentrations of NFZ. Kinetic Parameters for these enzymes can be seen in Tables 5.11, 5.12 and 5.13. As seen with CB1954 the apparent k_{cat} and $K_{m\ NFZ}$ increased with increasing NADH concentration and the apparent k_{cat} and $K_{m\ NADH}$ also increased with increasing NFZ concentration.

WT, F124N, T41L N71S and T41Q N71S F124T have been studied by a single NFZ assay for comparative purposes. Each enzyme was studied using 200 µM NADH with a range of NFZ concentrations as can be seen in Figure 5.30. Kinetic parameters showing K_m, k_{cat} and k_{cat}/K_m values were determined for each enzyme (see Table 5.14). Previous NFZ data for these enzymes have been compared to that obtained in this study (see Table 5.15 and Figure 5.31). Small differences were seen for WT and T41L N71S enzymes; these values are within error of fit. However, F124N and T41Q N71S F124T enzymes showed bigger differences. The K_m values for these two enzymes were double that previously determined; however the k_{cat} values were similar to previous data.

Global parameters for nitrofurazone were attempted however the data did not fit well and were not statistically consistent, data not shown.

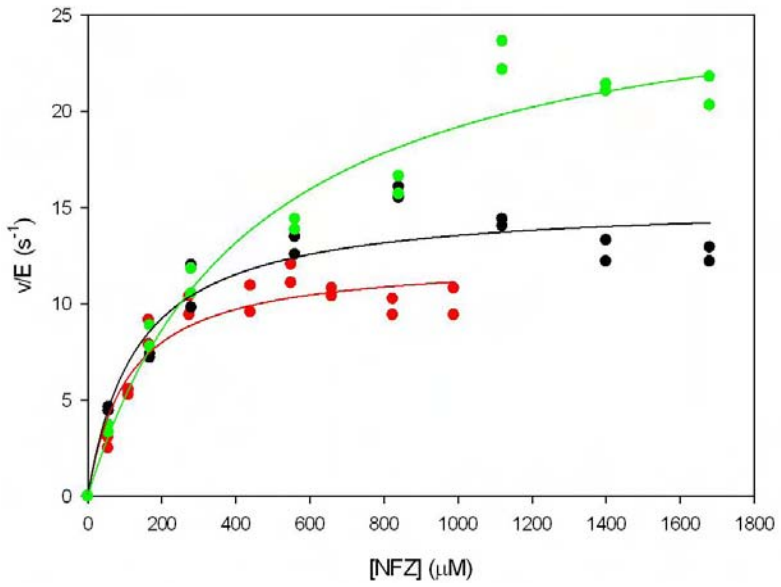

Figure 5.24 Plots of rate of reduction of nitrofurazone by T41G N71S, versus NFZ concentration
200 µM NADH (red), 500 µM NADH (black) and 1000 µM NADH (green). Lines were fitted to Equation 5.1

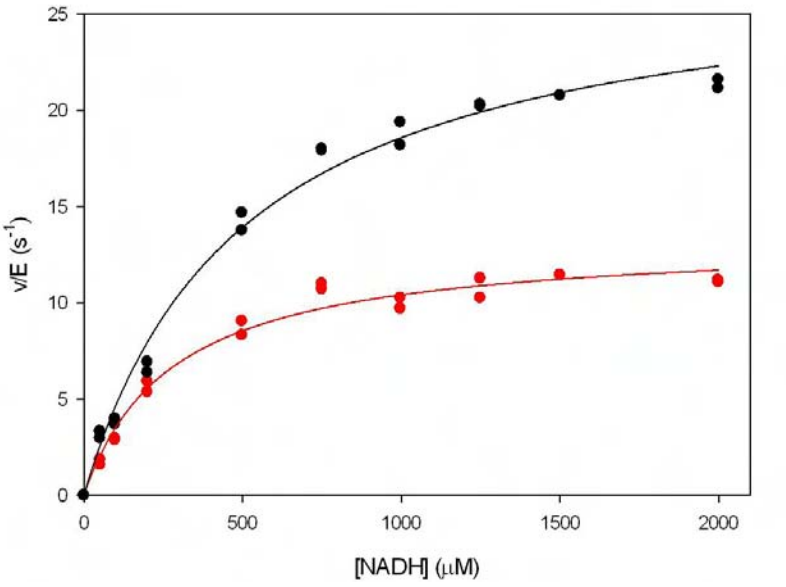

Figure 5.25 Plots of rate of reduction of nitrofurazone by T41G N71S, versus NADH concentration
500 µM NFZ (red) and 1000 µM NFZ (black). Lines were fitted to Equation 5.1

[NFZ] (μM)	[NADH] (μM)	$k_{cat\ app\ NFZ}$ (s^{-1})	t test	P	$K_{m\ app\ NFZ}$ (μM)	t test	P	$k_{cat}/K_{m\ NFZ}$ (μM s^{-1})	t test	P
0-1000	200	12 ± 1	18.7	<0.0001	110 ± 24	4.5	0.0003	0.113 ± 0.020	5.7	<0.0001
0-1700	500	15 ± 1	20.7	<0.0001	132 ± 30	4.3	0.0005	0.116 ± 0.023	5.2	<0.0001
0-1700	1000	41 ± 3	16.1	<0.0001	438 ± 80	5.5	<0.0001	0.095 ± 0.012	7.9	<0.0001

(A)

[NADH] (μM)	[NFZ] (μM)	$k_{cat\ app\ NADH}$ (s^{-1})	t test	P	$K_{m\ app\ NADH}$ (μM)	t test	P	$k_{cat}/K_{m\ NADH}$ (μM s^{-1})	t test	P
0-2000	500	13 ± 0.4	32.6	<0.0001	280 ± 32	8.8	<0.0001	0.048 ± 0.004	11.3	<0.0001
0-2000	1000	28 ± 1	30.0	<0.0001	503 ± 49	10.3	<0.0001	0.056 ± 0.004	14.9	<0.0001

(B)

Table 5.11 Kinetic Parameters of the reduction of nitrofurazone by T41G N71S
(A) NFZ concentration is varied at a range of fixed NADH concentrations (B) NADH concentration is varied at a range of fixed NFZ concentrations. Parameters for data were fitted to Equation 5.1 for a single substrate Menten equation and analysed statistically by calculating t test and P values for each regression curve, t equals the ratio of the regression coefficient to its standard error, indicating how much the rate of the reaction depends on the K_m and k_{cat}. A large t value indicates that the data fits the equation and that the rate of reaction can be predicted from the parameters. The P value is the probability that the parameters fit the curve by chance, the smaller the P value the less likely it occurred by chance. Ideally P values should be <0.05, which indicates a reliable fit to the experimental data

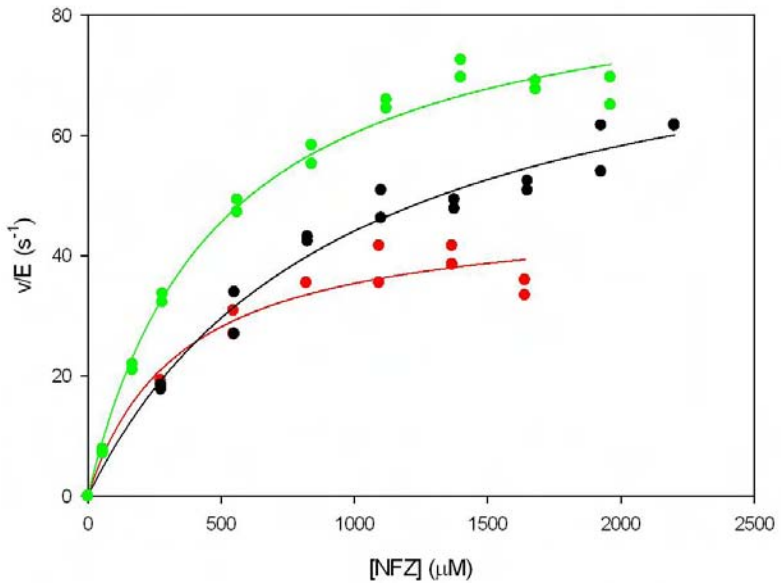

Figure 5.26 Plots of rate of reduction of nitrofurazone by T41L F70A, versus NFZ concentration
40 µM NADH (red), 60 µM NADH (black) and 200 µM NADH (green). Lines were fitted to Equation 5.1

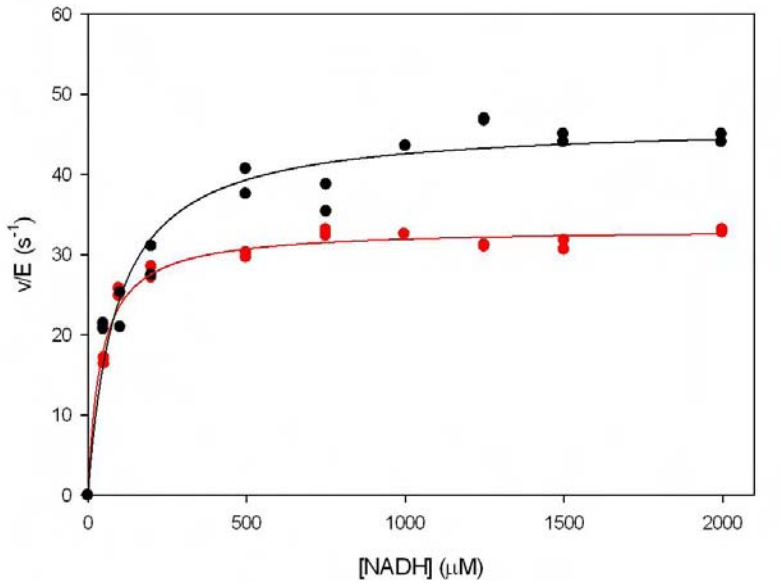

Figure 5.27 Plots of rate of reduction of nitrofurazone by T41L F70A, versus NADH concentration
500 µM NFZ (red) and 1000 µM NFZ (black). Lines were fitted to Equation 5.1

[NFZ] (μM)	[NADH] (μM)	$k_{cat\ app\ NFZ}$ (s^{-1})	t test	P	$K_{m\ app\ NFZ}$ (μM)	t test	P	$k_{cat}/K_{m\ NFZ}$ (μM s^{-1})	t test	P
0-1650	40	48 ± 4	13.7	<0.0001	347 ± 88	3.9	0.0020	0.138 ± 0.026	5.3	0.0002
0-2200	60	86 ± 5	16.5	<0.0001	953 ± 138	6.9	<0.0001	0.090 ± 0.008	11.4	<0.0001
0-2000	200	90 ± 3	31.9	<0.0001	481 ± 46	10.5	<0.0001	0.186 ± 0.013	14.9	<0.0001

(A)

[NADH] (μM)	[NFZ] (μM)	$k_{cat\ app\ NADH}$ (s^{-1})	t test	P	$K_{m\ app\ NADH}$ (μM)	t test	P	$k_{cat}/K_{m\ NADH}$ (μM s^{-1})	t test	P
0-2000	500	33 ± 0.4	79.7	<0.0001	41 ± 4	11.1	<0.0001	0.810 ± 0.067	12.0	<0.0001
0-2000	1000	46 ± 1	37.8	<0.0001	90 ± 13	6.9	<0.0001	0.517 ± 0.0065	7.9	<0.0001

(B)

Table 5.12 Kinetic Parameters of the reduction of nitrofurazone by T41L F70A
(A) NFZ concentration is varied at a range of fixed NADH concentrations (B) NADH concentration is varied at a range of fixed NFZ concentrations. Parameters for data were fitted to Equation 5.1 for a single substrate Menten equation and analysed statistically by calculating t test and P values for each regression curve, t equals the ratio of the regression coefficient to its standard error, indicating how much the rate of the reaction depends on the K_m and k_{cat}. A large t value indicates that the data fits the equation and that the rate of reaction can be predicted from the parameters. The P value is the probability that the parameters fit the curve by chance, the smaller the P value the less likely it occurred by chance. Ideally P values should be <0.05, which indicates a reliable fit to the experimental data

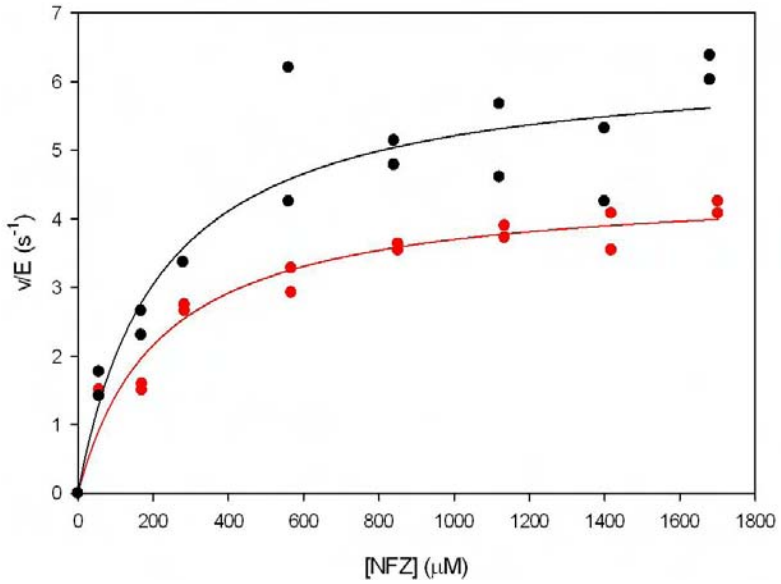

Figure 5.28 Plots of rate of reduction of nitrofurazone by 282, versus NFZ concentration
100 μM NADH (red) and 200 μM NADH (black). Lines were fitted to Equation 5.1

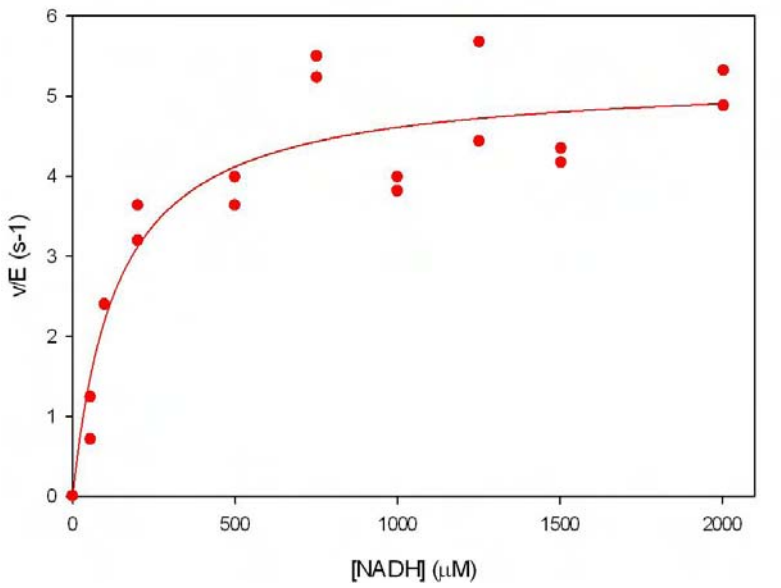

Figure 5.29 Plots of rate of reduction of nitrofurazone by 282, versus NADH concentration
500 μM NFZ. Lines were fitted to Equation 5.1

[NFZ] (μM)	[NADH] (μM)	$k_{cat\ app\ NFZ}$ (s^{-1})	t test	P	$K_{m\ app\ NFZ}$ (μM)	t test	P	$k_{cat}/K_{m\ NFZ}$ (μM s^{-1})	t test	P
0-1700	100	5 ± 0.2	22.8	<0.0001	217 ± 37	5.8	<0.0001	0.021 ± 0.003	7.3	<0.0001
0-1700	200	6 ± 0.4	14.8	<0.0001	216 ± 57	3.8	0.0017	0.029 ± 0.006	4.7	0.0002

(A)

[NADH] (μM)	[NFZ] (μM)	$k_{cat\ app\ NADH}$ (s^{-1})	t test	P	$K_{m\ app\ NADH}$ (μM)	t test	P	$k_{cat}/K_{m\ NADH}$ (μM s^{-1})	t test	P
0-2000	500	5 ± 0.3	19.2	<0.0001	136 ± 34	4.0	0.0008	0.039 ± 0.008	4.8	0.0002

(B)

Table 5.13 Kinetic Parameters of the reduction of nitrofurazone by 282
(A) NFZ concentration is varied at a range of fixed NADH concentrations (B) NADH concentration is varied at a range of fixed NFZ concentrations. Parameters for data were fitted to Equation 5.1 for a single substrate Menten equation and analysed statistically by calculating t test and P values for each regression curve, t equals the ratio of the regression coefficient to its standard error, indicating how much the rate of the reaction depends on the K_m and k_{cat}. A large t value indicates that the data fits the equation and that the rate of reaction can be predicted from the parameters. The P value is the probability that the parameters fit the curve by chance, the smaller the P value the less likely it occurred by chance. Ideally P values should be <0.05, which indicates a reliable fit to the experimental data

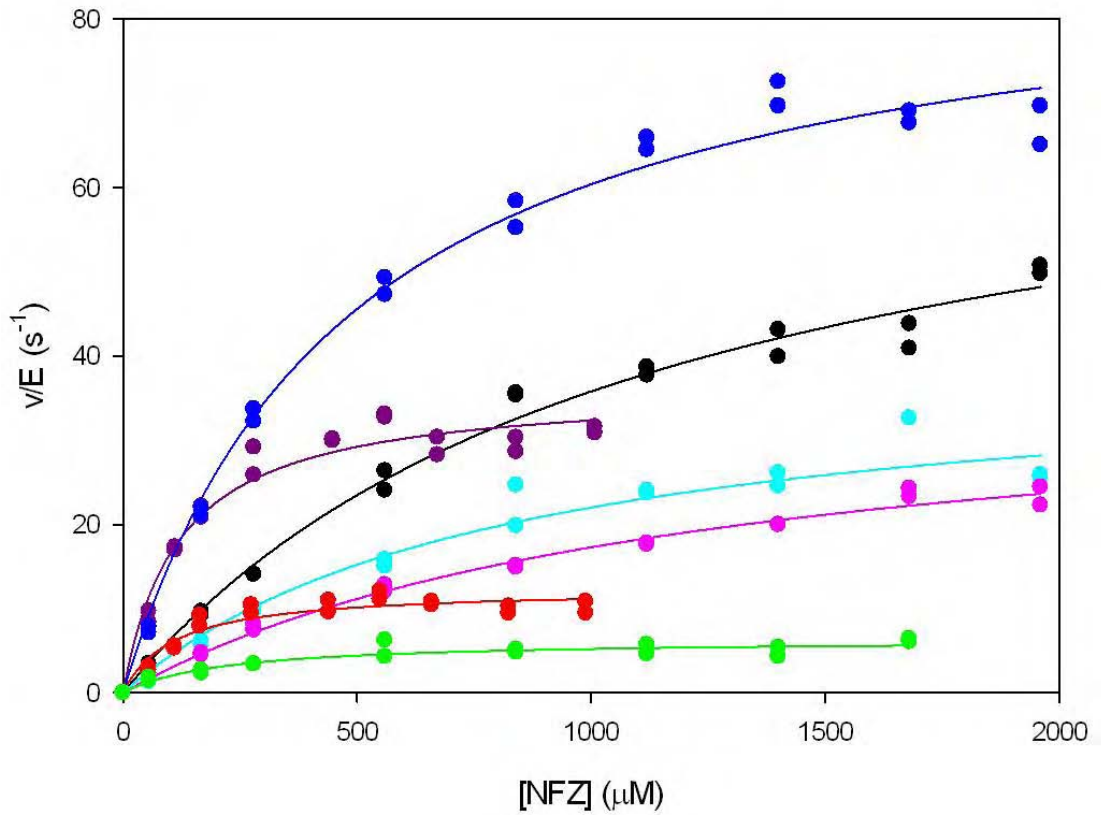

Figure 5.30 Plots of rate of reduction of nitrofurazone, versus NFZ concentration at 200 μM NADH

WT (black), F124N (cyan), T41L N71S (purple), T41Q N71S F124T (pink), T41G N71S (red), T41L F70A (blue) and 282 (green)

NTR	$k_{cat\ app\ NFZ}$ (s^{-1})	t test	P	$K_{m\ app\ NFZ}$ (μM)	t test	P	$k_{cat}/K_{m\ NFZ}$ (μM s^{-1})	t test	P
Wild Type	76 ± 4	17.3	<0.0001	1105 ± 134	8.2	<0.0001	0.068 ± 0.005	15	<0.0001
F124N	30 ± 4	11.4	<0.0001	609 ± 171	4.7	0.0002	0.049 ± 0.006	7.7	<0.0001
T41L N71S	36 ± 1	28.7	<0.0001	120 ± 17	7.2	<0.0001	0.302 ± 0.034	9.0	<0.0001
T41Q N71S F124T	28 ± 2	28.7	<0.0001	718 ± 141	8.6	<0.0001	0.038 ± 0.002	16.3	<0.0001
T41G N71S	12 ± 1	18.7	<0.0001	110 ± 24	4.5	0.0003	0.113 ± 0.020	5.7	<0.0001
T41L F70A	90 ± 3	31.9	<0.0001	481 ± 46	10.5	<0.0001	0.186 ± 0.013	14.9	<0.0001
282	6 ± 0.4	14.8	<0.0001	216 ± 57	3.8	0.0017	0.029 ± 0.006	4.7	0.0002

Table 5.14 Kinetic Parameters of WT and six *NfsB* mutants for the reduction of nitrofurazone at a constant NADH concentration of 200 μM
Parameters for data were fitted to Equation 5.1 for a single substrate Menten equation and analysed statistically by calculating t test and P values for each regression curve, t equals the ratio of the regression coefficient to its standard error, indicating how much the rate of the reaction depends on the K_m and k_{cat}. A large t value indicates that the data fits the equation and that the rate of reaction can be predicted from the parameters. The P value is the probability that the parameters fit the curve by chance, the smaller the P value the less likely it occurred by chance. Ideally P values should be <0.05, which indicates a reliable fit to the experimental data. New data highlighted in red

NTR	$k_{cat\ app\ NFZ}$ (s^{-1})	t test	P	$K_{m\ app\ NFZ}$ (μM)	t test	P	$k_{cat}/K_{m\ NFZ}$ (μM s^{-1})	t test	P
Wild Type	80 ± 2	36	<0.0001	1280 ± 70	19	<0.0001	0.063 ± 0.002	38	<0.0001
F124N	27 ± 2	13	<0.0001	350 ± 60	5.7	<0.0001	0.077 ± 0.008	9.4	<0.0001
T41L N71S	37 ± 1	27	<0.0001	120 ± 10	10	<0.0001	0.300 ± 0.020	15	<0.0001
T41Q N71S F124T	23 ± 2	15	<0.0001	320 ± 50	6.8	<0.0001	0.070 ± 0.006	12	<0.0001

Table 5.15 Kinetic Parameters of WT and three *NfsB* mutants for the reduction of nitrofurazone at a constant NADH concentration of 200 μM
Data from previous studies (Jarrom 2008), which have been included for comparison purposes

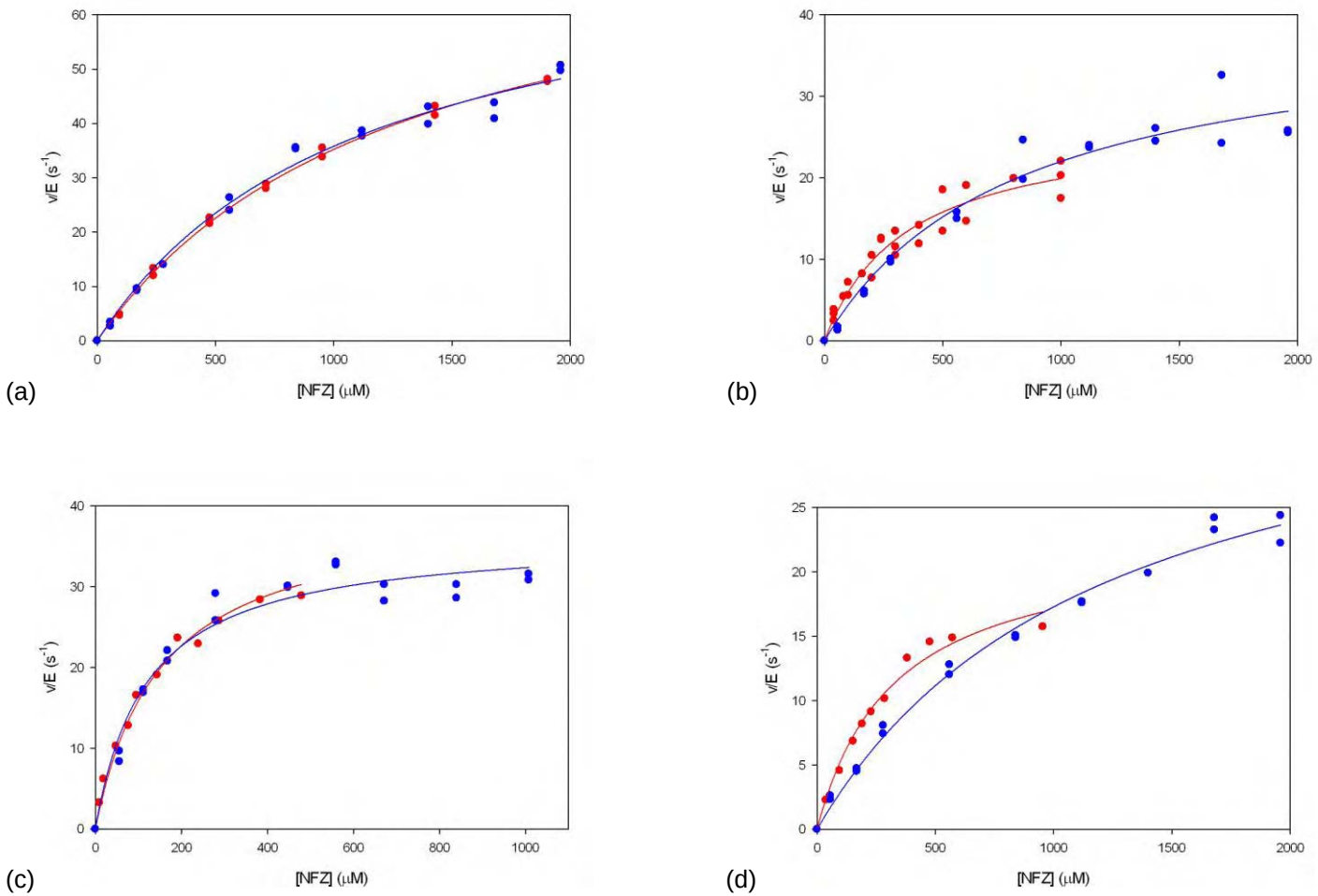

Figure 5.31 Plots of rate of reduction of nitrofurazone, versus NFZ concentration at 200 μM NADH
Graphical representation with the red lines showing previous data (Jarrom 2008) and the blue lines this study. (a) WT (b) F124N (c) T41L N71S and (d) T41Q N71S F124T

5.3.6.3 Menadione Kinetics

In addition to the reduction of nitroaromatic compounds NTR can reduce quinones to the corresponding quinols (see Section 1.4.3.1). Steady-state rates for the reduction of menadione were determined at a single fixed concentration of 500 µM NADH, varying the concentration of menadione for WT and all six mutants. This reaction was coupled with 100 µM cytochrome c. These were fitted to Equation 5.1 and a graph showing the rate of reaction constructed (see Figure 5.32). Kinetic parameters showing apparent K_m, k_{cat} and k_{cat}/K_m were determined for each enzyme (see Table 5.16).

Previous menadione data for WT, F124N, T41L N71S and T41Q N71S F124T enzymes have been compared to that obtained in this study (see Table 5.17 and Figure 5.33). A small difference was seen for each enzyme; however the k_{cat}/K_m for each was similar to previous data.

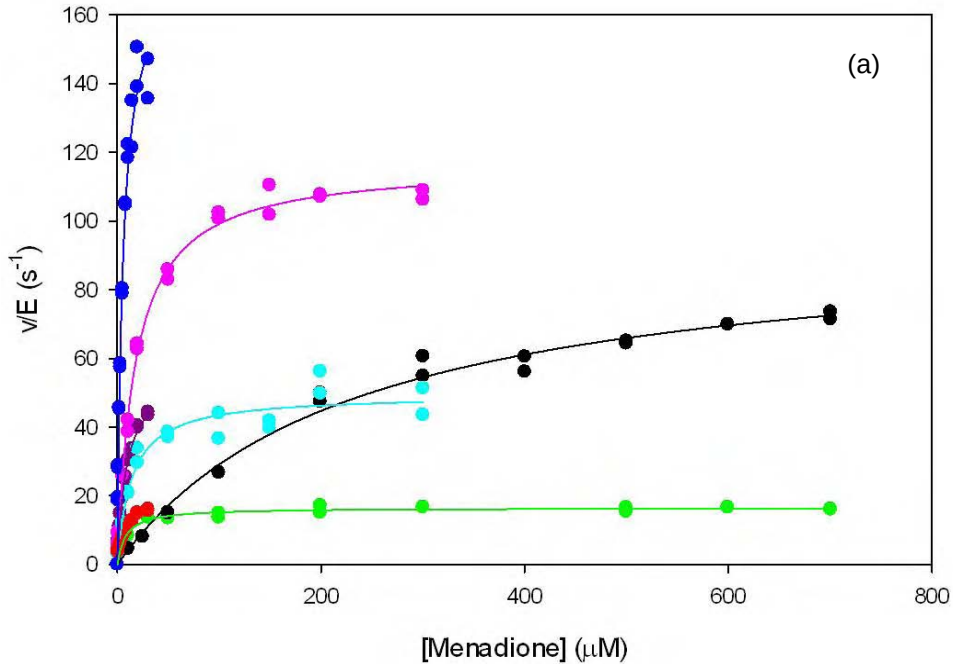

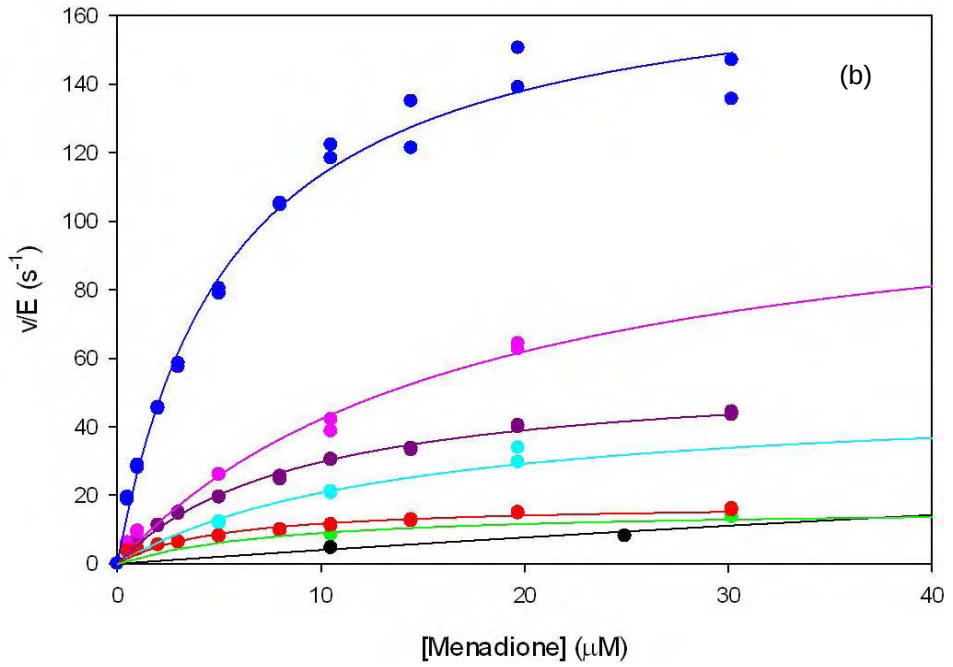

Figure 5.32 Plots of rate of reduction of menadione, versus menadione concentration at 500 µM NADH

WT (black), F124N (cyan), T41L N71S (purple), T41Q N71S F124T (pink), T41G N71S (red), T41L F70A (blue) and 282 (green). (a) Shows T41Q N71S F124T, WT and 282 (b) Shows detail T41L F70A, T41L N71S and T41G N71S

NTR	$k_{cat\ app\ MENADIONE}$ (s^{-1})	t test	P	$K_{m\ app\ MENADIONE}$ (μM)	t test	P	$k_{cat}/K_{m\ MENADIONE}$ (μM s^{-1})	t test	P
Wild Type	96 ± 3	28.8	<0.0001	231 ± 21	10.9	<0.0001	0.42 ± 0.03	16.6	<0.0001
F124N	50 ± 2	29.1	<0.0001	14 ± 2	6.3	<0.0001	3.57 ± 0.49	7.3	<0.0001
T41L N71S	57 ± 2	36.8	<0.0001	9 ± 1	15.3	<0.0001	6.23 ± 0.26	24.4	<0.0001
T41Q N71S F124T	117 ± 1	83.5	<0.0001	12 ± 1	19.0	<0.0001	9.75 ± 0.30	22.4	<0.0001
T41G N71S	18 ± 1	20.1	<0.0001	5 ± 1	6.8	<0.0001	3.43 ± 0.36	9.5	<0.0001
T41L F70A	170 ± 5	34.9	<0.0001	25 ± 1	12.1	<0.0001	6.80 ± 0.50	17.2	<0.0001
282	16 ± 0.4	45.4	<0.0001	8 ± 2	5.7	<0.0001	1.97 ± 0.32	6.1	<0.0001

Table 5.16 Kinetic Parameters of WT and six *NfsB* mutants for the reduction of menadione at a constant NADH concentration of 500 μM
Parameters for data were fitted to Equation 5.1 for a single substrate Menten equation and analysed statistically by calculating t test and P values for each regression curve, t equals the ratio of the regression coefficient to its standard error, indicating how much the rate of the reaction depends on the K_m and k_{cat}. A large t value indicates that the data fits the equation and that the rate of reaction can be predicted from the parameters. The P value is the probability that the parameters fit the curve by chance, the smaller the P value the less likely it occurred by chance. Ideally P values should be <0.05, which indicates a reliable fit to the experimental data. New data highlighted in red

NTR	$k_{cat\ app}$ MENADIONE (s^{-1})	t test	P	$K_{m\ app}$ MENADIONE (μM)	t test	P	$k_{cat}/K_{m\ MENADIONE}$ (μM s^{-1})	t test	P
Wild Type	80 ± 3	31	<0.0001	150 ± 15	9.8	<0.0001	0.58 ± 0.04	13	<0.0001
F124N	58 + 4	14	<0.0001	24 ± 6	3.9	0.005	2.8 ± 0.5	4.9	0.001
T41L N71S	53 ± 5	11.2	<0.0001	8 ± 2	3.6	0.0046	6.4 ± 1.2	5.3	0.0002
T41Q N71S F124T	107 ± 5	23	<0.0001	7 ± 1	5.4	0.0005	15 ± 2	6.3	0.0001

Table 5.17 Kinetic Parameters of WT and three *NfsB* mutants for the reduction of menadione at a constant NADH concentration of 500 μM
Data from previous studies (Jarrom 2008 and Anchal unpublished), which have been included for comparison purposes

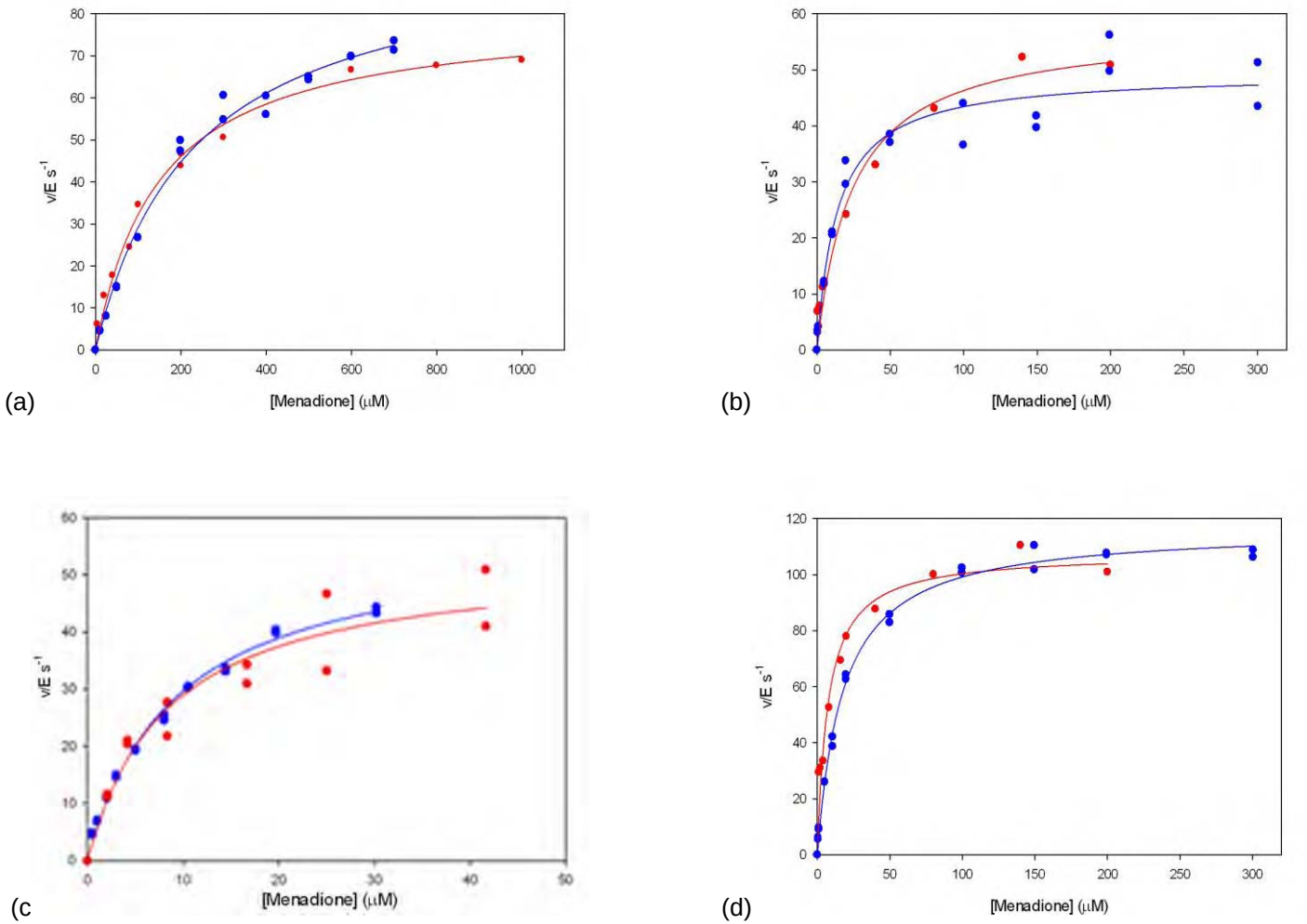

Figure 5.33 Plots of rate of reduction of menadione, versus menadione concentration at 500 μM NADH
Graphical representation with the red lines showing previous data (Jarrom 2008) and the blue lines this study. (a) WT (b) F124N (c) T41L N71S and (d) T41Q N71S F124T

5.3.7 Analysis and quantification of product ratios for the reduction of CB1954

WT *NfsB* enzyme reduces the prodrug CB1954 at both the 2-hydroxylamine and 4-hydroxylamine in equal ratios. The 4-hydroxylamine (4-HA) is highly cytotoxic being a difunctional alkylating agent (Anlezark *et al.* 1992). Whereas the 2-hydroxylamine (2-HA) is a less toxic monofunctional alkylating agent which allows greater spread of the active product known as the "bystander effect" (Helsby *et al.* 2004). It has previously been determined that most *NfsB* mutants produce a 50:50 ratio of the 2-HA and 4-HA, with the exception of mutants with a T41 mutation to Leucine. Both the mutant T41L and T41L N71S only produce the 4-HA.

Nuclear magnetic resonance spectroscopy (NMR) was used to analyse the product ratio for T41G N71S, T41L F70A and clone 282 NTR activation of CB1954. WT *NfsB*, T41L N71S and *NfsA* were also analysed for comparison purposes.

T41G N71S produces both the 4-HA and 2-HA with a slight preference for the 4-HA. Both T41L F70A and clone 282 dominantly produce the 4-HA. In the case of 282 a small amount of 2-HA is produced (see Figure 5.34).

(a)

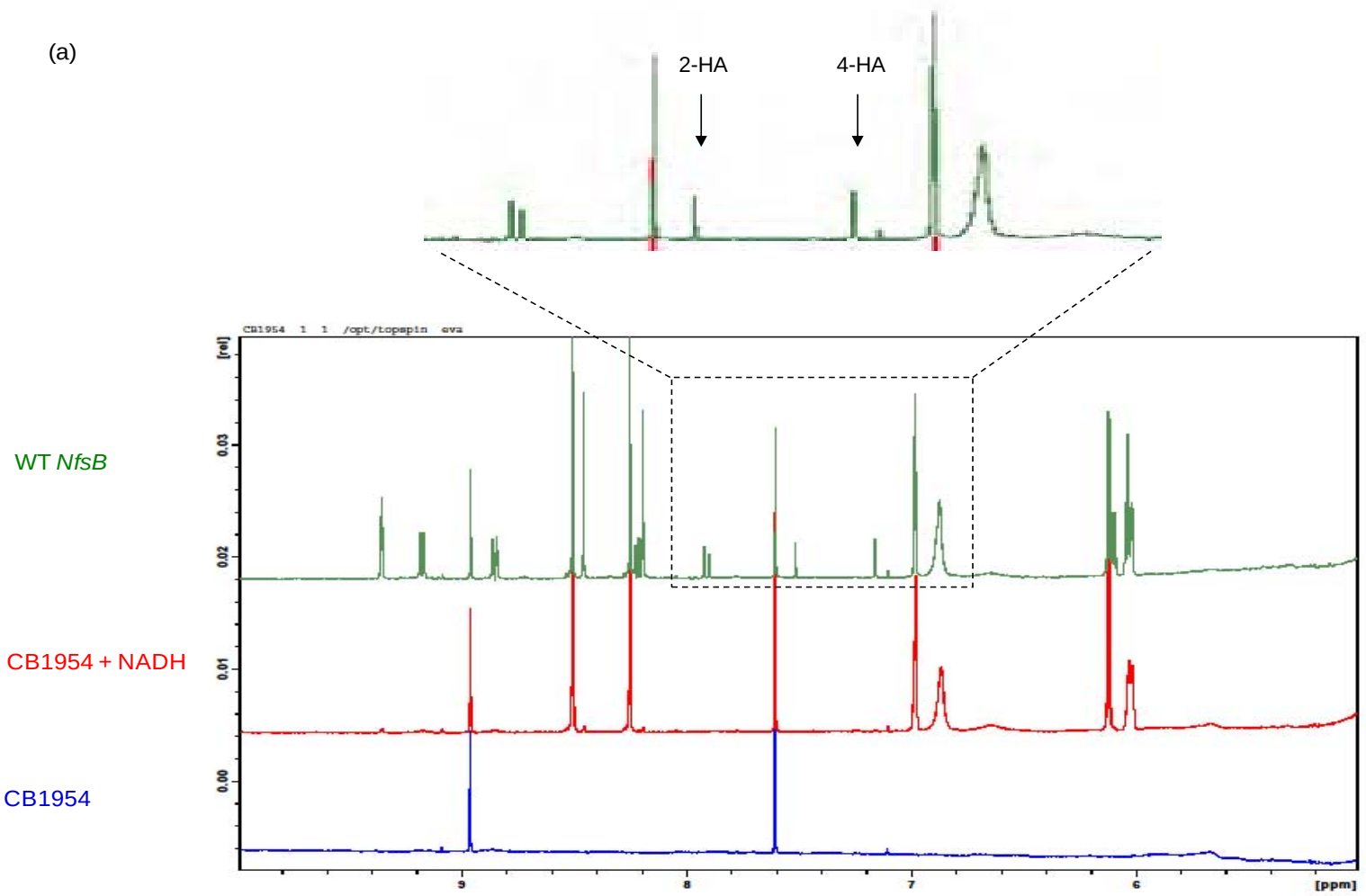
2-HA
4-HA
WT NfsB
CB1954 + NADH
CB1954
[rel]
0.03
0.02
0.01
0.00
9
8
7
6
[ppm]

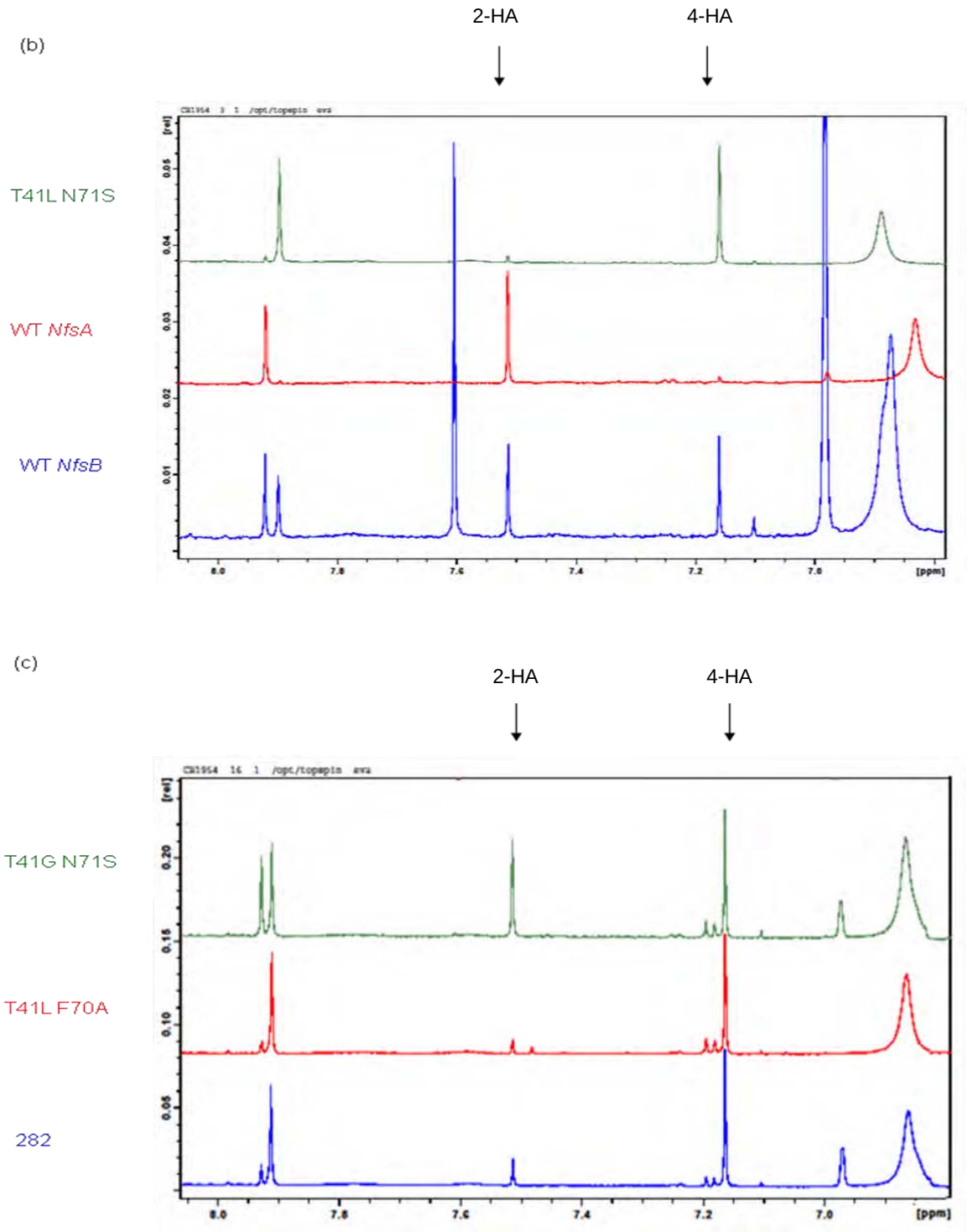

Figure 5.34 NMR spectra for the reduction of CB1954
(a) Control: CB1954 alone, CB1954 + NADH and CB1954 + NADH + WT *NfsB*, (b) Previous enzymes: WT *NfsB*, WT *NfsA* and T41L N71S, (c) New enzymes: N71S A113V R121V F123N F124V A125C K179R (282), T41L F70A and T41G N71S. NAD(P)H (1 mM final concentration) and CB1954 (0.5 mM final concentration, in 10% final DMSO) were mixed in 10 mM sodium phosphate buffer, pH 7.0, containing 10% D_2O. Approximately 0.1 µM of each enzyme was then added and spectrum taken within 5-10 minutes. NADH was used for all enzymes except WT *NfsA* which used NADPH. This work was carried out by Dr Eva Hyde using purified enzymes purified in this study

5.4 DISCUSSION

5.4.1 Column purification

Three NTR mutants T41G N71S, T41L F70A and clone 282 were purified by column chromatography. Firstly using a hydrophobic column (phenyl sepharose), which selectively binds hydrophobic proteins. Most of the T41G N71S NTR bound to the column at 0.5M ammonium sulphate. However most of the T41L F70A NTR slipped off the column and all of the 282 NTR washed straight through the column at 0.5M ammonium sulphate but bound to the column at 1M ammonium sulphate. This indicates that T41L F70A is less hydrophobic than T41G N71S and 282 is less hydrophobic than both T41G N71S and T41L F70A. In the case of T41L F70A there is a substitution of phenylalanine 70 to alanine and for 282 there were substitutions of phenylalanine 123 and 124 to asparagines and valine respectively.

The second column used was an ion-exchange column (Q-Sepharose column). T41L F70A, T41G N71S and 282 were further purified with a single Q-Sepharose column. All proteins bound tightly and eluted with a 0.1M NaCl/0.5M NaCl gradient (pH 7.0).

5.4.2 Kinetic Assays

The ideal NTR mutant would have an increased k_{cat} to allow faster conversion of prodrug, coupled with a reduced $K_{m\ CB1954}$ lowering the physiological concentrations required for efficient turnover. This would allow administration of a lower dose of the prodrug. The $K_{m\ NADH}$ values are also important, research shows that the physiological concentration of NADH is in the millimolar range (Garofalo *et al.* 1988). For WT *NfsB* millimolar concentrations mean that NADH is not rate limiting. However some of the best mutants have led to large increases in the $K_{m\ NADH}$. Ideally the mutant would also have an increased specificity for CB1954, with improved enzyme activity for CB1954, but reduced activity for other NTR substrates eg: nitrofurazone and menadione.

5.4.2.1 CB1954

The initial K_m and k_{cat} was determined for F124N, T41L N71S, T41G N71S, T41L F70A, T41Q N71S F124T and 282 at 500 µM NADH. However because CB1954 is a poor substrate for WT NTR, it was not possible to determine the K_m and k_{cat} for the WT reaction. To determine these values a high substrate concentration would be required. Substrate concentrations that high are not achievable, as CB1954 is only soluble to 4 mM in Tris buffer.

The reduction of CB1954 by WT, F124N, T41L N71S and T41Q N71S F124T NTR were then compared to previous data (see Figure 5.24 and Tables 5.9-5.10). Small differences within error were seen for each enzyme. Overall previous and current data are consistent with each other.

However the k_{cat}/K_m can reliably be determined for WT, as this parameter can be determined even if the substrate saturation is not achieved. The k_{cat}/K_m of all the mutants were better than WT enzyme, showing that T41L N71S (~70-fold increase) was kinetically the best at reducing CB1954, followed by T41G N71S (~50-fold increase), T41Q N71S F124T (~30-fold increase), T41L F70A (~10-fold increase), F124N (~3-fold increase) and 282 (~1-fold increase).

Finally global kinetic parameters were determined for T41G N71S, T41L F70A and 282. This allows the determination of K_m and k_{cat} values, for one substrate if the enzyme was saturated with the second substrate. T41G N71S has a k_{cat} ~3-fold lower than WT, however the K_m was ~200-fold lower. Only a small reduction in k_{cat} compared to a huge reduction in K_m means that the $k_{cat}/K_{m\ CB1954}$ for T41G N71S is ~80-fold higher than WT. Alternatively T41L F70A has a k_{cat} and K_m ~1.5-fold and ~25-fold lower, giving a k_{cat}/K_m ~15-fold higher than WT. Finally 282 has a k_{cat} and K_m ~7-fold and ~250-fold lower, giving a k_{cat}/K_m ~2.5-fold higher. Therefore all the mutants had a reduced K_m but they also all had reduced k_{cat} values.

5.4.2.2 Nitrofurazone

Initial K_m and k_{cat} parameters were determined for T41G N71S, T41L F70A and 282 for the reduction of nitrofurazone. These were compared to WT enzyme. T41G N71S has a k_{cat} ~6.3-fold lower than WT and K_m ~10-fold lower. T41L F70A has a k_{cat} ~1.2-fold higher than WT and K_m ~2.3-fold lower and 282 has a k_{cat} ~12.7-fold lower than WT and K_m ~5.1-fold lower.

Two of these mutants had an increase in specificity constant for nitrofurazone. In particular mutant T41L F70A showed a high specificity constant for nitrofurazone with a reduction in K_m and increase in k_{cat}. By contrast mutant 282 showed a decrease in specificity constant with a large drop in k_{cat} and only a small drop in K_m. Thus three of the mutant NTR's were better at reducing nitrofurazone than WT enzyme. T41L N71S (~4.4-fold increase) was kinetically the best, followed by T41L F70A (~2.7-fold increase) and T41G N71S (~1.7-fold increase). F124N (~1.4-fold decrease), T41Q N71S F124T (~1.8-fold decrease) and 282 (~2.3-fold decrease) were kinetically worse than WT NTR.

The reduction of nitrofurazone by WT, F124N, T41L N71S and T41Q N71S F124T was compared to previous data (see Figure 5.35 and Tables 5.16-5.17). Small differences within error were seen for WT and T41L N71S enzyme. However F124N and T41Q N71S F124T showed bigger differences. In both of these cases the k_{cat} is similar but the K_m is approximately double what was previously found, having a big effect on the k_{cat}/K_m. My data puts both T41Q N71S F124T and F124N as less sensitive to nitrofurazone but previous data has them as more sensitive than WT. The fact two of the enzymes give similar results indicates that consistent results are possible. However the big differences for the other two enzymes is still a little worrying. It is difficult to determine why such differences in data were seen. Different preparations of enzyme were used however if there had been contamination of some sort CB1954 results would also have also been different.

5.4.2.3 Menadione

K_m and k_{cat} parameters were also determined for T41G N71S, T41L F70A and 282 for the reduction of menadione at 500 µM NADH. These were compared to WT enzyme. T41G N71S has a k_{cat} ~5.3-fold lower than WT and K_m ~46.2-fold lower. T41L F70A has a k_{cat} ~1.8-fold higher than WT and K_m ~9.2-fold lower and 282 has a k_{cat} ~6-fold lower than WT and K_m ~28.9-fold lower. All three of these mutants had an increase in specificity constant for menadione. In particular mutant T41L F70A showed high specificity constant for menadione with a reduction in K_m and increase in k_{cat}.

The k_{cat}/K_m measurements were again used to determine the fold increase in activity of each mutant relative to WT NTR. T41Q N71S F124T (~23.2-fold increase) was kinetically the best, followed by T41L F70A (~16.2-fold increase), T41L N71S (~14.8-fold increase), F124N (~8.5-fold increase), T41G N71S (~8.2-fold increase) and 282 (~2.3-fold increase).

The reduction of menadione by WT, F124N, T41L N71S and T41Q N71S F124T NTR was compared to previous data (see Figure 5.37 and Tables 5.18-5.19). Small differences were seen for all enzymes, but the k_{cat}/K_m remained similar to that determined previously.

5.4.3 Product ratios for the reduction of CB1954

T41L F70A enzyme produced mostly the 4-HA, with negligible amounts of the 2-HA. This was expected. However N71S A113V R121V F123N F124V A125C K179R enzyme also produced mainly the 4-HA. This has only previously been seen for T41L mutants (Race *et al.* 2007 and Jarrom *et al.* 2009). This enzyme shows no mutation at position T41. Therefore it is feasible that the mutation of either A113, R121, F123, A125 or K179 or a combination of these also leads to a shift towards the 4-HA derivative. Enzyme T41G N71S produced both the 2-HA and 4-HA, with possibly a slight preference for the 4-HA.

Looking at activity based on k_{cat}/K_m, T41L N71S is kinetically the best mutant at reducing CB1954. Of the three mutants purified in this study, T41G N71S was kinetically the best mutant at reducing CB1954. This mutant showed clear improvement for CB1954 with a reduction in K_m, showing the tightest CB1954 data of all the mutants. However the NADH kinetic data for T41G N71S was poor with a large increase in K_m. This large increase in K_m could potentially make NADH rate limiting when in an in vivo setting.

CHAPTER 6: COMPARISON OF WT AND MUTANT NTR IN HUMAN CELLS

6.1 INTRODUCTION

VDEPT is a cancer gene therapy strategy which requires enzyme delivery by a viral vector. In the past, replication deficient adenoviruses and retroviruses have been used to express NTR in human tumour cells (Bridgewater *et al.* 1995, Green *et al.* 1997, McNeish *et al.* 1998, Weedon *et al.* 2000). As previously stated CB1954 is a poor substrate for NTR, however improving the catalytic efficiency of the system may produce therapeutic benefits. WT NTR and several improved mutants have previously been tested in human tumour cells lines (Grove *et al.* 2003, Jaberipour 2005 and Guise *et al.* 2007). Many of the mutants identified as improved in bacterial assays showed comparable improvement in human cells, however there have been exceptions. In particular NTR mutants N71S F124K and N71S F124N were poor in human cells due to poor expression.

During this study a number of improved NTR mutants have been isolated and tested in bacterial cells (Chapter 3 and 4 this study) and kinetic parameters determined in vitro (Chapter 5 this study). The main aim of this chapter is to assess the therapeutic potential of four improved mutants in human ovarian carcinoma cells (SKOV-3). Adenoviruses that express the four most promising NTR mutants T41G N71S, T41N N71S, N71S A125T and N71S A113V R121V F123N F124V A125C K179R (282) were constructed and compared with previous adenoviruses WT, T41L N71S and T41Q N71S F124T. These four new mutant NTRs were chosen based on their ability to sensitise bacterial cells to CB1954.

6.2 MATERIAL AND METHODS

6.2.1 NTR expression

6.2.1.1 Plasmid construction

λ lysogens encoding desired NTR mutants were streaked onto LB plates containing a fresh lawn of *E. coli* UT5600. The resulting lysis area was picked and used to provide a template for a PCR reaction, using Kod polymerase with primers JG138A and JG138B (see section 2.2.1) to generate NTR PCR fragments. JG138A introduces the Kozak sequence (CCACC) immediately preceding the ATG start codon of the NTR coding sequence (Kozak 1987) and JG138B spans the end of the coding region. PCR products were resolved by agarose gel electrophoresis to confirm DNA fragments of the correct size were amplified and purified using Roche High Pure PCR Product Purification Kit (Roche Applied Sciences, Germany).

A plasmid vector pPS1326B1 was digest with *Hpa* I and the appropriate size fragment was gel extracted using Qiagen QIA-Quick Gel Extraction Kit (Qiagen, West Sussex). The plasmid vector pPS1326B1 contains adenovirus type 5 genome sequence from the left end to *Xba* I site at 10589 bp of the genome, with the E1 region from 360 bp to 3525 bp deleted and replaced with CMV enhancer and promoter, and sequences from human β globin and complement C2 genes, which contain an intron and poly A site transcription termination signals, respectively. This plasmid was designed for the expression of open reading frames inserted into an *Hpa* I site downstream of the CMV promoter. Figure 6.1 shows a schematic of pPS1326B1 plasmid vector.

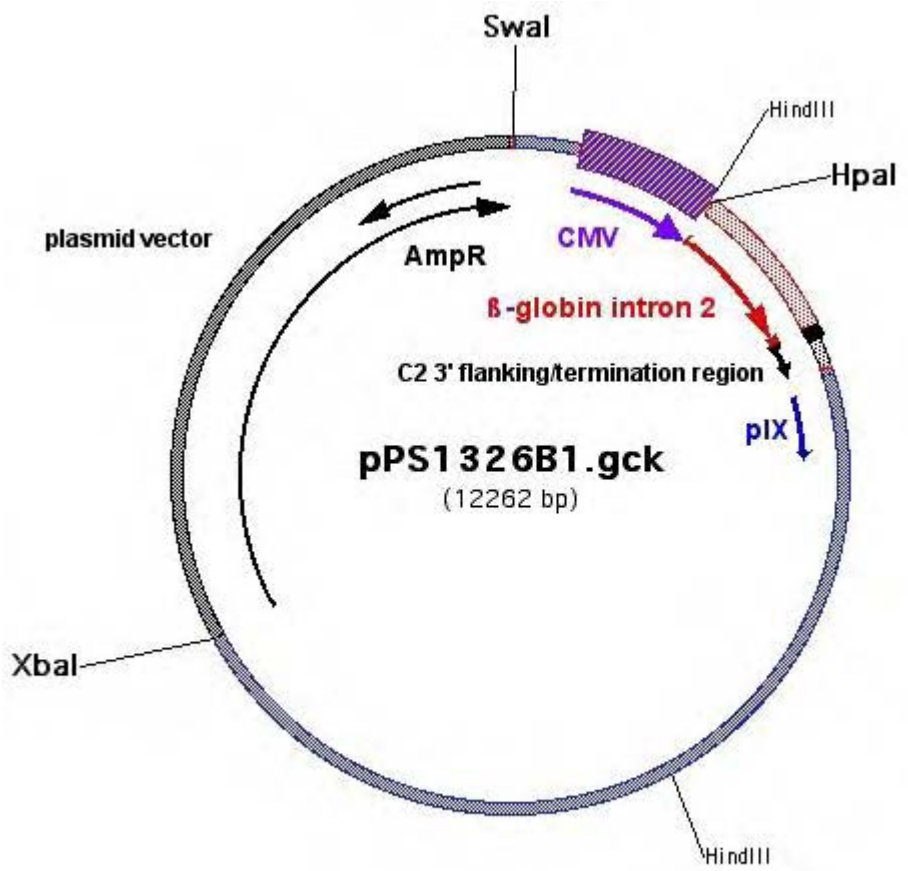

Figure 6.1 Schematic diagram of plasmid pPS1326B1 left end vector.
Plasmid pPS1326B1 contains adenovirus type 5 genome sequence from the left end to *Xba* I site at 10589 bp of genome, with an E1 deletion from 360 bp – 3525 bp. The deleted region has been replaced with a CMV enhancer and promoter, with sequences from human β globin and complement C2 genes, containing an intron and poly A transcription termination signal.

PCR products were ligated with the *Hpa* I digested pPS1326B1 (0.5 pico moles of PCR insert with 200 ng plasmid vector) and transformed into competent *E. coli* XL-2 blue cells. Individual colonies were picked and grown in 10 ml of LB Broth containing ampicillin. Mini Prep plasmid purification was performed on the bacterial cultures and the resulting plasmid preps were digested with *Nco* I, *Eco* RV and *Bgl* II and analysed by agarose gel electrophoresis. Plasmids with correct digestion patterns were taken on to large-scale cultures (1 µl of undigested Mini-Prep Plasmid DNA was re-transformed into *E. coli* XL-2 blue cells. A single colony was picked for each mutant NTR and grown in 300 ml of LB Broth containing ampicillin). Bulk Prep purification was performed on the bacterial cultures, and the resulting plasmid preps were again digested with *Nco* I, *Eco* RV and *Bgl* II.

Plasmids with correct digestion patterns were linearised with *Xba* I and the inserted NTR gene sequenced with primers PS1013A and PS1013B.

6.2.2 Generation of adenovirus vectors in HEK 293 cells

The adenoviruses were generated by co-transfection of DNA from plasmids carrying "left end" and "right end" of the adenoviral vector into HEK 293 cells. HEK 293 cells are derived from human embryonic kidney cells, which have been transformed with adenovirus DNA. They contain the E1 region of the adenovirus genome, which allows them to support the replication of E1-deleted adenovirus vectors (Graham *et al.* 1977). The resulting full length genome was therefore generated by homologous recombination (see Figure 6.2 and 6.3).

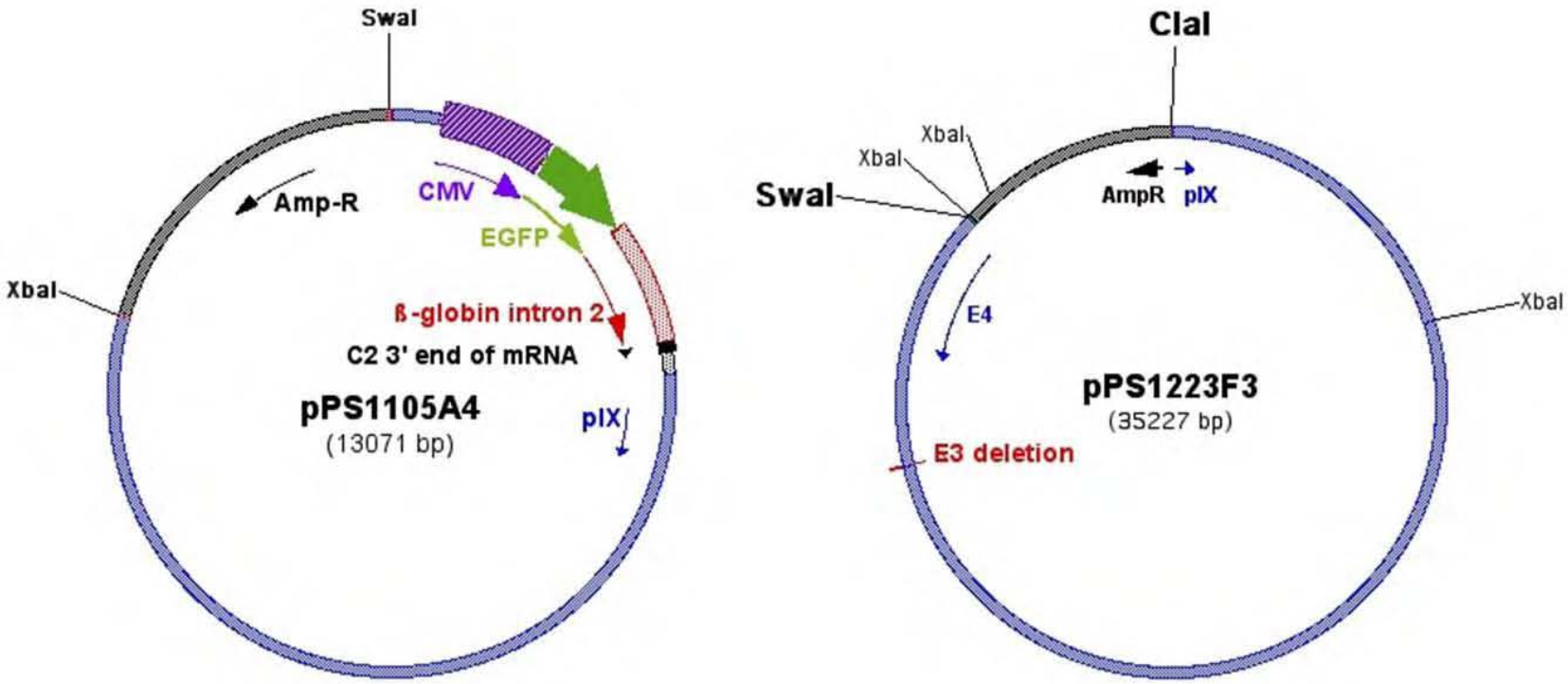

Figure 6.2 Schematic diagrams of plasmids pPS1105A4 and pPS1223F3
Plasmid pPS1105A4 contains Adenovirus left end with EGFP from CMV promoter and plasmid pPS1223F3 contains Ad5 sequence from the start of pIX to the right end, with E3 deletion

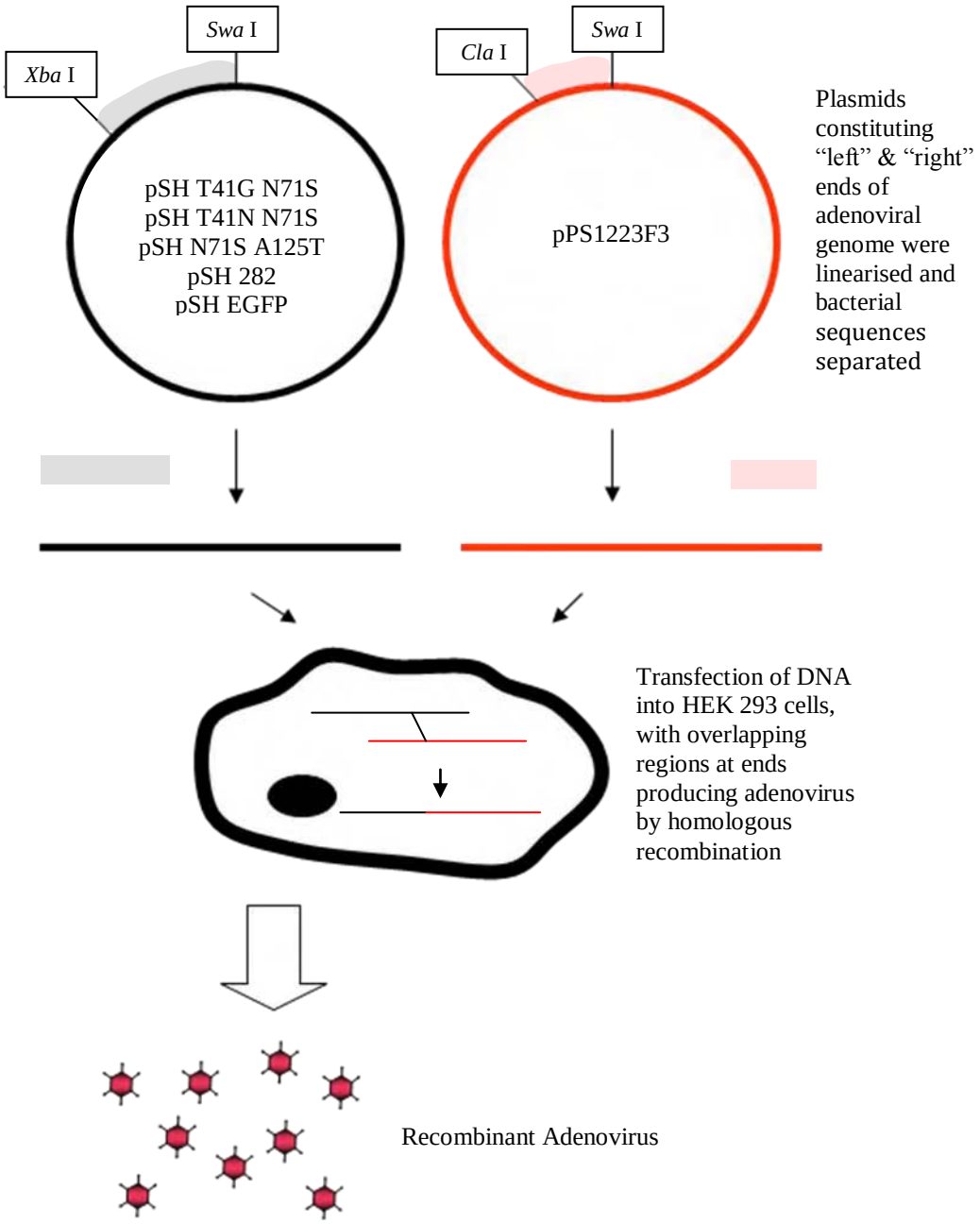

Figure 6.3 Homologous recombination of pSH T41G N71S, pSH T41N N71S, pSH N71S A125T, pSH 282, pSH EGFP with pPS1223F3, to produce non-replicating adenovirus
The plasmids pSH T41G N71S, pSH T41N N71S, pSH N71S A125T, pSH 282 (encoding mutant NTR), pSH EGFP (encoding green fluorescent protein) and pPS1223F3 were linearised and bacterial sequence separated by restriction digestion with *Xba* I/Swa I and *Cla* I/*Swa* I respectively. These plasmids were co-transfected into HEK 293 cells with FuGENE. Following homologous recombination within cells, adenoviruses encoding mutant NTR were produced

10 µg of the "left end" plasmid encoding mutant NTR (pSHT41GN71S, pSHT41NN71S, pSHN71SA125T or pSH282) and 10 µg of plasmid pPS1105A4 "left end" (encoding EGFP) were digested with *Xba* I and 50 µg of plasmid pPS1223F3 "right end" was digested with *Cla* I to linearise the DNA. These were cleaned by phenol/chloroform extraction and ethanol precipitation before digestion with *Swa* I allowing the removal of bacterial genome from the plasmids. The plasmids were again cleaned by phenol/chloroform extraction and ethanol precipitation and resuspended in 50 µl and 250 µl sterile $T_{10}E_1$ respectively.

10 µl FuGENE 6 transfection reagent was added to 206.5 µl DMEM (serum free) media. This mix was vortexed for 1 second and incubated for 5 minutes at room temperature. The two digested plasmids containing inserted DNA (5.0 µg left end, 1.7 µg right end) were mixed with the FuGENE/DMEM mixture and incubated for 30-60 minutes. The mixture was then pipetted gently onto 90% confluent HEK 293 cells growing in a 25 cm^2 tissue flask, and incubated while rocking occasionally for 5 hours in a 37 ^oC incubator. After 5 hours, 5 ml of 2% FBS DMEM plus 2 mM glutamine and pen/strep was added.

The following plasmid combinations were transfected, to generate the indicated viruses:

pSH T41G N71S left end with pPS1223F3 right end = vSH T41G N71S

pSH T41N N71S left end with pPS1223F3 right end = vSH T41N N71S

pSH N71S A125T left end with pPS1223F3 right end = vSH N71S A125T

pSH 282 left end with pPS1223F3 right end = vSH 282

pPS1105A4 left end with pPS1223F3 right end = vSH EGFP

A control of pPS1105A4 “left end” plasmid alone was also transfected. After 3-5 days reporter gene expression was checked for the control and vSH EGFP by fluorescence microscopy. Figure 6.4a shows background EGFP expression from the control and Figure 6.4b shows viral EGFP gene expression. Clear spread of virus can be seen.

a) b)

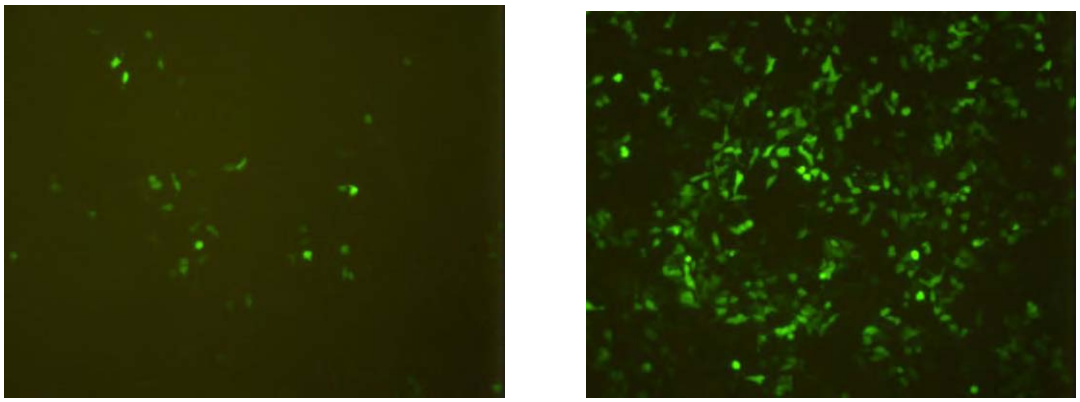

Figure 6.4 Photograph showing EGFP expression from control and EGFP virus using FuGENE transfection in HEK 293 cells
a) Control showing a small amount of background expression, b) EGFP viral gene expression 5 days after transfection. Clear viral spread can be seen

6.2.3 Adenoviral rescue

When most of the cells showed cytopathic effect, the cultures were harvested by tapping side of flask and or flushing with a Pasteur pipette. The sample was then centrifuged at 1,000 rpm for 5 minutes at 4 ^{o}C to pellet cells (Beckman GS-6R bench top centrifuge). Media was removed to leave approximately 1.5 ml. Virus particles were released from cells by three cycles of alternating freezing (in liquid nitrogen) and thawing (in 37 ^{o}C water bath). The sample was then centrifuged at 4,000 rpm for 10 minutes at 4 ^{o}C (Beckman GS-6R bench top centrifuge) to bring down the cell debris. The virus-containing supernatant was transferred to a new container and stored at -80 ^{o}C.

6.2.4 Expansion of adenovirus stocks

For virus titration a 75 cm^2 flask of confluent HEK 293 cells was trypsinised and suspended in 20 ml DMEM containing 10% FBS, 2 mM Glutamine and 20 mM HEPES. HEK 293 cells were counted using a Hycor KOVA Glasstic® Slide 10 Haemocytometer, and 5 x 10^5 cells were added to each well of three six well plates and made up to a total volume of 1 ml with DMEM. Three virus dilutions were used for each virus with 2 µl, 10 µl and 100 µl of virus prep added to 1 ml of DMEM. These virus dilutions were added to the cells and mixed thoroughly by swirling, before incubation at 37 ^oC until clear cytopathic effect was seen. The cells were then harvested and pelleted by centrifugation at 1,000 rpm for 5 minutes and resuspended in 1.5 ml of medium. A cleared virus lysate was made from freeze-thawed cells as above in section 6.2.3. The culture with clear CPE after 3-5 days was designated as P1 stock.

To propagate viral stocks three 75 cm^2 flasks of sub-confluent HEK 293 cells were infected with 1 µl, 4 µl and 10 µl of the P1 virus and incubated at 37 ^oC for 2-5 days until cytopathic effect was seen. The cells with most CPE were then harvested and pelleted by centrifugation at 4,000 rpm for 10 minutes at 4 ^oC and resuspended in 1 ml of medium. A cleared lysate was made from freeze-thawed cells as above in section 6.2.3 and designated as P2 stock.

Finally twenty 150 cm^2 flasks of sub-confluent HEK 293 cells were infected with 1 µl of the P2 stock. The resulting 10 ml of harvested cells were freeze thawed as above in section 6.2.3. A 1/100 volume of N-butanol was added before mixing thoroughly by inversion and left on ice for 1 hour, after which the mixture was centrifuged in a Beckman GS-6R centrifuge for 10 minutes at 2,000 rpm.

A caesium chloride gradient was prepared by firstly adding 2 ml of ρ=1.32 g/ml CsCl (32 g CsCl, 6.8 ml 0.5 M Tris pH 7.9, 61.2 ml sterile distilled water) to a 15 ml Beckman polycarbonate tube, followed by underlaying with 3 ml of ρ=1.45 g/ml CsCl (20.5 g CsCl, 2.9 ml 0.5 M Tris pH 7.9, 25.8 ml sterile distilled water). On top of this, 2 ml of 40% glycerol (40 g glycerol, 2 ml 0.5 M Tris pH 7.9, 0.5 ml 0.2 M EDTA, sterile distilled water to 100 ml) was slowly added, followed by the supernatant from the N-butanol/virus lysate centrifugation. The tubes were then topped up with medium to just below the brim. Balanced tubes were placed in an SW40 rotor in a Beckman Coulter Optima™ LE-80K ultracentrifuge and spun at 25,000 rpm for two hours. A clear white band of adenovirus could be seen and was removed by piercing the tube with a 21 gauge needle. Dialysis of the virus suspension to remove contaminating CsCl was then performed by inserting virus into Slidealyser (Pierce, PO Box 117, Rockford, IL, 61105) 5 ml dialysis cassettes. The virus was dialysed three times against PBS/10% glycerol. Virus was finally removed from the cassette and aliquoted into Sartstedt O ring sealed 1 ml tubes for storage at -85 °C.

6.2.5 Adenoviral DNA purification

Adenoviral DNA was extracted from banded preparations for each virus using Qiagen QIAamp DNA Mini Kit (Qiagen House, Fleming Way, Crawley, West Sussex). 200 µl of virus was used for each extraction, and extraction followed the manufacturer's instructions.

6.2.6 Virus titre determination

6.2.6.1 Virus Particle concentration

20 µl of dialysed virus stock was mixed with 20 µl SDS (0.1%) and heat inactivated by incubation at 56 °C for 30 minutes. The resulting virus lysate was serially diluted and the concentration of DNA determined using DNA binding reagent PicoGreen (Molecular Probes, Eugene, USA) (Murakami and McCaman 1999). The DNA concentration can then be converted to virus particles using the conversion factor:

$$1\ \mu g\ DNA = 2.74 \times 10^{10}\ virus\ particles$$

6.2.6.2 Plaque Assays

For plaque assays, the cell line HER 911 was used. These are human embryonic retina cells transfected with a fragment of Ad5 DNA spanning the E1 region (Fallaux *et al.* 1998). These support replication of E1-deleted adenovirus vectors in the same way as HEK 293 cells, but give a more uniform monolayer, making it easier to see viral plaques.

24 hours before infection, one 150 cm^2 flask of 90% confluent HER 911 cells was split into twenty 6 cm^2 tissue culture dishes. Serial, ten fold dilutions of virus were made in DMEM medium with 2% FBS down to 10^{-10}. 100 µl of each virus dilution ranging from 10^{-3} to 10^{-9} was added, in duplicate, to each 6 cm^2 dish of 911 cells. The dishes were incubated for 90 minutes with gentle agitation every 15 minutes to ensure cells did not dry and to allow gentle mixing.

After removal of virus, 4 ml of a 1:1 mixture of liquified 1.4% agar noble, and complete 2x DME medium (100 ml of 2x DME medium, 4 ml FBS, 2 ml 200 mM glutamine, 1 ml 0.5 M $NaHCO_3$, 1 ml 1 M $MgCl_2$ and 2 ml penicillin / streptomycin) were added gently. These solutions had been pre warmed to 37 °C. The agar was allowed to set at room temperature before incubation at 37 °C in 5% CO_2. The cells were fed at day 4, day 7 and day 10 with 2 ml further 1:1 mixture of complete 2x DME medium and agar noble. Plaques were usually counted between days 10-12 until no further plaques appear. The value for the plaque forming units per ml of virus (pfu/ml) was calculated using the following formula:

$$pfu / ml = \frac{number\ of\ plaques\ per\ dilution\ factor}{0.1}$$

6.2.6.3 Rapid titration of infectious virus (Adeno-X rapid titre kit)

As an alternative to plaque assays, adeno-X rapid titre kit (Clontech Laboratories Inc, 1290 Terra Bella Avenue, Mountain View, CA 94043) was used for the quantification of adenoviral stocks. This allows quick determination in approximately 48 hours taking advantage of the production of viral hexon protein. HEK 293 cells were used for infection, after 24 hours these were fixed and stained with hexon antibody. Methods followed manufacturer's instructions with the exception that virus was plated out first followed by HEK 293 cells; whereas the original protocol plated the cells first. The order was changed to allow greater mixing and to ensure even spread of virus and cells. Sixteen fields of brown/black positive cells were counted per well. For each virus duplicate wells were used for each virus concentration.

The mean numbers of brown/black positive cells or infectious units were determined as followed:

$$(ifu / ml) = \frac{(positive\ cells / field) \times (fields / well) \times (number\ of\ ml\ virus\ dilution)}{(volume\ virus\ ml) \times (dilution\ factor)}$$

Dilution factor = 10^{-7}

Volume = 100 µl (0.1 ml)

5x objective

10x Eye Piece lense

4 mm field diameter

12.5 mm^2 field area

= 16 Fields/well on a 24 well plate based on area being 2.0 cm^2

Figure 6.5 shows photographic examples of the brown/black positive cells examined for this study.

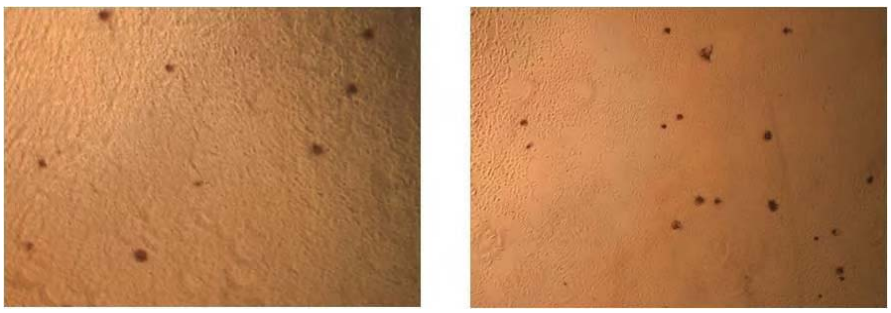

Figure 6.5 Photographs showing brown/black positive cells
The individual spots were counted and the mean number per field determined

6.2.7 Sensitisation of SKOV3 cells to CB1954 using adenovirus expressing NTR

Human ovarian carcinoma SKOV3 cells were used for prodrug sensitivity assays. Cells were trypsinised and resuspended in culture media and allowed to recover for 1 hour in suspension at 37 ^{o}C with intermittent mixing to prevent clumping. 1.33 x 10^{6} cells were infected with each adenovirus (expressing NTR) at 300, 100, 30, 10 and 0 infectious virus particles per cell (based on Adeno-X hexon staining) on day zero. The suspension was incubated at 37 ^{o}C for 90 minutes with gentle intermittent mixing before plating 1.5 x10^{4} cells (150 µl) per well into 96 well plates. The plates were then incubated at 37 ^{o}C. The medium was aspirated on day two and prodrug CB1954 was added in 150 µl medium to each well. Triplicates of each CB1954 concentration were used ranging from 0-300 µM. See Figure 6.6 for 96 well plate layout.

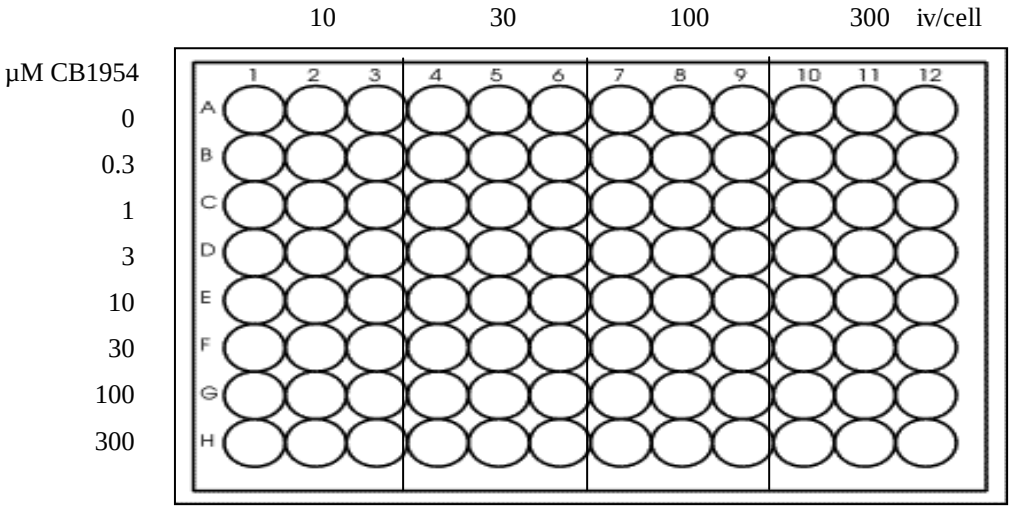

Figure 6.6 Plate layout for MTT Assay using Adenovirus encoding NTR

The prodrug was removed after 16 hours of incubation at 37 ^{o}C and replaced with 150 µl fresh medium. On day five, medium was removed and replaced with 150 µl fresh culture medium containing 0.5 mg/ml MTT, diluted fresh from a 5 mg/ml stock solution in PBS. Plates were incubated for three hours at 37 °C before the MTT solution was aspirated from the wells. Plates were dried for 30 minutes at room temperature before the addition of 150 µl DMSO to each well. Plates were left overnight to allow crystals to fully dissolve before reading the Absorbance at 490 nm using a Wallac Victor 1420 plate reader (Perkin Elmer, Monza, Italy).

6.2.8 Protein harvesting from virus infected tissue culture cells

In parallel to the sensitisation assay 5.1 x 10^5 SKOV3 cells were infected and plated in tissue culture dishes (6 cm) and incubated at 37 ^{o}C for 48 hours. The media was removed from the plates and washed twice with PBS. The cells were then scraped with a cell scraper into 1 ml of PBS and transferred to a screw topped 15 ml Sartstedt tube. The tubes were centrifuged at 1,500 rpm to pellet cells. The PBS was removed and 150 µl Urea (8M) was added, the pellet was dispersed by vortexing. The cells were incubated on ice for 10 minutes, before vortexing and transfer to a 1.5 ml microfuge tube. These cell lysates were stored at -20 ^{o}C until required. Protein concentrations were measured using bradford assay (see section 2.4.1).

6.2.9 SDS PAGE Gel Electrophoresis

Cell lysates were diluted 1:1 with 50 mM Laemmli loading buffer (4% SDS, 20% glycerol, 10% β-mercaptoethanol, 0.0004% bromophenol blue and 0.125 M Tris HCl) containing 1 M DTT before heating to 95 ^{o}C for 5 minutes and run on a 12% SDS PAGE gel as described in section 2.4.2. PageRuler™ Plus Prestained Protein Ladder (Fermentas, UK) was also run to verify molecular weights. Gels were run at 120 volts for approximately 2 hours (Laemmli 1970).

6.2.10 Western Blotting

Separated proteins were transferred to nitrocellulose membranes (see section 2.4.3). NTR and β-tubulin as a loading control were detected using primary and secondary antibodies listed in table 6.1. The secondary antibodies were peroxide conjugated and the bands were visualised using immobilon western detection reagents.

Protein	Primary Antibody	Secondary Antibody
Nitroreductase	NTR sheep	Anti sheep made in donkey
β-tubulin	β-tubulin mouse	Anti mouse made in sheep

Table 6.1 Primary and secondary antibodies used for western blotting

6.2.11 Sensitisation of SKOV3 cells to CB1954 using purified enzymes

Cells were seeded on day one at 1 x 10^4 cells per well in 96 well flat bottomed plates at a total volume of 150 µl. The cells were allowed to adhere overnight. The medium was aspirated from the plates on day two. Purified enzymes (see chapter 5 for purification of enzymes) were diluted with a range from 0-3000 nM final concentration in culture medium.

Each enzyme's concentration was tested in triplicate in a total volume of 50 µl. CB1954 prodrug at a final concentration of 10 µM and 50 µM was added with 0.1 µM FMN and either 100 µM or 200 µM NADH/NADPH in a volume of 100 µl. See Figure 6.7 for 96 well plate layout. Columns 1-6 indicate final enzyme concentrations from 0-3000 nM and columns 7-12 indicate final enzyme concentrations from 0-1000 nM.

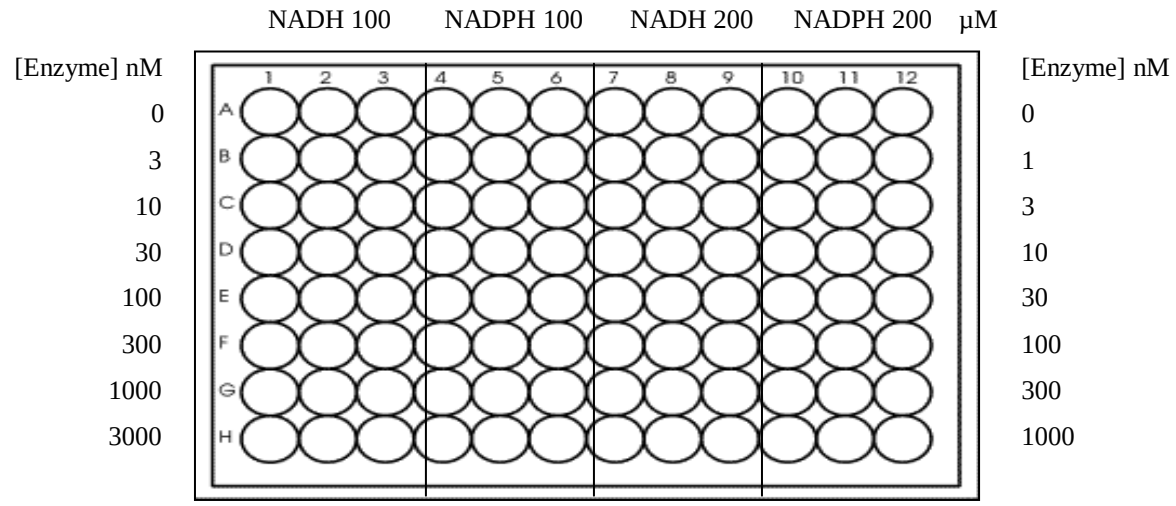

Figure 6.7 Plate layout used for MTT Assay using purified enzymes

The medium containing enzyme and substrate was removed after 4 hours of incubation at 37 ^{o}C and replaced with 150 µl fresh medium. On day five, medium was removed and replaced with 150 µl fresh culture medium containing 0.5 mg/ml MTT, diluted fresh from a 5 mg/ml stock solution. Plates were incubated for three hours at 37 °C before the MTT solution was aspirated from the wells. Plates were dried for 30 minutes at room temperature before the addition of 150 µl DMSO to each well. Plates were left overnight to allow crystals to fully dissolve before reading the Absorbance at 490 nm using a Wallac Victor 1420 plate reader.

6.3 RESULTS

6.3.1 NTR expression

6.3.1.1 Plasmid construction

PCR products were resolved by agarose gel electrophoresis to confirm DNA fragments of the correct size were amplified (see Figure 6.8). Bands of the correct size were the major products of each PCR reaction and were gel purified.

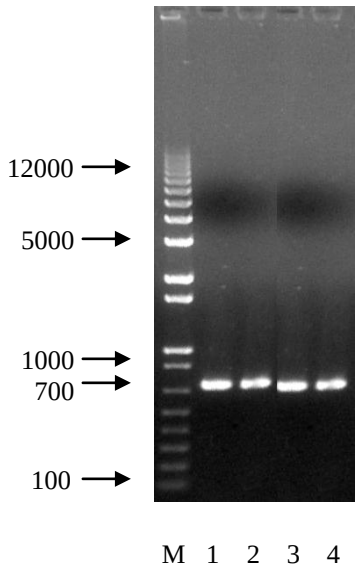

Figure 6.8 Agarose gel of PCR fragments for plasmid construction using primers JG138A and JG138B
Total PCR products amplified from NTR. PCR products were run on 0.7% agarose gel. M = Marker 1 kb plus ladder, Lanes 1-4 NTR fragments T41G N71S, T41N N71S, N71S A125T and 282 respectively. A single fragment of approximately 700 bp observed for each PCR

The purified PCR products were ligated with pPS1326B1 plasmid vector and transformed. Plasmid preps were generated from individual colonies and the resulting plasmid DNA digested with *Nco* I, *Eco* RV and *Bgl* II to ensure the correct plasmids were isolated. Digestion products were resolved by agarose gel electrophoresis (see Figure 6.9).

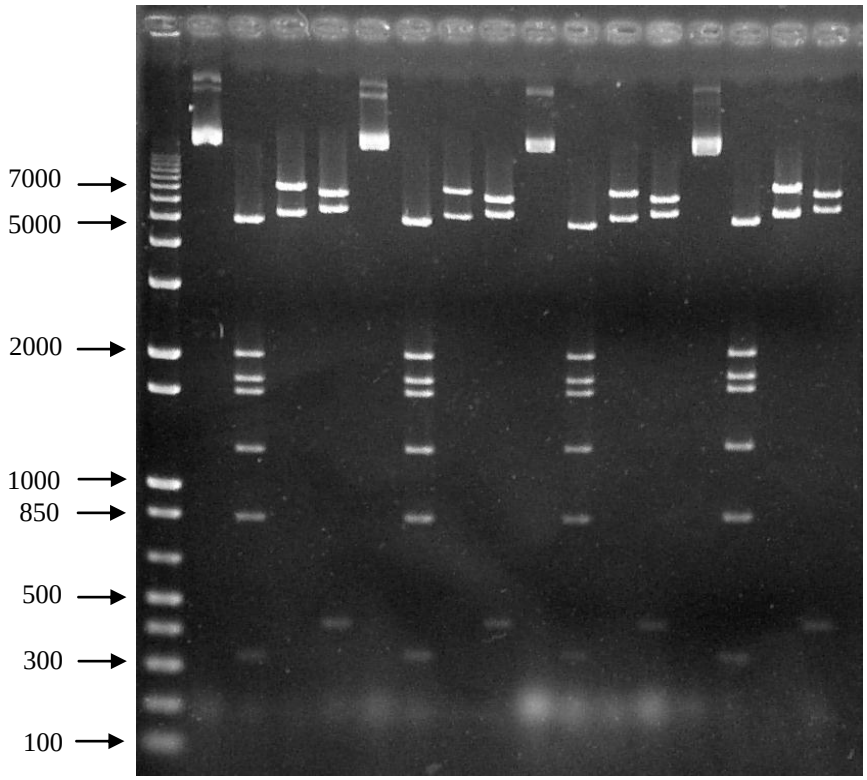

Nco I	*Eco* RV	*Bgl* II
5036	7559	6892
2038	5397	5638
1765		426
1670		
1240		
857		
330		

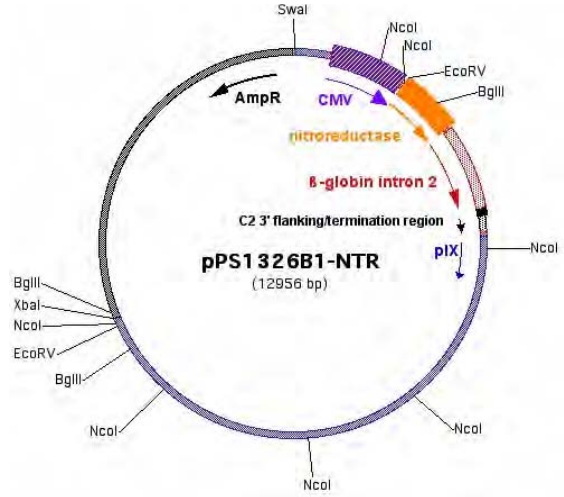

Figure 6.9 Restriction enzyme digests of plasmid bulk preparation DNA
Plasmid digests were run on 0.7% agarose gel. M = Marker 1kb plus ladder (Invitrogen, UK), Lanes 1-4 pSH282, Lanes 5-8 pSHT41GN71S, Lanes 9-12 pSHT41NN71S and Lanes 13-16 pSHN71SA125T. Each set of four showed undigested, *Nco* I, *Eco* RV and *Bgl* II digests from left to right. The table on the right shows expected band sizes for each enzyme digestion. The schematic diagram shows the fully constructed plasmid with *Nco* I, *Eco* RV and *Bgl* II restriction sites labelled. Correct digestion patterns were observed for all four plasmids.

Plasmids with correct digestion patterns were digested with *Xba I* and sequenced with primers PS1013A and PS1013B to ensure the NTRs they encode were correct.

6.3.2 Generation of adenovirus vectors in HEK 293 cells

Co-transfection was used to generate five viruses, vSH T41G N71S, vSH T41N N71S, vSH 282, vSH N71S A125T, and vSH EGFP. Each virus was rescued, propagated and caesium chloride-banded (as described in Section 6.2.4). DNA was extracted from each banded virus, digestion patterns were checked by *Hind* III digestion. Predicted fragment sizes and agarose gel results can be seen in Figure 6.10.

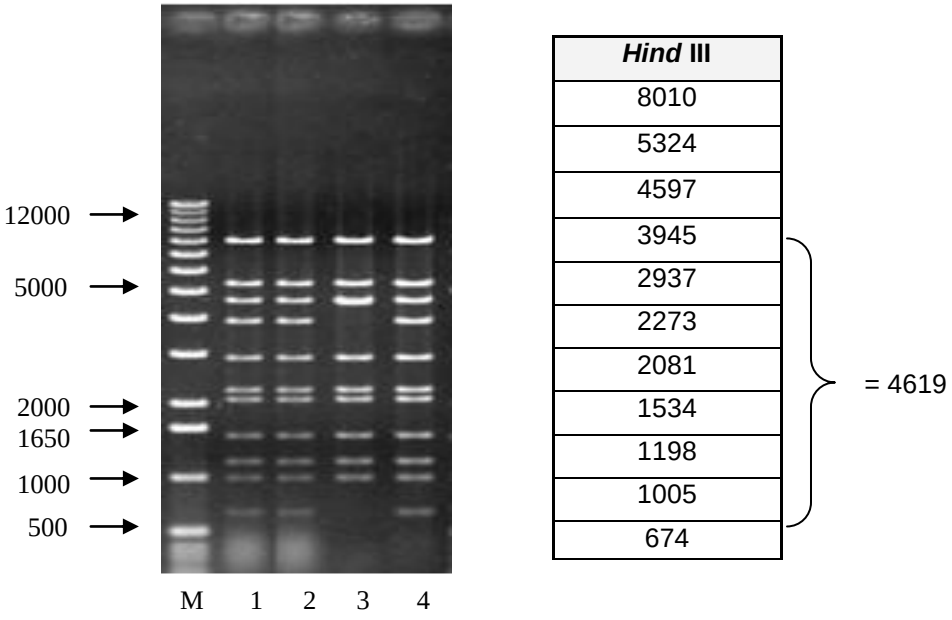

Figure 6.10 Restriction enzyme digests of viral DNA

Each virus was digested with *Hind* III and run on 0.7% agarose gel. Bands of the correct size were observed for virus preparations 1, 2 and 4. Virus preparation 3 has a stronger band at ~4600bp and absent bands at 3945bp and 674bp. The darker band at ~4600 bp correlates with the band expected at 4597 bp and a further band at ~ 4619 bp, which could result from loss of the *Hind* III site between the adjacent 3945 bp and 674 bp fragments. M = Marker 1kb plus ladder (Invitrogen, UK) Lanes 1 vSH 282, Lanes 2 vSH T41G N71S, Lane 3 vSH T41N N71S and Lanes 4 vSH N71S A125T

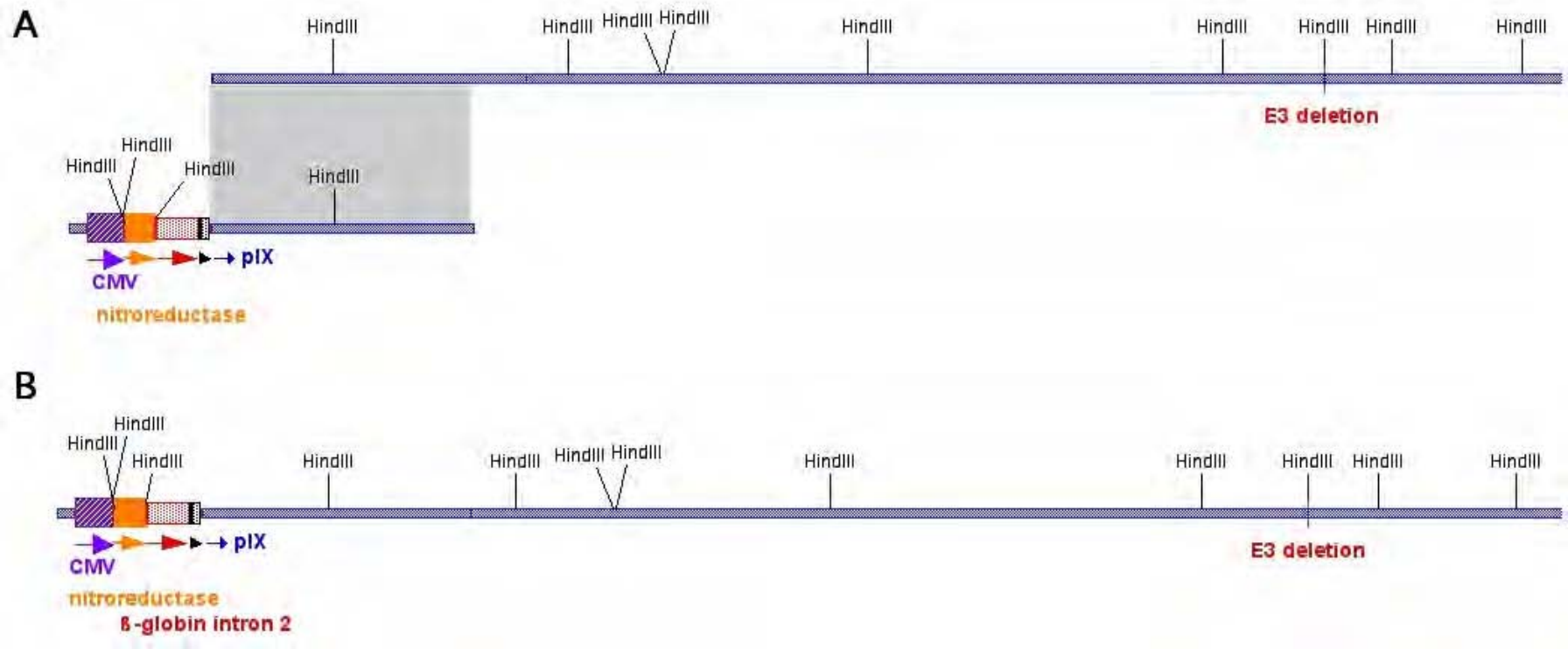

Figure 6.11 Schematic diagrams of recombination between plasmids pPS1326B1 NTR (T41G N71S, N71S A125T, T41N N71S and 282) and pPS1223F3

Co-transfection of pPS1326B1 NTR (T41G N71S, N71S A125T, T41N N71S and 282) "right end" virus with pPS1223F3 "left end" virus. A: Indicates the two linearised plasmids, showing the region of overlap for recombination. B: Full length NTR virus. *Hind* III sites have been marked, which were used for test digestion to ensure correct viruses generation

Figure 6.11 shows schematic diagrams of the two plasmids used for co-transfection and the fully constructed virus with *Hind* III sites highlighted.

The restriction pattern for vSH T41N N71S shows absence of bands, 3945 bp and 674 bp. These two fragments are adjacent in the viral DNA indicating a missing *Hind* III site shortly after the inserted NTR gene, and would generate a fragment of 4619 bp if joined. The increased intensity of the band at ~ 4619 bp probably results from comigration of this 4619 bp band, and the predicted 4597 bp fragment. The vSH T41G N71S, vSH N71S A125T and vSH 282 showed expected digestion patterns. The DNA for each virus was sequenced; the correct NTR sequence was seen for each with no additional base changes, additions or deletions. A single base substitution was shown within the *Hind* III site just downstream of NTR for vSH T41N N71S. This was in a non-coding region, therefore not expected to influence function, therefore it was decided that this virus could be used.

6.3.3 Virus validation

To allow comparison of generated adenoviruses, the titre of each virus needed to be determined. Three methods were used to determine virus concentrations, initially by virus particle number. This give a good indication of the amount of viral DNA present, however not all virus particles can infect cells and therefore this is not an ideal method for determining a viruses titre. Plaque Assays were performed for each virus and the particle to infectivity ratios determined. These ratios are a little high (see Table 6.2).

Virus	Particles/ml	pfu/ml	Particle to infectivity (P:I) ratio
vWT	6.5×10^{12}	8.1×10^{10}	80.3
vT41L N71S	7.3×10^{12}	8.9×10^{9}	820.2
vT41Q N71S F124T	5.8×10^{11}	7.2×10^{8}	805.6
vSH T41G N71S	4.6×10^{12}	6.0×10^{10}	76.7
vSH T41N N71S	1.1×10^{12}	7.0×10^{9}	157.1
vSH N71S A124T	2.3×10^{12}	3.0×10^{10}	76.7
vSH 282	2.0×10^{12}	6.1×10^{10}	32.8

Table 6.2 Particles per ml, Plaque forming units (pfu) per ml from plaque assay and Particle to infectivity (P:I) ratio for each virus

It has previously been found that viruses encoding some mutant NTRs can be impaired in their growth and fail to produce good plaques (Jaberipour 2005). It is believed that NTR can be toxic, killing some cell early in the infectious cycle, thus inhibiting plaque formation. In this situation the plaque assay may underestimate the number of viruses able to infect a target cell and express the inserted gene. A reliable method that will not be affected by NTR toxicity was required. Adeno-X rapid titer kit was used to determine infectious units per ml. This method is based on hexon protein staining 48 hours after infection of a HEK 293 monolayer, when virus is in its first infection cycle, thus, unlike the plaque assay, cell to cell spread of virus is not required. A further advantage to this method is that more "events" are counted than a plaque assay, therefore expect greater accuracy. Tighter particle to infectivity ratios were determined using this kit, with Ifu/ml values being higher than Pfu/ml, as expected, and this is probably a better reflection of the number of virus particles that can enter a cell to express NTR (See Table 6.3).

Virus	Particles/ml	ifu/ml	Particle to infectivity (P:I) ratio
vWT	6.5×10^{12}	1.10×10^{11}	59.1
vT41L N71S	7.3×10^{12}	2.66×10^{11}	27.4
vT41Q N71S F124T	5.8×10^{11}	1.36×10^{10}	42.7
vSH T41G N71S	4.6×10^{12}	2.06×10^{11}	22.3
vSH T41N N71S	1.1×10^{12}	3.53×10^{11}	3.1
vSH N71S A124T	2.3×10^{12}	5.59×10^{11}	4.1
vSH 282	2.0×10^{12}	1.75×10^{11}	11.4

Table 6.3 Particles per ml, Infectious units (ifu) per ml based on Adeno-X titre and Particle to infectivity (P:I) ratio for each virus

6.3.4 MTT prodrug Sensitivity Assay

The efficiency of adenoviruses expressing WT and mutant NTR's at sensitising human tumour cell line SKOV3 to CB1954 were compared by prodrug sensitivity assays. SKOV3 cells were infected with each virus at various MOI's (based on adeno-X titre) and the cell survival was assessed by MTT Assay. Figure 6.12 shows survival curves for each individual virus at various MOI's and Figure 6.13 shows survival curves for all viruses at specific MOI's.

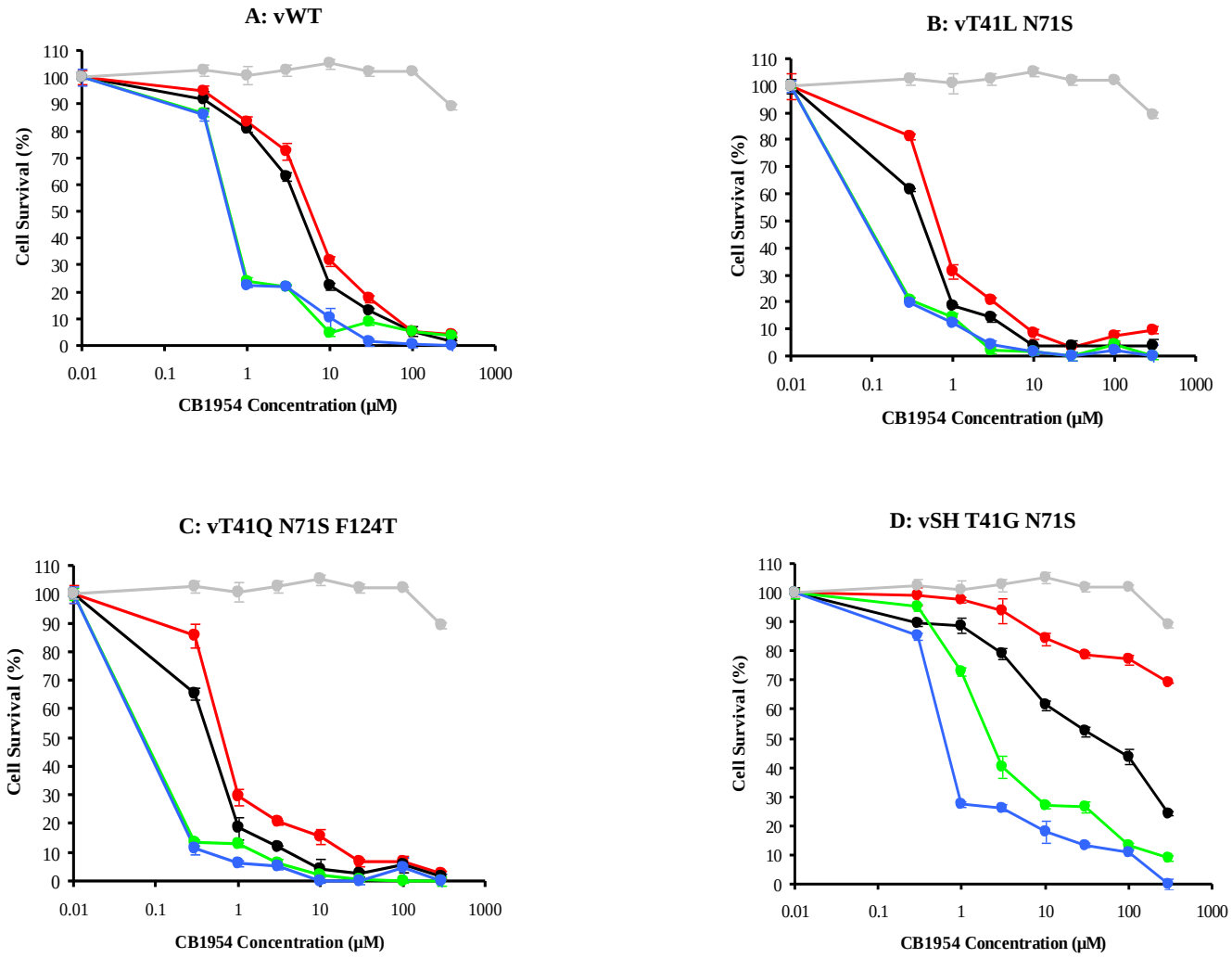
A: vWT
B: vT41L N71S
C: vT41Q N71S F124T
D: vSH T41G N71S
Cell Survival (%)
CB1954 Concentration (µM)
0.01
0.1
1
10
100
1000
0
10
20
30
40
50
60
70
80
90
100
110

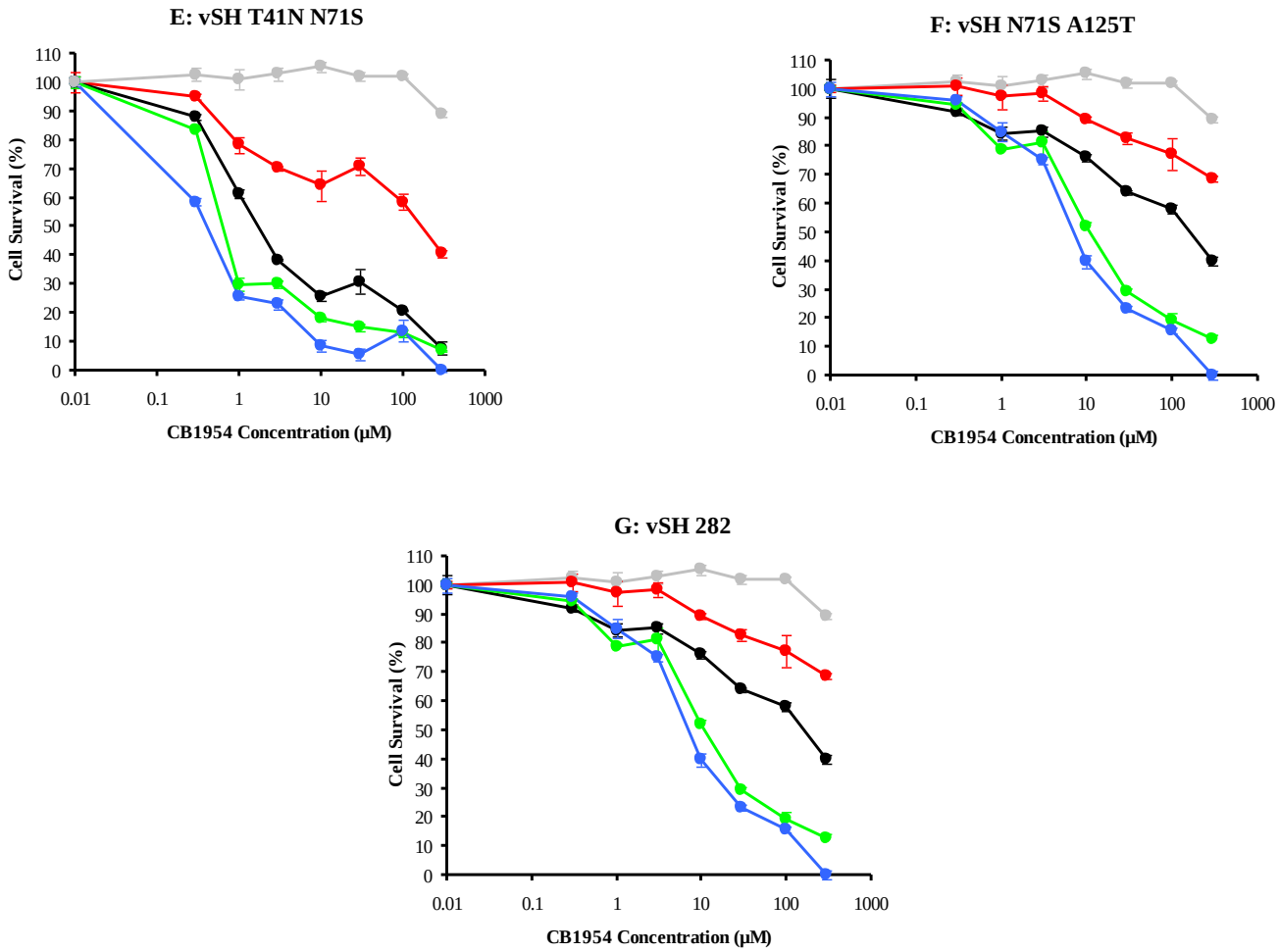

Figure 6.12 Survival curves for adenoviruses expressing WT and mutant NTR's A: vWT, B: vT41L N71S, C: vT41Q N71S F124T, D: vSH T41G N71S, E: vSH T41N N71S, F: vSH N71S A125T and G: vSH 282 at MOI 0 (grey), 10 (red), 30 (black), 100 (green), 300 (blue) based on ifu/cell
The percentage cell survival was determined by MTT, normalised to cell survival with no prodrug. Error bars shown are standard errors of the mean based on measurement of three replicate wells within the same experiment

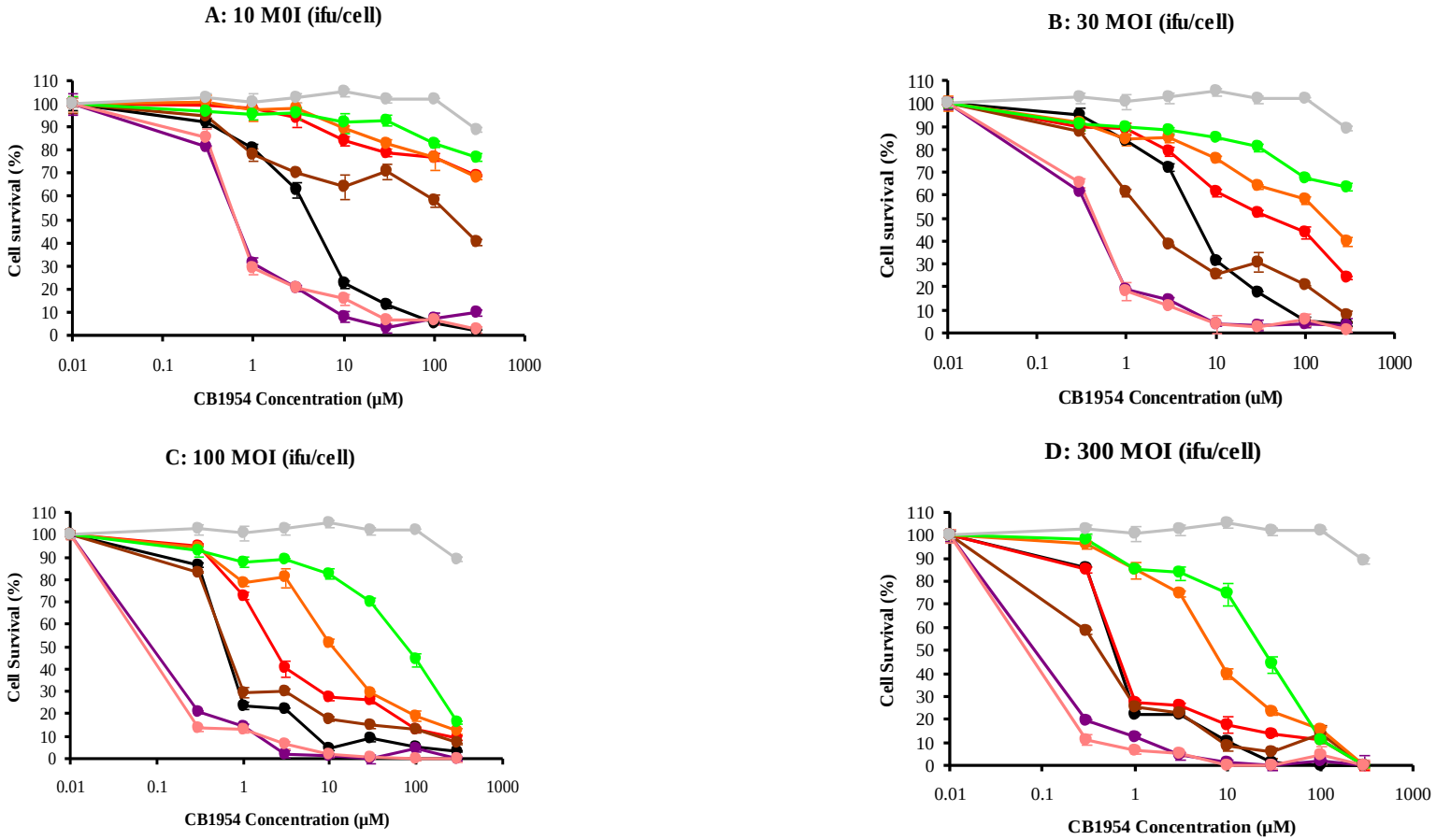

Figure 6.13 Survival curves for adenoviruses expressing WT and mutant NTR's vWT (black), vT41L N71S (purple) and vT41Q N71S F124T (pink), vSH T41G N71S (red), vSH T41N N71S (brown), vSH N71S A125T (orange), vSH 282 (green)

The different plots show cells exposed to different MOI A: 10 ifu/cell, B: 30 ifu/cell, C: 100 ifu/cell and D: 300 ifu/cell. The percentage cell survival was determined by MTT, normalised to cell survival with no prodrug. Error bars shown are standard errors of the mean based on measurement of three replicate wells within the same experiment

Percentage cell survival for each enzyme was determined and survival curves constructed using four different MOI's of 10, 30, 100 and 300 ifu/cell (see Figures 6.13). As expected very little killing was seen when no virus was used (grey) and all the viruses showed the least killing at 10 ifu/cell (red) and the most at 300 ifu/cell (blue).

Survival curves for each MOI (ifu/cell) can be seen in Figure 6.13. At the highest MOI 300 ifu/cell vT41Q N71S F124T showed greatest killing, ~9-fold improvement relative to WT. This was closely followed by vT41L N71S, ~8-fold better, then vT41N N71S ~1-fold better. vT41G N71S showed similar sensitisation as WT enzyme. Finally vN71S A125T and v282 were ~10-fold and ~60-fold less sensitive than WT. However at a lower MOI of 30 ifu/cell vT41Q N71S F124T and vT41L N71S have similar sensitisation and vT41G N71S is less sensitive to WT enzyme.

6.3.4.1 NTR expression levels

One of the major contributing factors to the degree of cell sensitisation to CB1954 is the level of NTR expression. Previous viruses have sometimes shown differences in expression levels. Either the NTR degrades more quickly or is expressed at a lower level. To quantify the amount of NTR being expressed by each virus western blotting was used as previously described. To confirm even loading of cell lysate, the blots were also probed for the protein β-tubulin (Westermann and Weber 2003). The western blots of these samples (MOI 10 ifu/cell) probed with antibodies against both NTR and β-tubulin is shown in Figure 6.14.

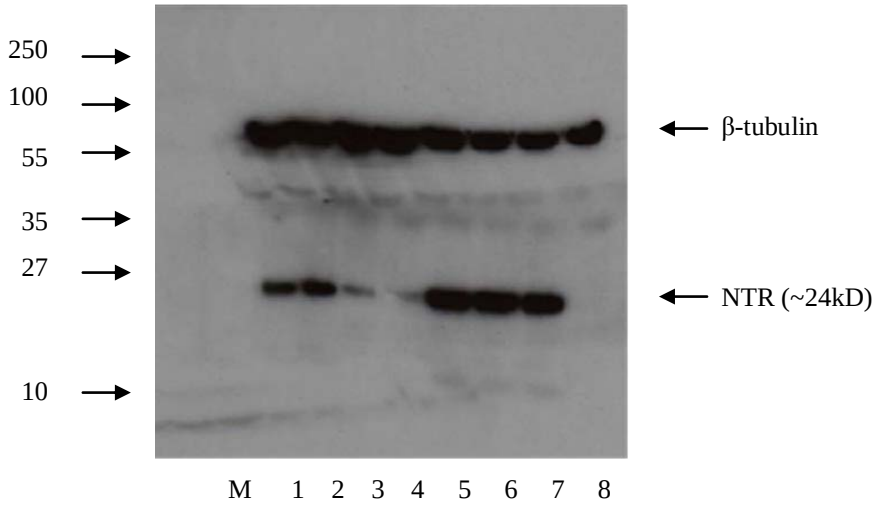

Figure 6.14 Western blots of cell lysates
M: Marker, 1: vSH T41G N71S, 2: vSH T41N N71S, 3: vSH N71S A125T, 4: vSH 282, 5: vT41L N71S, 6: vT41Q N71S F124T, 7: vWT, 8: Control no virus, at MOI 10 ifu/cell and exposure for 1 minute

The intensity of the NTR band showed a considerable variation between samples. There was much less variation in the β-tubulin band, and the two didn't correlate, rather the β-tubulin showed greater intensity in the samples with less NTR detected. Therefore this result shows that the viruses expressing WT, T41L N71S and T41Q N71S F124T produce more NTR in infected cells than those expressing T41G N71S and T41N N71S, while N71S A125T and 282 appear to be particularly poorly expressed.

In order to compare the viruses further, western blot analysis was performed at four different MOI's 10, 30, 100 and 300 ifu/cell. This makes it possible to identify which MOI's of the different viruses give the most closely matched levels of NTR expression. This allows comparison of NTR expression levels, giving a crude overview. Western blots for this showing both NTR and β-tubulin can be seen in Figure 6.15.

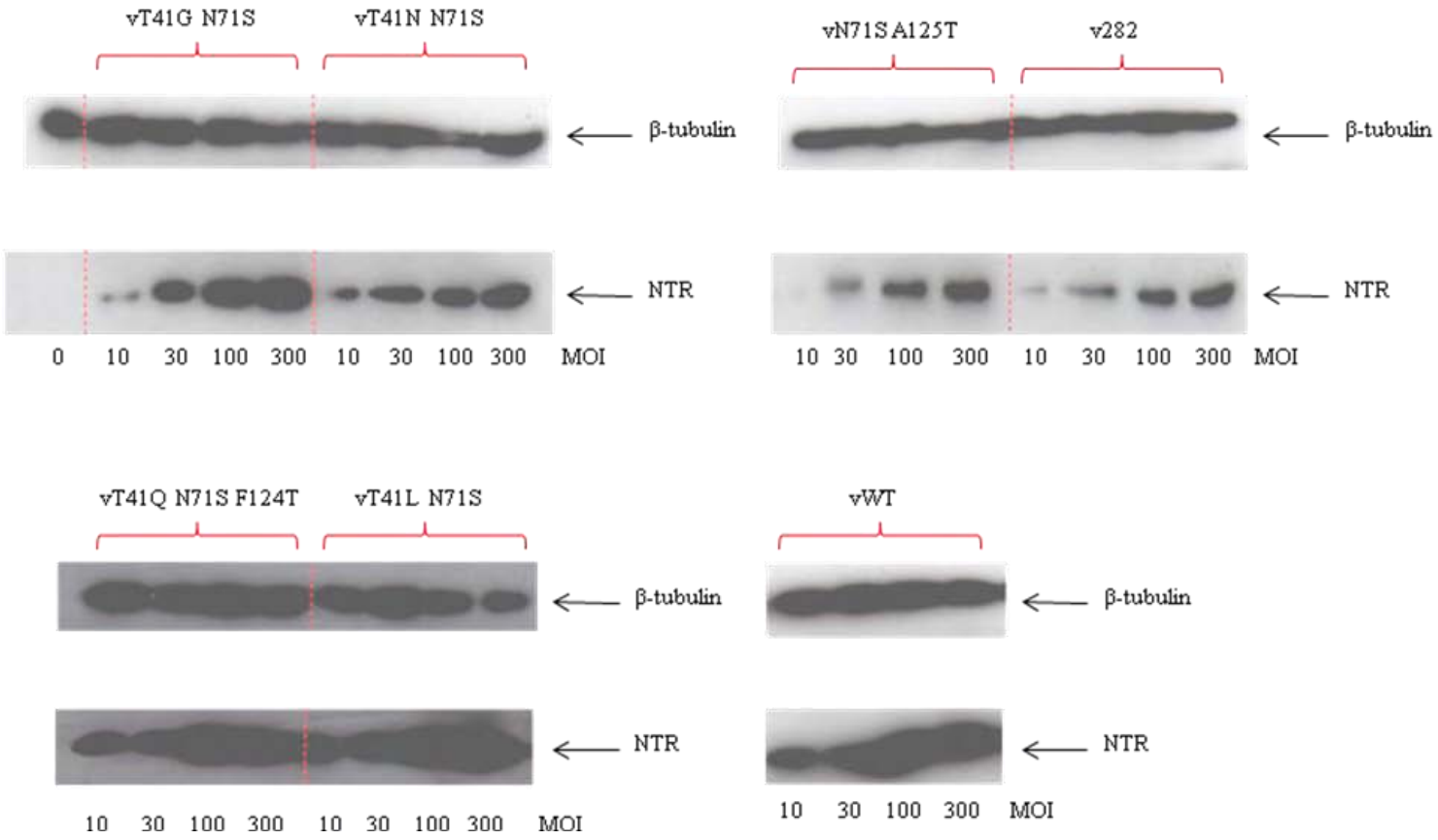

Figure 6.15 Western blots of cell lysates
vT41G N71S, vT41N N71S, vN71S A125T, v282, vT41L N71S, vT41Q N71S F124T, and vWT at MOI 10, 30, 100, 300 based on ifu/cell

Comparison of these blots indicates that 10 ifu/cell for vWT, vT41L N71S and vT41Q N71S F124T express approximately the same amount of NTR as 100 ifu/cell for vT41G N71S and vT41N N71S and 300 ifu/cell for v282 and vN71S A125T. Figure 6.16 shows survival curves for each individual virus at the MOI (ifu/cell) that best approaches normalisation of NTR expression for each virus, using existing data.

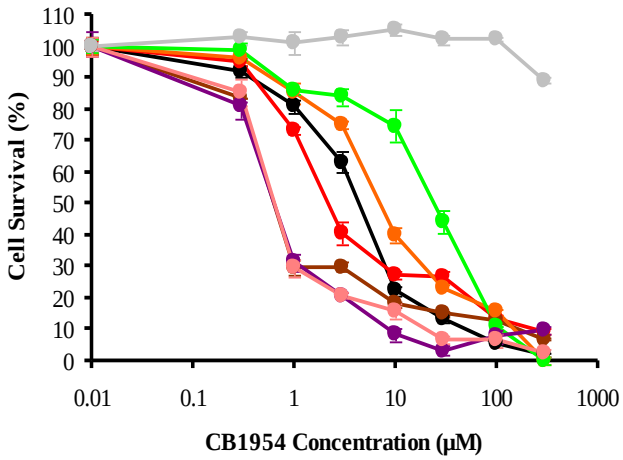

Figure 6.16 Survival curves for adenoviruses expressing WT and mutant NTR's
vWT 10 ifu/cell (black), vT41L N71S 10 ifu/cell (purple) and vT41Q N71S F124T 10 ifu/cell (pink), vT41G N71S 100 ifu/cell (red), vT41N N71S 100 ifu/cell (brown), vN71S A125T 300 ifu/cell (orange), v282 300 ifu/cell (green) and control no virus (grey). The percentage cell survival was determined by MTT, normalised to cell survival with no prodrug. Error bars shown are standard errors of the mean based on measurement of three replicate wells within the same experiment

Cell survival curves were constructed based on MOI's (ifu/cell) that showed best normalisation of NTR expression in this case vT41Q N71S F124T, vT41L N71S and vT41N N71S showed similar sensitisation with ~9-fold improvement over WT enzyme. vT41G N71S was also better than WT with ~2-fold improvement observed. However vN71S A125T and v282 remain less sensitive than WT at ~1-fold and ~5-fold respectively.

6.3.5 Sensitisation of SKOV3 cells to CB1954 using purified enzymes

An alternative way of comparing NTR mutants with WT is to use purified enzymes of known concentration. The benefit of this is the ability to compare appropriately matched, controlled enzyme concentrations. WT, F124N, T41L N71S and T41Q N71S F124T have been previously purified and T41G N71S, T41L F70A and 282 were purified for this study (see Chapter 5). F124N and T41L F70A viruses were not used previously however purified enzyme was available so they were included.

The abilities of purified WT and mutant NTR to sensitise human tumour cell line SKOV3 to CB1954 were compared. SKOV3 cells were plated out and NTR protein dilutions were added along with 0.1 μM FMN, appropriate concentrations of either NADH or NADPH and appropriate concentrations of CB1954. Cell survival was assessed by MTT Assay. Figures 6.17 shows survival curves for each NTR and Figure 6.18 show survival curves at each reaction condition.

A: T41L F70A

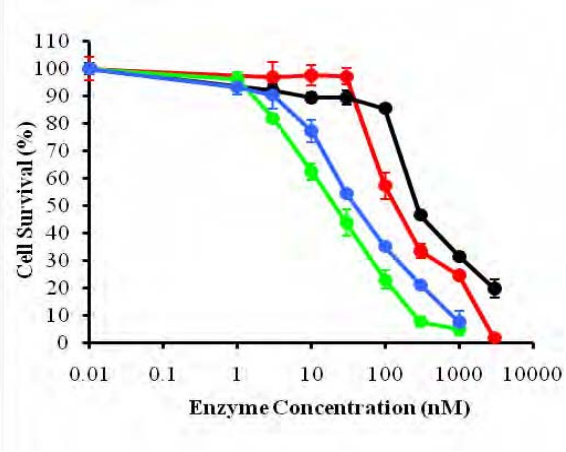

B: 282

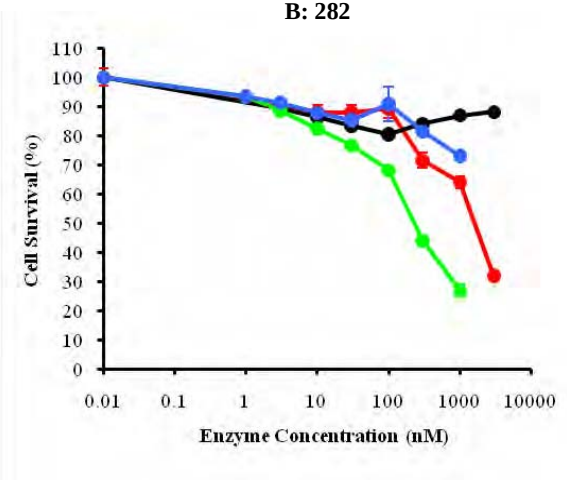

C: T41Q N71S F124T

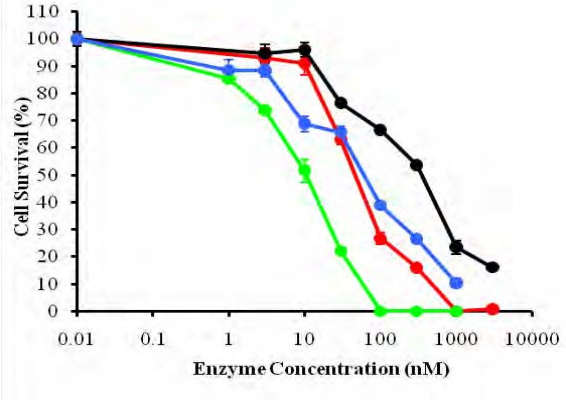

D: WT

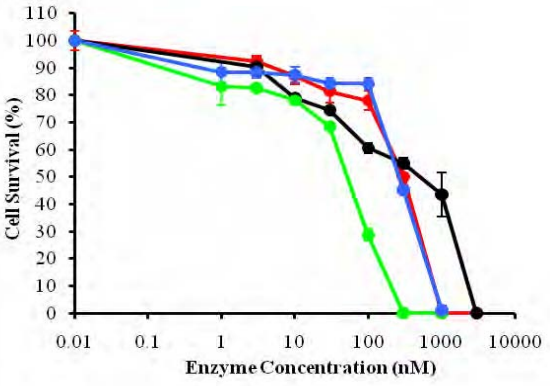

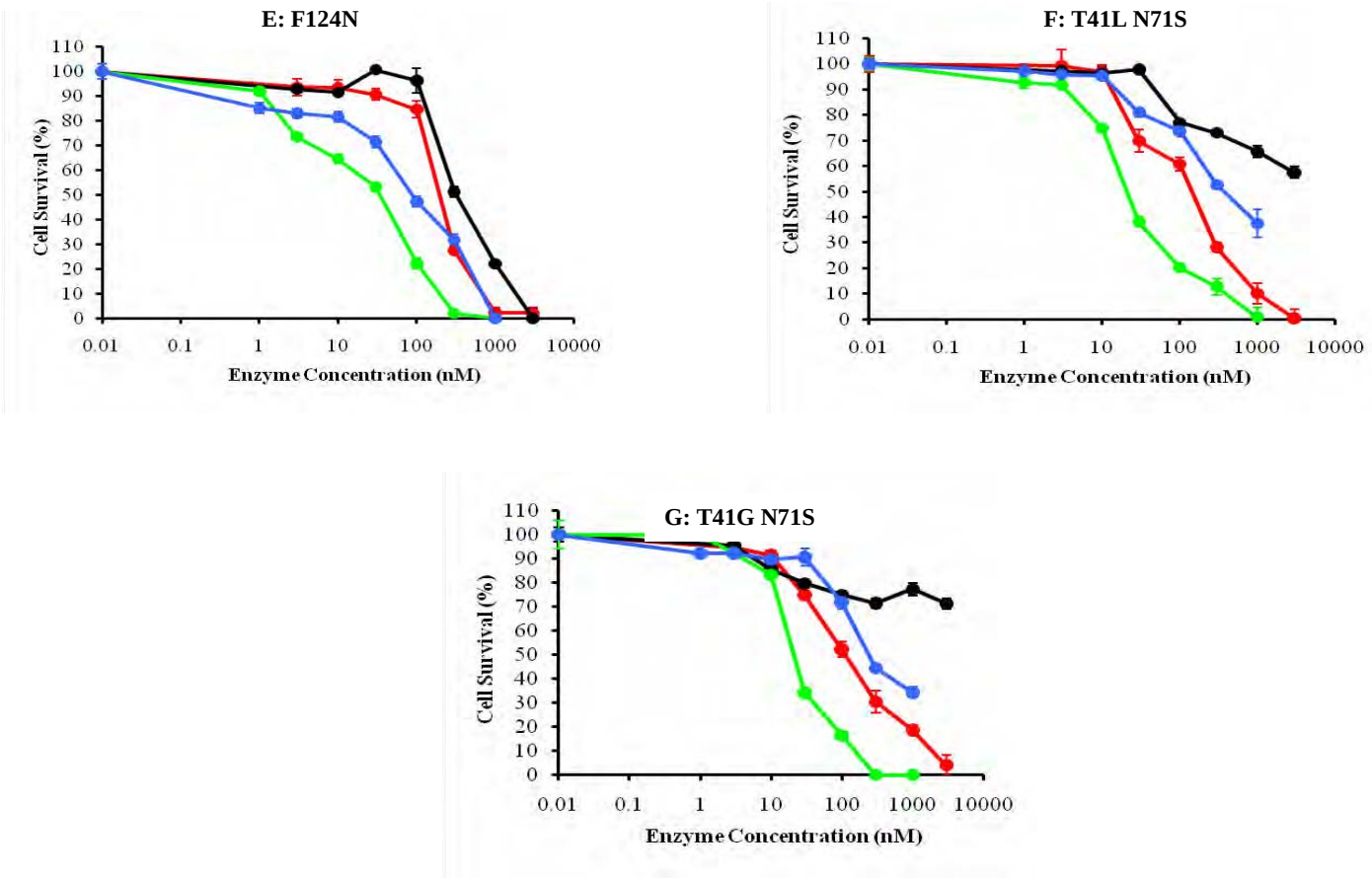

Figure 6.17 Survival curves for WT and mutant enzymes A: T41L F70A, B: 282, C: T41Q N71S F124T, D: WT, E: F124N, F: T41L N71S and G: T41G N71S using 100 µM NADH 10 µM CB1954 (red), 100 µM NADPH 10 µM CB1954 (black), 200 µM NADH 50 µM CB1954 (green), 200 µM NADPH 50 µM CB1954 (blue)

Percentage cell survival was determined by MTT, normalised to cell survival with no prodrug. Error bars shown are standard errors of the mean based on measurement of three replicate wells within the same experiment

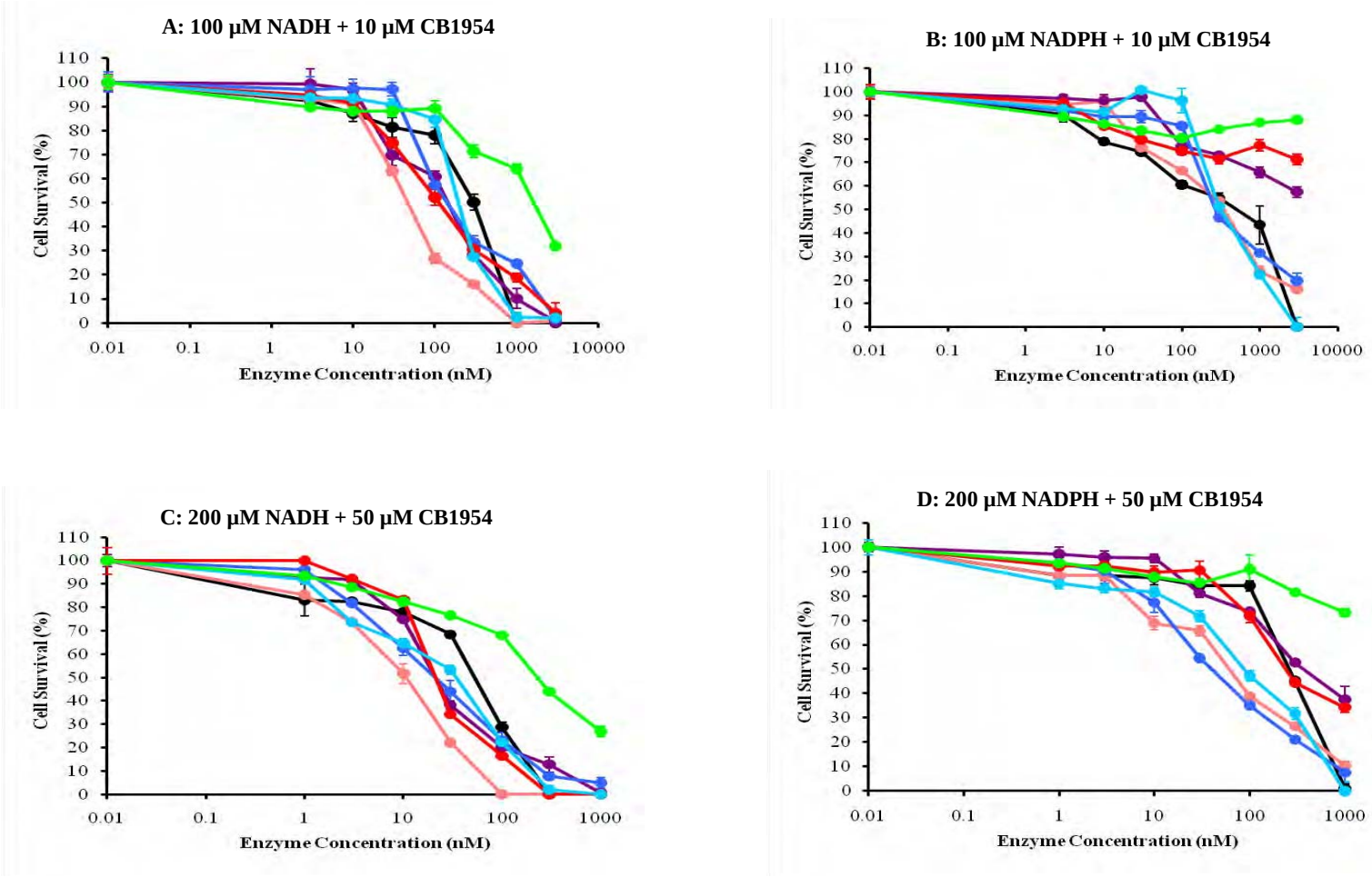

Figure 6.18 Survival curves for WT (black), F124N (cyan), T41L N71S (purple), T41Q N71S F124T (pink), T41G N71S (red), T41L F70A (blue) and 282 (green) enzymes

A: 100 µM NADH 10 µM CB1954, B: 100 µM NADPH 10 µM CB1954 C: 200 µM NADH 50 µM CB1954 and D: 200 µM NADPH 50 µM CB1954. Percentage cell survival was determined by MTT Assay. Error bars shown are standard errors of the mean based on measurement of three replicate wells within the same experiment

Percentage cell survival for each enzyme was determined and survival curves constructed using NADH and NADPH as cofactor (see Figures 6.17). All enzymes were better with NADH than with NADPH, with ~5-fold difference for WT and T41Q N71S F124T. Two of the mutant enzymes T41L F70A and F124N showed less difference with ~2-fold difference. The remaining two enzymes showed greater than WT preference for NADH over NADPH with T41L N71S and T41G N71S showing ~18-fold difference.

Survival curves for each condition can be seen in Figure 6.18. For both 100 µM and 200 µM NADH T41Q N71S F124T was the best at sensitising SKOV3 cells to CB1954 being ~ 9-fold better than WT NTR. All the other mutants except 282 were better than WT with T41G N71S, T41L N71S and T41L F70A showing similar values at ~2.6-fold better and F124N being ~1.4-fold improved. However with 200 µM NADPH T41L F70A was best (~7-fold) followed by T41Q N71S F124T (~5-fold), then F124N (~4.5-fold) and when looking at 100 µM NADPH it is less clear which enzymes worked best with WT, T41L F70A, F124N and T41Q N71S F124T showing similar results.

6.4 DISCUSSION

6.4.1 Adenovirus

Four replication defective adenoviruses expressing NTR were generated (vSH T41G N71S, vSH T41N N71S, vSH N71S A125T and vSH 282). Prodrug sensitivity assays for CB1954 were performed for each as well as several previous viruses (expressing WT, T41L N71S and T41Q N71S F124T) in SKOV3 cells.

Initial results showed that T41Q N71S F124T was the best mutant at sensitising SKOV3 cells to the prodrug CB1954 followed by T41L N71S. This was consistent with previous tissue culture results (Guise *et al.* 2007 and Jaberipour 2005). At 300 ifu/cell T41N N71S was better than WT but at 10 ifu/cell WT appears better. This may show that WT has a better bystander effect than T41N N71S. None of the three other new mutants were better than WT NTR. This contradicts bacterial and kinetics data which showed that T41G N71S should be similar to T41L N71S and 282 marginally better than WT. Protein expression of NTR showed different expression levels for the viruses making it difficult to compare the different mutants. Using previous data, but comparing the dose-response curves at the MOI that gave most closely matched levels of NTR expression allowed better comparison of mutant NTR's relative to WT. In this case T41Q N71S F124T, T41L N71S and T41N N71S appeared to have similar sensitisation in SKOV3 cells followed by T41G N71S. N71S A125T and 282 remained less sensitive than WT NTR.

6.4.2 Purified Enzyme

An alternative way of comparing NTR mutants with WT in tissue culture cells is to use purified enzymes of known concentration. When using the cofactor NADH, T41Q N71S F124T was found to be the best mutant at sensitising SKOV3 cells to the prodrug CB1954, closely followed by T41G N71S, T41L F70A and T41L N71S which showed similar sensitisation to each other. This was followed by F124N the best single mutant. However when using the cofactor NADPH, very different results were observed. In this case T41L F70A gave greatest sensitisation followed by T41Q N71S F124T, F124N and then WT. Several of the best NTR mutants (T41G N71S and T41L N71S) using the cofactor NADH, were less sensitive than WT using NADPH as cofactor. The NTR mutant 282 was poor with both NADH and NADPH being less sensitive than WT in both cases.

Human cells contain varying amounts of NADH and NADPH. Combined NAD^+ and NADH levels are reported typically to be ~10-fold higher than $NADP^+$ and NADPH (Garofalo *et al.* 1988). Therefore mutants that work well with and favour NADH as a cofactor, such as T41Q N71S F124T, T41G N71S and T41L N71S should work particularly well in human cells. T41Q N71S F124T, T41G N71S and T41L N71S showed good sensitisation in SKOV 3 cells. However, considering only the reduced cofactors, Pollak *et al* found NADH levels in HEK293 cells were just 1-2 times that of NADPH (Pollak *et al.* 2007). The similar sensitisation of SKOV 3 cells to CB1954 by virus expressing either T41Q N71S F124T or T41L F70A is consistent with both reduced cofactors being available to NTR expressed in the cell.

When using NADH as cofactor the order of sensitisation to CB1954 reassuringly follow a similar pattern to that determined kinetically (using NADH as cofactor) with the exception of mutants T41Q N71S F124T and 282. Kinetic parameters for mutant 282 were slightly better than WT with a 1.8-fold increase in sensitivity; however in all tissue culture experiments WT was more efficient at sensitising cells to CB1954. Mutant T41Q N71S F124T was kinetically the third best mutant behind T41L N71S and T41G N71S. However, in a tissue culture setting, using both virus and purified enzyme, T41Q N71S F124T worked more efficiently being the best mutant at sensitising SKOV 3 cells to CB1954.

CHAPTER 7: DISCUSSION

7.1 VDEPT

Virus-directed enzyme prodrug therapy (VDEPT) is an emerging strategy against cancer, using a virus to administer a gene encoding an activating enzyme to tumour cells (McNeish *et al.* 1997). Phase I/II clinical trials, using *NfsB* NTR enzyme and the prodrug CB1954 have been completed here in Birmingham, using a replication defective adenovirus CTL102 for delivery (Palmer *et al.* 2004, Patel *et al.* 2009). No patients were cured, but a reduction in PSA implies a delay in tumour burden and progression. Kinetic analysis of NTR has shown that CB1954 is a poor substrate with a $k_{cat} \sim 140\ s^{-1}$ and a $K_{m\ CB1954} \sim 17200\ \mu M$ (Jarrom *et al.* 2009). Therefore low enzymatic efficiency plus low gene transfection efficiencies are likely to have limited the effectiveness of the therapy. Improvement to the system would be highly beneficial, with the aim to take refinements into future clinical trials.

It was proposed that engineering *NfsB* NTR enzyme to better catalyse CB1954 could greatly improve the efficacy of this system.

7.2 ENGINEERING NTR ENZYME

A series of improved *NfsB* NTR mutants have previously been generated based on the crystal structure (Lovering *et al.* 2001). Initially residues round the active site were targeted (Grove *et al.* 2003). F124N showed modest improvement with a k_{cat}/K_m 5-fold greater than WT NTR (Jarrom *et al.* 2008). A second generation combining beneficial mutants were generated with T41L N71S and T41L F70A being the most improved, with the k_{cat}/K_m for T41L N71S being 100-fold greater (Jaberipour *et al.* 2010). A direct positive selection system (Guise *et al.* 2007) has allowed further improvements; with T41Q N71S F124T having a k_{cat}/K_m that is 50-fold greater than WT NTR (Jarrom *et al.* 2008).

7.2.1 Generating new mutants

This system was taken forward in this study to generate further improved NTR mutants. Firstly three small libraries were generated with mutations around the active site at adjacent positions S40/T41 ± N71S and E165/G166 ± N71S and the single position K14. From these libraries three double NTR mutants of interest were determined T41G N71S, T41N N71S and N71S A125T giving improved sensitivity to CB1954 in bacterial cells.

These three libraries have improved our knowledge of the contribution of active site residues of NTR to the efficacy of CB1954 activation. Only a few isolated mutants contained a mutation at position S40. Single mutations at this residue resulting in alanine, glycine or threonine all led to NTRs with improved CB1954 activation (Grove *et al.* 2003). All the mutations isolated at S40 were threonine and these appeared to be tolerated mutations. This indicates that amino acid changes at both S40 and T41 do not work well together. It is likely changes at both these residues may sterically hinder each other. No mutants were isolated with amino acid changes at residues E165 and or G166. Previous work indicated that all single amino acid substitutions at these residues were detrimental to CB1954 activation (Grove *et al.* 2003). This work indicates that no combination of substitutions at these two sites can allow efficient CB1954 activation. No amino acid changes were seen at residue K14, indicating that all amino acid substitutions were detrimental to CB1954 activation.

Using this understanding a large library was constructed with mutations at up to six residues around the active site. This large library contained a maximum diversity of 6.3×10^6 possible nucleotide sequences. One mutant N71S A113 R121V F123N F124V A125C K179R (282) analysed showed improvement over WT.

7.2.1.1 Kinetic Analysis of mutant NTR

T41L F70A from a previous study (Jaberipour *et al.* 2010) and two of the promising mutants T41G N71S and clone 282 were purified and kinetically characterised and compared with WT and other previously purified mutant *NfsB* NTR enzymes. K_m and k_{cat} were calculated for CB1954, nitrofurazone and menadione and the specificity constant k_{cat}/K_m has been used to compare the activity of each enzyme.

Looking at enzyme activity T41L N71S was the best mutant at reducing CB1954. When looking at the three mutants purified in this study T41G N71S was the best mutant at reducing CB1954 being the second best mutant analysed just slightly behind T41L N71S.

7.2.1.1.1 Substrate specificity of NTR mutants

Although activity for CB1954 is important a good enzyme should also demonstrate good selectivity for CB1954 compared to other substrates. In order to calculate specificity each mutant was tested with nitrofurazone and menadione. The hope is that an improvement in CB1954 reducing activity is not reciprocated in the other substrates, to reduce substrate competition in human cells. The specificity constant for CB1954 has been compared with the specificity constants for nitrofurazone and menadione, allowing ratios for each enzyme and substrate combination to be calculated (see Table 7.1).

k_{cat}/K_m μM^{-1} s^{-1}

	WT	F124N	T41L N71S	T41G N71S	T41L F70A	T41Q N71S F124T	282
CB1954	**0.009**	**0.027**	**0.628**	**0.457**	**0.103**	**0.277**	**0.010**
NFZ	**0.068**	**0.049**	**0.302**	**0.113**	**0.186**	**0.038**	**0.038**
MENADIONE	**0.42**	**3.57**	**6.23**	**3.43**	**6.80**	**9.75**	**1.97**

$(k_{cat}/K_m)/(k_{cat}/K_m)$

	WT	F124N	T41L N71S	T41G N71S	T41L F70A	T41Q N71S F124T	282
CB1954:NFZ	**0.13**	**0.55**	**2.08**	**4.04**	**0.55**	**7.29**	**0.26**
CB1954:MENADIONE	**0.016**	**0.013**	**0.048**	**0.032**	**0.027**	**0.004**	**0.019**

Table 7.1 Specificity constants and ratios of specificity constants comparing CB1954 with Nitrofurazone and Menadione
WT, F124N, T41L N71S, T41G N71S, T41L F70A, T41Q N71S F124T

The higher the k_{cat}/K_m value the greater the likelihood that the reaction will be catalysed. Therefore specificity constant ratios can be used to determine which reaction is most likely to proceed. When comparing CB1954 and NFZ mutants T41Q N71S F124T, T41G N71S and T41L N71S showed greater specificity for CB1954 with a value greater than 1. All the mutants showed improvement over WT. My best mutant T41G N71S showed ~30-fold improvement relative to WT (see Table 7.1).

When comparing CB1954 and Menadione all the enzymes showed greater specificity for Menadione with values less than 1. However T41L N71S, T41G N71S, T41L F70A and 282 showed improvement over WT being between 1- and 3-fold better (see Table 7.1).

This specificity data indicate that T41Q N71S F124T, T41L N71S and T41G N71S are the most promising nitroreductases. T41L N71S and T41G N71S are particularly promising as they both show an increase in CB1954:NFZ and CB1954:MENADIONE specificity constants.

7.2.1.1.2 CB1954 product ratios

CB1954 reduction products were determined for the three new enzymes. T41L F70A and clone 282 produced mostly the 4-hydroxylamine (4-HA), with a small amount of 2-hydroxylamine (2-HA) being produced by the latter. T41G N71S however produced approximately equal amounts of the 4-HA and 2-HA products.

Several previous mutants have also shown a shift towards the production of 4-HA. All of these enzymes had a T41L mutation (Race *et al.* 2007 and Jarrom *et al.* 2009). It was therefore a little surprising that clone 282 also favours the 4-HA as this enzyme doesn't have a substitution at residue T41. It is feasible that the mutation of A113, R121, F123, A125 or K179 or a combination has lead to this shift. It is unclear why leucine at T41 affects the ratio of products. Glycine and glutamine at this position both produce equal ratios of 2-HA and 4-HA.

7.2.1.2 Sensitisation of SKOV3 cells to CB1954

7.2.1.2.1 Adenovirus

Four adenoviral vectors expressing the NTR mutants T41G N71S, T41N N71S, N71S A125T and clone 282 were generated and their therapeutic potential tested in SKOV3 cells relative to previous mutants and WT enzyme. vT41Q N71S F124T was best at sensitising SKOV3 cells to CB1954 followed by vT41L N71S. Contrary to bacterial and kinetics data, vT41G N71S and v282 confer less sensitivity to CB1954 than vWT. However NTR expression levels make a major contribution to the degree of sensitisation. Western blotting showed considerable variation between the viruses with vWT, vT41L N71S and vT41Q N71S F124T producing much higher levels of NTR. Western blotting at four different MOI's was used in order to identify which MOI of each virus most closely matched NTR expression. Survival curves for vWT, vT41L N71S and vT41Q N71S F124T at 10 ifu/cell were compared with 100 ifu/cell for vT41G N71S and vT41N N71S and 300 ifu/cell for v282 and vN71S A125T. These demonstrated the best normalisation of NTR possible with these viruses using current data. vT41Q N71S F124T, vT41L N71S and vT41N N71S showed similar sensitisation with ~9-fold improvement and vT41G N71S was ~2-fold improved relative to WT.

7.2.1.2.2 Purified Enzyme

Purified enzymes were also used to sensitise SKOV3 cells to CB1954 using both NADH and NADPH as cofactor. When using NADH as cofactor mutant T41Q N71S F124T gave greatest sensitisation of SKOV3 cells to CB1954. This was followed by T41G N71S, T41L F70A and then T41L N71S. By contrast for NADPH, T41L F70A gave greatest sensitisation. Two of the best NTR mutants (T41G N71S and T41L N71S) provided less sensitisation than WT.

7.2.1.3 Comparison of in vitro and in vivo performance

Kinetic activity of mutant enzymes T41Q N71S F124T, F124N and clone 282 show a direct relationship with their ability to sensitise bacterial cells to CB1954. However a direct relationship cannot be seen for T41L N71S and T41G N71S (see Table 7.2). In both these cases a greater fold increase in sensitivity was seen kinetically compared to bacterial cells.

There are several factors which will have an effect on cell sensitisation. CB1954 in the cell will have to compete with endogenous substrates and inhibitors for nitroreductase. Although T41L N71S and T41G N71S showed improvement for CB1954 compared to NFZ and Menadione we do not know what substrates and inhibitors are present within human cells and at what concentrations. It should be noted that crystal structure work has shown that nicotinic acid, acetate and dicoumarol can bind to the NTR active site, as crystals containing these compounds have been resolved (Lovering *et al.* 2001 and Johansson *et al.* 2003).

NTR must interact with at least one substrate in human and bacterial cells as growth inhibition due to NTR toxicity has been observed in both. In human cells it is harder to generate stable cell clones expressing NTR compared to EGFP; it has not been possible to rescue some NTR mutant viruses. When doing plaque assays smaller plaques are produced by NTR expressing viruses and λ bacteriophage.

All kinetic parameters were determined with NADH as cofactor; however both NADH and NADPH are available in cells. Human cells contain varying amounts of NADH and NADPH. Combined NAD^+ and NADH levels are reported typically to be ~ 10 fold higher than $NADP^+$ and NADPH (Garofalo *et al.* 1988). However when considering only the reduced cofactors used for CB1954 reduction, NADH levels in HEK293 cells were just 1-2 times that of NADPH (Pollak *et al.* 2007).

Tissue culture studies in this thesis have shown that both T41L N71S and T41G N71S have a big preference for NADH, whereas some of the other nitroreductases show less of a preference.

T41G N71S has a high K_m NADH of ~305 μM. This is 9.7-fold higher than WT NTR and between 1.7-5.5-fold higher than the other NTR mutants. Therefore the amount of NADH in the cell may be low enough for NADH to be rate limiting for T41G N71S. NADH is probably what limits this enzyme's overall success in human cells.

	In vitro Kinetics		In vivo *E. coli* bacterial cells		In vivo SKOV3 human cells	
Enzyme	**$k_{cat}/K_{m\ CB1954}$ μM s^{-1}**	**Fold improvement**	**$IC_{50\ CB1954}$ μM**	**Fold improvement**	**$IC_{50\ CB1954}$ μM**	**Fold improvement**
WT	0.0072	1	143	1	7	1
T41L N71S	0.90	125	14	10	0.8	9
T41G N71S	0.52	72	8	18	4	2
T41Q N71S F124T	0.32	44	4	36	0.8	9
F124N	0.031	4.3	25	6	-	-
282	0.018	2.5	18	8	60	NO IMPROVEMENT

Table 7.2 Comparison of in vitro and in vivo efficacy of *NfsB* mutants with the prodrug CB1954
Enhancement values are the fold improvement relative to WT *NfsB*

Finally, different NTRs have different bystander effects, the ability of the toxic product to spread to surrounding cells. WT *NfsB* and most of the mutants produce a 50:50 ratio of the 2-HA and 4-HA products for CB1954 reduction. The 4-HA is known to be more toxic being a difunctional DNA alkylating agent. However the less toxic 2-HA monofunctional alkylating agent has recently been stated as having a greater contribution to the bystander effect (Helsby *et al.* 2004). The mutant T41L N71S produces only the 4-hydroxylamine product. Therefore T41L N71S could plausibly have a lesser bystander effect, with a reduction in spread of the toxic product and less killing of surrounding tumour cells. T41G N71S however produces both the 2-HA and 4-HA and therefore should have a good bystander effect.

It was more difficult to compare kinetic activity with sensitising SKOV 3 cells to CB1954. In all cases the improvement in cell sensitisation was a lot lower than predicted by kinetic activity. However clone 282 was less sensitive than WT in SKOV 3 cells, which is contradictory to both bacterial *E. coli* cells and kinetic assays. However clone 282 only produces the 4-HA product; therefore it is likely that the bystander effect for this enzyme would be poor. In tissue culture much of the killing relies on the spread of the activated prodrug to surrounding cells. So NTRs with good bystander effects will be better in tissue culture assays. This was also the case with T41L N71S. This enzyme was kinetically the best. However, T41Q N71S F124T was better at sensitising SKOV3 cells. As with clone 282 enzyme T41L N71S only produces the 4-HA product. This shows that enzymes that produce both the 2-HA and 4-HA are favourable for VDEPT as they produce the highly cytotoxic derivative but also have a good bystander effect killing large portions of surrounding cells. It is not currently possible to target every cancerous cell so a good bystander effect would be essential for a cure.

When analysing all data from this thesis, T41Q N71S F124T *NfsB* enzyme appears to be the best enzyme for use in a CB1954/NTR VDEPT strategy. Although it was not the best enzyme kinetically it was consistently best in human cancer cell lines. However the T41Q N71S F124T virus had at least 8 fold lower titres, when compared to other NTR viruses. The particle to infectivity ratio for the T41Q N71S F124T virus was very high when looking at both plaque forming units and infectious units (see Figures 6.2 and 6.3). A GMP clinical grade viral stock with a high particle to infectivity ratio would need to be manufactured for any clinical trial using these viruses. For T41Q N71S F124T this would be very difficult and expensive to produce making this NTR enzyme too costly.

There are three remaining NTR mutants T41G N71S, T41N N71S and F124N, which have shown potential. T41G N71S is somewhat limited by its poor NADH kinetics but still showed 2-fold improvement over WT in SKOV3 cells. However T41N N71S was 3.8-fold better than T41G N71S and 7.8-fold than WT. Further work to determine kinetic parameters and ratio of products would need to be determined for this enzyme before it could be considered, but T41N N71S NTR has potential as a prodrug-activating enzyme for VDEPT with CB1954.

There are several alternative ways to improve an enzyme prodrug system, to use an alternative enzyme or prodrug and to improve the viral vector and delivery method. Each of these will be discussed further.

7.3 ALTERNATIVE ENZYMES

Several alternative enzymes have been examined with CB1954. *Escherichia coli* enzyme *NfsA* has been cloned and characterised by our group. *NfsA* is considered as the major nitroreductase with good nitrofurazone metabolism (Whiteway *et al.* 1998). The activity of *NfsA* with CB1954 was examined and was found to have a 25 fold higher activity than WT *NfsB* (Vass *et al.* 2009). An adenovirus expressing *NfsA* in SKOV3 human cells showed 3.5-, 6.3- and 8.1-fold lower IC_{50} values than an adenovirus expressing *NfsB* NTR. However this enzyme has a strong preference for NADPH which may limit its efficiency in human cells. Several of the *NfsB* mutants T41Q N71S F124T, T41L N71S, T41G N71S and T41L F70A showed greater sensitivity than *NfsA*.

The nitrobenzene nitroreductase enzyme *NbzA* from *Pseudomonas pseudoalcaligenes* has also been proposed as an alternative enzyme. This enzyme shares moderate sequence homology with *E. coli* nitroreductase *NfsA* and is able to reduce nitrobenzene to hydroxylaminobenzene. This enzyme has low affinity for nitrofurazone relative to other nitroreductases at 1763 µM. *NbzA* enzyme was found to have a much lower $K_{m\ CB1954}$ than *NfsB* at 11.7 µM. However kinetic data was determined by HPLC which is less reliable than steady state kinetics. There is no published in vivo data for *NbzA* (Berne *et al.* 2006).

A further nitroreductase enzyme *YwrO* from *Bacillus amyloliquefaciens* which is unrelated to *NfsB* but shares some sequence homology with mammalian NQO1 has been considered with CB1954. This enzyme only produces the 4-HA product and favours NADPH as cofactor. Kinetic parameters for CB1954 showed that both the k_{cat} and K_m are similar to those for *NfsB* NTR with a k_{cat} 618 µM and K_m 8.2 µM (Anlezark *et al.* 2002). However as with some of the *NfsB* mutants, kinetic data was not transferable to in vitro tissue culture assays. Purified *YwrO* enzyme required more CB1954 to kill V79 cells relative to *NfsB* enzyme. This is most probably due to a poor bystander effect, due to failure to produce 2-HA product, and preference for NADPH which reduces the amount of available cofactor.

A further *E. coli* enzyme *YieF* a chromate reductase has shown CB1954 reducing activity. Initially *YieF* mutants were screened to identify genes that encoded enzymes with superior chromate reductase activity. However it wasn't until later that several enzymes with improved chromate reductase activity where found to also possess superior prodrug-reducing activity. One of these *YieF* mutants has been compared to *NfsA*. Purified enzymes were used to compare the enzymes in HeLa cells. *YieF* was found to be a 5-fold improvement relative to *NfsA* (Barak *et al.* 2006). A more recent published paper has attempted to determine kinetic parameters for this enzyme using stop flow kinetics, however *YieF* failed to give detectable levels of activity with CB1954 (Prosser *et al.* 2010).

Prosser and colleagues used SOS chromotest (use of genetically modified *E. coli* encoding β-gal gene, the β-gal gene becomes activated by the SOS response upon DNA damage) to survey eleven *E. coli* CB1954 NTR candidates. This has allowed independent confirmation that *NfsA* is an effective CB1954 activating enzyme and has identified two other previously unreported enzymes with CB1954 reductase activity *AzoR* and *NemA* (Prosser *et al.* 2010). Stop flow kinetic data has shown that *NfsA* was 10-fold more active with CB1954 than *NfsB*, which was in turn approximately 2-fold more active than *NemA* and 60-fold more active than *AzoR*. IC_{50} assays showed *NfsA* (331 μM) then *NfsB* (490 μM) were best at sensitising *E. coli* SOS-R1 cells to CB1954. These were closely followed by *NemA* (502 μM).

Further examination would be required before *NbzA*, *YieF*, *YwrO*, *NemA* and *AzoR* could be considered as an alternative to *NfsB*; however it is unlikely these enzymes will be better than *NfsB* mutant enzymes.

7.4 ALTERNATIVE PRODRUGS

Two other classes of compounds have been used as prodrugs for NTR: dinitrobenzamide mustards (DNBM) and nitroaromatic phosphoramide mustards.

DNBM are analogues of CB1954 which have nitrogen mustard instead of an aziridine ring. The most well known is SN23862 which was originally designed to be activated in hypoxic tumour cells (Palmer *et al.* 1992 and Palmer *et al.* 1994). SN23862 was later tested with NTR, producing only a 2-HA product (see Figure 7.1a) (Anlezark *et al.* 1995). A range of further DNBM prodrugs have been generated by Wilson and colleagues. The prodrug SN24927 was found to have superior therapeutic activity to CB1954 (see Figure 7.1b) (Wilson *et al*. 2002).

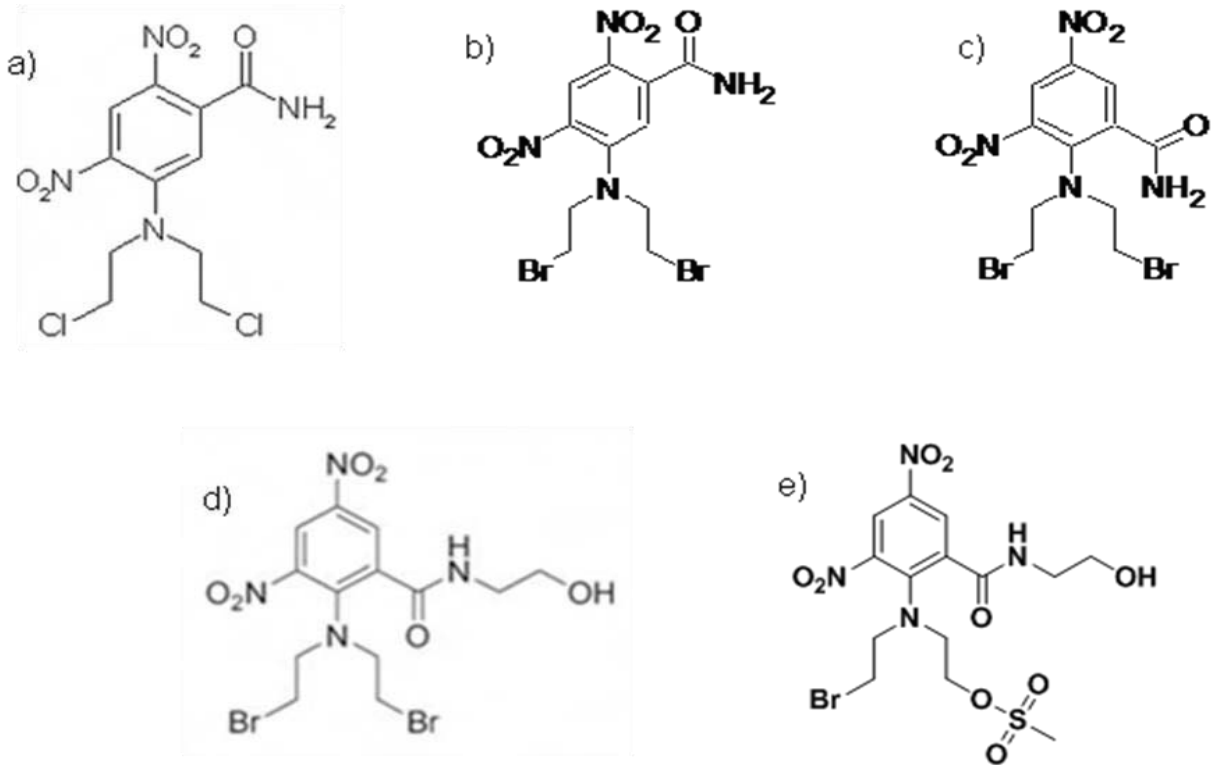

Figure 7.1 Dinitrobenzamide mustard prodrugs
a) SN23862, b) SN24927, c) SN26209, d) SN27686 and e) PR-104

In collaboration with the Wilson group several DNBM prodrugs have been tested with both *NfsA* and *NfsB*. SN24927 and SN26209 were found to be better than CB1954 (see Figure 7.1b and 7.1c). All the prodrugs tested were found to be better with *NfsA* than with *NfsB* (Vass *et al.* 2009). A further prodrug has been designed, SN27686, which also shows more dose potency and selectivity than CB1954 and also provide a superior bystander effect (see Figure 7.1d) (Singleton *et al.* 2007).

However, first generation DNBMs have poor aqueous solubility which limited *in vivo* application and prompted the development of DNBM phosphate esters, such as PR-104 which act as a 'pre-prodrug'. Systemic phosphatase activity generates the corresponding alcohols (prodrug PR-104A), which are then able to be reduced by hypoxic reductases or *NfsB* (see Figure 7.1e) (Patterson *et al.* 2007). PR-104 recently entered a Phase I clinical trial which showed that the prodrug was well tolerated (Jameson *et al*. 2010). PR-104 is now entering a Phase II clinical trial.

The most well known phosphoramide mustard, cyclophosphamide has been successfully used as an anticancer agent for many years. A number of nitroaromatic phosphoramide prodrugs have been designed to allow activation of the phosphoramide mustard by NTR. The best of these, LH7, contains a simple nitrobenzene ring, connected to the phosphoramide mustard moiety, allowing NTR reduction to release phosphoramide mustard (see Figure 7.2a). Hu and colleagues have shown that LH7 is a better substrate for NTR than CB1954, with an IC_{50} about 10-fold lower, and a greater differential toxicity between control and NTR expressing cells (Hu *et al.* 2003).

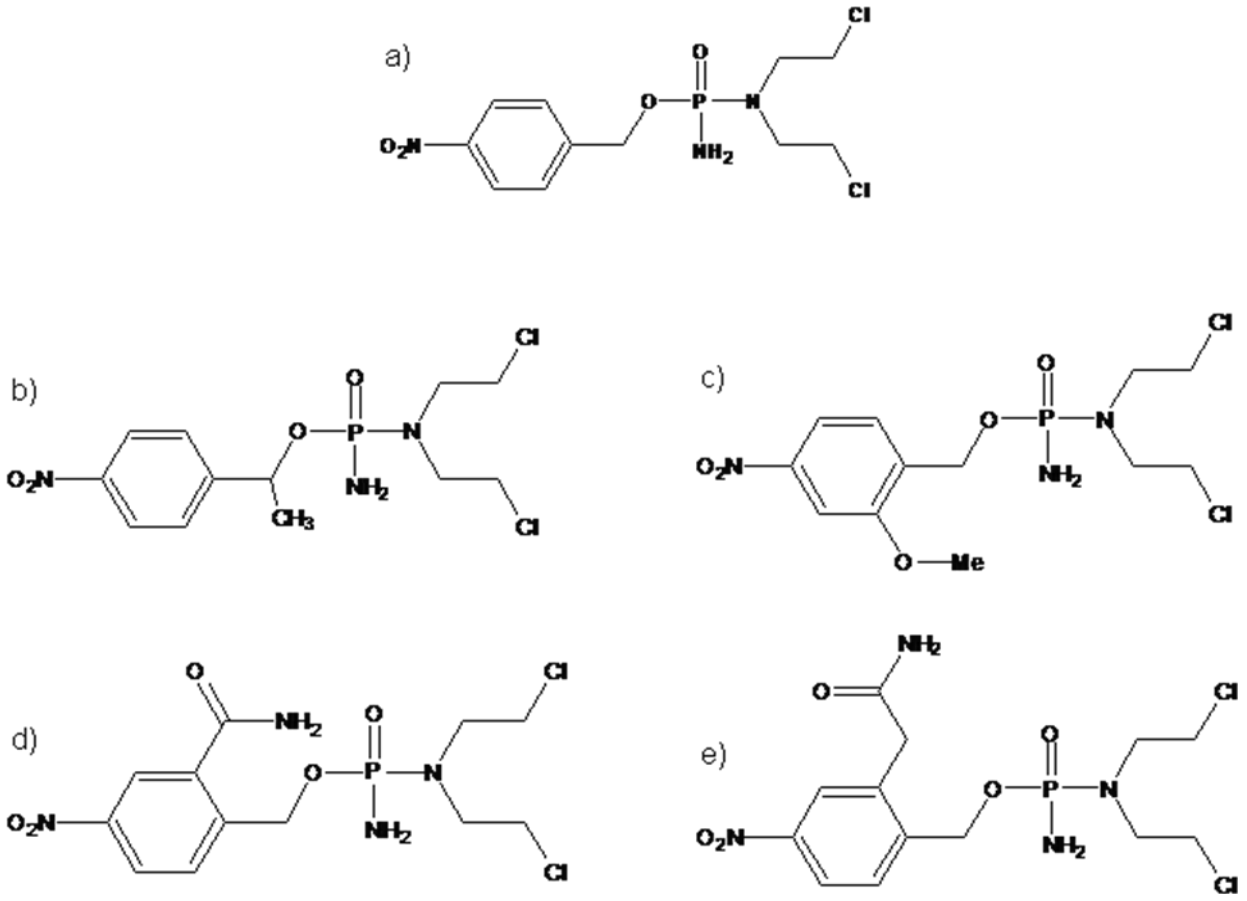

Figure 7.2 Phosphoramide mustard prodrugs
a) LH7, b) LH14, c) LH17, d) LH25 and e) LH26

In collaboration with the Hu group a large number of LH7 analogue phosphoramide prodrugs have been test with *NfsB*. Most were less sensitive than LH7 and CB1954. LH7 still remained most sensitive closely followed by LH17 then LH14 (see Figure 7.2b and 7.2c) (Vass 2007). A further set of prodrugs engineered to have good bystander effects have been tested with *NfsB*. None of these were better than LH7 and CB1954. However LH25 and LH26 were only marginally worse than CB1954 with *NfsB* (see Figure 7.2d and 7.2e) (Vass 2007).

Therefore SN27686, SN26209 and LH7 could prove good alternative to CB1954 when using *NfsB* NTR.

7.5 ALTERNATIVE SYSTEMS

The most clinically advanced enzyme/prodrug combinations for VDEPT are herpes simplex virus thymidine kinase (TK) for activation of the prodrug ganciclovir (GCV) and cytosine deaminase (CD) for conversion of 5-fluorocytosine to the antineoplastic agent 5-fluorouracil (Dachs *et al.* 2005 and Dachs *et al.* 2009).

HSV-TK with ganciclovir (GCV) is the only GDEPT combination to have reached phase III human trials. Patients with glioblastoma were treated with an HSV-TK-expressing replication defective retrovirus followed by GCV and radiotherapy (Rainov *et al.* 2000). However this treatment failed to improve patient survival. A subsequent phase II trial utilising a replication defective adenovirus for delivery of HSV-TK into patients has shown some success. The adenoviral vector was injected into the wound bed after glioma resection. A clinically and statistically significant increase in median survival over standard therapy was observed. (Immonen *et al.* 2004).

Adenovirally delivered HSV-TK has been granted Orphan Drug Status by the European Committee for Orphan Medicinal Products under the name of Cerepro. Their most recent Phase III clinical trial showed promising results (Arktherapeutics website www.arktherapeutics.com/CEREPRO September 2010).

HSV-TK mutants and ganciclovir (GCV) derivatives have been developed in an attempt to reduce toxicity, owing to HSV-TK having a higher affinity for its natural substrate thymidine (Field *et al.* 1983, Balzarini *et al.* 1993 and Munir *et al.* 1994). Ten thymidine kinase variants were selected from a random mutagenesis library consisting of over 1 million thymidine kinases. All ten showed increased activity to both GCV and ACV (Black *et al.* 1996). Further remodelling has further improved substrate specificity for GCV, giving improved prodrug-mediated tumour cell killing (Black *et al.* 2001 and Wiewrodt *et al.* 2003). It should be noted that these improvements to HSV-TK have resulted from a reduction in binding to thymidine (the natural substrate) rather than an improvement in activity with the prodrug. Therefore any improvement made stems from a reduction in substrate competition in contrast to improvements made by my group, which have improved the activity with the prodrug CB1954.

Cytosine deaminase (CD) and 5-fluorocytosine (5-FC) in combination has been tested in several Phase I clinical trials (Huber *et al.* 1993 and Padha *et al.* 1999). Initial work used bacterial CD cloned from *E. coli*, which has been shown in a number of *in vitro* studies to enhance mammalian cell sensitivity to 5-FC (Ge *et al.* 1997). CD from *Saccharomyces cerevisiae* has since been found to have a higher affinity for 5-FC (Kievit *et al.* 1999 and Kievit *et al.* 2000).

More recent studies have used the yeast enzyme or have attempted to improve the bacterial enzyme. Alanine-scanning mutagenesis and random mutagenesis of CD by error prone PCR has produced several CD mutants with favourable properties (Mahan *et al.* 2004a and Mahan *et al.* 2004b).

Uracil phosphoribosyl transferase (UPRT) has been used to help sensitise cells to lower concentrations of 5-FU by converting 5-FU to 5-FUMP, increasing the cytotoxic effects of 5-FC (Koyama *et al.* 2000). A fusion of the CD and UPRT genes has been created resulting in greater sensitisation to 5-FC (Erbs *et al.* 2000 and Chung-Faye *et al*. 2001b).

Over the last 7 years a double suicide gene therapy system has been proposed, looking at synergistic cytotoxicity, using a combination of cytosine deaminase and herpes simplex virus thymidine kinase enzymes. This system used a replication competent adenovirus delivering the two enzymes as a fusion gene (Freytag *et al.* 2002a). A second generation replication competent adenovirus has been constructed which contains an improved yeast cytosine deaminase, the herpes simplex virus thymidine kinase gene and the adenovirus death protein gene (Barton *et al.* 2006). This system has entered phase I clinical trials for prostate cancer (Freytag *et al.* 2002b and Freytag *et al.* 2007). A recent study has shown a synergistic cytotoxic interaction (Boucher *et al.* 2006).

7.6 VIRAL VECTORS AND THEIR DELIVERY

The clinical trial here in Birmingham used a replication defective adenovirus CTL102 (Palmer *et al.* 2004, Patel *et al.* 2009). Low efficiency of gene delivery and poor distribution of the virus was seen. Ideally the perfect vector system would be administered by a non-invasive route, would target only desired cells within the target tissue, and would express a therapeutic amount of transgene product with desired regulation for a desired length of time (Vorburger and Hunt 2002). No vector with all these properties is currently available.

A conditionally replicating virus ONYX-015 has been developed which was expected to target cells containing dysfunctional p53 (Barker and Berk 1987, Heise *et al.* 1997 and Freytag *et al.* 1998). The mechanism of tumour selectivity is now believed to depend more on complementation by tumour cells with defects in nuclear export of viral RNA in the absence of E1B 55K protein (O'Shea *et al.* 2004). Modest anti-tumour activity was observed; particularly when combined with chemotherapy (Khuri *et al.* 2000). In 2005 a modified version of the oncolytic ONYX-015 virus was approved for the treatment of head and neck cancer in Shanghai (Garber 2006). Survival data was not given but combination with chemotherapy showed an improvement relative to chemotherapy alone.

Further research here in Birmingham using a virus (CRAd), similar to ONYX-015, encoding *NfsB* NTR showed oncolytic growth properties and the virus expressed substantially more NTR than a comparable replication-defective adenovirus. The combination of viral oncolysis and NTR expression resulted in significantly greater sensitization of colorectal cancer cells to the prodrug CB1954 in vitro (Chen *et al.* 2004).

Onyx Pharmaceuticals have engineered a second oncolytic virus ONYX-411 which selectively replicates in tumor cells, depending upon the status of the cells' retinoblastoma tumour suppressor protein (pRB) pathway. Early and late viral gene expression was significantly reduced, resulting in a restricted replication profile similar to that of nonreplicating adenoviruses in normal cells both in vitro and in vivo (Johnson *et al.* 2002). ONYX-411 is also better at expressing in tumour cells compared to ONYX-015 (Zhan *et al.* 2005). Reddi and colleagues have report that ONYX-411 is able to induce cell death in eight human anaplastic carcinoma cell lines in vitro (Reddi *et al.* 2008). ONYX-411^{NTR} has been tested in combination with the prodrug SN27686. Robust, durable NTR expression was seen in ONYX-411^{NTR} infected neoplastic cell lines, but not primary human cell lines. The water-soluble phosphate ester SN28343 was substantially more active than CB1954 against xenografts containing a minority of stable NTR-expressing cells (Singleton *et al.* 2007).

Systemic administration of oncolytic viruses have so far been limited by the cellular immune response. Adenoviruses are readily cleared from the bloodstream after interacting with blood clotting factors and neutralisation by pre-existing antibodies. Lyons and colleagues have shown that the highest level of adenovirus binding was in erythrocytes (accounting for 70-95%), however binding was also seen in human neutrophils and peripheral blood mononuclear cells (PBMCs) (Lyons *et al.* 2006). Therefore any virus administered systemically must be protected from the immune system. A possible way around this would be to polymer-shield viral vectors to prevent interaction with antibodies, but to still allow viral production once in the target tumour cells.

Modification of adenoviruses with hydrophilic synthetic polymers such as N-(2-hydroxypropyl) methacrylamide copolymer (HPMA) significantly prolongs plasma circulation times and prevents non-specific cell entry. In mouse studies a polymer-coated adenovirus showed nearly 50% plasma circulation, representing 3.5-fold greater levels when compared to unmodified adenovirus. This has allowed active and passive targeting to tumour cells (Green *et al.* 2004 and Fisher *et al.* 2007). Polymers have been further improved by including side chains bearing reactive carbonyl thiazolidine-2-thione groups and the inclusion of side chains bearing positively charged quaternary ammonium groups (Subr *et al.* 2009). Antibody-resistant polymer coated viruses that circulate well in plasma and can be targeted directly to tumour cells have real potential for the treatment of metastatic cancer. First generation vectors are currently being developed which could prove to be a big step towards curative cancer gene therapy (Fisher and Seymour 2010).

7.7 GENE THERAPY PROGRESS

Gene therapy has come a long way since it was originally conceived as a treatment for monogenic disease in 1989. Rapid progress has allowed greater understanding of disease processes, with the first gene therapy trial being performed in 1990 for children with adenosine deaminase deficiency (ADA) (Blaese *et al.* 1995). As our knowledge has improved, research has moved towards more complex diseases with cancer now being the focus for the vast majority of gene therapy clinical trials.

There have been many successes and failures during the last 20 years of gene therapy. The death of a clinical trial patient in 1999 was a major blow to gene therapy research. Jesse Gelsinger suffered from a partial deficiency of ornithine transcarbamylase (OTC). Gelsinger suffered an adverse reaction to the adenovirus used in the trial which lead to multiple organ failure (Thomas *et al.* 2003).

In 2000 the successful treatment of ten patients with SCID was probably the highest point for gene therapy (Cavazzana-Calvo *et al.* 2000). However the excitement turned to alarm at the end of 2002 when two of the ten children developed leukaemia-like conditions, linked to the retroviral vector used during the treatment (Hacein-Bey-Abina *et al.* 2003a and Hacein-Bey-Abina *et al.* 2003b). Regulatory bodies halted the trial, but in 2004 the trial was reopened on the grounds that benefits outweigh the risks. This gave fresh hope that gene therapy can offer a realistic chance of survival to babies born with SCID. However this incident has spawned much further work to understand retrovirus integration site preferences and to allow the development of vectors less likely to result in oncogene activation.

In 2003 Gendicine (recombinant adenovirus encoding human tumor suppressor gene p53) gene therapy and in 2005 Oncorine (Recombinant oncolytic virus) gene therapy have both been made commercially available in China for the treatment of a large range of cancers (Guo and Xin 2006). In 2009 HSV-TK with ganciclovir prodrug activation therapy was granted orphan drug status, showing clinical efficacy (Arktherapeutics website www.arktherapeutics.com/CEREPRO September 2010).

Despite a huge amount of research over the last 20 years further improvement would be required before gene therapy could be used as a curative procedure for cancer. Ideally improved vectors and delivery systems could prove crucial to future gene therapy successes.

In conclusion, I have further improved the NTR/CB1954 enzyme prodrug system by generating improve NTR variants. These improved enzymes have been kinetically determined and their ability to sensitise human cancer cell lines examined. The merits of these enzymes should be considered when designing future clinical trials, using NTR for prodrug activation.

CHAPTER 8: APPENDIX

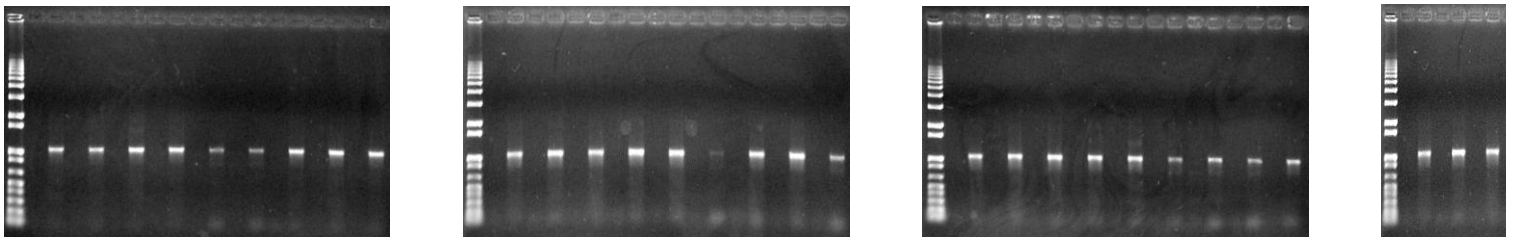

WT

30/30 100% *NfsB* NTR

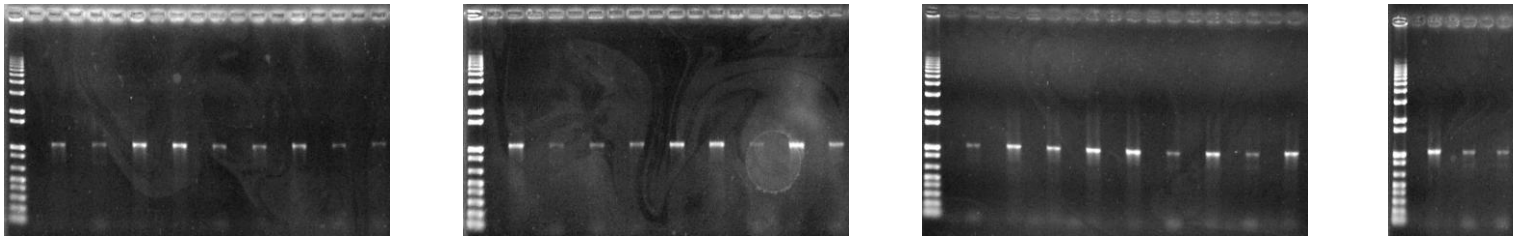

N71S

30/30 100% *NfsB* NTR

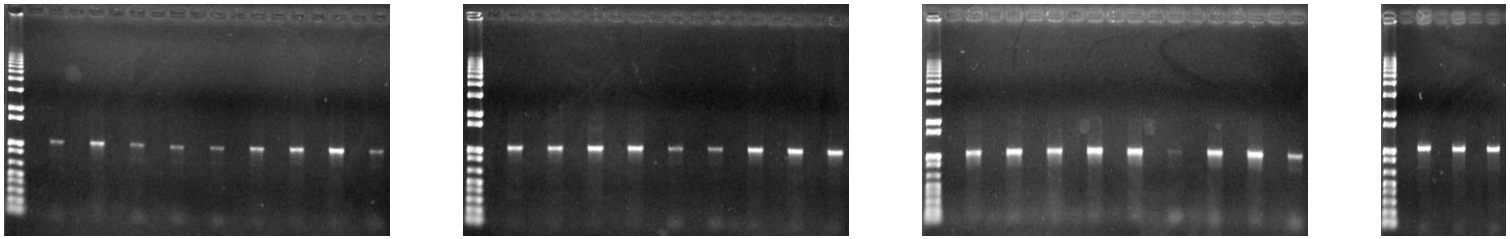

T41L N71S

30/30 100% *NfsB* NTR

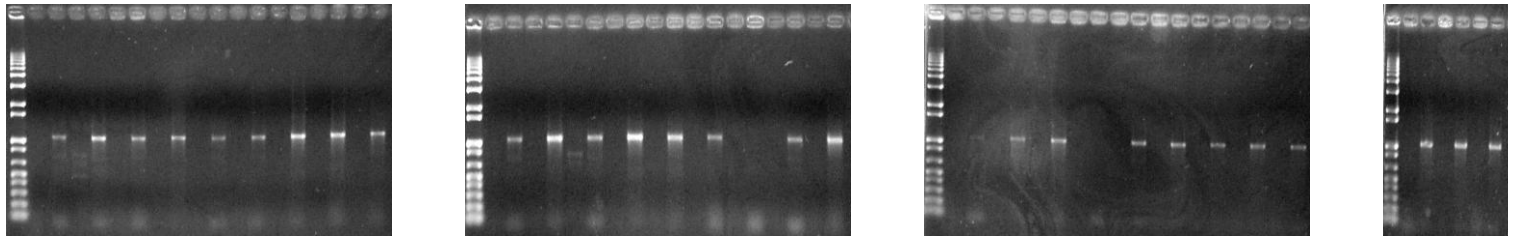

T41N N71S

28/28 100% *NfsB* NTR

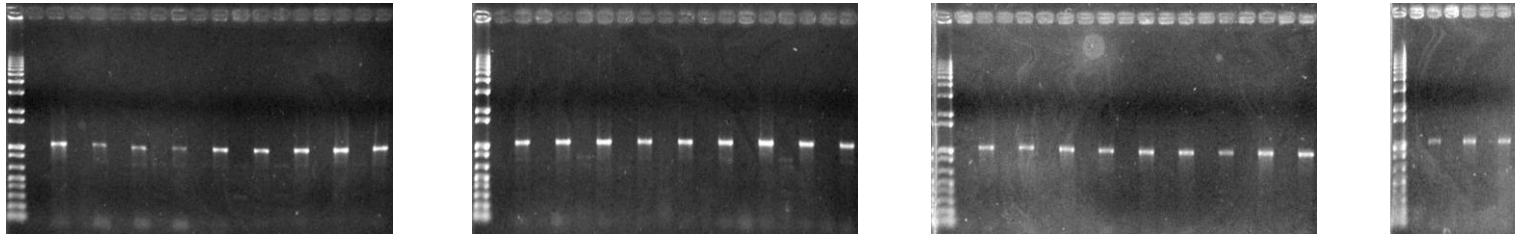

T41Q N71S

30/30 100% *NfsB* NTR

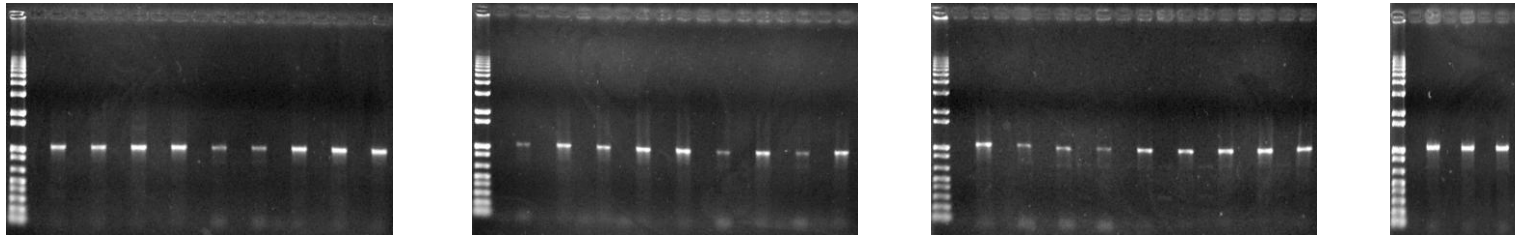

T41G N71S

30/30 100% *NfsB* NTR

Figure 8.1 Agarose gels of PCR's using primers JG2A with PS1296F and JG2A with JG2B
PCR products were run on 0.7% agarose gel. JG2A/PS1296F: *NfsB* insert no band, *NfsA* insert expect band of 607 bp and empty vector no band. JG2A/JG2B: *NfsB* insert expert band of 1093 bp, *NfsA* insert expect band of 1126 bp and empty vector 385 bp. *NfsB* NTR and empty vector can't prime with PS1296F

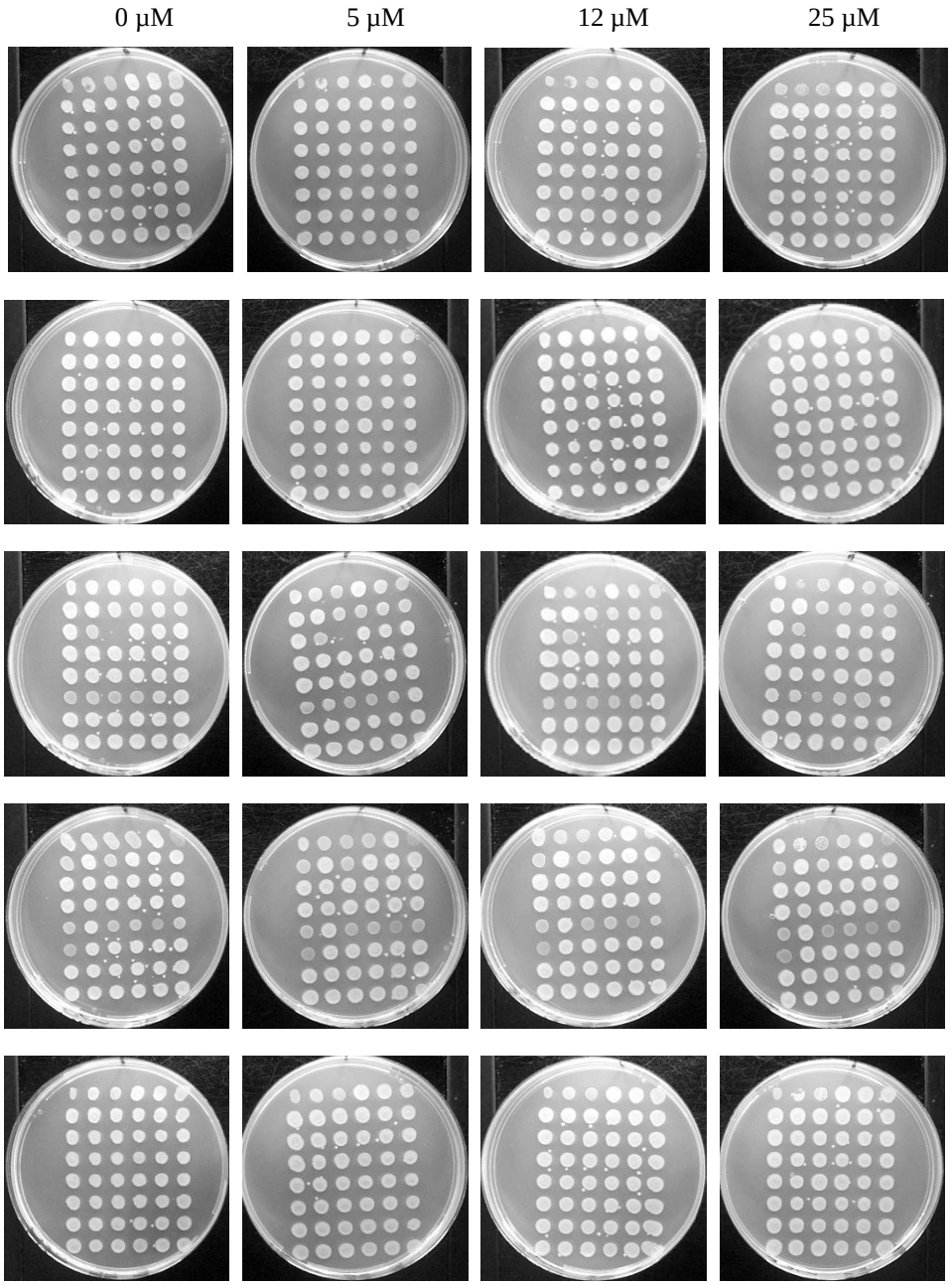

Figure 8.2 Replica plating of individual lysogens after twenty-one rounds of selection using 25 µM CB1954
No CB1954, 5 µM, 12 µM and 25 µM CB1954 was used for replica plating. The first two lysogens on the top left of each plate are controls WT and T41G N71S respectively

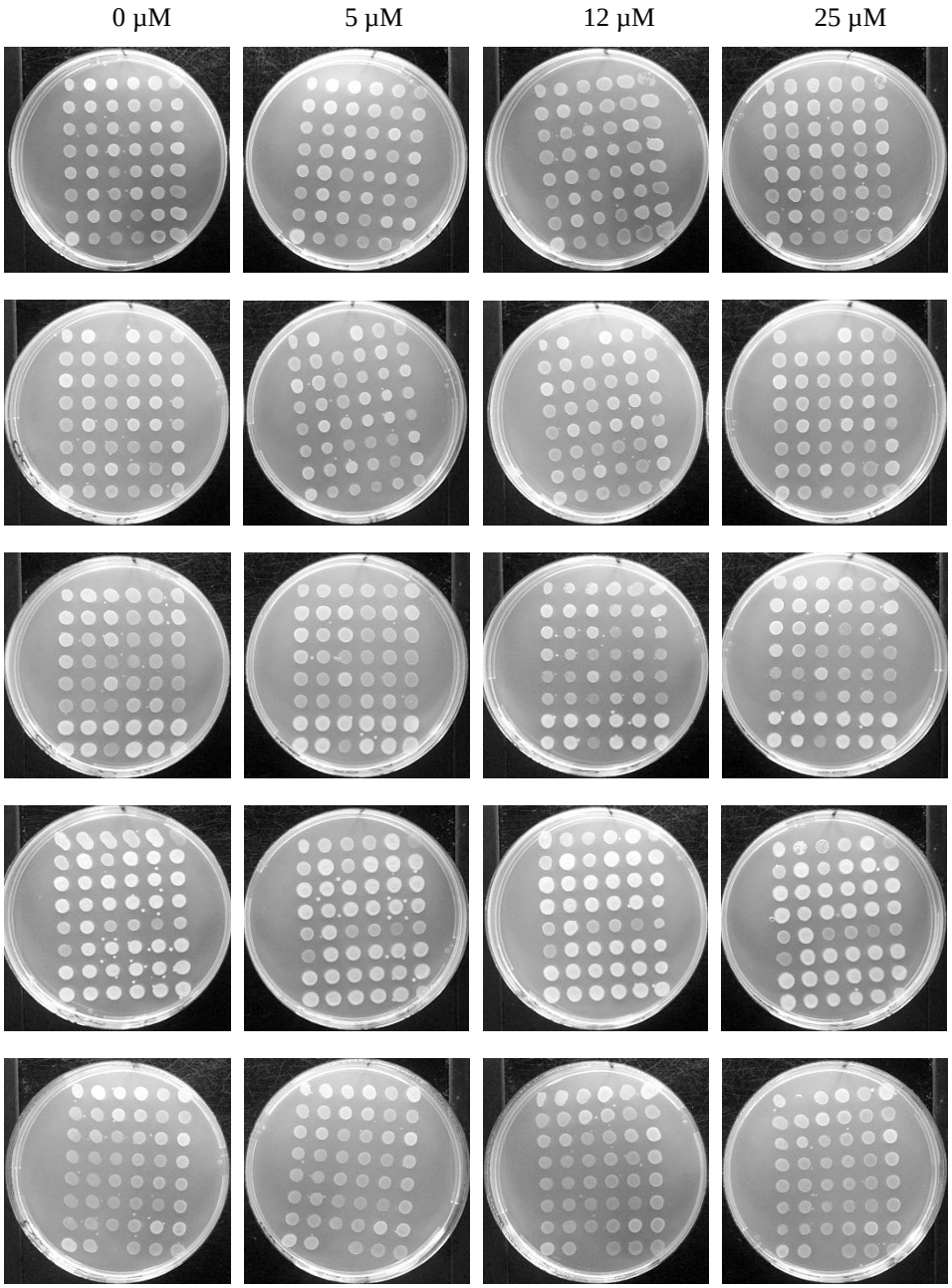

Figure 8.3 Replica plating of individual lysogens after twenty-one rounds of selection using 50 µM CB1954
No CB1954, 5 µM, 12 µM and 25 µM CB1954 was used for replica plating. The first two lysogens on the top left of each plate are controls WT and T41G N71S respectively

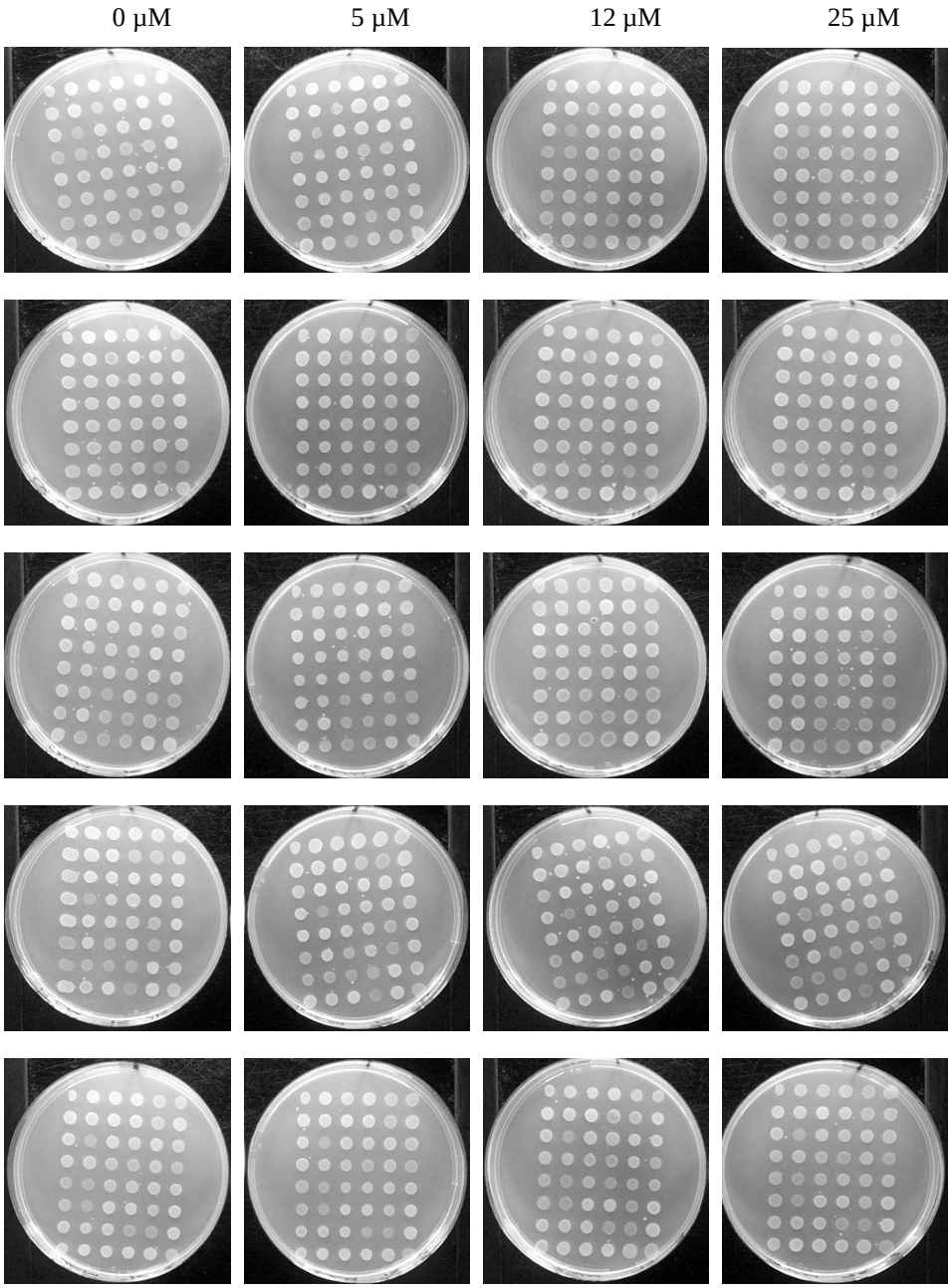

Figure 8.4 Replica plating of individual lysogens after twenty-one rounds of selection using 75 µM CB1954
No CB1954, 5 µM, 12 µM and 25 µM CB1954 was used for replica plating. The first two lysogens on the top left of each plate are controls WT and T41G N71S respectively

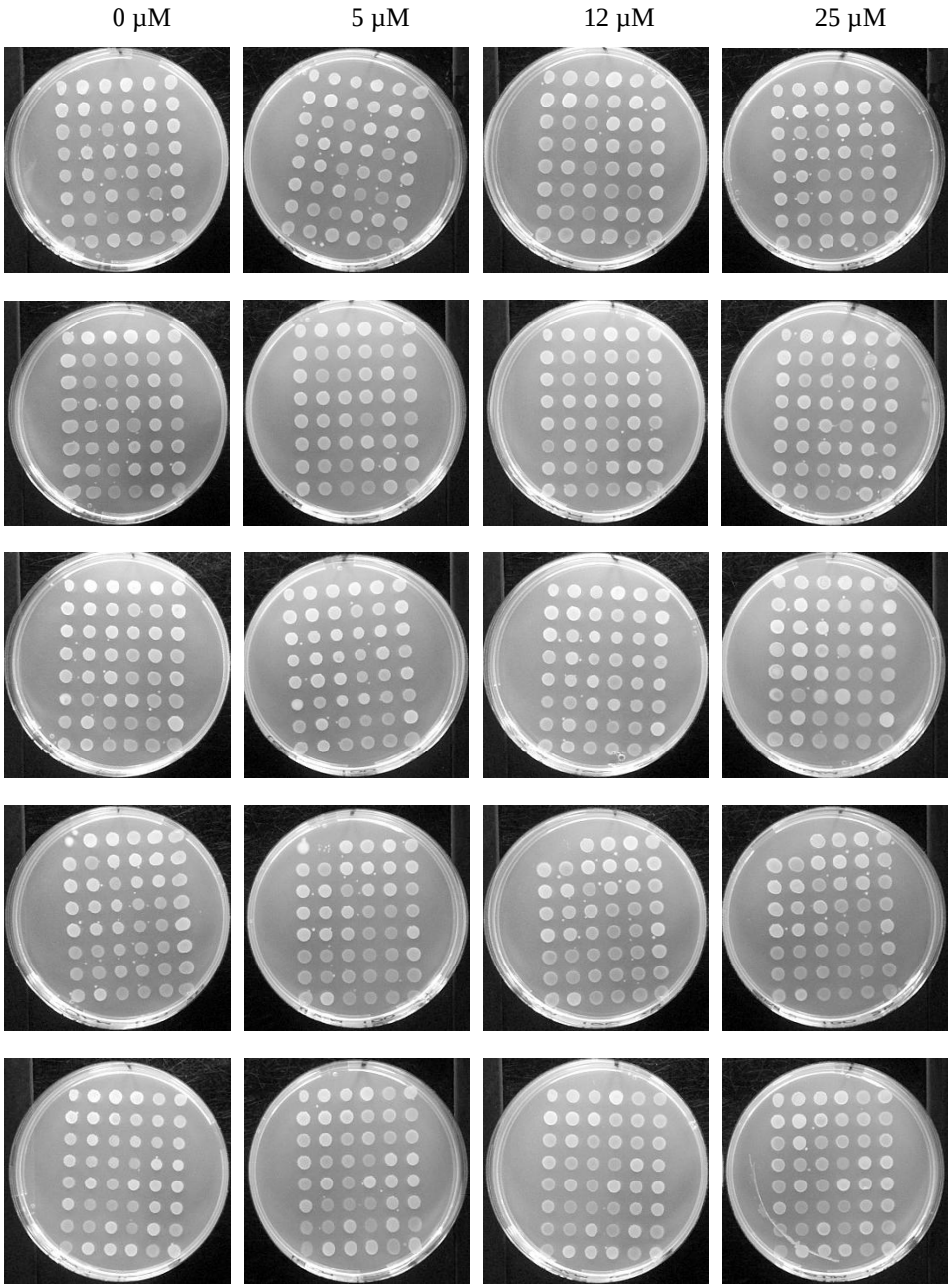

Figure 8.5 Replica plating of individual lysogens after twenty-one rounds of selection using 100 µM CB1954
No CB1954, 5 µM, 12 µM and 25 µM CB1954 was used for replica plating. The first two lysogens on the top left of each plate are controls WT and T41G N71S respectively

CHAPTER 9: REFERENCES

www.cancerhelp.org.uk Cancer Research UK (October 2009)

info.cancerresearchuk.org Cancer Research UK (October 2009)

www.wiley.co.uk/genmed/clinical/ Gene Therapy Clinical Trials World Wide (October 2009)

www.arktherapeutics.com/CEREPRO CEREPRO Trial (October 2009/September 2010)

Agarwal K.C, Agarwal R.P, Stoeckler J.D, & Parks R.E Jr 1975. Purine Nucleoside Phosphorylase. Microheterogeneity and Comparison of Kinetic Behaviour of the Enzyme from Several Tissues and Species. *Biochemistry*, 14(1): 79-84.

Alberts B, Bray D, Lewis J, Raff M, Roberts K, & Watson J.D 1994. *Molecular Biology of the Cell*. Garland Publishing.

Alvarez R.D, Barnes M.N, Gomez-Navarro J, Wang M, Strong T.V, Arafat W, Arani R.B, Johnson M.R, Roberts B.L, Siegal G.P, & Curiel D.T 2000a. A Cancer Gene Therapy Approach Utilizing an Anti-erbB-2 Single-Chain Antibody-encoding Adenovirus (AD21): A Phase I Trial. *Clinical Cancer Research*, 6: 3081-3087.

Alvarez R.D, Gomez-Navarro J, Wang M, Barnes M.N, Strong T.V, Arani R.B, Arafat W, Hughes J.V, Siegal G.P, & Curiel D.T 2000b. Adenoviral-Mediated Suicide Gene Therapy for Ovarian Cancer. *Molecular Therapy*, 2(5): 524-530.

Anlezark G.M, Melton R.G, Sherwood R.F, Coles F, Friedlos F, & Knox R.J 1992. The Bioactivation of 5-(Aziridin-1-yl)-2,4-Dinitrobenzamide (CB1954)-I. *Biochemical Pharmacology*, 44(12): 2289-2295.

Anlezark G.M, Melton R.G, Sherwood R.F, Wilson W.R, Denny W.A, Palmer B.D, Knox R.J, Friedlos F, & Williams A 1995. Bioactivation of Dinitrobenzamine Mustards by an *E. coli* B Nitroreductase. *Biochemical Pharmacology*, 50(5): 609-618.

Anlezark G.M, Vaughan T, Fashola-Stone E, Michael P.N, Murdoch H, Sims M.A, Stubbs S, Wigley S, & Minton N.P 2002. *Bacillus amyloliquefaciens* orthologue of *Bacillus subtilis yrwO* encodes a nitroreductase enzyme activates the prodrug CB1954. *Microbiology*, 148: 297-306.

Arber W 1983. *A Beginner's Guide to Lambda Biology*. *Lambda II*: 381-391. Cold Spring Harbor.

Asnis R.E 1957. The reduction of Furacin by cell-free extracts of Furacin-resistant and parent-susceptible strains of *Escherichia coli*. *Archives of Biochemistry and Biophysics*, 66(1): 208-216.

Bagshawe K.D, Sharma S.K, Springer C.J, & Rogers G.T 1994. Antibody directed enzyme prodrug therapy (ADEPT). *Annals of Oncology*, 5: 879-891.

Bainbridge J.W.B, Smith A.J, Barker S.S, Robbie S, Henderson R, Balaggan K, Viswanathan A, Holder G.E, Stockman A, Tyler N, Peterson-Jones S, Bhattacharya S.S, Thrasher A.J, Fitzke F.W, Carter B.J, Rubin G.S, Moore A.T, & Ali R.R 2008. Effect of Gene Therapy on Visual Function in Leber's Congenital Amaurosis. *The New England Journal of Medicine*, 358(21): 2231-2239.

Balzarini J, Bohman C, & De Clerq E 1993. Differential Mechanism of Cytostatic Effect of (*E*)-5-(2-Bromovinyl)-2'-deoxyuuridine, 9-(1,3-Dihydroxy-2-propxymethyl)guanine, and Other Antiherpetic Drugs on Tumor Cells Transfected by the Thymidine Kinase Gene of Herpes Simplex Virus Type 1 or Type 2. *The Journal of Biological Chemistry*, 268(9): 6332-6337.

Bansal K & Engelhard H.H 2000. Gene therapy for brain tumors. *Current Oncology Reports*, 2(5): 463-472.

Barak Y, Thorne S.H, Ackerley D.F, Lynch S.V, Contag C.H, & Matin A 2006. New enzyme for reductive cancer chemotherapy, YieF, and its improvement by directed evolution. *Molecular Cancer Therapeutics*, 5(1): 97-103.

Barker D.D & Berk A.J 1987. Adenovirus proteins from both E1B reading frames are required for transformation of rodent cells by viral infection and DNA transfection. *Virology*, 156(1): 107-121.

Barton K.N, Paielli D, Zhang Y, Koul S, Brown S.L, Lu M, Seely J, Kim J.H, & Freytag S.O 2006. Second-Generation Replication-Competent Oncolytic Adenovirus Armed with Improved Suicide Genes and ADP Gene Demonstrates Greater Efficacy without Increased Toxicity. *Molecular Therapy*, 13(2): 347-356.

Bernards R, Brummelkamp T.R, & Beijersbergen R.L 2006. shRNA libraries and their use in cancer genetics. *Nature Methods*, 3: 701-706.

Berne C, Betancor L, Luckarift H.R, & Spain J.C 2006. Application of a Microfluidic Reactor for Screening Cancer Prodrug Activation Using Silica-Immobilized Nitrobenzene Nitroreductase. *Biomacromolecules*, 7: 2631-2636.

Bilsland A.E, Anderson C.J, Fletcher-Monaghan A.J, McGregor F, Jeffry Evans T.R, Ganly I, Knox R.J, Plumb J.A, & Nicol K.W 2003. Selective ablation of human cancer cells by telomerase-specific adenoviral suicide gene therapy vectors expressing bacterial nitroreductase. *Oncogene*, 22: 370-380.

Black M.E, Newcomb T.G, Wilson H-M.P, & Loeb L.A 1996. Creation of drug-specific herpes simplex virus type 1 thymidine kinase mutants for gene therapy. *Proceedings of the National Academy of Sciences of the United States of America*, 93: 3525-3529.

Black M.E, Kokoris M.S, & Sabo P 2001. Herpes Simplex Virus-1 Thymidine Kinase Mutants Created by Semi-Random Sequence Mutagenesis Improve Prodrug-mediated Tumor Cell Killing. *Cancer Research*, 61: 3022-3026.

Blaese R.M, Culver K.W, Miller A.D, Carter C.S, Fleisher T, Clerici M, Shearer G, Chang L, Chiang Y, Tolstoshev P, Greenblatt J.J, Rosenberg S.A, Klein H, Berger M, Mullen C.A, Ramsey W.J, Muul L, Morgan R.A, & Anderson W.F 1995. T Lymphocyte-Directed Gene Therapy for ADA SCID: Initial Trial Results After 4 Years. *Science*, 270: 475-480.

Bos J.L, Toksoz D, Marshall C.J, Verlaan-de Vries M, Veeneman G.H, Van der Eb A.J, Van Boom J.H, Janssen Johannes W.G, & Steenvoorden Ada C.M 1985. Amino-acid substitutions at codon 13 of the N-ras oncogene in human acute myeloid leukaemia. *Nature*, 315: 726-730.

Boucher P.D, Im M.M, Freytag S.O, & Shewach D.S 2006. A Novel Mechanism of Synergistic Cytotoxicity with 5-Fluorocytosine and Ganciclovir in Double Suicide Gene Therapy. *Cancer Research*, 66(6): 3230-3237.

Boucher R.C, Knowles M.R, Johnson L.G, Olsen J.C, Pickles R, Wilson J.M, Engelhardt J, Yang Yiping, & Grossman M 1994. Clinical Protocol - Gene Therapy for Cystic Fibrosis Using E1-Deleted Adenovirus: A Phase I Trial in the Nasal Cavity. *Human Gene Therapy*, 5: 615-639.

Bradford M.M 1976. Rapid and sensitive method for quantitation of microgram quantities of protein utilizing principle of protein-dye binding. *Analytical Biochemistry*, 72: 248-254.

Braybrooke J.P, Slade A, Deplanque G, Harrop R, Madhusuan S, Forster M.D, Gibson R, Makris A, Talbot D.C, Steiner J, White L, Kan O, Naylor S, Carroll M.W, Kingsman S.M, & Harris A.L 2005. Phase I Study of MetXia-P450 Gene Therapy and Oral Cyclophosphamide for Patients with Advanced Breast Cancer or Melanoma. *Clinical Cancer Research*, 11: 1512-1520.

Brenner S & Malech H.L 2003. Current developments in the design of onco-retrovirus and lentivirus vector systems for hematopoietic cell gene therapy. *Biochimica Et Biophysica Acta*, 1640: 1-24.

Bridgewater J.A, Springer C.J, Knox R.J, Minton N.P, Michael N.P, & Collins M.K 1995. Expression of the Bacterial Nitroreductase Enzyme in Mammalian Cells Renders Them Selectively Sensitive to Killing by the Prodrug CB1954. *European Journal of Cancer*, 31A(13/14): 2362-2370.

Bryant C, Hubbard L, & McElroy W.D 1991a. Cloning, Nucleotide Sequence, and Expression of the Nitroreductase Gene from *Enterobacter cloacae*. *The Journal of Biological Chemistry*, 266(7): 4126-4130.

Bryant C & DeLuca M 1991b. Purification and Characterization of an Oxygen-insensitive NAD(P)H Nitroreductase from *Enterobacter cloacae*. *The Journal of Biological Chemistry*, 266(7): 4119-4125.

Bryant D.W, McCalla D.R, Leeksma M, & Laneuville P 1981. Type I nitroreductases of *Escherichia coli*. *Canadian Journal of Microbiology*, 27(1): 81-86.

Buchschacher G.L Jr 2001. Introduction to Retroviruses and Retroviral Vectors. *Somatic Cell and Molecular Genetics*, 26(1-6): 1-11.

Buckley R.H, Schiff R.I, Schiff S.E, Markert L.M, Williams L.W, Harville T.O, Roberts J.L, & Puck J.M 1997. Human severe combined immunodeficiency: Genetic phenotypic, and functional diversity in one hundred and eight infants. *The Journal of Pediatrics*, 130: 378-387.

Buckley R.H, Schiff S.E, Schiff R.I, Markert L.M, Williams L.W, Roberts J.L, Myers L.A, & Ward F.E 1999. Hematopoietic stem-cell transplantation for the treatment of severe combined immunodefieciency. *The New England Journal of Medicine*, 340(7): 508-516.

Campbell N.A, Reece J.B, & Mitchell L.G 1999. *Biology*. Addison Wesely Longman Inc.

Cavazzana-Calvo M, Hacein-Bey S, de Saint Basile G, De Coene C, Selz F, Le Deist F, & Fischer A 1996. Role of interleukin-2 (IL-2), IL-7, and IL-15 in natural killer cell differentiated from cord blood hematopoietic progenitor cells and from gamma c transduced severe combined immunodeficiency X1 bone marrow cells. *Blood*, 88(10): 3901-3909.

Cavazzana-Calvo M, Hacein-Bey S, Saint Basile G, Gross F, Yvon E, Nusbaum P, Selz F, Hue C, Certain S, Casanova J, Bousso P, Le Deist F, & Fischer A 2000. Gene Therapy of Human Severe Combined Immunodeficiency (SCID)-X1 Disease. *Science*, 288: 669-672.

Chen L & Waxman D.J 1995. Intratumoral Activation and Enhanced Chemotherapeutic Effect of Oxazaphosphorines following Cytochrome P-450 Gene Transfer: Development of a Combined Chemotherapy/Cancer Gene Therapy Strategy. *Cancer Research*, 55: 581-589.

Chen M-J, Green N.K, Reynolds G.M, Flavell J.R, Mautner V, Kerr D.J, Young L.S, & Searle P.F 2004. Enhanced efficacy of Escherichia coli nitroreductase/CB1954 prodrug activation gene therapy using an E1B-55K-deleted oncolytic adenovirus vector. *Gene Therapy*, 11: 1126-1136.

Chen Y, Bathula S.R, Li J, & Huang L 2010. Multi-functional Nanoparticles Delivering siRNA and Doxorubicin Overcome Drug Resistance in Cancer. *The Journal of Biological Chemistry*, 285: 22639-22650.

Chung-Faye G, Palmer D, Anderson D, Clark J, Downes M, Baddeley J, Hussain S, Murray P.I, Searle P, Seymour L, Harris P.A, Ferry D, & Kerr D.J 2001a. Virus-directed, Enzyme Prodrug Therapy with Nitroimidazole Reductase: A Phase I and Pharmacokinetic Study of its Prodrug, CB1954. *Clinical Cancer Research*, 7: 2662-2668.

Chung-Faye G.A, Chen M-J, Green N.K, Burton A, Anderson D, Mautner V, Searle P.F, & Kerr D.J 2001b. In vivo gene therapy for colon cancer using adenovirus-mediated, transfer of the fusion gene cytosine deaminase and uracil phosphoribosyltransferase. *Gene Therapy*, 8: 1547-1554.

Cobb L.M, Connors T.A, Elson L.A, Khan A.H, Mitchley B.C.V, Ross W.C.J, & Whisson M.E 1969. 2,4-Dinitro-5-ethyleneiminobenzamide (CB1954): A Potent and Selective Inhibitor of the Growth of the Walker Carcinoma 256. *Biochemical Pharmacology*, 18: 1519-1527.

Connors T.A 1995. The choice of prodrugs for gene directed enzyme prodrug therapy of cancer. *Gene Therapy*, 2(10): 702-709.

Cooper M.D, Lanier L.L, Conley M.E, & Puck J.M 2003. Immunodeficiency Disorders. *American Society of Haematology*, 314-330.

Court D.L, Oppenheim A.B, & Adhya S.L 2007. REVIEW - A New Look at Bacteriophage lambda Genetic Networks. *Journal of Bacteriology*, 189(2): 298-304.

Cowen R.L, Williams J.C, Emery S, Blakey D, Darling J.L, Lowenstein P.R, & Castro M.G 2002. Adenovirus vector-mediated delivery of the prodrug-converting enzyme carboxypeptidase G2 in a secreted or GPI-anchored form: High-level expression of this active conditional cytotoxic enzyme at the plasma membrane. *Cancer Gene Therapy*, 9: 897-907.

Crystal R.G 1995. Clinical Protocol - A phase I Study in Cystic Fibrosis Patients, of the Safety, Toxicity, and Biological Efficiency of a Single Administration of a Replication Deficient, Recombinant Adenovirus Carrying the cDNA of the Normal Cystic Fibrosis Transmembrane Conductance Regulator Gene in the Lung. *Human Gene Therapy*, 6: 643-666.

Dachs G.U, Tupper J, & Tozer G.M 2005. From bench to bedside for gene-directed enzyme prodrug therapy of cancer. *Anticancer Drugs*, 16(4): 349-359.

Dachs G.U, Hunt M.A, Syddall S, Singleton D.C, & Patterson A.V 2009. Bystander or No Bystander for Gene Directed Enzyme Prodrug Therapy. *Molecules*, 14: 4517-4545.

Davis M.E, Zuckerman J.E, Choi C.H.J, Seligson D, Tolcher A, Alabi C.A, Yen Y, Heidel J.D, & Ribas A 2010. Evidence of RNAi in humans from systemically administered siRNA via targeted nanoparticles. *Nature Letters*, 464: 1067-1071.

DeWeese T.L, Van der Poel H, Li S, Mikhak B, Drew R, Goemann M, Hamper U, DeJong R, Detorie N, Rodriguez R, Haulk T, DeMarzo A.M, Piantadosi S, Yu D.C, Chen Y, Henderson D.R, Carducci M.A, Nelson W.G, & Simons J.W 2001. A Phase I Trial of CV706, a replication-competent, PSA Selective Oncolytic Adenovirus, for the Treatment of Locally Recurrent Prostate Cancer following Radiation Therapy. *Cancer Research*, 61: 7464-7472.

DiPaola R.S, Plante M, Kaufman H, Petrylak D.P, Israeli R, Lattime E, Manson K, & Schuetz T 2006. A Phase I Trial of Pox PSA vaccines (PROSTVAC-VF) with B7-I, ICAM-I, and LFA-3 co-stimulatory molecules (TRICOM) in Patients with Prostate Cancer. *Journal of Translational Medicine*, 4(1): 1-5.

Eder J.P, Kantoff P.W, Roper K, Xu G.X, Bubley G.J, Boyden J, Gritz L, Mazzara G, Oh W.K, Arlen P, Tsang K.Y, Panicali D, Schlom J, & Kufe D.W 2000. A Phase I Trial of a Recombinant Vaccinia Virus Expressing Prostate-specific Antigen in Advanced Prostate Cancer. *Clinical Cancer Research*, 6: 1632-1638.

Efstathiou S & Minson A.C 1995. Herpes virus-based vectors. *British Medical Bulletin*, 51(1): 45-55.

Elo J.P & Visakorpi T 2001. Molecular genetics of prostate cancer. *Annals of Medicine*, 33(2): 130-141.

Embleton M.L, Williams S.A, Watson M.A, & Halford S.E 1999. Specificity from the Synapsis of DNA Elements by the *Sfi* I Endonuclease. *Journal of Molecular Biology*, 289: 785-797.

Embleton M.L, Vologodskii A.V, & Halford S.E 2004. Dynamics of DNA Loop Capture by the *Sfi* I Restriction Endonuclease on Supercoiled and Relaxed DNA. *Journal of Molecular Biology*, 339: 53-66.

Engel P.C 1981. *Enzyme Kinetics: the steady-state approach*. Chapman Hall.

Erbs P, Regulier E, Kintz J, Leroy P, Poitevin Y, Exinger F, Jund R, & Mehtali M 2000. In Vivo Cancer Gene Therapy by Adenovirus-mediated Transfer of a Bifunctional Yeast Cytosine Deaminase/Uracil Phosphoribosyltransferase Fusion Gene. *Cancer Research*, 60: 3813-3822.

Fallaux F.J, Bout A, Van der Velde I, Van den Wollenberg D.J.M, Hehir K.M, Keegan J, Auger C, Cramer S.J, Ormondt H.V, Van der Eb A.J, Valerio D, & Hoeben R.C 1998. New Helper Cells and Matched Early Region 1-Deleted Adenovirus Vectors Prevent Generation of Replication-Competent Adenoviruses. *Human Gene Therapy*, 9: 1909-1917.

Ferrari S, Pettenazzo A, Garbati N, Zacchello F, Behr J, & Scarpa M 1999. Polyethylenimine shows properties of interest for cystic fibrosis gene therapy. *Biochemica Et Biophysica Acta (BBA) - Gene Structure and Expression*, 1447(2-3): 219-225.

Field A.K, Davies M.E, DeWitt C, Perry H.C, Liou R, Germershausen J, Karkas J.D, Ashton W.T, Johnston D.B.R, & Tolman R.L 1983. 9-{[2-Hydroxy-1-(hydroxymethyl)ethoxy]methyl}guanine: A selective inhibitor of herpes group virus replication. *Proceedings of the National Academy of Sciences of the United States of America*, 80: 4139-4143.

Firth M.E & Wickner S.H 1983. *Lambda DNA Replication*. *Lambda II*: 145-173. Cold Spring Harbor.

Fischer A, Hacein-Bey S, & Cavazzana-Calvo M 2002. Gene therapy of severe combined immunodeficiencies. *Nature Reviews Immunology*, 2: 615-621.

Fisher K.D, Green N.K, Hale A, Subr V, Ulbrich K, & Seymour L.W 2007. Passive tumour targeting of polymer-coated adenovirus for cancer gene therapy. *Journal of Drug Targeting*, 15(7-8): 546-551.

Fisher K.D & Seymour L.W 2010. HPMA copolymers for masking and retargeting of theraeutic viruses. *Advanced Drug Delivery Reviews*, 62: 240-245.

Flotte T, Carter B, Conrad C, Guggino W, Reynolds T, Rosenstein B, Taylor G, Walden S, & Wetzel R 1996. Clinical Protocol - A phase I Study of an Adeno-Associated Virus-CFTR Gene Vector in Adult CF Patients with Mild Lung Disease. *Human Gene Therapy*, 7: 1145-1159.

Fogh J, Wright W.C, & Loveless J.D 1977. Absence of HeLa cell contamination in 169 cell lines derived from human tumors. *Journal of National Cancer Institute*, 58(2): 209-214.

Friedlos F, Davies L, Scanlon I, Ogilvie L.M, Martin J, Stribbling S.M, Spooner R.A, Niculescu-Duvaz I, Marais R, & Springer C.J 2002. Three New Prodrugs for Suicide Gene Therapy Using Carboxypeptidase G2 Elicit Bystander Efficacy in Two Xenograft Models. *Cancer Research*, 62: 1724-1729.

Friedlos F, Lehouritis P, Ogilvie L, Hedley D, Davies L, Bermudes D, King I, Martin J, Marais R, & Springer C.J 2008. Attenuated *Salmonella* Targets Prodrug Activating Enzyme Carboxypeptidase G2 to Mouse Melanoma and Human Breast and Colon Carcinomas for Effective Suicide Gene Therapy. *Clinical Cancer Research*, 14(13): 4259-4266.

Freytag S.O, Rogulski K.R, Paielli D.L, Gilbert J.D, & Kim J.H 1998. A Novel Three-Pronged Approach to Kill Cancer Cells Selectively: Concomitant Viral, Double Suicide Gene, and Radiotherapy. *Human Gene Therapy*, 9: 1323-1333.

Freytag S.O, Paielli D.L, Wing M, Rogulski K, Brown S, Kolozsvary A, Seely J, Barton K, Dragovic A, & Kim J.H 2002a. Efficacy and Toxicity of Replication-Competent Adenovirus-Mediated Double Suicide Gene Therapy in Combination with Radiation Therapy in an Orthotopic Mouse Prostate Cancer Model. *International Journal of Radiation Oncology, Biology, Physics*, 54(3): 873-885.

Freytag S.O, Khil M, Stricker H, Peabody J, Menon M, DePeralta-Venturina M, Nafziger D, Pegg J, Paielli D, Brown S, Barton K, Lu M, Aguilar-Cordova E, & Kim J.H 2002b. Phase I Study of Replication-competent Adenovirus-mediated Double Suicide Gene Therapy for the Treatment of Locally Recurrent Prostate Cancer. *Cancer Research*, 62: 4968-4976.

Freytag S.O, Stricker H, Pegg J, Paielli D, Pradhan D.G, Peabody J, DePeralta-Venturina M, Xia X, Brown S, Lu M, and Kim J.H 2003. Phase I Study of Replication-Competent Adenovirus-Mediated Double-Suicide Gene Therapy in Combination with Conventional-Dose Three-Dimensional Conformal Radiation Therapy for the Treatment of Newly Diagnosed, Intermediate- to High-Risk Prostate Cancer. *Cancer Research*, 63: 7497-7506.

Freytag S.O, Stricker H, Peabody J, Pegg J, Paielli D, Movsas B, Barton K.N, Brown S.L, Lu M, & Kim J.H 2007. Five-year Follow-up of Trial of Replication-competent Adenovirus-mediated Suicide Gene Therapy for Treatment of Prostate Cancer. *Molecular Therapy*, 15(3): 636-642.

Friedman D.I & Gottesman M 1983. *Lytic Mode of Lambda Development*. *Lambda II*: 21-51. Cold Spring Harbor.

Garber K 2006. China Approves World's First Oncolytic Virus Therapy For Cancer Treatment. *Journal of the National Cancer Institute*, 98(5): 298-300.

Garofalo O, Cox D.W, & Bachelard H.S 1988. Brain levels of NADH and NAD^+ under hypoxic and hypoglycaemic conditions in vitro. *Journal of Neurochemistry*, 51(1): 172-176.

Gaspar B.H, Parsley K.L, Howe S, King D, Gilmour K.C, Sinclair J, Brouns G, Schmidt M, Von Kalle C, Barington T, Jakobsen M.A, Christensen H.O, Al Ghonaium A, White H.N, Smith J.L, Levinsky R.J, Ali R.R, Kinnon C, & Thrasher A.J 2004. Gene therapy of X-linked severe combined immunodeficiency by use of a pseudotyped gammaretroviral vector. *Lancet*, 364: 2181-2187.

Ge K, Xu L, Zheng Z, Xu D, Sun L, & Liu X 1997. Transduction of cytosine deaminase gene makes rat glioma cells highly sensitive to 5-fluorocytosine. *International Journal of Cancer*, 71: 675-679.

Georgopoulos C, Tilly K, & Casjens S 1983. *Lamboid Phage Head Assembly*. *Lambda II*: 279-303. Cold Spring Harbor.

Ginsberg H.S, Pereira H.G, Valentine R.C, & Wilcox W.C 1966. A proposed terminology for the adenovirus antigens and virion morphological subunits. *Virology*, 28(4): 782-783.

Glick B.R & Pasternak J.J 1998. *Molecular Biotechnology: Principles and Applications of Recombinant DNA*. ASM Press.

Goktas S, Ziada A, & Crawford E.D 1999. Combined androgen blockade for advanced prostatic carcinoma. *Prostate Cancer and Prostatic Diseases*, 2: 172-179.

Goncalves M.A.F.V 2005. Adeno-associated virus: from defective virus to effective vector. *Proceedings of the National Academy of Sciences of the United States of America*, 2(43).

Grabenstein J.D, Pittman P.R, Greenwood J.T, & Engler J.M 2006. Immunization to Protect the US Armed Forces: Heritage, Current Practice, and Prospects. *Epidemiology Review*, 28: 3-26.

Graham F.L, Smiley J, Russell W.C, & Nairn R 1977. Characteritics of a human cell line transformed by DNA from human adenovius type 5. *Journal of General Virology*, 36(1): 59-74.

Green N.K, Youngs D.J, Neoptolemos J.P, Friedlos F, Knox R.J, Springer C.J, Anlezark G.M, Michael P, Melton R.G, Ford M.J, Young L.S, Kerr D.J, & Searle P.F 1997. Sensitization of colorectal and pancreatic cancer cell lines to the prodrug 5-(aziridin-1-yl)-2,4-dinitrobenzamide (CB1954) by retroviral transduction and expression of the *E. coli* nitroreductase gene. *Cancer Gene Therapy*, 4(4): 229-238.

Green N.K, Herbert C.W, Hale S.J, Hale A.B, Mautner V, Harkins R, Hermiston T, Ulbrich K, Fisher K.D, & Seymour L.W 2004. Extended plasma circulation time and decreased toxicity of polymer-coated adenovirus. *Gene Therapy*, 11: 1256-1263.

Griffiths A.J, Miller J.H, Suzuki D.T, Lewontin R.C, & Gelbart W.M 2002. *An Introduction to Genetic Analysis*. W.H Freeman and Company.

Grove J.I, Lovering A.L, Guise C, Race P.R, Wrighton C.J, White S.A, Hyde E.I, & Searle P.F 2003. Generation of *Escherichia Coli* Nitroreductase Mutants Conferring Improved Cell Sensitization to the Prodrug CB1954. *Cancer Research*, 63: 5532-5537.

Guise C.P, Grove J.I, Hyde E.I, & Searle P.F 2007. Direct positive selection for improved nitroreductase variants using SOS triggering of bacteriophage lambda lytic cycle. *Gene Therapy*, 14: 690-698.

Gulley J, Chen A.P, Dahut W, Arlen P.M, Bastian A, Steinberg S.M, Tsang K, Panicali D, Poole D, Schlom J, & Hamilton M 2002. Phase I study of a vaccine using recombinant vaccinia virus expressing PSA (rv-PSA) in patients with metastatic androgen-independent prostate cancer. *The Prostate*, 53(2): 109-117.

Guo J & Xin H 2006. Slicing Out The West? *Science*, 314: 1232-1235.

Hacein-Bey-Abina S, Le Deist F, Carlier F, Bouneaud C, Hue C, De Villartay J, Thrasher A.J, Wulffraat N, Sorensen R, Dupuis-Girod S, Fischer A, & Cavazzana-Calvo M 2002. Sustained Correction of X-linked Severe Combined Immunodeficiency by Ex Vivo Gene Therapy. *The New England Journal of Medicine*, 346(16): 1185-1195.

Hacein-Bey-Abina S, Von Kalle C, Schmidt M, Le Deist F, Wulffraat N, McIntyre E, Radford I, Villeval J, Fraser C.C, Cavazzanna-Calvo M, & Fischer A 2003a. A Serious Adverse Event after Successful Gene Therapy for X-Linked Severe Combined Immunodeficiency. *The New England Journal of Medicine*, 348(3): 255-256.

Hacein-Bey-Abina S, Von Kalle C, Schmidt M, McCormack M.P, Wulffraat N, Leboulch P, Lim A, Osborne C.S, Pawliuk R, Morillon E, Sorensen R, Forster A, Fraser P, Cohen J.I, de Saint Basile G, Alexander I, Wintergerst U, Frebourg T, Aurias A, Stoppa-Lyonnet D, Romana S, Radford-Weiss I, Gross F, Valensi F, Delabesse E, Macintyre E, Sigaux F, Soulier J, Leiva L.E, Wissler M, Prinz C, Rabbitts T.H, Le Deist F, Fischer A, & Cavazzana-Calvo M 2003b. LMO2-Associated Clonal T Cell Proliferation in Two Patients after Gene Therapy for SCID-X1. *Science*, 302: 415-419.

Hanahan D 1983. Studies on transformation of *Escherichia coli* with plasmids. *Journal of Molecular Biology*, 166(4): 557-580.

Hardy S, Kitamura M, Harris-Stansil T, Dai Y, & Phipps L 1997. Construction of Adenovirus Vectors through Cre-*lox* Recombination. *Journal of Virology*, 71(3): 1842-1849.

Hartl D.L & Jones E.W 1999. *Genetics: Analysis of Genes and Genomes*. Jones and Bartlett Publishers.

Hasenburg A, Tong X, Rojas-Martinez A, Nyberg-Hoffman C, Kieback C.C, Kaplan A, Kaufman R.H, Ramzy I, Aguilar-Cordova E, & Kieback D.G 2000. Thymidine kinase gene therapy with concomitant topotecan chemotherapy for recurrent ovarian cancer. *Cancer Gene Therapy*, 7: 839-852.

Haynes C.A, Koder R.L, Miller A, & Rodgers D.W 2002. Structures of Nitroreductase in Three States. *The Journal of Biological Chemistry*, 277(13): 11513-11520.

Hedley D, Ogilvie L, & Springer C 2007. Carboxypeptidase G2-based gene-directed enzyme-prodrug therapy: a new weapon in the GDEPT armoury. *Nature Reviews*, 7: 870-879.

Heise C, Sampson-Johannes A, Williams A, McCormick F, Von Hoff D.D, & Kim D.H 1997. ONYX-015, an E1B gene-attenuated adenovirus, causes tumor-specific cytolysis and antitumoral efficacy that can be augmented by standard chemotherapeutic agents. *Nature Medicine*, 6: 639-645.

Heise CC, Williams A, Olesch J, & Kirn D.H 1999. Efficacy of a replication-competent adenovirus (ONYX-015) following intratumoral injection: Intratumoral spread and distribution effects. *Cancer Gene Therapy*, 6(6): 499-504.

Herman J.R, Adler H.L, Aguilar-Cordova E, Rojas-Martinez A, Woo S, Timme T.L, Wheeler T.M, Thompson T.C, & Scardino P.T 1999. In situ gene therapy for adenocarcinoma of the prostate: a phase I clinical trial. *Human Gene Therapy*, 10(7): 1239-1249.

Hershey A.D & Dove W 1971. *Introduction to Lambda. The Bacteriophage Lambda*: 3-11. Cold Spring Harbor.

Hinata N, Shirakawa T, Terao S, Goda K, Tanaka K, Yamada Y, Hara I, Kamidono S, Fujisawa M, & Gotoh A 2006. Progress report on phase I/II clinical trial of Ad-OC-TK plus VAL therapy for metastatic or locally recurrent prostate cancer: Initial experience at Kobe University. *International Journal of Urology*, 13: 834-837.

Hohn O, Krause H, Babarotto P, Niederstadt L, Beimforde N, Denner J, Miller K, Kurth R, & Bannert N 2009. Lack of evidence for xenotropic murine leukemia virus-related virus (XMRV) in German prostate cancer patients. *Retrovirology*, 6(92): 1-11.

Hortobagyi G.N, Ueno N.T, Xia W, Zhang S, Wolf J.K, Putnam J.B, Weiden P.L, Willey J.S, Carey M, Branham D.L Payne J.Y, Tucker S.D, Bartholomeusz C, Kilbourn R.G, De Jager R.L, Sneige N, Katz R.L, Anklesaria P, Ibrahim N.K, Murray J.L, Theriault R.L, Valero V, Gershenson D.M, Bevers M.W, Huang L, Lopez-Berestein G, & Hung M 2001. Cationic Liposome-Mediated E1A Gene Transfer to Human Breast and Ovarian Cancer Cells and Its Biologic Effects: A Phase I Clinical Trial. *Journal of Clinical Oncology*, 19: 3422-3433.

Horwitz M.S, Edited by Fields B.N, Knipe D.M, Howley P.M, Chanock R.M, Melnick J.L, Monath T.P, Roizman B, & Straus S.E 1996. *Adenoviruses. Fields Virology*: 2149-2169. Lippincott - Raven.

Hu L, Yu C, Jiang Y, Han J, Li Z, Browne P, Race P.R, Knox R.J, Searle P.F, & Hyde E.I 2003. Nitroaryl Phosphoramides as Novel Prodrugs for *E. coli* Nitroreductase Activation in Enzyme Prodrug Therapy. *Journal of Medicinal Chemistry*, 46(23): 4818-4821.

Huber B.E, Austin E.A, Good S.S, Knick V.C, Tibbels S, & Richards C.A 1993. *In Vivo* Antitumor Activity of 5-Fluorocytosine on Human Colorectal Carcinoma Cells Genetically Modified to Express Cytosine Deaminase. *Cancer Research*, 53: 4619-4626.

Hughes B.W, Wells A.H, Bebok Z, Gadi V.K, Garver R.I Jr, Parker W.B, & Sorscher E.J 1995. Bystander Killing of Melanoma Cells Using the Human Tyrosinase Promoter to Express the Escherichia coli Purine Nucleoside Phosphorylase Gene. *Cancer Research*, 55: 3339-3345.

Hurley J.B, Simon M.I, Teplow D.B, Robishaw J.D, & Gilman A.G 1984. Homologies Between Signal Transducing G Proteins and *ras* Gene Products. *Science*, 226(4676): 860-862.

Hwang T.L & Shaka A.J 1995. Water Suppression That Works. Excitation Sculpting Using Arbitary Wave-Forms and Pulsed-Field Gradients. *Journal of Magnetic Resonance, Series A*, 112(2): 275-279.

Hyde S.C, Southern K.W, Gileadi U, Fitzjohn E.M, Mofford K.A, Waddell B.E, Gooi H.C, Goddard C.A, Hannavy K, Smyth S.E, Egan J.J, Sorgi F.L, Huang L, Cuthbert A.W, Evans M.J, Colledge W.H, Higgins C.F, Webb A.K, & Gill D.R 2000. Repeat administration of DNA/liposomes to the nasal epithelium of patients with cystic fibrosis. *Gene Therapy*, 7: 1156-1165.

Immonen A, Vapalahti M, Tyynela K, Hurskainen H, Sandmair A, Vanninen R, Langford G, Murray N, & Yla-Herttuala S 2004. AdHSV-TK Gene Therapy with Intravenous Ganciclovir Improves Survival in Human Malignant Glioma: A Randomised, Controlled Study. *Molecular Therapy*, 10(5): 967-972.

Iorns E, Lord C.J, & Ashworth A 2009. Parallel RNAi and compound screens identify the PDK1 pathway as a target for tamoxifen sensitization. *Biochemical Journal*, 417: 361-370.

Irving J, Wang Z, Powell S, O'Sullivan C, Mok M, Murphy B, Cardoza L, Lebkowski J.S, & Majumdar A.S 2004. Conditionally replicative adenovirus driven by the human telomerase promoter provides broad-spectrum antitumor activity without liver toxicity. *Cancer Gene Therapy*, 11: 174-185.

Ishii-Morita H, Agbaria R, Mullen C.A, Hirano H, Koeplin D.A, Ram Z, Oldfield E.H, Johns D.G, & Blaese R.M 1997. Mechanism of 'bystander effect' killing in the herpes simplex thymidine kinase gene therapy model of cancer treatment. *Gene Therapy*, 4: 244-251.

Jaberipour M 2005. PhD Thesis *Cancer Studies*. University of Birmingham.

Jaberipour M, Vass S.O, Guise C.P, Grove J.I, Knox R.J, Hu L, Hyde E.I, & Searle P.F 2010. Testing double mutants of the enzyme nitroreductase for enhanced cell sensitisation to prodrugs: effects of combining beneficial single mutations. *Biochemical Pharmacology*, 79(2): 102-111.

Jameson M.B, Rischin D, Pegram M, Gutheil J, Patterson A.V, Denny W.A, & Wilson W.R 2010. A phase I trial of PR-104, a nitrogen mustard prodrug activated by both hypoxia and aldo-keto reductase 1C3, in patients with solid tumors. *Cancer Chemotherapy and Pharmacology*, 65(4): 791-801.

Janion C 2001. Some aspects of the SOS response system - A critical survey. *Acta Biochimica Polonica*, 48(3): 599-610.

Jarrom D 2008. PhD Thesis *Biosciences.* University of Birmingham.

Jarrom D, Jaberipour M, Guise C.P, Daff S, White S.A, Searle P.F, & Hyde E.I 2009. Steady-state and stopped-flow kinetic studies of three E. coli NfsB mutants with enhanced activity for the prodrug CB1954. *Biochemistry*, 48(32): 7665-7672.

Jenks P.J & Edwards D.I 2002. Metronidazole resistance in *Helicobacter pylori*. *International Journal of Antimicrobial Agents*, 19: 1-7.

Johansson E, Parkinson G.N, Denny W.A, & Neidle S 2003. Studies on the Nitroreductase Prodrug-Activating System. Crystal Structures of Complexes with the Inhibitor Dicoumoral and Dinitrobenzamide Prodrugs and of the Enzyme Active Form. *Journal of Medicinal Chemistry*, 46(19): 4009-4020.

Johnson L.G, Olsen J.C, Sarkadi B, Moore K.L, Swanstrom R, & Boucher R.C 1992. Efficiency of gene transfer for restoration of normal airway epithelial function in cystic fibrosis. *Nature Genetics*, 2: 21-25.

Johnson L.G 1995. Gene Therapy for Cystic Fibrosis. *Chest*, 107: 77S-83S.

Johnson L, Shen A, Boyle L, Kunich J, Pandey K, Lemmon M, Hermiston T, Giedlin M, McCormick F, & Fattaey A 2002. Selectively replicating adenoviruses targeting deregulated E2F activity are potent, systemic antitumor agents. *Cancer Cell*, 1: 325-337.

Katsura I 1983. *Tail Assembly and Injection. Lambda II*: 331-345. Cold Spring Harbor.

Kaufman H.L, Wang W, Manola J, DiPaola R.S, Ko Y, Sweeney C, Whiteside T.L, Schlom J, Wilding G, & Weiner L.M 2004. Phase II Randomized Study of Vaccine Treatment of Advanced Prostate Cancer (E7897): A Trial of the Eastern Cooperative Oncology Group. *Journal of Clinical Oncology*, 22(11): 2122-2132.

Keilholz U, Conradt C, Legha S.S, Khayat D, Scheibenbogen C, Thatcher N, Hoo Goey S, Gore M, Darval T, Hancock B, Punt C.J.A, Drummer R, Avril M, Bröcker E.B, Benhammouda A, Eggermont A.M.M, & Pritsch M 1998. Results of Interleukin-2-Based Treatment in Advanced Melanoma: A Case Record-Based Analysis of 631 Patients. *Journal of Clinical Oncology*, 16: 2921-2929.

Kershaw M.H, Westwood J.A, Parker L.L, Wang G, Eshhar Z, Mavroukakis S.A, White D.E, Wunderlich J.R, Canevari S, Rogers-Freezer L, Chen C.C, Yang J.C, Rosenberg S.A, & Hwu P 2006. A phase I Study on Adoptive Immunotherapy Using Gene-Modified T Cells for Ovarian Cancer. *Clinical Cancer Research*, 12(20): 6106-6115.

Khuri F.R, Nemunaitis J, Ganly I, Arseneau J, Tannock I.F, Romel L, Gore M, Ironside J, MacDougall R.H, Heise C, Randlev B, Gillenwater A.M, Bruso P, Kaye S.B, Hong W.K, & Kirn D.H 2000. A controlled trial of intratumoral ONYX-015, a selectively-replicating adenovirus, in combination with cisplatin and 5-fluorouracil in patients with recurrent head and neck cancer. *Nature Medicine*, 6(8): 879-885.

Kievit E, Bershad E, Ng E, Sethna P, Dev I, Lawrence T.S, & Rehemtulla A 1999. Superiority of Yeast over Bacterial Cytosine Deaminase for Enzyme/Prodrug Gene Therapy in Colon Cancer Xenografts. *Cancer Research*, 59: 1417-1421.

Kievit E, Nyati M.K, Ng E, Stegman L.D, Parsels J, Ross B.D, Rehemtulla A, & Lawrence T.S 2000. Yeast Cytosine Deaminase Improves Radiosensitization and Bystander Effect by 5-Fluorocytosine of Human Colorectal Cancer Xenografts. *Cancer Research*, 60: 6649-6655.

Kim J, Zeller K.I, Wang Y, Jegga A.G, Aronow B.J, O'Donnell K.A, & Dang C.V 2004. Evaluation of Myc E-box Phylogenetic Footprints in Glycolytic Genes by Chromatin Immunoprecipitation Assays. *Molecular and Cellular Biology*, 24(13): 5923-5936.

Knox R.J, Boland M.P, Friedlos F, Coles B, Southan C, & Roberts J.J 1988. The Nitroreductase enzyme in Walker cells that activates 5-(aziridin-1-yl)-2,4-dinitrobenzamide (CB1954) to 5-(aziridi-1-yl)-4-hydroxlamine-2-nitrobenzamide is a form of NAD(P)H dehydrogenase (quinone). *Biochemical Pharmacology*, 37(24): 4671-4677.

Knox R.J, Friedlos F, Jarman M, & Roberts J.J 1988. A New Cytotoxic, DNA Interstrand Crosslinking Agent, 5-(Aziridin-1-yl)-4-hydroxlamine-2-Nitrobenzamide, is Formed from 5-(Aziridin-1-yl)-2,4-Dintrobenzamide (CB1954) by a Nitroreductase Enzyme in Walker Carcinoma Cells. *Biochemical Pharmacology*, 37(24): 4661-4669.

Knox R.J, Friedlos F, Sherwood R.F, Melton R.G, & Anlezark G.M 1992. The bioactivation of 5-(aziridin-1-yl)-2,4-dinitrobenzamide (CB1954)--II. A comparison of an Escherichia coli nitroreductase and Walker DT diaphorase. *Biochemical Pharmacology*, 44(12): 2297-2301.

Kobori T, Sasaki H, Lee W.C, Zenno S, Saigo K, Murphy M.E.P, & Tanokura M 2001. Structure and Site-directed Mutagenesis of a Flavoprotein from *Escherichia coli* That Reduces Nitrocompounds. *The Journal of Biological Chemistry*, 276(4): 2816-2823.

Kon O.L, Sivakumar S, Teoh Khay L, Lok S.H.L, & Long Yun C 1999. Naked Plasmid-Mediated Gene Transfer to Skeletal Muscle Ameliorates Diabetes Mellitus. *The Journal of Gene Medicine*, 1: 186-194.

Koyama F, Sawada H, Hirao T, Fujii H, Hamada H, & Nakano H 2000. Combined suicide gene therapy for human colon cancer cells using adenovirus-mediated transfer of *Escherichia coli* cytosine deaminase gene and *Escherichia coli* uracil phosphoribosyltransferase gene with 5-fluorocytosine. *Cancer Gene Therapy*, 7: 1015-1022.

Kozak M 1987. At least six nucleotides preceding AUG initiator codon enhance translation in mammalian cells. *Journal of Molecular Biology*, 196(4): 947-950.

Krisky D.M, Wolfe D, Goins W.F, Marconi P.C, Ramakrishnan R, Mata M, Rouse R.J.D, Fink D.J, & Glorioso J.C 1998. Deletion of multiple immediate-early genes from herpes simplex virus reduces cytotoxicity and permits long-term gene expression in neurons. *Gene Therapy*, 5: 1593-1603.

Kubo H, Gardner T.A, Wada Y, Koeneman K.S, Gotoh A, Yang L, Kao C, Lin S.D, Amin M.B, Yang H, Black M.E, Matsubara S, Nakagawa M, Gillenwater J.Y, Zhau H.E, & Chung L.W 2003. Phase I dose escalation clinical trial of adenovirus vector carrying osteocalcin promoter-driven herpes simplex virus thymidine kinase in localized and metastatic hormone-refactory prostate cancer. *Human Gene Therapy*, 14(3): 227-241.

Laemmli U.K 1970. Cleavage of structural proteins during the assembly of the head of bacteriophage T4. *Nature*, 227: 680-685.

Lanson N.A Jr, Friedlander P.L, Schwarzenberger P, Kolls J.K, & Wang G 2003. Replication of an Adenoviral Vector Controlled by the Human Telomerase Reverse Transcriptase Promoter Causes Tumor-Selective Tumor Lysis. *Cancer Research*, 63: 7936-7941.

Lewin B 2000. *Genes VII*. Oxford University Press.

Li C, Bowles D.E, Van Dyke T, & Samulski R.J 2005. Adeno-associated virus vectors: potential applications for cancer gene therapy. *Cancer Gene Therapy*, 12: 913-925.

Liu M, Acres B, Balloul J, Bizouarne N, Paul S, Slos P, & Squiban P 2004. Gene-based vaccines and immunotherapeutics. *Proceedings of the National Academy of Sciences of the United States of America*, 101(2): 14567-14571.

Liu Y, Huang R, Han L, Ke W, Shao K, Ye L, & Lou J Jiang C 2009. Brain-targeting gene delivery and cellular internalization mechanisms for modified rabies virus glycoprotein RVG29 nanoparticles. *Biomaterials*, 30(25): 4195-4202.

Lovering A.L, Hyde E.I, Searle P.F, & and White S.A 2001. The Structure of *Escherichia coli* Nitroreductase Complexed with Nicotinic Acid: Three Crystal Forms at 1.7Å, 1.8Å and 2.4 Å Resolution. *Journal of Molecular Biology*, 309: 203-213.

Lyons M, Onion D, Green N.K, Aslan K, Rajaratnam R, Bazan-Peregrino M, Phipps S, Hale S, Mautner V, Seymour L.W, & Fisher K.D 2006. Adenovirus Type 5 Interactions with Human Blood Cells May Compromise Systemic Delivery. *Molecular Therapy*, 14(1): 118-128.

Mabjeesh N.J, Zhong H, & Simons J.W 2002. Gene therapy of prostate cancer: current and future directions. *Endocrine-Related Cancer*, 9(2): 115-139.

Mahan S.D, Ireton G.C, Knoeber C, Stoddard B.L, & Black M.E 2004a. Random mutagenesis and selection of *Escherichia coli* cytosine deaminase for cancer gene therapy. *Protein Engineering, Design and Selection*, 17(8): 625-633.

Mahan S.D, Ireton G.C, Stoddard B.L, & Black M.E 2004b. Alanine-Scanning Mutagenesis Reveals a Cytosine Deaminase Mutant with Altered Substrate Preference. *Biochemistry*, 43: 8957-8964.

Maloy S, Stewart V, & Taylor R 1996. *Genetic analysis of pathogenic bacteria*. Cold Spring Harbor.

Marais R, Spooner R.A, Light Y, Martin J, & Springer C.J 1996. Gene-directed Enzyme Prodrug Therapy with a Mustard Prodrug/Carboxypeptidase G2 Combination. *Cancer Research*, 56: 4735-4742.

Mastrangelo M.J, Maguire H.C Jr, Eisenlohr L.C, Laughlin C.E, Monken C.E, McCue P.A, Kovatich A.J, & Lattime E.C 1998. Intratumoral recombinant GM-CSF-encoding virus as gene therapy in patients with cutaneous melanoma. *Cancer Gene Therapy*, 6(5): 409-422.

Mastrangelo M.J, Eisenlohr L.C, Gomella L, & Lattime E.C 2000. Poxvirus vectors: orphaned and underappreciated. *The Journal of Clinical Investigation*, 105(8): 1031-1034.

Matic I, Taddei F, & Radman M 2000. No Genetic Barriers between *Salmonella enterica* Serovar Typhimurium and *Escherichia coli* in SOS-Induced Mismatch Repair-Deficient Cells. *Journal of Bacteriology*, 182(20): 5922-5924.

Mayer A, Francis R.J, Sharma S.K, Tolner B, Springer C.J, Martin J, Boxer G.M, Bell J, Green A.J, Hartley J.A, Cruickshank C, Wren J, Chester K.A, & Begent R.H.J 2006. A Phase I Study of Single Administration of Antibody-Directed Enzyme Prodrug Therapy with the Recombinant Anti-Carcinoembryonic Antigen Antibody-Enzyme Fusion Protein MFECP1 and a Bis-Iodo Phenol Mustard Prodrug. *Clinical Cancer Research*, 12(21): 6509-6516.

McCall P, Witton C.J, Grimsley S, Nielsen K.V, & Edwards J 2008. Is PTEN loss associated with clinical outcome measures in human prostate cancer? *British Journal of Cancer*, 99: 1296-1301.

McCalla D.R, Reuvers A, & Kaiser C 1970. Mode of Action of Nitrofurazone. *Journal of Bacteriology*, 104(3): 1126-1134.

McCalla D.R, Olive P, Tu Y, & Fan M.L 1975. Nitrofurazone-reducing enzymes in *E. Coli* and their role in drug activation in vivo. *Canadian Journal of Microbiology*, 21(10): 1484-1491.

McNeish I.A, Searle P.F, Young L.S, & Kerr D.J 1997. Gene directed enzyme prodrug therapy for cancer. *Advanced Drug Delivery Reviews*, 26: 173-184.

McNeish I.A, Green N.K, Gilligan M.G, Ford M.J, Mautner V, Young L.S, Kerr D.J, & Searle P.F 1998. Virus directed enzyme prodrug therapy for ovarian and pancreatic cancer using retrovirally delivered *E. coli* nitroreductase and CB1954. *Gene Therapy*, 5: 1061-1069.

Meany H.J, Seibel N.L, Sun J, Finklestein J.Z, Sato J, Kelleher J, Sondel P, & Reaman G 2008. Phase 2 trial of recombinant tumor necrosis factor-alpha in combination with dactinomycin in children with recurrent Wilms tumor. *Journal of Immunotherapy*, 31(7): 679-683.

Merlin J, N'Doye A, Bouriez T, & Dolivet G 2002. Polyethylenimine Derivatives as Potent Nonviral Vectors for Gene Transfer. *Drug News and Perspectives*, 15(7): 445-451.

Mesnil M & Yamasaki H 2000. Bystander Effect in Herpes Simplex Virus-Thymidine Kinase/Ganciclovir Cancer Gene Therapy: Role of Gap-junctional Intercellular Communication. *Cancer Research*, 60: 3989-3999.

Michael N.P, Brehm J.K, Anlezark G.M, & Minton N.P 1994. Physical characterisation of the *Escherichia coli* B gene encoding nitroreductase and its over-expression in *Escherichia coli* K12. *FEMS Microbiology Letters*, 124: 195-202.

Michel B 2005. After 30 Years of Study, the Bacterial SOS Response Still Suprises Us. *PLoS Biology*, 3(7): 1174-1176.

Miles B.J, Shalev M, Aguilar-Cordova E, Timme T.L, Lee H.M, Yang G, Adler H.L, Kernen K, Pramudji C.K, Satoh T, Gdor Y, Ren C, Ayala G, Wheeler T.M, Butler E.B, Kadmon D, & Thompson T.C 2001. Prostate-specific antigen response and systemic T cell activation after in situ gene therapy in prostate cancer patients failing radiotherapy. *Human Gene Therapy*, 12(16): 1955-1967.

Moolten F.L 1986. Tumor Chemosensitivity Conferred by Inserted Herpes Thymidine Kinase Genes: Paradigm for a Prospective Cancer Control Strategy. *Cancer Research*, 46: 5276-5281.

Moroziewicz D & Kaufman H.L 2005. Gene therapy with poxvirus vectors. *Current Opinion Molecular Therapy*, 4: 317-325.

Munir K.M, French D.C, Dube D.K, & Loeb L.A 1994. Herpes thymindine kinase mutants with altered catalytic efficiencies obtained by random sequence selection. *Protein Engineering*, 7(1): 83-89.

Murakami P & McCarnan M.T 1999. Quantitation of Adenovirus DNA and Virus Particles with the PicoGreen Fluorescent Dye. *Analytical Biochemistry*, 274: 283-288.

Murray N.E & Gann A 2007. What has phage lambda ever done for us? *Current Biology - Magazine*, 17(9): R305-R312.

Nasu Y, Saika T, Ebara S, Kusaka N, Kaku H, Abarzua F, Manabe D, Thompson T.C, & Kumon H 2007. Suicide gene therapy with adenoviral delivery of HSV-TK gene for patients with local recurrence of prostate cancer after hormonal therapy. *Molecular Therapy*, 15(4): 834-840.

Nobbs T.J, Szczelkun M.D, Wentzell L.M, & Halford S.E 1998. DNA Excision by the *Sfi* I Restriction Endonuclease. *Journal of Molecular Biology*, 281: 419-432.

Noguchi M, Yi H, Rosenblatt H.M, Filipovich A.H, Adelstein S, Modi W.S, McBride W.O, & Leonard W.J 1993. Interleukin-2 receptor γ chain mutation results in X-linked severe combined immunodeficiency in humans. *Cell*, 73(1): 147-157.

O'Shea C.C, Johnson L, Bagus B, Choi S, Nicholas C, Shen A, Boyle L, Pandey K, Soria C, Kunich J, Shen Y, Habets G, Ginzinger D, & McCormick F 2004. Late Viral RNA export, rather than p53 inactivation, determines ONYX-015 tumor selectivity. *Cancer Cell*, 6: 611-623.

Oppenheim A.B, Kobiler O, Stavans J, Court D.L, & Adhya S 2005. Switches in Bacteriophage Lambda Development. *Annual Review of Genetics*, 39: 409-429.

Palmer B.D, Wilson W.R, Cliffe S, & Denny W.A 1992. Hypoxia-selective antitumor agents. 5. Synthesis of water-soluble nitroaniline mustards with selective cytotoxicity for hypoxic mammalian cells. *Journal of Medicinal Chemistry*, 35(17): 3214-3222.

Palmer B.D, Wilson W.R, Atwell G.J, Schultz D, Xu X.Z, & Denny W.A 1994. Hypoxia-Selective Antitumor Agents. 9. Structure-Activity Relationships for Hypoxia-Selective Cytotoxicity among Analogues of 5-[N,N-Bis(2-chloroethyl)amino]-2,4-dinitrobenzamide. *Journal of Medicinal Chemistry*, 37: 2175-2184.

Palmer D.H, Mautner V, Mirza D, Oliff S, Gerritsen W, Van der Sijp J.R.M, Hubscher S, Reynolds G, Bonney S, Rajaratnam R, Hull D, Horne M, Ellis J, Mountain A, Hill S, Harris P.A, Searle P.F, Young L.S, James N.D, & Kerr D.J 2004. Virus-Directed Enzyme Prodrug Therapy: Intertumoral Administration of a Replication-Deficient Adenovirus Encoding Nitroreductase to Patients With Resectable Liver Cancer. *Journal of Clinical Oncology*, 22(9): 1546-1552.

Pan J, Zhang S, Chen C, Xiao S, Sun Y, Liu C, Su X, Li D, Xu G, Xu B, & Lu Y 2009. Effect of Recombinant Adenovirus-p53 Combined With Radiotherapy on Long-Term Prognosis of Advanced Nasophayngeal Carcinoma. *Journal of Clinical Oncology*, 27(5): 799-804.

Pandha H.S, Martin L, Rigg A, Hurst H.C, Stamp G.W.H, Sikora K, & Lemoine N.R 1999. Genetic Prodrug Activation Therapy for Breast Cancer: A Phase I Clinical Trial of *erb*B-2-Directed Suicide Gene Expression. *Journal of Clinical Oncology*, 17: 2180-2189.

Paoletti E 1996. Applications of pox virus vectors to vaccination: An update. *Proceedings of the National Academy of Sciences of the United States of America*, 93: 11349-11353.

Parkinson D.R, Abrams J.S, Wiernik P.H, Rayner A.A, Margolin K.A, Van Echo D.A, Sznol M, Dutcher J.P, Aronson F.R, Doroshow J.H, Atkins M.B, & Hawkins M.J 1990. Interleukin-2 Therapy in Patients With Metastatic Malignant Melanoma: A Phase II Study. *Journal of Clinical Oncology*, 8: 1650-1656.

Parkinson G.N, Skelly J.V, & Neidle S 2000. Crystal Structure of FMN-Dependent Nitroreductase from *Escherichia coli* B: A Prodrug-Activating Enzyme. *Journal of Medicinal Chemistry*, 43: 3624-3631.

Parks R.J, Chen L, Anton M, Sankar U, Rudnicki M.A, & Graham F.L 1996. A helper-dependent adenovirus vector system: Removal of helper virus by Cre-mediated excision of the viral packaging signal. *Proceedings of the National Academy of Sciences of the United States of America*, 93: 13565-13570.

Patel P, Young G, Mautner V, Ashdown D, Bonney S, Pineda R, Collins S.I, Searle P.F, Hull D, Peers E, Chester J, Wallace M.D, Doherty A, Leung H, Young L.S, & James N.D 2009. A phase I/II clinical trial in localised prostate cancer of an adenovirus expressing Nitroreductase with CB1954 [correction of CB1984]. *Molecular Therapy*, 17(7): 1292-1299.

Patterson A.V, Ferry D.M, Edmunds S.J, Gu Y, Singleton R.S, Patel K, Pullen S.M, Hicks K.O, Syddall S.P, Atwell G.J, Yang S, Denny W.A, & Wilson W.R 2007. Mechanism of Action and Preclinical Antitumor Activity of the Novel Hypoxia-Activated DNA Cross-Linking Agent PR-104. *Clinical Cancer Research*, 13(13): 3922-3932.

Pisters L.L, Pettaway C.A, Troncoso P, McDonnell T.J, Stephens L.C, Wood C.G, Do K, Brisbay S.M, Wang X, Hossan E.A, Evans R.B, Soto C, Jacobson M.G, Parker K, Merritt J.A, Steiner M.S, & Logothetis C.J 2004. Evidence That Transfer of Functional p53 Protein Results in Increased Apoptosis in Prostate Cancer. *Clinical Cancer Research*, 10: 2587-2593.

Pitard B, Oudrhiri N, Lambert O, Vivien E, Masson C, Wetzer B, Hauchecorne M, Scherman D, Rigaud J, Vigneron J, Lehn J, & Lehn P 2001. Sterically stabilized BGTC-based lipoplexes: structural features and gene transfection into the mouse airways *in vivo*. *The Journal of Gene Medicine*, 3: 478-487.

Pollak N, Niere M, & Ziegler M 2007. NAD Kinase Levels Control the NADPH Concentration in Human Cells. *The Journal of Biological Chemistry*, 282(46): 33562-33571.

Prosser G.A, Copp J.N, Syddall S.P, Williams E.M, Smaill J.B, Wilson W.R, Patterson A.V, & Ackerley D.F 2010. Discovery and evaluation of *Escherichia coli* nitroreductases that activate the anti-cancer prodrug CB1954. *Biochemical Pharmacology*, 79: 678-687.

Puck J.M, Deschenes S.M, Porter J.C, Dutra A.S, Brown C.J, Willard H.F, & Henthorn P.S 1993. The interleukin-2 receptor gamma chain maps to Xq13.1 and is mutated in X-linked severe combined immunodeficiency, SCIDX1. *Human Molecular Genetics*, 2(8): 1099-1104.

Purves W.K, Orians G.H, Heller H.C, & Sadava D 1999. *Life: The Science of Biology*. W.H Freeman and Company.

Putnam D, Gentry C.A, Pack D.W, & Langer R 2001. Polymer-based gene delivery with low cytotoxicity by a unique balance of side-chain termini. *Proceedings of the National Academy of Sciences of the United States of America*, 98(3): 1200-1205.

Qiu Z, Cang Y, & Goff S.P 2009. c-Abl tyrosine kinase regulates cardiac gowth and development. *Proceedings of the National Academy of Sciences of the United States of America*, 107(3): 1136-1141.

Race P.R 2003. PhD Thesis *Biosciences.* University of Birmingham.

Race P.R, Lovering A.L, Green R.M, Ossor A, White S.A, Searle P.F, Wrighton C.J, & Hyde E.I 2005. Structural and Mechanistic Studies of *Escherichia coli* Nitroreductase with the Antibiotic Nitrofurazone Reversed binding orientations in different redox states of the enzyme. *The Journal of Biological Chemistry*, 280(14): 13256-13264.

Race P.R, Lovering A.L, White S.A, Grove J.I, Searle P.F, Wrighton C.W, & Hyde E.I 2007. Kinetic and Structural Characterisation of *Escherichia coli* Nitroreductase Mutants Showing Improved Efficacy for the Prodrug Substrate CB1954. *Journal of Molecular Biology*, 368: 481-492.

Rainov N.G 2000. A phase III Clinical Evaluation of Herpes Simplex Virus Type I Thymidine Kinase and Ganciclovir Gene Therapy as an Adjuvant to Surgical Resection and Radiation in Adults with Previously Untreated Glioblastoma Multiforme. *Human Gene Therapy*, 11: 2389-2401.

Rakhmilevich A.L, Janssen K, Turner J, Culp J, & Yang N.S 1997. Cytokine Gene Therapy of Cancer Using Gene Gun Technology: Superior Antitumor Activity of Interleukin-12. *Human Gene Therapy*, 8: 1303-1311.

Rang H.P, Dale M.M, Ritter J.M, & Moore P.K 2003. *Pharmacology*. Churchill Livingstone.

Reddi H.V, Madde P, Reichert-Eberhardt A.J, Galanis E.C, Copland J.A, McIver B, Grebe S.K.G, & Eberhardt N.L 2008. ONYX-411, a conditionally replicative oncolytic adenovirus, induces cell death in anaplastic thyroid carcinoma cell lines and suppresses the growth of xenograft tumors in nude mice. *Cancer Gene Therapy*, 15: 750-757.

Rodenhuis S & Slebos R.J 1990. The ras oncogenes in human lung cancer. *The American Review of Respiratory Disease*, 142(6 pt 2): S27-S30.

Rodriguez R, Schuur E.R, Yeong Lim H, Henderson G.A, Simons J.W, & Henderson D.R 1997. Prostate Attenuated Replication Competent Adenovirus (ARCA) CN706:A Selective Cytotoxic for Prostate-specfic Antigen-positive Prostate Cancer Cells. *Cancer Research*, 57: 2559-2563.

Roth J.A, Nguyen D, Lawrence D.D, Kemp B.L, Carrasco C.H, Ferson D.Z, Hong W.K, Komaki R, Lee J.J, Nesbitt J.C, Pisters K.M.W, Putnam J.B, Schea R, Shin D.M, Walsh G.L, Dolormente M.M, Han C.I, Martin F.D, Yen N, Xu K, Stephens L.C, McDonnell T.J, Mukhopadhyay T, & Cai D 1996. Retrovirus-mediated wild-type p53 gene transfer to tumors of patients with lung cancer. *Nature Medicine*, 2(9): 985-991.

Roth J.A & Cristiano R.J 1997. Gene Therapy for Cancer: What Have We Done and Where Are We Going? *Journal of the National Cancer Institute*, 89: 21-39.

Rowe W.P, Huebner R.J, Gilmore L.K, Parrott R.H, & Ward T.G 1953. Isolation of a cytopathogenic agent from human adenoids undergoing spontaneous degeneration in tissue culture. *Proceedings of the Society for Experimental Biology and Medicine*, 84(3): 570-573.

Sambrook J, Fritsch E.F, & Maniatis T 1989. *Moleular Cloning: A Laboratory Manual*.

Sanda M.G, Ayyagari S.R, Jaffee E.M, Epstein J.I, Clift S.L, Cohen L.K, Dranoff G, Pardoll D.M, Mulligan R.C, & Simons J.W 1994. Demonstration of a rational strategy for human prostate cancer gene therapy. *The Journal of Urology*, 151(3): 622-628.

Sanda M.G, Smith D.C, Charles L.G, Hwang C, Pienta K.J, Schlom J, Milenic D, Panicali D, & Montie J.E 1999. Recombinant vaccinia-PSA (PROSTVAC) can induce a prostate-specific immune response in androgen-modulated human prostate cancer. *Urology*, 53(2): 260-266.

Saz A.K & Slie R.B 1954. The inhibition of organic nitro reductase by aureomycin in cell-free extracts. II. Cofactor requirements for the nitro reductase enzyme complex. *Archives of Biochemistry and Biophysics*, 51(1): 5-16.

Schlaberg R, Choe D.J, Brown K.R, Thaker H.M, & Singh I.R 2009. XMRV is present in malignant prostatic epithelium and is associated with prostate cancer, especially high-grade tumors. *Proceedings of the National Academy of Sciences of the United States of America*, 106(38): 16351-16356.

Searle P.F, Chen M, Hu L, Race P.R, Lovering A.L, Grove J.I, Guise C, Jaberipour M, James N.D, Mautner V, Young L.S, Kerr D.J, Mountain A, White S.A, & Hyde E.I 2004. Nitoreductase: A prodrug-activating enzyme for cancer gene therapy. *Clinical and Experimental Pharmacology and Physiology*, 31: 811-816.

Shalev M, Miles B.J, Thompson T.C, Ayala G, Butler E.B, Aguilar-Cordova E, & Kadmon D 2000. Suicide gene therapy for prostate cancer using a replication-deficient adenovirus containing the herpesvirus thymidine kinase gene. *World Journal of Urology*, 18: 125-129.

Shenk T, Edited by Fields B.N, Knipe D.M, Howley P.M, Chanock R.M, Melnick J.L, Monath T.P, Roizman B, & Straus S.E 1996. *Adenoviridae: The Viruses and Their Replication. Fields Virology*: 2111-2148. Lippincott - Raven.

Shirakawa T, Terao S, Hinata N, Tanaka K, Takenaka A, Hara I, Sugimura K, Matsuo M, Hamada K, Fuji K, Okegawa T, Higashihara E, Gardner T.A, Kao C, Chung L.W, Kamidono S, Fujisawa M, & Gotoh A 2007. Long-term outcome of phase I/II clinical trial of Ad-OC-TK/VAL gene therapy for hormone-refractory metastatic prostate cancer. *Human Gene Therapy*, 18(12): 1225-1232.

Simons J.W, Mikhak B, Chang J, DeMarzo A.M, Carducci M.A, Lim M, Weber C.E, Baccala A.A, Goemann M.A, Clift S.M, Ando D.G, Levitsky H.I, Cohen L.K, Sanda M.G, Mulligan R.C, Partin A.W, Carter B, Piantadosi S, Marshall F.F, & Nelson W.G 1999. Induction of Immunity to Prostate Cancer Antigens: Results of a Clinical Trial of Vaccination with Irradiated Autologous Prostate Tumor Cells Engineered to Secrete Granulocyte-Macrophage Colony-stimulating Factor Using *ex vivo* Gene Transfer. *Cancer Research*, 59: 5160-5168.

Singleton D.C, Li D, Bai S.Y, Syddall S.P, Smaill J.B, Shen Y, Denny W.A, Wilson W.R, & Patterson A.V 2007. The nitroreductase prodrug SN 28343 enhances the potency of systemically administered armed oncolytic adenovirus ONYX-411^{NTR}. *Cancer Gene Therapy*, 14: 953-967.

Small E.J, Carducci M.A, Burke J.M, Rodriguez R, Fong L, Van Ummersen L, Yu DC, Aimi J, Ando D, Working P, Kirn D, & Wilding G 2006. A phase I trial of intraveous CG7870, a replication-selective, prostate-secific antigen-targeted oncolytic adenovirus, for the treatment of hormone-refractory, metastatic prostate cancer. *Molecular Therapy*, 14(1): 107-117.

Snyder L & Champness W 2003. *Molecular Genetics of Bacteria*. ASM Press.

Sorscher E.J, Peng S, Bebok Z, Allan P.W, Bennett L.L Jr, & Parker W.B 1994. Tumor cell bystander killing in colonic carcinoma utilizing the Escherichia coli DeoD gene to generate toxic purines. *Gene Therapy*, 1(4): 233-238.

Sterman D.H, Gillespie C.T, Carroll R.G, Coughlin C.M, Lord E.M, Sun J, Haas A, Recio A, Kaiser L.R, Coukos G, June C.H, Albelda S.M, & Vonderheide R.H 2006. Interferon beta adenoviral gene therapy in a patient with ovarian cancer. *Nature Clinical Practice Oncology*, 3(11): 633-639.

Subr V, Kostka L, Selby-Milic T, Fisher K, Ulbrich K, Seymour L.W, & Carlisle R.C 2009. Coating of adenovirus type 5 with polymers containing quaternary amines prevents binding to blood components. *Journal of Controlled Release*, 135: 152-158.

Sudbery P 2002. *Human Molecular Genetics*. Prentice Hall - Pearson Education.

Sutter G & Moss B 1992. Nonreplicating vaccinia vector efficiently expresses recombinant genes. *Proceedings of the National Academy of Sciences of the United States of America*, 89: 10847-10851.

Swisher S.G, Roth J.A, Nemunaitis J, Lawrence D.D, Kemp B.L, Carrasco C.H, Connors D.G, El-Naggar A.K, Fossella F, Glisson B.S, Hong W.K, Khuri F.R, Kurie J.M, Lee J.J, Lee J.S, Mack M, Merritt J.A, Nguyen D.M, Nesbitt J.C, Perez-Soler R, Pisters K.M.W, Putnam J.B Jr, Richli W.R, Savin M, Schrump D.S, Shin D.M, Shulkin A, Walsh G.L, Wait J, Weill D, Kimberly M, & Waugh A 1999. Adenovirus-Mediated p53 Gene Transfer in Advanced Non-Small-Cell Lung Cancer. *Journal of the National Cancer Institute*, 91(9): 763-771.

Tait D.L, Obermiller P.S, Redlin-Frazier S, Jensen R.A, Welcsh P, Dann J, King M, Johnson D.H, & Holt J.T 1997. A Phase I Trial of Retroviral BRCA1sv Gene Therapy in Ovarian Cancer. *Clinical Cancer Research*, 3: 1959-1968.

Tait D.L, Obermiller P.S, Hatmaker A.R, Redlin-Frazier S, & Holt J.T 1999. Ovarian Cancer BRCA1 Gene Therapy: Phase I and II Trial Differences in Immune Response and Vector Stability. *Clinical Cancer Research*, 5: 1708-1714.

Tal J 2000. Adeno-Associated Virus-Based Vectors in Gene Therapy. *Journal of Biomedical Science*, 7: 279-291.

Teh B.S, Aguilar-Cordova E, Kernen K, Chou C.C, Shalev M, Vlachaki M.T, Miles B, Kadmon D, Mai YY, Caillouet J, Davis M, Ayala G, Wheeler T, Brady J, Carpenter L.S, Lu H.H, Chiu J.K, Woo S.Y, Thompson T, & Butler E.B 2001. Phase I/II trial evaluating combined radiotherapy and in situ gene therapy with or without hormonal therapy in the treatment of prostate cancer--a preliminary report. *International Journal of Radiation Oncology, Biology, Physics*, 51(3): 605-613.

Teh B.S, Ayala G, Aguilar L, Mai W, Timme T.L, Vlachaki M.T, Miles B, Kadmon D, Wheeler T, Caillouet J, Davis M, Carpenter L.S, Lu H.H, Chiu J.K, Woo S.Y, Thompson T, Aguilar-Cordova E, & Butler E.B 2004. Phase I-II trial evaluating combined intensity-modulated radiotherapy and in situ gene therapy with or without hormonal therapy in treatment of prostate cancer - interim report on PSA response and biopsy data. *International Journal of Radiation Oncology, Biology, Physics*, 58(5): 1520-1529.

Thomas C.E, Ehrhardt A, & Kay M.A 2003. Progress and problems with the use of viral vectors for gene therapy. *Nature Reviews Genetics*, 4: 346-358.

Titomirov A.V, Sukharev S, & Kistanova E 1991. In vivo electroporation and stable transformation of skin cells of newborn mice by plasmid DNA. *Biochimica Et Biophysica Acta*, 1088(1): 131-134.

Trudel S, Trachtenberg J, Toi A, Sweet J, Li Z.H, Jewett M, Tshilias J, Zhuang L.H, Hitt M, Wan Y, Gauldie J, Graham F.L, Dancey J, & Stewart A.K 2003. A phase I trial of adenovector-mediated delivery of interleukin-2 (AdIL-2) in high-risk localized prostate cancer. *Cancer Gene Therapy*, 10: 755-763.

Tsuneoka M, Nakano F, Ohgusu H, & Mekada E 1997. c-myc activates RCC1 gene expression through E-box elements. *Oncogene*, 14: 2301-2311.

Tupin E, Poirier B, Bureau M.F, Khallou-Laschet J, Vranckx R, Caligiuri G, Gaston A.T, Duong Van Huyen J.P, Scherman D, Bariety J, Michel J.B, & Nicoletti A 2003. Non-viral gene transfer of murine spleen cells achieved by in vivo electroporation. *Gene Therapy*, 10: 569-579.

Turner P.C, McLennan A.G, Bates A.D, & White M.R.H 1997. *Instant Notes in Molecular Biology*. Bios Scientific Publishers.

Van Duijn P.W, Ziel-van der Made A.C, Van der Korput J.A, & Trapman J 2010. PTEN-mediated G1 cell-cycle arrest in LNCaP prostate cancer cells is associated with altered expression of cell-cycle regulators. *The Prostate*, 70(2): 135-146.

Vass S.O 2007. PhD Thesis *Cancer Studies*. University of Birmingham.

Vass S.O, Jarrom D, Wilson W.R, Hyde E.I, & Searle P.F 2009. *E.coli* NfsA: an alternative nitroreductase for prodrug activation gene therapy in combination with CB1954. *British Journal of Cancer*, 100: 1903-1911.

Vollmer C.M, Ribas A, Butterfield L.H, Dissette V.B, Andrews K.J, Eilber F.C, Montejo L.D, Chen A.Y, Hu B, Glaspy J.A, McBride W.H, & Economou J.S 1999. p53 Selective and Nonselective Replication of an E1B-deleted Adenovirus in Hepatocellular Carcinoma. *Cancer Research*, 59: 4369-4374.

Vorburger S.A & Hunt K.K 2002. Adenoviral Gene Therapy. *The Oncologist*, 7: 46-59.

Walhout A.J.M, Gubbels J.M, Bernards R, van der Vliet P.C, & Timmers H.T.M 1997. c-Myc/Max heterodimers bind cooperaively to the E-box sequences located in the first intron of the rat ornithine decarboxylase (ODC) gene. *Nucleic Acids Research*, 25(8): 1493-1501.

Walker G.C 1984. Mutagenesis and Inducible Responses to Deoxyribonucleic Acid Damage in *Escherichia coli*. *Microbiological Reviews*, 48(1): 60-93.

Watanabe M, Ishidate M, & Nohmi T 1990. Nucleotide sequence of *Salmonella typhimurium* nitroreductase gene. *Nucleic Acids Research*, 18(4): 1059.

Watanabe M, Nishino T, Takio K, Sofuni T, & Nohmi T 1998. Purification and Characterization of Wild-type and Mutant "Classical" Nitroreductases of *Salmonella typhimurium*. *The Journal of Biological Chemistry*, 273(37): 23922-23928.

Watson M.A, Gowers D.M, & Halford S.E 2000. Alternative Geometries of DNA Looping: an Analysis using the *Sfi* I Endonuclease. *Journal of Molecular Biology*, 298: 461-475.

Weedon S.J, Green N.K, McNeish I.A, Gilligan M.G, Mautner V, Wrighton C.J, Mountain A, Young L.S, Kerr D.J, & Searle P.F 2000. Sensitisation of Human Carcinoma Cells to the Prodrug CB1954 by Adenovirus Vector-Mediated Expression of *E. coli* Nitroreductase. *International Journal of Cancer*, 86: 848-854.

Wentzell L.M & Halford S.E 1998. DNA Looping by the *Sfi* I Restriction Endonuclease. *Journal of Molecular Biology*, 281: 433-444.

Westermann S & Weber K 2003. Post-translational modifications regulate microtubulin function. *National Review of Molecular Cell Bilogy*, 4: 938-947.

Whiteway J, Koziarz P, Veall J, Sandhu N, Kumar P, Hoecher B, & Lambert I.B 1998. Oxygen-Insensitive Nitroreductases: Analysis of the Roles of *nfsA* and *nfsB* in Development of Resistance to 5-Nitrofuran Derivatives n *Escherichia coli*. *Journal of Bacteriology*, 180(21): 5529-5539.

Wiewrodt R, Amin K, Kiefer M, Jovanovic V.P, Kapoor V, Force S, Chang M, Lanuti M, Black M.E, Kaiser L.R, & Albelda S.M 2003. Adenovirus-mediated gene transfer of enhanced Herpes simplex virus thymdine kinase mutants improves prodrug-mediated tumor cell killing. *Cancer Gene Therapy*, 10: 353-364.

Wilson J.M, Englehardt J.F, Grossman M, Simon R.H, & Yang Y 1994. Clinical Protocol: Gene Therapy of Cystic Fibrosis Lung Disease Using E1 Deleted Adenoviruses: A Phase I Trial. *Human Gene Therapy*, 5: 501-519.

Wilson W.R, Pullen S.M, Hogg A, Helsby N.A, Hicks K.O, & Denny W.A 2002. Quantitation of Bystander Effects in Nitroreductase Suicide Gene Therapy Using Three-Dimensional Cell Cultures. *Cancer Research*, 62: 1425-1432.

Wilson W.R, Pullen S.M, Hogg A, Hobbs S.M, Pruijin F.B, & Hicks K.O 2004. In Vitro and In Vivo Models for Evaluation of GDEPT. *Methods in Molecular Medicine*, 90: 403-431.

Wolf J.K, Bodurka D.C, Gano J.B, Deavers M, Ramondetta L, Ramirez P.T, Levenback C, & Gershenson D.M 2004. A phase I study of Adp53 (INGN 201, ADVEXIN) for patients with platinum- and paclitaxel-resistant epthelial ovarian cancer. *Gynaecology Oncology*, 94(2): 442-448.

Wolff J.A, Malone R.W, Williams P, Chong W, Acsadi G, Jani A, & Felgner P.L 1990. Direct Gene Transfer into Mouse Muscle in Vivo. *Science*, 247(4949): 1465-1468.

Wu G.Y & Wu C.H 1987. Receptor-mediated in Vitro Gene Transformation by a Soluble DNA Carrier System. *The Journal of Biological Chemistry*, 262(10): 4429-4432.

Yang JP & Huang L 1996. Direct gene transfer to mouse melanoma by intratumor injection of free DNA. *Gene Therapy*, 3(6): 542-548.

Zabner J, Couture L.A, Gregory R.J, Graham S.M, Smith A.E, & Welsh M.J 1993. Adenovirus-mediated gene transfer transiently corrects the chloride transport defect in nasal epithelia of patients with cystic fibrosis. *Cell*, 75(2): 207-216.

Zenno S, Koike H, Kumar A.N, Jayaraman R, Tanokura M, & Saigo K 1996a. Biochemical Characterization of NfsA, the *Escherichia coli* Major Nitroreductase Exhibiting a High Amino Acid Sequence Homology to Frp, a *Vibrio harveyi* Flavin Oxidoreductase. *Journal of Bacteriology*, 178(15): 4508-4514.

Zenno S, Koike H, Tanokura M, & Saigo K 1996b. Conversion of NfsB, a Minor *Escherichia coli* Nitroreductase, to a Flavin Reductase Similar in Biochemical Properties to FRase I, the Major Flavin Reductase in *Vibrio fischeri*, by a single Amino Acid Substitution. *Journal of Bacteriology*, 178(15): 4731-4733.

Zhan J, Gao Y, Wang W, Shen A, Aspelund A, Young M, Laquerre S, Post L, & Shen Y 2005. Tumor-specific intravenous gene delivery using oncolytic adenoviruses. *Cancer Gene Therapy*, 12: 19-25.

Zhang Y, Mukhopadhyay T, Donehower L.A, Georges R.N, & Roth J.A 1993. Retroviral Vector-Mediated Transduction of K-ras Antisense RNA into Human Lung Cancer Cells Inhibits Expression of the Malignant Phenotype. *Human Gene Therapy*, 4: 451-460.

Zheng L.D, Jiang G.S, Pu J.R, Mei H, Dong J.H, Hou X.H, & Tong Q.S 2009. Stable knockdown of herparanase expression in gastric cancer cells *in vitro*. *World Journal of Gastroenterology*, 15(43): 5542-5448.

Zipfel P.A, Grove M, Blackburn K, Fujimoto M, Tedder T.F, & Pendergast A.M 2000. The c-Abl Tyrosine Kinase Is Regulated Downstream of the B Cell Antigen Receptor and Interacts with CD19. *The Journal of Immunology*, 165: 6872-6879.